AFAPL-TR-72-18

20 WATT-HOUR PER POUND REGENERATIVE FUEL CELL

R. L. Costa and S. S. Tomter

TECHNICAL REPORT AFAPL-TR-72-18

MARCH 1972

Approved for public release; distribution unlimited

Air Force Aero Propulsion Laboratory
Air Force Systems Command
Wright-Patterson Air Force Base, Ohio

NOTICE

When Government drawings, specifications, or other data are used for any purpose other than in connection with a definitely related Government procurement operation, the United States Government thereby incurs no responsibility nor any obligation whatsoever; and the fact that the government may have formulated, furnished, or in any way supplied the said drawings, specifications, or other data, is not to be regarded by implication or otherwise as in any manner licensing the holder or any other person or corporation, or conveying any rights or permission to manufacture, use, or sell any patented invention that may in any way be related thereto.

Copies of this report should not be returned unless return is required by security considerations, contractual obligations, or notice on a specific document.

Unclassified

Security Classification

DOCUMENT CONTROL DATA - R & D

(Security classification of title, body of abstract and indexing annotation must be entered when the overall report is classified)

1 ORIGINATING ACTIVITY (Corporate author)	2a. REPORT SECURITY CLASSIFICATION
Xerox Corporation/Electro-Optical Systems 300 North Halstead Street Pasadena, California	Unclassified
	2b. GROUP

3 REPORT TITLE

20 Watt-Hour Per Pound Regenerative Fuel Cell

4 DESCRIPTIVE NOTES (Type of report and inclusive dates)

Final Technical Report 22 June 1970 through 22 December 1971

5. AUTHOR(S) (First name, middle initial, last name)

Raymond L. Costa
Scott S. Tomter

6 REPORT DATE	7a. TOTAL NO. OF PAGES	7b. NO. OF REFS
3 April 1972	181	0

8a. CONTRACT OR GRANT NO	9a. ORIGINATOR'S REPORT NUMBER(S)
F33615-70-C-1671 b. PROJECT NO 3145 c. Task No. 314521 d. Work Unit No. 314521-018	4058-FR 9b. OTHER REPORT NO(S) (Any other numbers that may be assigned this report) AFAPL-TR-72-18

10 DISTRIBUTION STATEMENT

Approved for public release; distribution unlimited

11 SUPPLEMENTARY NOTES	12. SPONSORING MILITARY ACTIVITY
	Air Force Aero Propulsion Laboratory Wright-Patterson Air Force Base, Ohio 45433

13 ABSTRACT

Xerox Corporation, Electro-Optical Systems, has conducted an analytical and experimental program in the continued exploratory development of regenerative hydrogen-oxygen fuel cells. All work was on cylindrical single cells rated at 40 ampere-hours actually delivered, with the charge-discharge sequence simulating that of a satellite in synchronous orbit. It was demonstrated that regenerative fuel cells of the design described in the report are capable of cyclical storage and release of 20 watt-hours of electrical energy per pound of energy storage system. Preliminary environmental tests indicated that lightweight cells will withstand vibrational, thermal, and space vacuum conditions. A four-cell breadboard system was fabricated and tested through 23 cycles of a simulated synchronous orbit eclipse period prior to delivery of the breadboard as a contract hardware item.

DD FORM 1 NOV 65 1473

Unclassified

Security Classification

14. KEY WORDS	LINK A		LINK B		LINK C	
	ROLE	WT	ROLE	WT	ROLE	WT
Regenerative Fuel Cell						
Electrochemical Energy Storage System						
Cylindrical Fuel Cell						
Secondary Battery						

20 WATT-HOUR PER POUND REGENERATIVE FUEL CELL

R. L. Costa and S. S. Tomter

FOREWORD

The exploratory development described in this report was conducted by Xerox Corporation, Electro-Optical Systems, Pasadena, California, and was performed under Air Force Contract F33615-70-C-1671, Project No. 3145, Task No. 314521. The period of performance was 22 June 1970 through 22 December 1971.

This report was submitted by the authors on 15 December 1971 as Electro-Optical Systems Report 4058-FR. The work was done under the direction of L. S. Harootyan, Jr. and I. F. Luke, AFAPL/POE-1, Air Force Aero Propulsion Laboratory, Air Force System Command.

The publication of this report does not constitute Air Force approval of the report's findings or conclusions. It is published only for the exchange and stimulation of ideas.

James D. Reams, Chief
Energy Conversion Branch
Aerospace Power Division
Aero Propulsion Laboratory

ABSTRACT

Xerox Corporation, Electro-Optical Systems, has conducted an analytical and experimental program in the continued exploratory development of regenerative hydrogen-oxygen fuel cells. All work was on cylindrical single cells rated at 40 ampere-hours actually delivered, with the charge-discharge sequence simulating that of a satellite in synchronous orbit. It was demonstrated that regenerative fuel cells of the design described in the report are capable of cyclical storage and release of 20 watt-hours of electrical energy per pound of energy storage system. Preliminary environmental tests indicated that lightweight cells will withstand vibrational, thermal, and space vacuum conditions. A four-cell breadboard system was fabricated and tested through 23 cycles of a simulated synchronous orbit eclipse period prior to delivery of the breadboard as a contract hardware item.

TABLE OF CONTENTS

		PAGE
I.	INTRODUCTION	1
II.	SUMMARY OF THE ACTIVITIES	3
III.	SINGLE CELL EVALUATION	5
	3.1 Test Cell Design	5
	3.2 Parametric Studies of Electrochemical Performence	11
	3.2.1 Temperature Tests	25
	3.2.2 Pressure Tests	29
	3.2.3 Life Testing	40
	3.3 Cell Component Optimization	45
	3.3.1 Mechanical Components	49
	3.3.1.1 Bellows	49
	3.3.1.1.1 Electroformed Bellows	49
	3.3.1.1.2 Hypalon Rubber Diaphragm	49
	3.3.1.1.3 Welded Metal Bellows	49
	3.3.1.2 Pressure Housing	60
	3.3.1.3 Core Support	60
	3.3.1.3.1 Standard Perforated Core Support	60
	3.3.1.3.2 Core With No Support	60
	3.3.1.3.3 Sintered Nickel Core Support	64
	3.3.1.4 Insulated Feedthrough Connectors	66
	3.3.2 Electrochemical Components	72
	3.3.2.1 Oxygen Electrodes	72
	3.3.2.2 Electrical Connections	75
	3.3.2.3 Matrix and Electrolyte Loading	77
	3.3.2.4 Temperature Measurements	82
	3.4 Deliverable Single Cells	83

TABLE OF CONTENTS (Continued)

	PAGE
IV. LIGHTWEIGHT CELLS	92
4.1 Cell Design and Analysis	92
4.1.1 Stress and Dynamic Analysis	92
4.1.2 Thermodynamic Analysis	92
V. FABRICATION AND TESTING OF LIGHTWEIGHT CELLS	93
5.1 Prototype Fabrication and Checkout	93
5.1.1 Vibration Test	93
5.1.2 Temperature Test	94
5.1.3 Vacuum Test	94
VI. BREADBOARD REGENERATIVE FUEL CELL ENERGY STORAGE SYSTEM	99
6.1 Design and Fabrication	99
6.2 Performance of Breadboard Cells/System	99
6.2.1 Cell Acceptance Tests	101
6.2.2 System Cyclic Testing	102
VII. CONCLUSIONS AND RECOMMENDATIONS	107
APPENDIX I - SCOPE OF WORK	109
APPENDIX II - BOILER-PLATE DESIGN ANALYSIS	129
APPENDIX III - RANDOM VIBRATION ANALYSIS	145
APPENDIX IV - THERMODYNAMIC ANALYSIS	165

LIST OF ILLUSTRATIONS

FIGURE		PAGE
1.	Boiler Plate Test Fixture	6
2.	Perforated Plate (Core Support)	7
3.	40 Ampere-Hour, 600 psig Fuel Cell Core	8
4.	Fuel Cell Bellows (Diaphragm)	9
5.	External Component Assembly	10
6.	Cell No. 4058-2 - Discharge Performance	26
7.	Top Views of Boiler Plate Cell Assembly	28
8.	Cell No. 4058-11 - Charge Performance	30
9.	Cell No. 4058-11 - Discharge Performance	31
10.	Cell No. 4058-11 - Polarization Scans	32
11.	Cell No. 4058-13 - Charge Performance	33
12.	Cell No. 4058-13 - Discharge Performance	34
13.	Cell No. 4058-13 - Polarization Scans	35
14.	Cell No. 4058-15 - Charge Performance	36
15.	Cell No. 4058-15 - Discharge Performance	37
16.	Cell No. 4058-14 - Charge Performance	38
17.	Cell No. 4058-14 - Discharge Performance	39
18.	Set Positions of Bellows (Diaphragm)	41
19.	Cell No. 4058-6 - Charge Performance	42
20.	Cell No. 4058-6 - Discharge Performance	43
21.	Cell No. 4058-6 - Polarization Scans	44
22.	Cell No. 4058-10 - Charge Performance	46
23.	Cell No. 4058-10 - Discharge Performance	47
24.	Cell No. 4058-10 - Polarization Scans	48
25.	Fuel Cell Bellows Test Fixture	50
26.	Electroformed Bellows Design	51
27.	Welded Metal Bellows Design	52
28.	Cell No. 4058-19 - Charge Performance	54
29.	Cell No. 4058-19 - Discharge Performance	55

LIST OF ILLUSTRATIONS (Continued)

FIGURE		PAGE
30.	Cell No. 4058-18 - Charge Performance	57
31.	Cell No. 4058-18 - Discharge Performance	58
32.	Cell No. 4058-18 - Polarization Scans	59
33.	Fuel Cell Shell Hydroburst Test	63
34.	Cell No. 4058-33 - Charge Performance	67
35.	Cell No. 4058-33 - Discharge Performance	68
36.	Cell No. 4058-33 - Polarization Scans	69
37.	Ceramic Feedthrough Designs	70
38.	Feedthrough Test Assembly	71
39.	Comparative Cell Polarization Scans	74
40.	Cell No. 4058-29 - Charge Performance	78
41.	Cell No. 4058-29 - Discharge Performance	79
42.	Cell No. 4058-29 - Polarization Scans	80
43.	Cell No. 4058-29 - Performance Degradation	81
44.	Cell No. IR&D-3 - Temperature Profile During Charge	84
45.	Cell No. IR&D-3 - Temperature Profile During Discharge	85
46.	Boiler Plate Fuel Cell - External Plumbing	87
47.	Cell No. 4058-22 - Charge Performance	88
48.	Cell No. 4058-22 - Discharge Performance	89
49.	Cell No. 4058-27 - Charge Performance	90
50.	Cell No. 4058-27 - Discharge Performance	91
51.	Cell No. 4058-31 - Discharge Performance	95
52.	Cell No. 4058-32 - Discharge Performance	97
53.	E.S.S. Switching Arrangement	100
54.	4 Cell Breadboard System - Discharge Performance	106
55.	Random Vibration Environment	123
56.	Single Eclipse Season	128
57.	Formulas for Stresses and Deformation in Pressure Vessels	133
58.	Fuel Cell Configuration	135

LIST OF ILLUSTRATIONS (Continued)

FIGURE		PAGE
59.	Cyclindrical Regenerative Fuel Cell Construction	146
60.	Random Vibration Environment	147
61.	Outer Shell Free-Body Diagram	149
62.	Outer Shell Natural Frequency	151
63.	Outer Shell Stress	151
64.	Typical Perforated Core Surface	154
65.	Model of Top Cap	155
66.	Lateral Vibration of Core	156
67.	Natural Frequency of Core (Conf. 1)	157
68.	Natural Frequency of Core (Conf. 2)	157
69.	Tube Stress from Lateral Vibration	161
70.	Core Stress from Lateral Vibration	161
71.	Recommended Core Support Design	164
72.	Pressure Plots of Boilerplate Fuel Cell Discharge Cycle	167
73.	Pressure Differential Plots of Boilerplate Fuel Cell Discharge Cycle	168
74.	Gas Pressure Plots of a Balanced System	169

SECTION I

INTRODUCTION

The electrolytically regenerative fuel cell is an electrochemical energy storage device, wherein the energy density per unit weight substantially exceeds present acceptable power sources. This concept of an energy storage device, offering reduced weight for a given required energy storage package, is potentially attractive for orbital and interplanetary space application. Xerox Corporation, Electro-Optical Systems, has been conducting a program to design, develop, and test a Regenerative Fuel Cell Energy Storage System (ESS), utilizing the available technology gained in the development of the EOS-RHO-24 A.H. cylindrical fuel cell. The effort of this program has been conducted under the auspices of the Air Force Aero Propulsion Laboratory, Air Force System Command.

The EOS cylindrical regenerative hydrogen oxygen fuel cell is a basic electrochemical cell serving the dual function of a primary fuel cell and a water electrolysis cell. The cell consists of a capillary matrix, containing electrolyte, sandwiched between two catalytically activated porous electrodes. The configuration of the cell is cylindrical, which utilizes the inner core volume as the hydrogen gas reservoir and the space external to the core and within the outer pressure vessel as the oxygen gas reservoir. During the charge operation, the cell functions as a water electrolysis cell, whereby water in the electrolyte contained matrix is electrolyzed producing hydrogen at the cathode and oxygen at the anode. The gases so evolved are stored at pressure in intimate contact with the respective electrodes. During discharge, in the fuel cell mode, the stored gases react at the electrodes to form water, which is absorbed into the electrolyte containing matrix. The electrolyte employed is a 30 percent aqueous potassium hydroxide solution of a quantity which is completely absorbed in the matrix with no free liquid in the system. The entire fuel cell is a completely sealed self-contained unit. The design of a Regenerative Fuel Cell Energy Storage System requires the grouping of a number of individual cells in a circuitry pattern to deliver power at some desired voltage-amperage level.

The Program Plan, as initiated, consisted of the design, development, and testing of a 20 watt hour per pound regenerative fuel cell energy storage system. During the program, a number of modifications and additions to the work scope had to be made. The scope of work is shown in Appendix I.

Task I of the program involved thorough review of Contract F33615-70-C-1671 and preparation of a program master schedule as a milestone forecast. Tasks II, III, and IV entailed the design and fabrication of boilerplate test cells to allow greater flexibility and simplicity for test cell fabrication. The boilerplate test cells were used for parametric studies of the electrochemical performance of the materials and components used in

the EOS regenerative fuel cell. Cell optimization of the various cell components, both mechanical and electrochemical components, was undertaken during this portion of the work scope. Task V and Task VI comprised the design effort of a complete breadboard regenerative fuel cell energy storage system, modular at the single cell level, that would be fully representative of a larger system in all performance aspects. This effort was to include the selection and identification of all components of the ESS.

Task VII involved the design of lightweight cells and was divided into two major subtasks. The first includes the work required to optimize the single cell configuration, with special emphasis on stress and dynamic analysis, thermodynamic analysis, material analysis, and the incorporation of the recommendations of the analyses into documentation as required for the manufacture of the breadboard cells. The second effort of this task included parametric analyses, spacecraft integration considerations, and the generation of a conceptual design of a 1 kw energy storage system. Functional and environmental testing of the critical components of the energy storage system was undertaken in Tasks VIII and IX. This effort included the fabrication of several prototype lightweight cells. Tasks X and XI constituted the final design and design review, based on the technological data and information generated during all previous tasks. The complete breadboard system, fabrication and assembly, was accomplished in Task XII; and the system was tested to the cyclic regime as specified in the contract, modified to permit two cycles per day. The delivery of the tested breadboard regenerative fuel cell energy storage system to the Air Force Aero Propulsion Laboratory was the scope of Task XIII.

SECTION II

SUMMARY OF THE ACTIVITIES

This report describes the effort and results of a program to develop a 20 watt hour/pound regenerative fuel cell energy storage system under Contract F33615-70-C-1671 for the United States Air Force, Air Force Systems Command, Air Force Aero Propulsion Laboratory, Wright-Patterson Air Force Base, Ohio 45433.

The program initially concentrated on electrochemical performance of the materials and components used in the EOS Rechargeable Fuel Cell Model RHO-24AH-Mod. I. The cylindrical configuration of the Model RHO-24AH fuel cell was retained, but an increase in the length of newly designed boiler-plate shells and core assemblies increased the cell rating to 40 A.H. Using the boiler-plate configuration, cells were tested using Allis-Chalmers Type VI oxygen electrodes, an EOS composite potassium titanate matrix, an EOS platinized sintered nickel plaque for the hydrogen electrode, and a 30 percent by weight potassium hydroxide solution as the electrolyte. The materials and components of the test cells have been selected, based on the results of previous development and evaluation work done at Electro-Optical Systems. Parametric studies of cell performance at varying environmental temperatures and increased pressure for added capacity were made to determine the optimum conditions for enhancing increased cycle life. The test cells were cycled on a 10 hour charge at 4.0 amps/72 minute discharge at 33.3 amps test regime. The results of these tests was the attainment of some cells to be life tested for over 100 cycles and one cell to surpass 200 cycles with some degree of performance deterioration. An analysis of the failure modes of the cells indicate a catastrophic combustion within the cells due to the combination of hydrogen and oxygen gas. The cross leak sources in the cell have been through the matrices, due to loss of liquid (electrolyte) or excessive pressure differentials, or through the edge seals of the inner core cell assembly.

During the final phase of the program, it was determined that it would be more advantageous to deemphasize the effort required to deliver the specified hardware (12 cell breadboard ESS), and utilize this effort to advance the integrity of the cells as to cycle life. This contract modification resulted in a more thorough analysis of the failure modes of the cell, with a resultant edge seal design modification which greatly reduced the seal leak problem. The final hardware delivery was reduced to a 4 cell breadboard SS, made up of cells incorporating the new edge seal design. The breadboard has been subjected to a limited number of test cycles and yielded approximately 16 to 17 watt hours per pound without an investigation into weight optimization.

The feasibility of using the cylindrical regenerative fuel cell concept as a modular building block to fabricate large energy storage systems has been demonstrated in this contract, but further technological advancements are required, on the cell level, to increase cycle life and minimize performance degradation.

SECTION III

SINGLE CELL EVALUATION

3.1 TEST CELL DESIGN

Early in the program, it was determined that a heavy weight or "boiler-plate" cell assembly would be beneficial as a test bed for accumulating necessary data for the anticipated many cells to be tested. The "boiler-plate" assembly has the advantage of being reusable, less effort in assembly, and readily accessible for internal cell modification or inspection. The design of the "boiler-plate" shell included the capability of the vessel to withstand internal pressures of at least four times the pressure anticipated in the fully charged condition of lightweight cells. Pressure tests of the shell at 2500 psig showed no leaks or deformation. For simplicity of fabrication, the boiler-plate shell is comprised of a heavy walled stainless steel pipe with flanges at both ends, perforated for all connections to be made at the top. The support core is a perforated inconel sheet which is rolled and welded into a tube, upon which the cylindrical cell assembly (H_2 electrode, matrix, O_2 electrode) is assembled. A bellows is employed at the base of the support tube which isolates the hydrogen and oxygen gases, and allows for pressure compensation due to thermal gradients. The bellows employed is made of Hypalon, and has been tested for a total of over 3500 cycles with no damage to the diaphragm. The cycle test comprised subjecting the diaphragm to pressure differentials, in alternate directions, from 3 psid to a maximum of 15 psid, in 1 psi increments.

The design of the boiler-plate cell was based on a 40 A.H. capacity (200 to 600 psig total gas pressure) at a 33.3 amperes discharge current rate at 0.85 volt for a duration of 72 minutes. The internal volume of the core assembly (Hydrogen reservoir) is 36.4 in^3 and the remaining volume of the pressure vessel (oxygen reservoir) is 17.95 in^3. The schematics of the "boiler-plate" cell components are illustrated in Figures 1, 2, 3, and 4. Additional monitoring and control components have been applied to the external plumbing portion of the cell as schematically shown in Figure 5. This section of the "boiler-plate" is comprised of a pressure switch which is activated at 600 psig to shut off the source of power during the charging mode. In addition, a burst diaphragm has been incorporated into the vessel as a safety measure with a 1000 psig rupture rating. The total pressure within the cell, which is related to the state of charge of the cell, is monitored with a pressure transducer. A differential pressure transducer is incorporated to monitor the pressure differential of the hydrogen and oxygen gases across the cell. It is important to closely control the pressure differential to prevent leakage and consequent intermixing of the gases which recombine slowly to form water and a resultant pressure drop, or which recombine quickly as an explosion and a catastrophic cell failure.

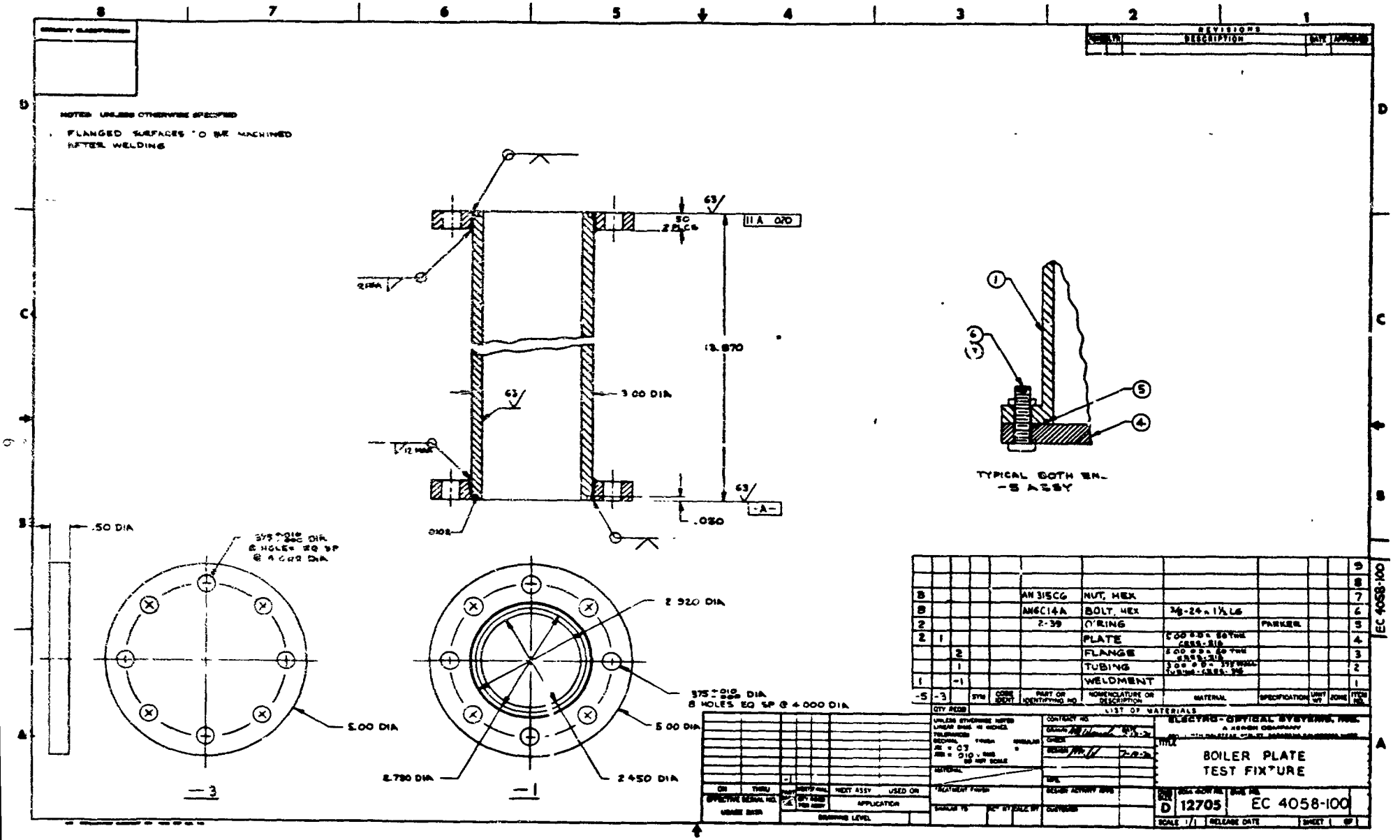

FIGURE 1. BOILER PLATE TEST FIXTURE

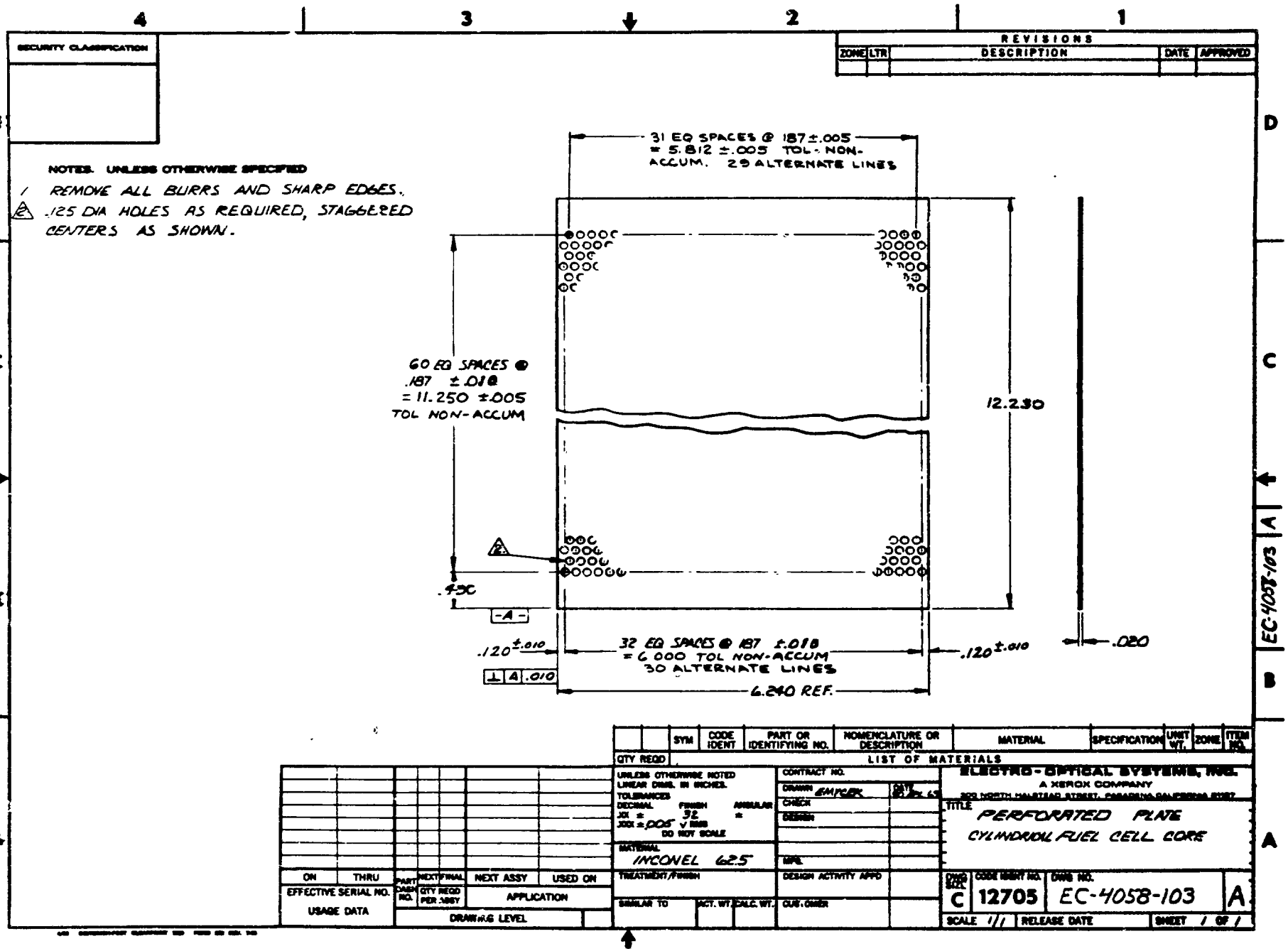

FIGURE 2. PERFORATED PLATE (CORE SUPPORT)

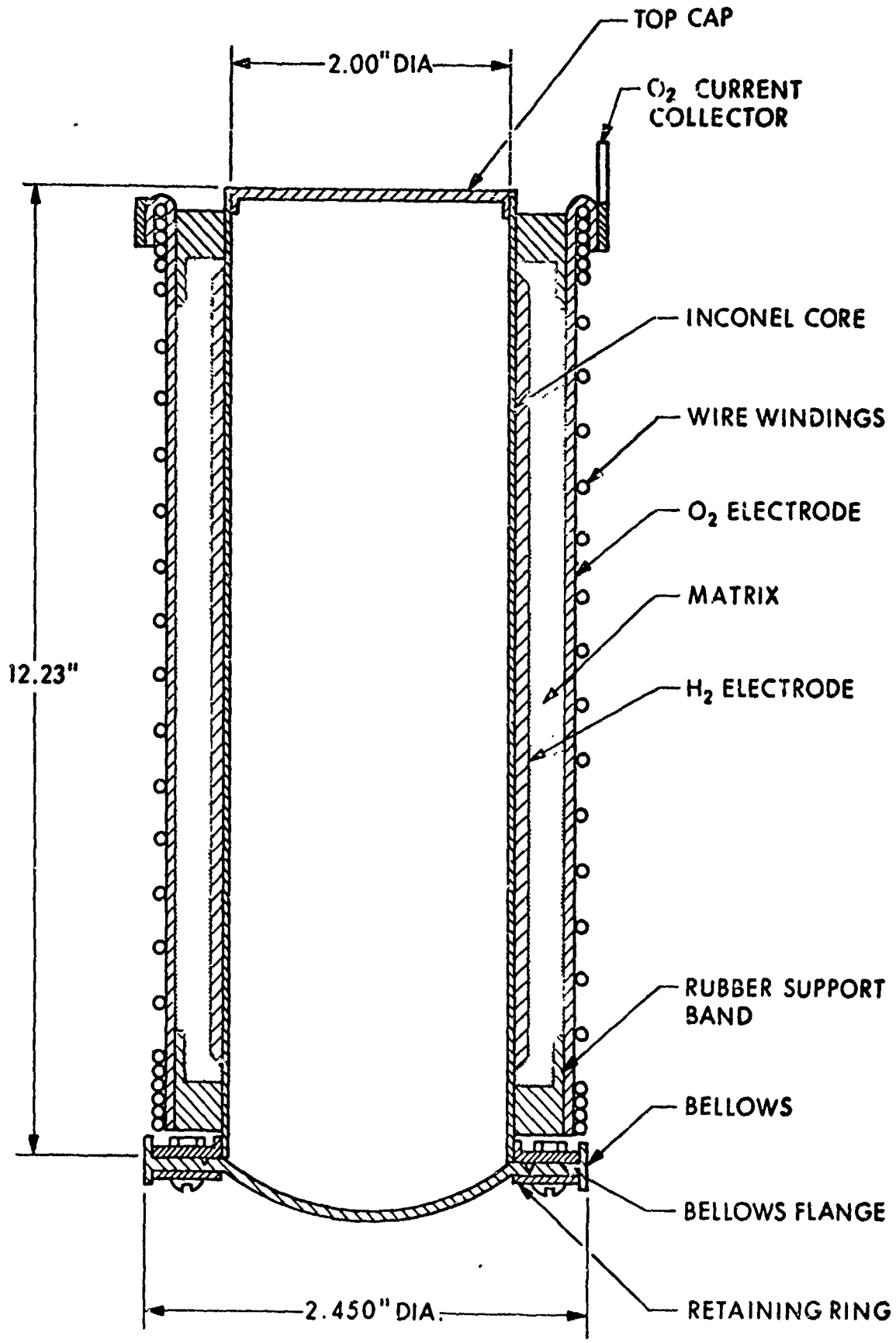

41721

FIGURE 3. 40 AMPERE-HOUR, 600 psig FUEL CELL CORE

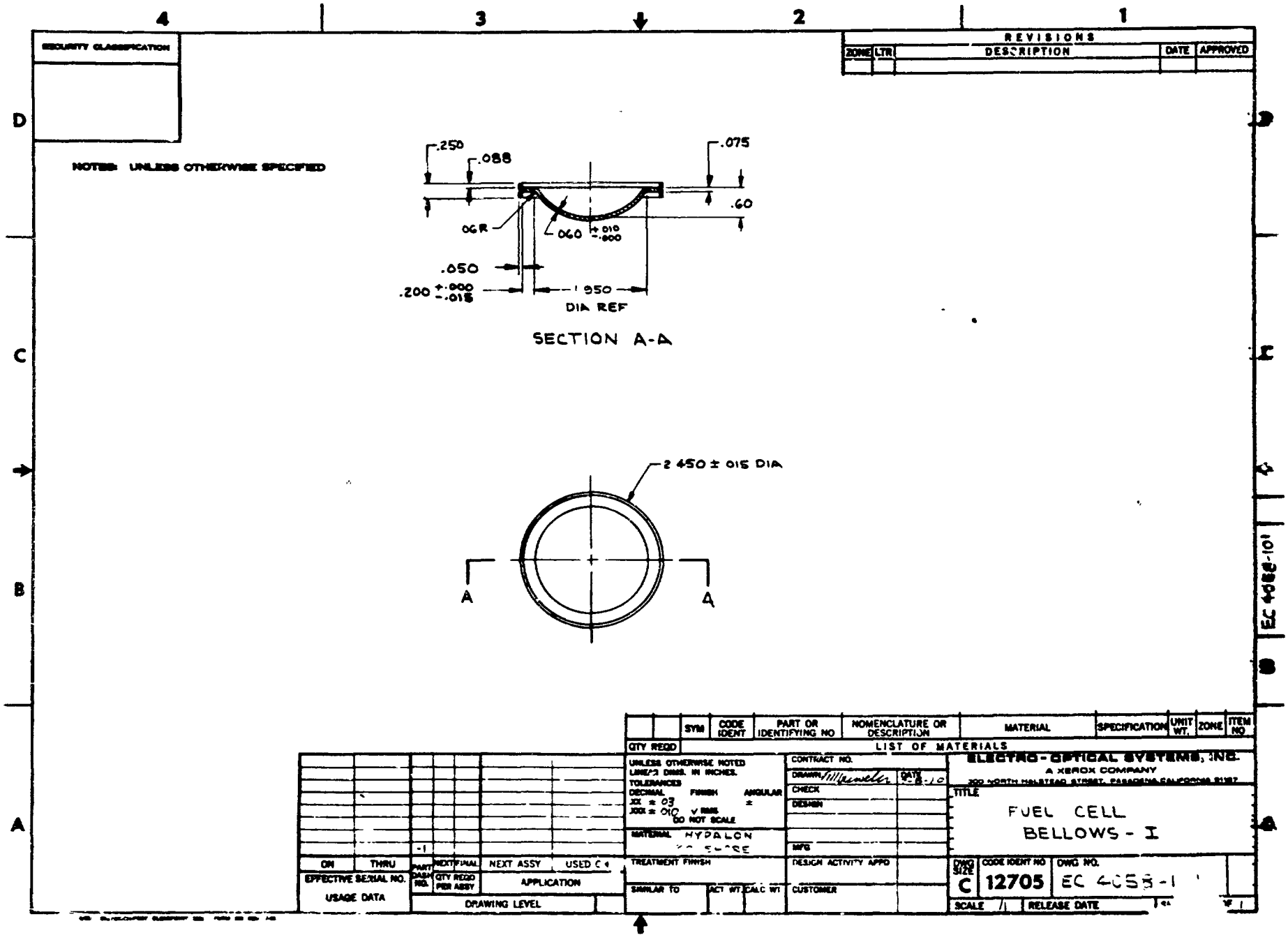

FIGURE 4. FUEL CELL BELLOWS (DIAPHRAGM)

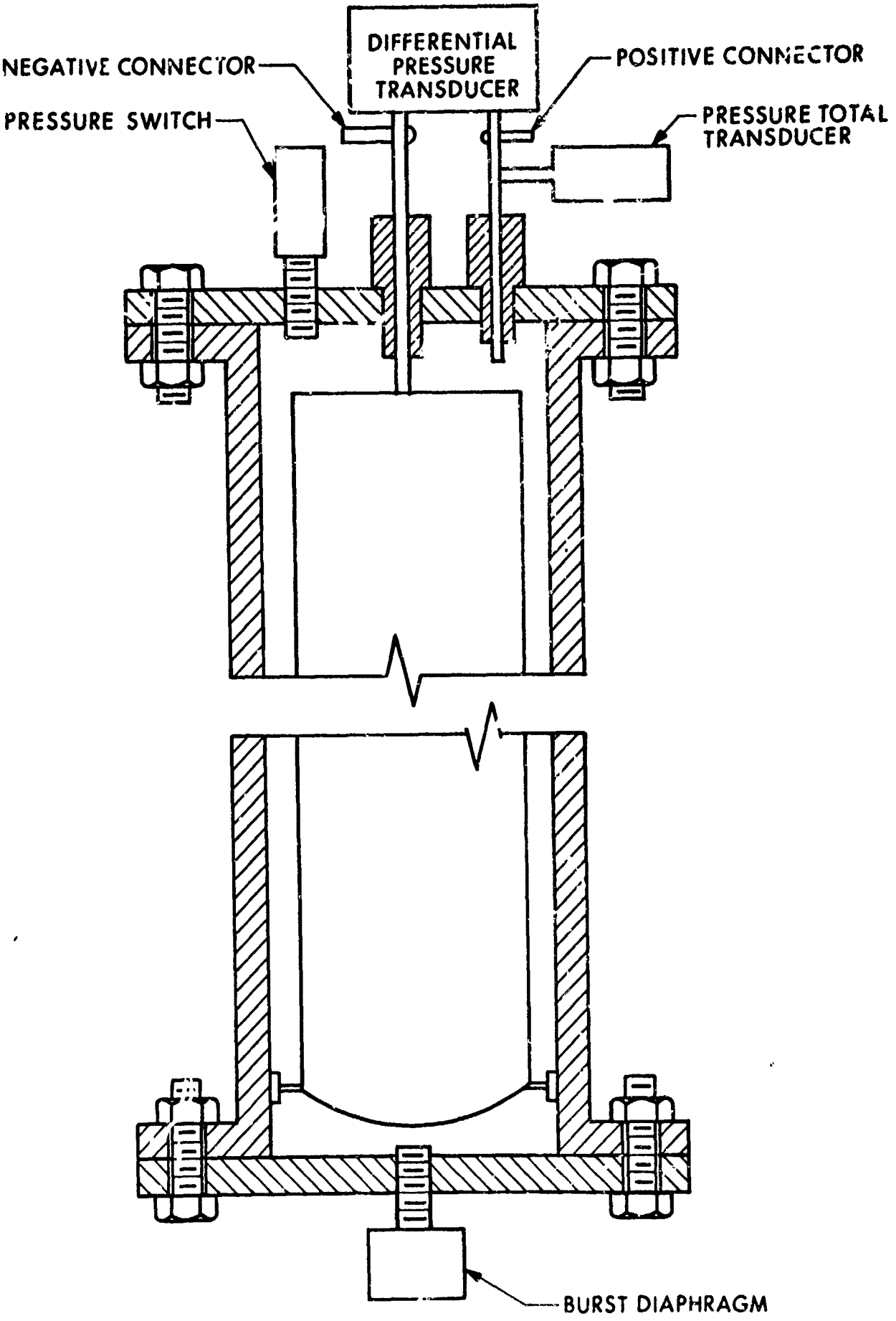

FIGURE 5. EXTERNAL COMPONENT ASSEMBLY

4172C

A preliminary "boiler-plate" design analysis task was undertaken which is included in this report - Appendix II. The analysis report includes volume calculations to establish proper component dimensions, stress analysis of the pressure vessel, and thermodynamic analysis of the EOS regenerative fuel cell.

3.2 PARAMETRIC STUDIES OF ELECTROCHEMICAL PERFORMANCE

Using the boiler-plate shell and internal configuration as previously described, 15 cells have been assembled for evaluation of the electrochemical performance of the materials and components used in EOS Rechargeable Fuel Cell Model RHO-24AH-Mod I.

These are:

Oxygen Electrode	-	Allis Chalmers Type VI, or equivalent.
Hydrogen Electrode	-	EOS sintered nickel plaque with 20 mg Pt/cm^2.
Matrix	-	EOS composite, containing 80 percent potassium titanate (KT), 10 percent Teflon, and 10 percent asbestos fiber.
Electrolyte	-	Potassium hydroxide solution, 30 percent by weight, with no additives.

The materials and components listed above have been chosen based on the results of extensive test work and evaluation performed under Contract No. NAS 3-10948, "Development of Hydrogen-Oxygen Electrolytic Regenerative Fuel Cell", for National Aeronautics and Space Administration, Lewis Research Center. The Final Report on this work has been approved by NASA and has been published for preliminary distribution.

The initial portion of the test program was devoted to tasks of evaluating EOS regenerative fuel cell performance characteristics as a function of environmental temperature, pressure, and life cycle capabilities. The secondary phase of the test program consisted of fabricating and testing cells to optimize various cell components and/or design modifications to advance the technological state-of-the-art and subsequently increase cycle life and reliability. Table I is a complete list of all the cells which were fabricated during this program, with cell description and results obtained. Table I includes the prototype and deliverable flight hardware (lightweight) cells as well as the "boiler-plate" test cells.

The test cells were operated on a 12 hour cycle, which consists of a 4.0 ampere charge rate for approximately 10.8 hours duration, followed by a 72 minute discharge at a rate of 33.3 amperes. The total pressure of the cell ranges from approximately 100 psig at the end of discharge and beginning of charge, to approximately 600 psig at the full charge mode. A 600 psig rated pressure switch automatically removes the cell from the charging power source. During this described cycle regime, the cell is continually monitored and the data recorded periodically through each test.

TABLE I

SUMMARY OF SINGLE CELL TESTS

CELL NUMBER	NO. OF CYCLES	OPER. TEMP. °C	CELL TYPE AND TEST HISTORY	FAILURE ANALYSIS
4058-1	0	--	Standard "boilerplate" fabrication. Failed during initial charge cycle	Rubber edge seal was inadvertently damaged (burned) while welding metal bellows mount.
4058-2	9	50	Standard "boilerplate" fabrication. Failed during charge mode of Cycle #10 while unattended, prior to the installation of the recording equipment.	No data available on charge/discharge condition at time of failure. Both top and bottom seals burned severely. Crack in Hypalon bellows may have been either the cause or effect of failure.
4058-3	15	80	Standard "boilerplate" fabrication. Test to evaluate performance characteristics at elevated temperature. Failed due to oxygen leak in nylon tubing which acts as insulator to differential pressure transducer (ΔPt), causing extreme ΔP. Data prior to failure indicates cell reversal caused by O_2 differential.	Top rubber edge seal was burned through along a 1½" section.
4058-4	--	--	Damaged in processing core; never completed.	
4058-5	--	50	Pellon covered core assembly. Pellon in direct contact with oxygen electrode. The cell failed to discharge and was limited to 4 amps at less than 0.5 volts.	

TABLE I (Continued)

CELL NUMBER	NO. OF CYCLES	OPER. TEMP. °C	CELL TYPE AND TEST HISTORY	FAILURE ANALYSIS
4058-6	42	50	Standard "boilerplate" fabrication. Preliminary test cycling indicated internal leak;defective bellows replaced. Records shortly before failure indicate differential pressure on the hydrogen side in excess of 5 psi, possibly caused by leak at nylon insulator. During the 41st cycle, total pressure dropped from 518 psi to 132 psi in 10 minutes, indicating internal leak and gas recombination.	Post-failure inspection revealed a hole burned through matrix and both electrodes about one inch from top.
4058-7	3	80	Standard "boilerplate fabrication. Druing 3rd discharge, current was at 37 amps instead of 33.3. Operator did not notice pressure going too low near end of 72 minutes, and power supply kept current "on" into reverse charge mode. Excessive differential pressure on oxygen side damaged bellows. In trying to locate leak, core was inadvertently immersed in water, with unknown effect on electrolyte and matrix. Removed from test.	
4058-8	0	50	Standard "boilerplate" fabrication. Failed in initial testing.	

TABLE I (Continued)

CELL NUMBER	NO. OF CYCLES	OPER. TEMP., °C	CELL TYPE AND TEST HISTORY	FAILURE ANALYSIS
4058-	10	80	Standard "boilerplate" fabrication. Performance of cell below normal for 10 cycles. Cell failed when the nylon tube, which acts as an insulator to the differential pressure transducer, broke causing a larger pressure differential across the cell.	The bellows was completely blown out; however, no visual damage occurred to the core assembly.
4058-10	221	50	Standard "boilerplate" fabrication. On the 222 charge cycle, a sudden drop in total pressure of the cell was noted. Test discontinued to analyze the problem. This cell was on standby from 5 April to 28 April 1971 between discharge Cycle 221 and charge cycle 222.	A series of leaks through the matrix were evident. The wire windings were very loose, and the matrix was not properly supported. Apparently, leakage occurred because of the matrix no longer being contained.
4058-11	60	80	Standard "boilerplate" fabrication. Cycle tested at elevated temperature. During 61st charge, near end of charge, pressure dropped rapidly indicating internal failure. Differential pressure of zero showed bellows failure.	Examination confirmed bellows failure, with signs of severe degradation on oxygen side of bellows.

TABLE I (Continued)

CELL NUMBER	NO. OF CYCLES	OPER. TEMP. °C	CELL TYPE AND TEST HISTORY	FAILURE ANALYSIS
4058-12	6	80	Standard "boilerplate" fabrication. Cycle tested at elevated temperature. During 4th discharge, high differential pressure developed on hydrogen side after about 60 minutes into 72 minute discharge cycle, rose to over 3 psid at 68 minutes, discharge discontinued. In 5th discharge, same observation, but a few minutes earlier with differential pressure going to over 3 at 64 minutes, discharge discontinued. In 6th cycle, operator set end of discharge at 64 minutes, but high differential pressure occurred sooner and cell failed.	Cell apparently had a very slight leak on oxygen side, accounting for progressively shorter times to high differential pressure; testing should have been discontinued for leak test and pressure balancing prior to failure.
4058-13	127	30	Standard "boilerplate" fabrication. Cycle tested at depressed temperature. Developed leak through the matrix. Would not charge over approximately 440 psig total pressure on the 128th charge cycle. Removed from test to be inspected. This cell was on standby from 5 April to 28 April 1971 between discharge cycle 127 and charge cycle 128.	Cell inspection revealed a series of leaks through the matrix at a Δ pressure of 2 psi. Removal of oxygen electrode showed a clean matrix. The general condition of the core assembly was good, but the matrix appeared to be on the dry side.
4058-14	--	50	Standard "boilerplate fabrication. High pressure test. Cycled successfully at 600,700,800, & 900 psig. Failed at 980 psig, probably due to ignition of Hypalon or EP in high pressure oxygen. Discharge at 33.3 amps for more than 72 minutes, to approximately 100 psig each cycle.	Catastrophic failure.

TABLE I (Continued)

CELL NUMBER	NO. OF CYCLES	OPER. TEMP. °C	CELL TYPE AND TEST HISTORY	FAILURE ANALYSIS
4058-15	30	100	Standard "boilerplate" fabrication. Cycle tested at elevated temperature. Hypalon bellows burned in 26th cycle, after unscheduled excursion to 890 psig. Bellows replaced. Failed in 31st cycle due to damage to oxygen electrode causing internal short circuit.	
4058-16	50	50	"Boilerplate" cell using a high platinum loaded oxygen electrode, 20 mg/cm^2. This cell was off test from 5 April to 12 May 1971 for test instrument calibration and repair of leaky feedthrough on the cell. During charge cycle #51, a sudden pressure drop followed by a sudden voltage drop resulted in discontinuance of the test for failure analysis.	Burn through matrix and electrodes at upper edge seal indicates initial leakage at edge seal, with a hot spot developing in the matrix with drying and gross leakage occurring.
4058-17	--	50	"Boilerplate" cell incorporating .016 x .250" nickel strips as current collectors on the oxygen electrodes. Cell failed on initail charge cycle at a cell pressure of 420 psig.	Rubber seal and Hypalon bellows badly charred and disintegrated. Failure due to leak at lower edge seal.

TABLE I (Continued)

CELL NUMBER	NO. OF CYCLES	OPER. TEMP. °C	CELL TYPE AND TEST HISTORY	FAILURE ANALYSIS
4058-18	79	50	"Boilerplate" cell employing a welded metal bellows. Cell operated for 37 cycles at the 33 amp discharge rate (40 A.H.). Cell operated an additional 40 cycles at a 40 amp discharge rate (48 A.H.). Cell failed about 10 minutes after reaching the shut-off pressure of 772 psig.	The oxygen electrode and matrix were severely burned at the lower edge seal, and a good portion of the rubber seal was charred and crumbled away. Cause of failure due to leak at lower edge seal.
4058-19	113	50	"Boilerplate" cell employing a welded metal bellows. Cell operated for 113 cycles when small cross leak in the cell developed. The cell analysis disclosed a minor cross leak through the matrix as the cause of failure. An attempt to salvage this cell by patching the matrix and saturating the core with KOH solution allowed the cell to be tested for several more cycles. The performance of the cell was upgraded to the level which characterized the cell initially.	Initial failure due to local hot spot causing matrix to become hard and dry, and a source of gas cross leakage. Repaired cell failed after two additional cycles, due to a leak in an external fitting causing a pressure differential of > 50 psi.
4058-20	--	50	"Boilerplate" cell employing Allis-Chalmers Type VI wetproofed electrodes for both the hydrogen and oxygen electrodes. Cell failed on initial charge cycle at a total pressure of 380 psig.	Hole burned through electrode and matrix at midpoint of core. Difficulty in forming and wetting of matrix using wetproofed electrodes may account for cross leakage in this cell.
4058-21	--	50	Standard "boilerplate" fabrication employing a welded metal bellows. Cell failed on initial charge cycle.	Bottom of core assembly burned. Failure due to bottom edge seal.

TABLE I (Continued)

CELL NUMBER	NO. OF CYCLES	OPER. TEMP. °C	CELL TYPE AND TEST HISTORY	FAILURE ANALYSIS
4058-22	9	50	Standard "boilerplate" cell fabrication with a metal bellows welded to the bottom of the inconel core. The failure of Cell 4058-21 on the initial charge cycle resulted in close analysis of this cell during fabrication which revealed the charred bottom rubber seal after welding the bellows to the core. The rubber seal was replaced and the cell subjected to 3 conditioning cycles to adjust electrolyte volume for optimum performance and then subjected to 6 functional cycles. This cell has been delivered to WPAFB.	
4058-23	2	50	Standard cell fabrication with a metal bellows welded to the bottom of the inconel core. Replaced bottom rubber seal which was also slightly charred during welding of the bellows to the core. Cell was tested during 2 conditioning cycles, but developed a leak during the 3rd charge cycle at approximately 410 psig.	A severe burn at the upper seal edge had developed which shorted the cell, burned the rubber edge seal, and burned the winding wire. Failure due to upper edge seal leak.
4058-24	--	--	This cell was inadvertently subject to failure during fabrication. In the process of pressing the matrix, whereby the matrix is subject to a pressure of 250 psig, the perforated inconel core was crushed. An undersize support core was inserted into the perforated inconel core, which was the reason for this failure.	

TABLE I (Continued)

CELL NUMBER	NO. OF CYCLES	OPER. TEMP. °C	CELL TYPE AND TEST HISTORY	FAILURE ANALYSIS
4058-25	--	50	Standard "boilerplate" fabrication incorporating a welded metal bellows. This cell failed on the initial charge cycle at a pressure of 320 psig and a pressure differential of approximately 1.2 psi.	Analysis revealed a burned section at the lower rubber seal. Failure due to edge seal leak.
4058-26	--	50	During fabrication of this cell, a modification of wire winding the core assembly was incorporated to insure a better end seal. The cell was put on test but failed on initial charge cycle at approximately 450 psig, with a pressure differential less than 1.0 psid.	The visual examination disclosed a small burn hole through the hydrogen electrode at a perforation in the core just above the lower rubber seal. Failure appears to be cross leakage through the matrix.
4058-27	7	50	This "boilerplate" cell was fabricated the same as Cell No. 4058-26, incorporating the same wire winding technique. The cell was subjected to 6 functional test cycles and delivered to WPAFB.	
4058-28	--	--	A standard "boilerplate" fabrication, with a thin plated nickel on the perforated inconel core support to reduce ohmic resistance. Cell was not put on test.	

TABLE I (Continued)

CELL NUMBER	NO. OF CYCLES	OPER. TEMP. °C	CELL TYPE AND TEST HISTORY	FAILURE ANALYSIS
4058-29	120	50	This "boilerplate" cell was fabricated and identified as a low resistant cell. The perforated inconel core was nickel plated, and a nickel screen was wrapped around the oxygen electrode to act as a current collector. The new wire winding technique for the edge seal was utilized.	No failure occurred after 120 cycles of operation. The termination of the contract resulted in test discontinuation.
4058-30	1	50	This "boilerplate" cell has been fabricated, using a sintered nickel core as the H_2 electrode as well as the support mechanism. A small external leak developed in a weld in the oxygen plumbing. The cell was removed from test and the proper repair was made. The cell was then subject to a leak test at which time the rupture diaphragm in the boilerplate assembly failed at approximately 500 psig. The cell was damaged beyond repair.	Cell failure due to a faulty pressure diaphragm which ruptured at approximately 500 psig.
IR&D-1	--	--	This "boilerplate" cell was fabricated in the standard method, substituting a platinum plated nickel plaque for the standard oxygen electrode. A leak in the weld of the cap prevented testing of this cell, which was then rebuilt as Cell No. IR&D-4.	

TABLE I (Continued)

CELL NUMBER	NO. OF CYCLES	OPER. TEMP. °C	CELL TYPE AND TEST HISTORY	FAILURE ANALYSIS
IR&D-2	2	50	This "boilerplate" cell was fabricated using a platinum plated nickel plaque for the oxygen electrode and an asbestos matrix approximately .043" thick. This cell was constructed with a Hypalon bellows. This cell was removed from test after two cycles because of excessive oxidation of the oxygen electrode, resulting in excessive pressure differentials in the cell.	No cell failure, but test verifies the prohibitiveness of using nickel oxygen electrodes.
IR&D-3	--	50	This cell was fabricated essentially the same as Cell No. IR&D-2. The asbestos matrix measured approximately .026" thick. No bellows was used in this cell, but thermocouples were employed to monitor temperature during charge and discharge. The operation of this cell was to merely monitor thermal effects within the cell.	
IR&D-4	24	50	This "boilerplate" cell was fabricated with an asbestos matrix which measured approximately .037" thick. After 20 cycles of operation, the cell was removed from test to provide a strip of wicking material to reduce performance degradation due to loss of liquid from the matrix. After two additional cycles, a minute cross leak was detected. After two more additional cycles, a gross cross leak developed which resulted in cell failure.	A burn condition through the electrode and matrix occurred approximately 1" above the bottom seal. Cell failure was due to leakage through the matrix. A drying condition of the matrix may have occurred during application of a wick into the cell, after having operated successfully for 20 cycles.

TABLE I (Continued)

CELL NUMBER	NO. OF CYCLES	OPER. TEMP. °C	CELL TYPE AND TEST HISTORY	FAILURE ANALYSIS
4058 31	6	50	This cell was fabricated to flight hardware design as one of two cells to be used for environmental testing. Used electrodes were used in the construction of this cell, because the nature of the tests did not necessarily warrant the use of new ones. This cell functioned for 6 cycles and was then subjected to the specified random vibration spectrum in three axis for 5 minutes duration in each axis. The cell failed on the initial post vibration test during discharge after a 2 minute reading had been recorded.	Cell failed due to lower edge seal, which may or may not have been a result of the random vibration exposure.
4058-32	8	50	Same construction as Cell No. 4058-32. Cell operated for 6 functional test cycles followed by a nonoperational thermal soak at 100°F and -20°F. A post thermal cycle was performed, followed by a complete operational cycle in a vacuum chamber at 1×10^{-5} mm Hg.	No cell failure was experienced throughout these environmental tests.
4058-33	117	50	This "boilerplate" cell contains a sintered nickel core as the H_2 electrode as well as the core support. It is a duplication of Cell No. 4058-30, and was put on test after failure of the mate cell due to failure of the rupture diaphragm. The cell has operated for 117 cycles to the termination of the contract.	No failure occurred after 117 cycles of operation. Test discontinued at termination of contract.

TABLE I (Continued)

CELL NUMBER	NO. OF CYCLES	OPER. TEMP. °C	CELL TYPE AND TEST HISTORY	FAILURE ANALYSIS
4058-34	2	50	Flight hardware design to be used in breadboard energy storage system. Acceptance tested for 2 cycles, but rejected for breadboard because of additional external volume required to balance gas volumes.	No failure.
4058-35	28	50	Flight hardware cell used in breadboard energy storage system. Acceptance tested for 4 cycles, and tested an additional 24 cycles as part of the breadboard.	No failure.
4058-36	26	50	Flight hardware cell used in breadboard energy storage system. Acceptance tested for 2 cycles, and tested an additional 24 cycles as part of the breadboard.	No failure.
4058-37	25	50	Flight hardware cell used in breadboard energy storage system. Acceptance tested for 1 cycle, and tested an additional 24 cycles as part of the breadboard.	No failure.
4058-38	25	50	Flight hardware cell used in breadboard energy storage system. Acceptance tested for 1 cycle, and tested an additional 24 cycles as part of the breadboard.	No failure.

TABLE I (Concluded)

CELL NUMBER	NO. OF CYCLES	OPER. TEMP. °C	CELL TYPE AND TEST HISTORY	FAILURE ANALYSIS
4058-39	1	50	Flight hardware cell to be used in breadboard energy storage system. Acceptance tested for 1 cycle. Cell was inadvertently subjected to a high pressure differential causing cell failure.	Cell failed when manually subjected to a high differential pressure. Cell has not been opened for inspection.

Each test cell is instrumented as follows:

1.	Voltmeter	± 1%
2.	Ammeter	± 1%
3.	Total Pressure Transducer	± 2%
4.	Differential Pressure Transducer	± 2%
5.	Cell Wall Temperature Thermocouple	± 1%
6.	Test Chamber Temperature Thermocouple	± 1%

A polarization scan (volt-amp curve) on charge and discharge was periodically performed to help define the overall electrochemical operation of the cell. The voltage ampere scan was performed, during a discharge cycle by manually varying the load on the fuel cell from 1.0 amps to 50 amps, in approximately 10 amp increments, and recording the stabilized voltage at each of the load increments. The charge and discharge polarization scans were performed during the discharge mode of a cycle.

3.2.1 Temperature Tests

Cell No. 4058-2 was flushed and set up in a test station regulated at 50°C. The cell was charged at 10 amps to check out the internal volume balance. The cell showed an increase in differential pressure on the H_2 side. The volumes were corrected by adding stainless steel tubing, externally, to the hydrogen chamber.

On the first cycle, the cell was charged at 15 amps for 3.42 hours. The pressure rose from zero to 590 psig where the pressure switch removed the cell from charge. The charge voltage rose from 1.73 to 1.78. Figure 6 shows the cell discharged at a plateau voltage of 0.83 to 0.82 at 33 amps for the first 40 minutes, then fell off during the remaining 32 minutes of the cycle. The second and third cycles were run in 24-hour periods. The cell was charged at 2 amps until the pressure switch removed it from charge, then switched to a 72 minute discharge after the elapse of 27.8 hours. Figure 6 shows an average discharge of 0.81 volts on cycle No. 3. The three cycles were considered sufficient to qualify the boiler-plate design.

The cell was allowed to operate for a total of 9 cycles. The cell was then completely discharged and transferred to another station so that part of the test area could be worked on. During recalibration of the transducers, it was discovered that the cell contained an internal leak. The core was removed from the pressure vessel and a leak was found in the bellows seal area. Tightening the bellows mount screws eliminated the leak. The cell was reassembled and placed on test for additional cycles. On cycle No. 12, a catastrophic failure occurred during the night. No further cycle data is available because the data scanning system was not yet operating.

DISCHARGE RATE: 33.3 AMPS:
TEMPERATURE: 50° C.

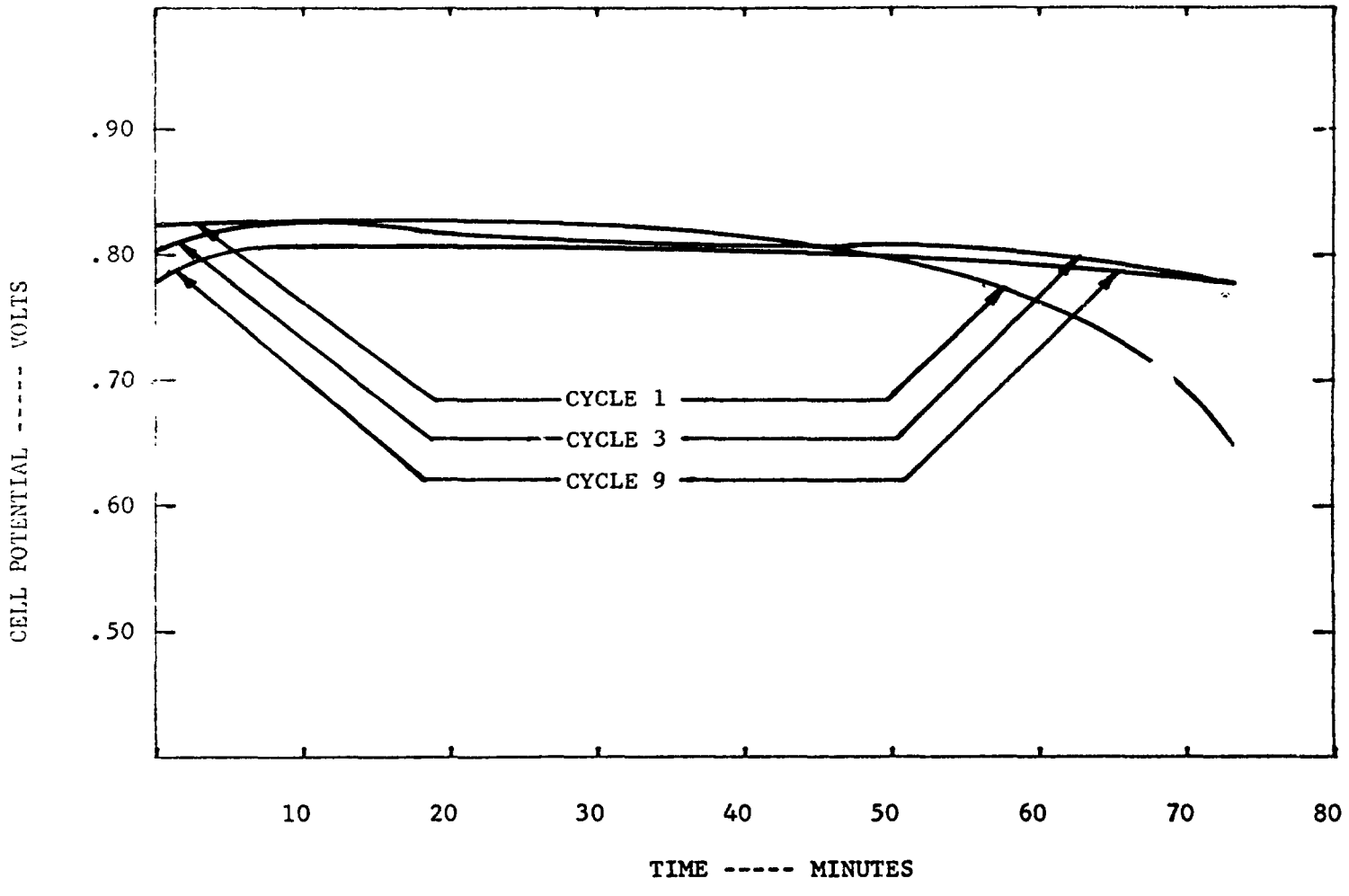

FIGURE 6. CELL NO. 4058-2 DISCHARGE PERFORMANCE

An inspection analysis of this cell revealed a burned area approximately 0.5 inch long just below the upper edge seal. The burn section extended through the matrix and the hydrogen electrode. Both the top and bottom Ethylene Propylene edge seals were charred and the Hypalon bellows was badly burned. The cause of failure was a faulty or inadequate edge seal or a defective bellows.

Cell No. 4058-3 was fabricated and instrumented in the same manner as Cell No. 4058-2. The cell was placed on test on a 12-hour cycle regime at 80°C rather than 50°C as in the case of Cell No. 4058-2. The cell was found to be lacking H_2 volume on the preliminary cycles. The 1.0 in^3 of volume was added to the hydrogen side. The cell failed catastrophically on the 20th cycle. On the 19th cycle, the pressure differential went to the O_2 side probably because of external leakage. The cell voltage dropped to zero and it was reversed charged by the series batteries twice during the 19th cycle. On the 20th cycle, the cell was fully charged. During the subsequent discharge, the cell again reversed because of the low H_2 differential and then failed.

Cell No. 4058-7 was fabricated and instrumented in the same manner as the other cells. During the preliminary cycles, this cell was found lacking in hydrogen volume. One in^3 of volume was added to the hydrogen side of the cell. The cell was put on a 12-hour cycle at 80°C; on the third discharge cycle, the load was at 37 amps. The cell totally discharged and was reverse charged. This condition subjected the cell to a 5.25 psi differential on the H_2 side. The cell would not take the subsequent charge. Examination revealed that the bellows was leaking, but the rest of the cell was undamaged. Since the core was inadvertently in water while locating the leak, this cell was not put back on test.

Cell No. 4058-9 was fabricated and instrumented in the same manner as the other cells. One in^3 of volume was added to the H_2 side of this cell after the preliminary cycles. The cell was put on a 12-hour cycle at 80°C. The cell ran 10 cycles, then failed when the nylon tube, which acts as an insulator to the differential transducer, broke. The nylon tubing has been replaced with a ceramic insulated feedthrough on the remaining cells. Figure 7 shows this modification of the top plumbing assembly.

Cell No. 4058-11 was fabricated and instrumented in the same manner as the previous cells. This cell was put on a 12-hour cycle at 80°C. 1.5 in^3 of volume was added to the hydrogen side of this cell in order to balance volumes. This cell completed the prescribed 30 cycles at the elevated temperature and was retained on cycle test for life evaluation. The cell failed on the 61st charge cycle due to bellows failure caused by chemical attack on the oxygen side of the Hypalon diaphragm.

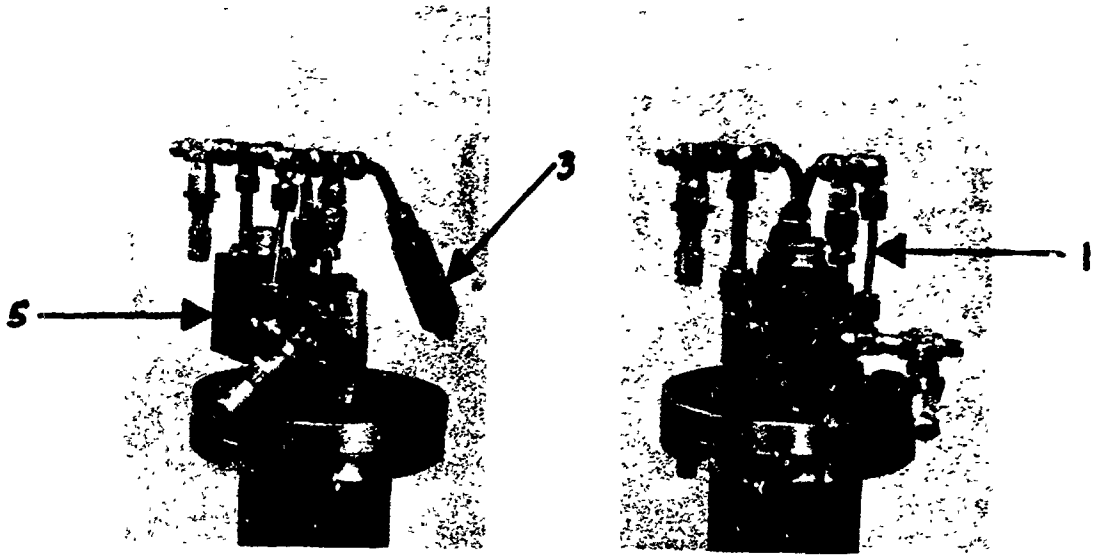

1. Nylon Tube Feedthrough
2. Ceramic Insulated Feedthrough
3. Total Pressure Transducer
4. Total Pressure Switch
5. Differential Pressure Transducer

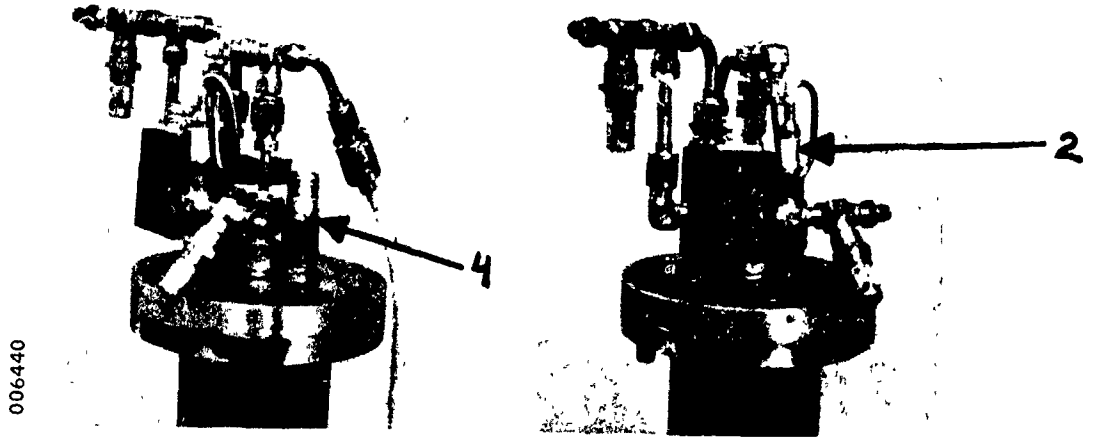

Figure 7. Top Views of Boiler Plate Fuel Cell Assembly

The data, Figures 8, 9, and 10, indicates that the operation of the cell at 80°C results in electrical performance which is superior to the operation at 50°C by approximately 50 mv in both the charge and discharge mode. The rate of voltage degradation was 0.83 millivolts per cycle in the charge mode and 0.46 millivolts per cycle in the discharge mode. The combined degradation, for the same cycle duration, is higher than that seen in Cell No. 4058-10 which had operated at a lower temperature; however, the voltage efficiency of the cell at 54 cycles was greater (46.0%) because of the increased performance at higher temperature.

Cell No. 4058-13 was fabricated and instrumented in the same manner as the previous cells. This cell was put on a 12-hour cycle at 30°C. 1.75 in^3 of volume was added to the hydrogen side of this cell in order to balance out volumes. This cell had completed 127 cycles prior to shutdown on 5 April 1971. This cell was opened for inspection and a new Hypalon bellows was substituted. The cell was put back on test on 29 April 1971 after flushing five times with hydrogen and oxygen from 10 to 95 psig. During the charge cycle, the total pressure of the cell reached 444 psig. The final 2 hours of charge resulted in only a 17 psig rise. After final discharge, the cell was inspected and leakage through the electrodes-matrix assembly was evident at a 2 psid. In the 128th cycle, the voltage efficiency was approximately 42 percent as compared to the efficiency of slightly over 43 percent in the 92nd cycle. The cell performance characteristics are demonstrated in Figures 11, 12, and 13.

Cell No. 4058-15 was fabricated and instrumented in the same manner as the previous cells. This cell was put on a 12-hour cycle at 100°C. 2.0 in^3 of volume was added to the hydrogen side in order to balance the volumes of this cell. Figures 14 and 15 show that there has been little change in electrical performance over the first ten cycles. The average degradation over the first 23 cycles was 5.10μ volts per hour on the discharge mode at 400 psi. The current efficiency as of Cycle No. 9 was 51.6%. This was the highest efficiency rate which was accomplished up to this time; the lowest was that of the 30°C cell. These efficiency rate differences show that higher efficiency is accomplished at higher temperatures.

3.2.2 Pressure Tests

Cell No. 4058-14, a standard 40 A.H. fuel cell designed for 600 psig, was put on the 12-hour cycle at 50°C. It was cycled 6 times between the pressures of 600 and 124. Figure 16 and 17 show typical performance on Cycle 3 under these conditions for charge and discharge. On Cycle 7, the cell was charged from 374 psig to 700 psig and then discharged at 33 amps down to 132 psig in 95 minutes. The cell performance remained unchanged and a gain of 12.7 amp hours was achieved. On Cycle 8, the cell was charged from 120 psig to 804 psig, then discharged down to 133 psig in 108 minutes. A gain of 20 amp hours was achieved with no loss in performance. On Cycle 9, the cell was charged from 120 psig to 903 psig and discharged down to 125 psig in 125 minutes. A gain of 29.3 amp hours or a total of 69 amp hours

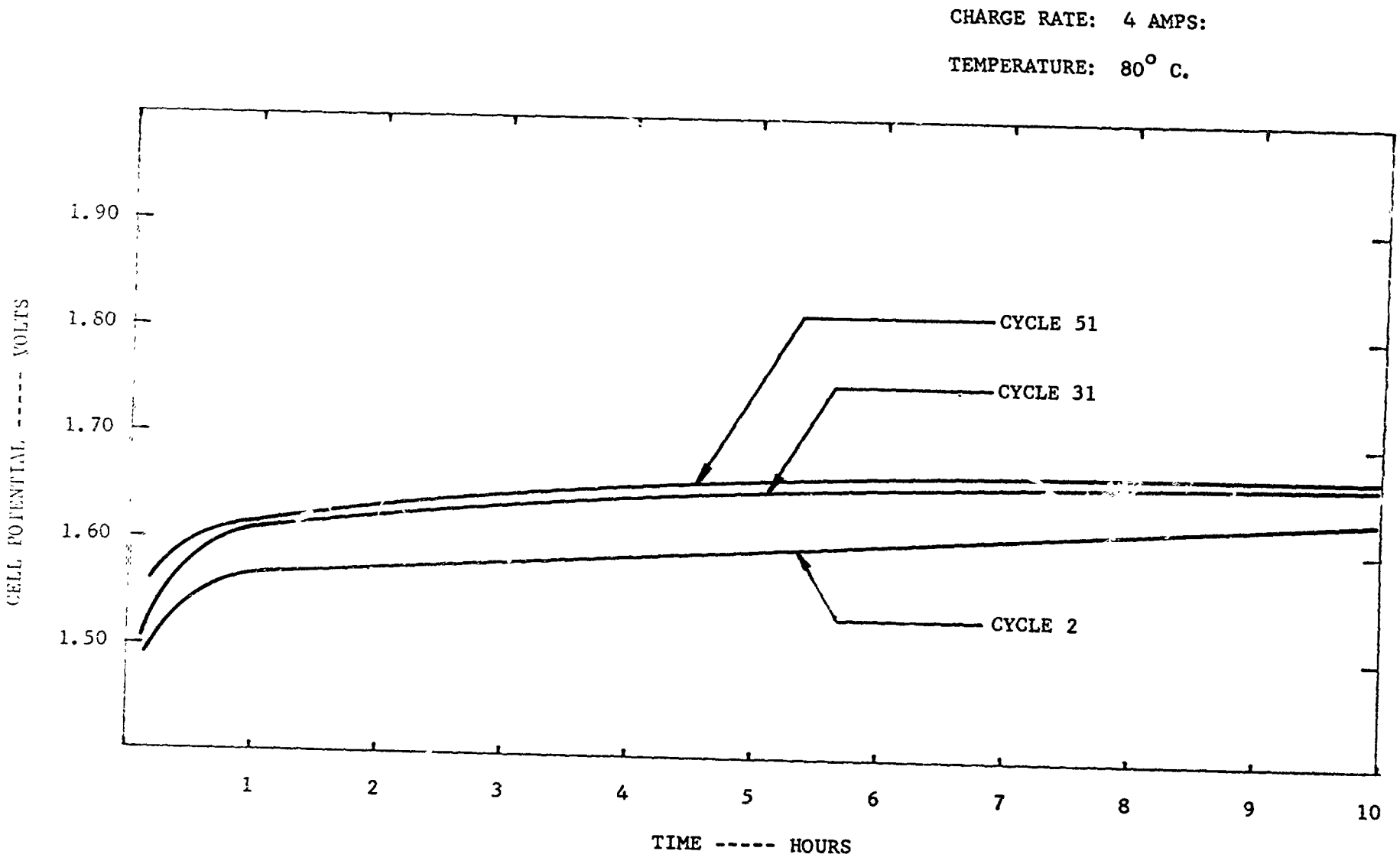

FIGURE 8 . CELL NO. 4058-11 CHARGE PERFORMANCE

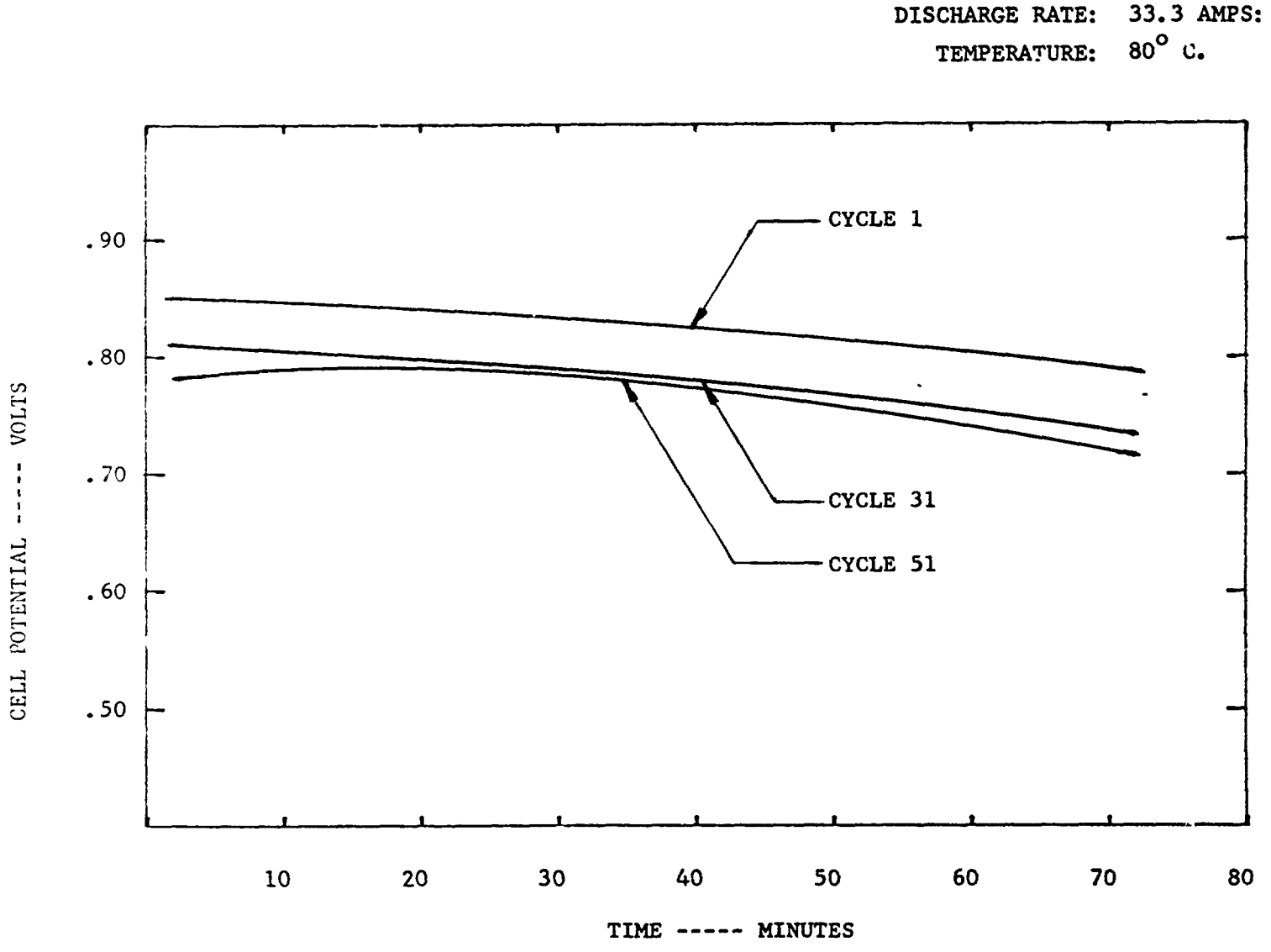

FIGURE 9. CELL NO. 4058-11 DISCHARGE PERFORMANCE

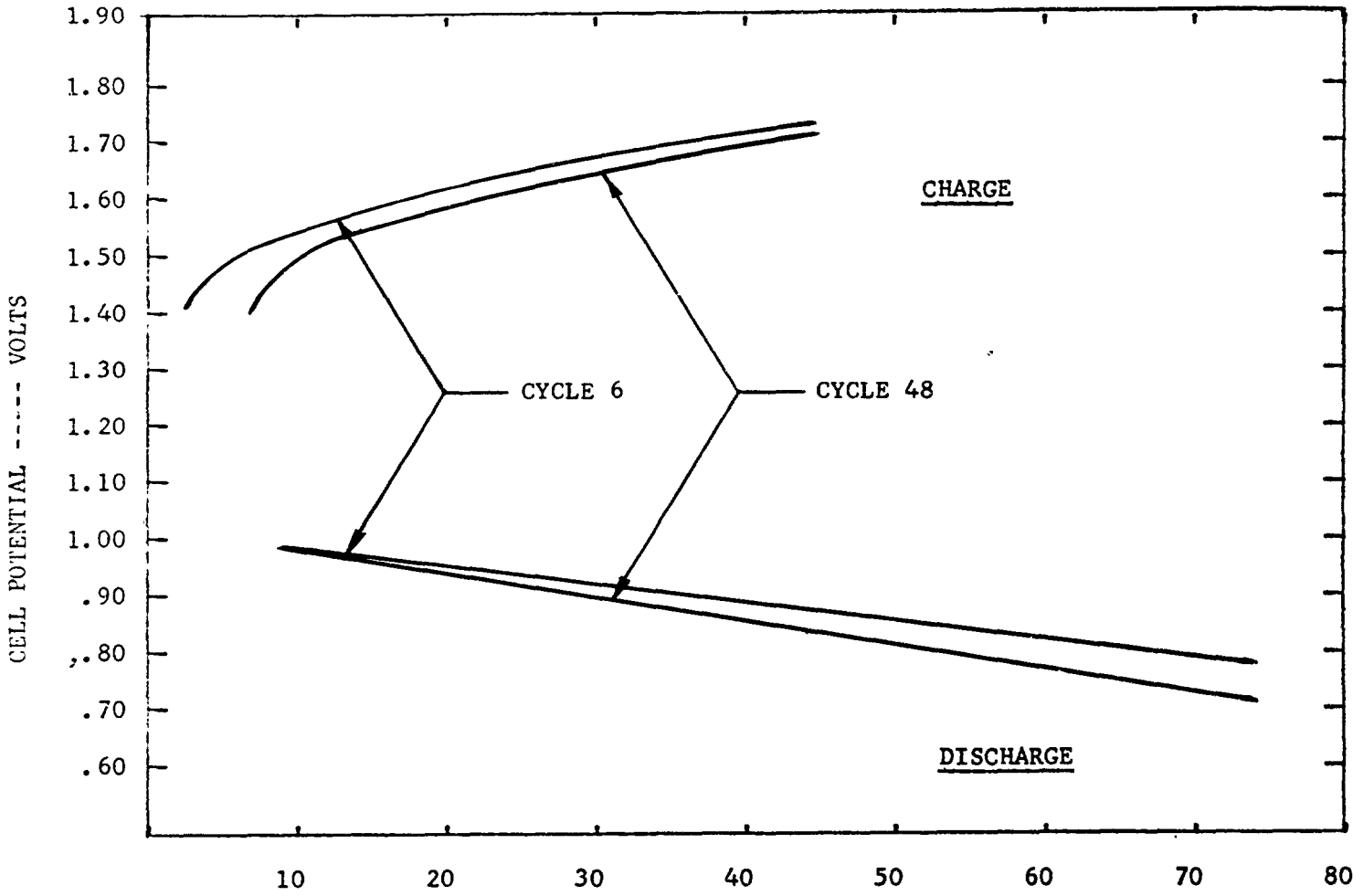

FIGURE 10. CELL NO. 4058-11 POLARIZATION SCANS

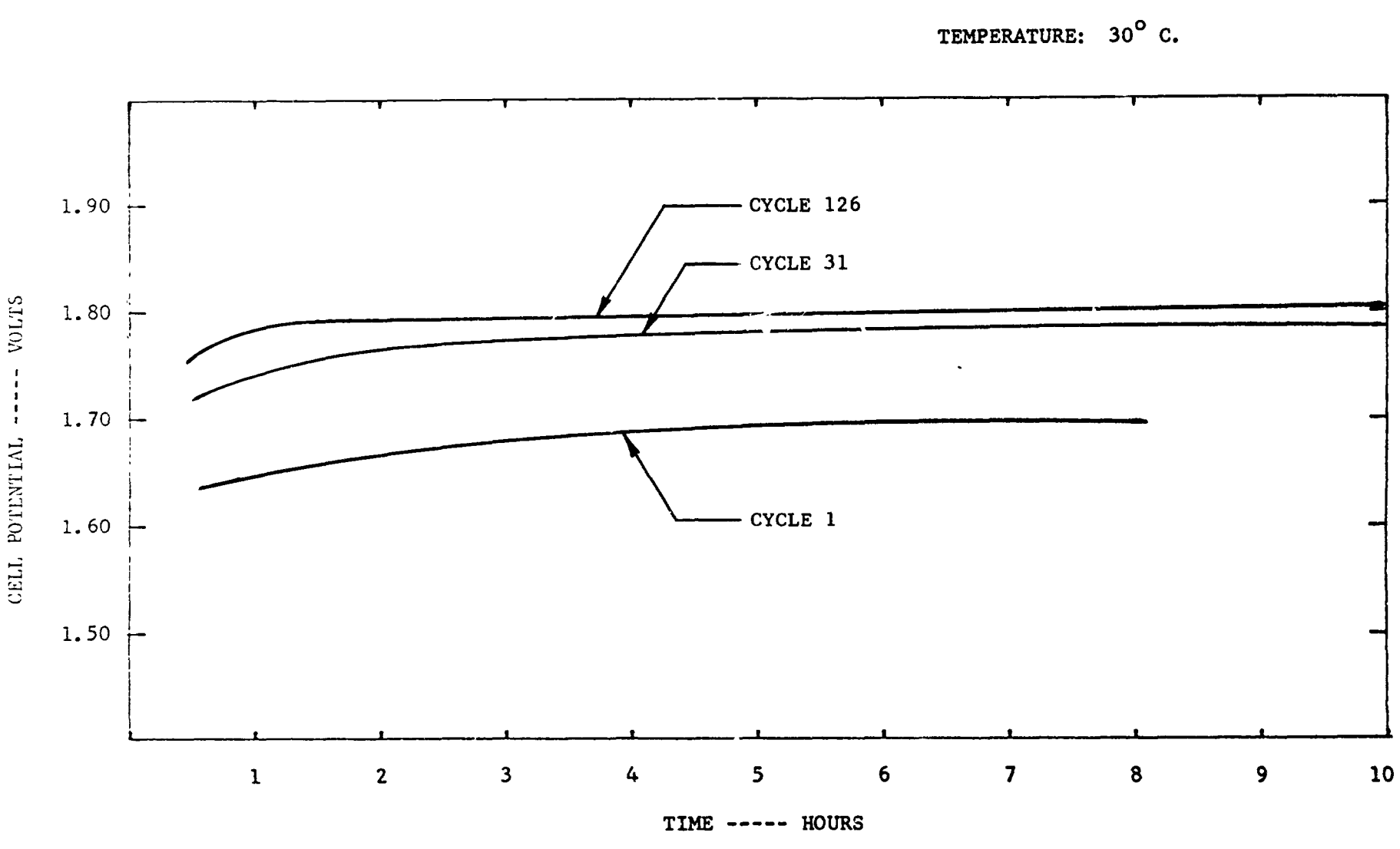

FIGURE 11. CELL NO. 4058-13 CHARGE PERFORMANCE

DISCHARGE RATE: 33.3 AMPS:
TEMPERATURE: 30° C.

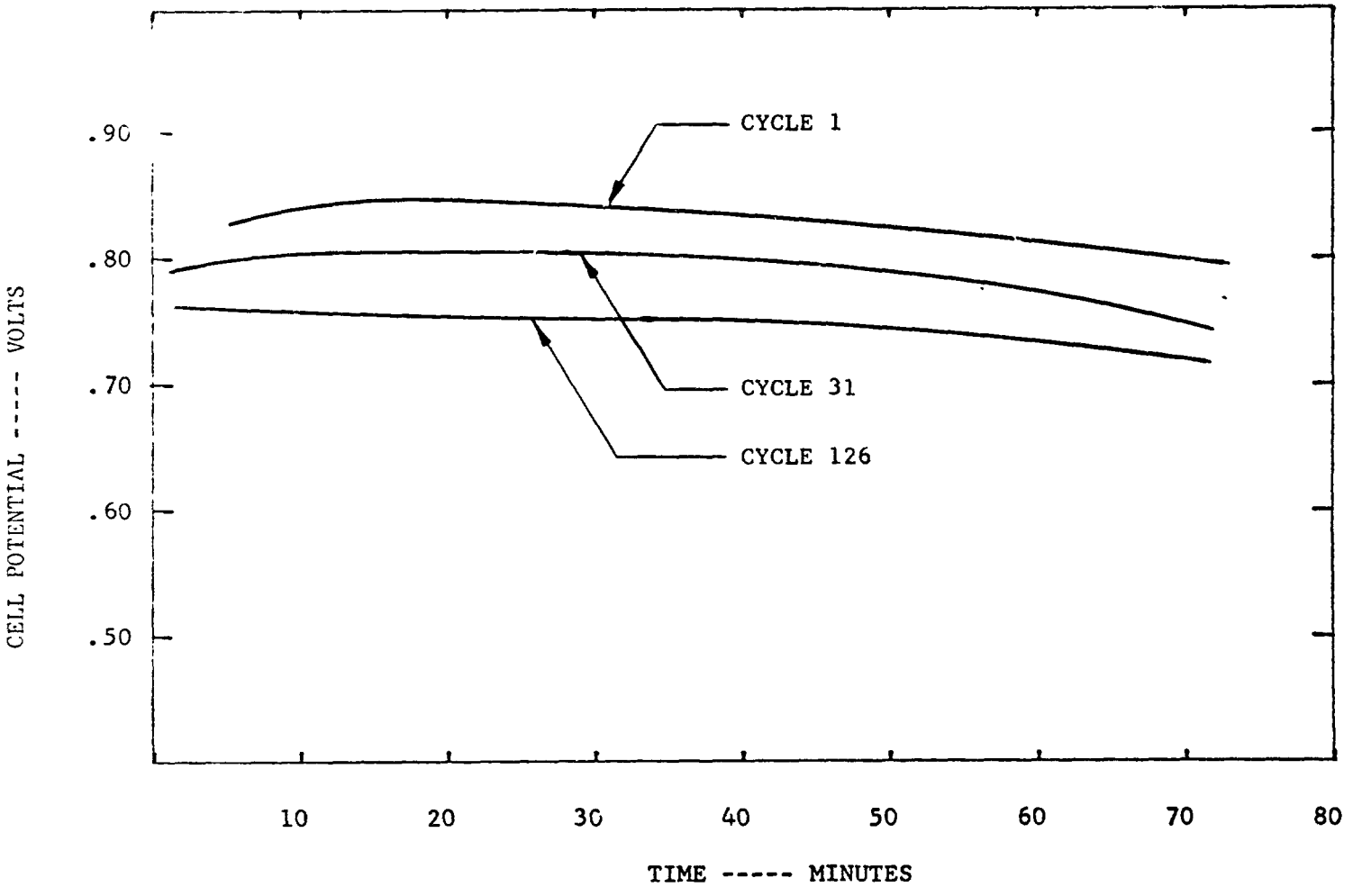

FIGURE 12. CELL NO. 4058-13 DISCHARGE PERFORMANCE

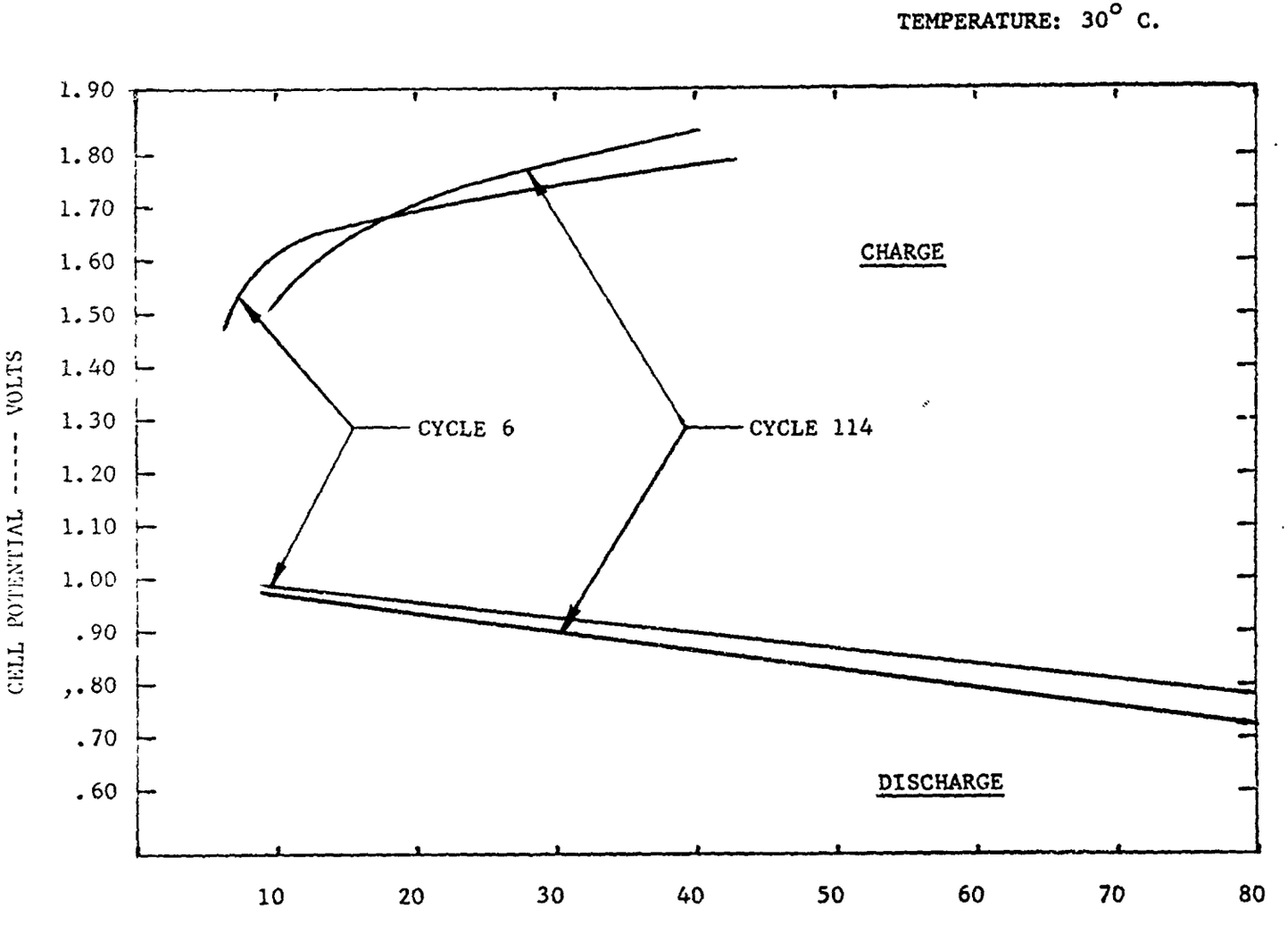

FIGURE 13 . CELL NO. 4C58-13 POLARIZATION SCANS

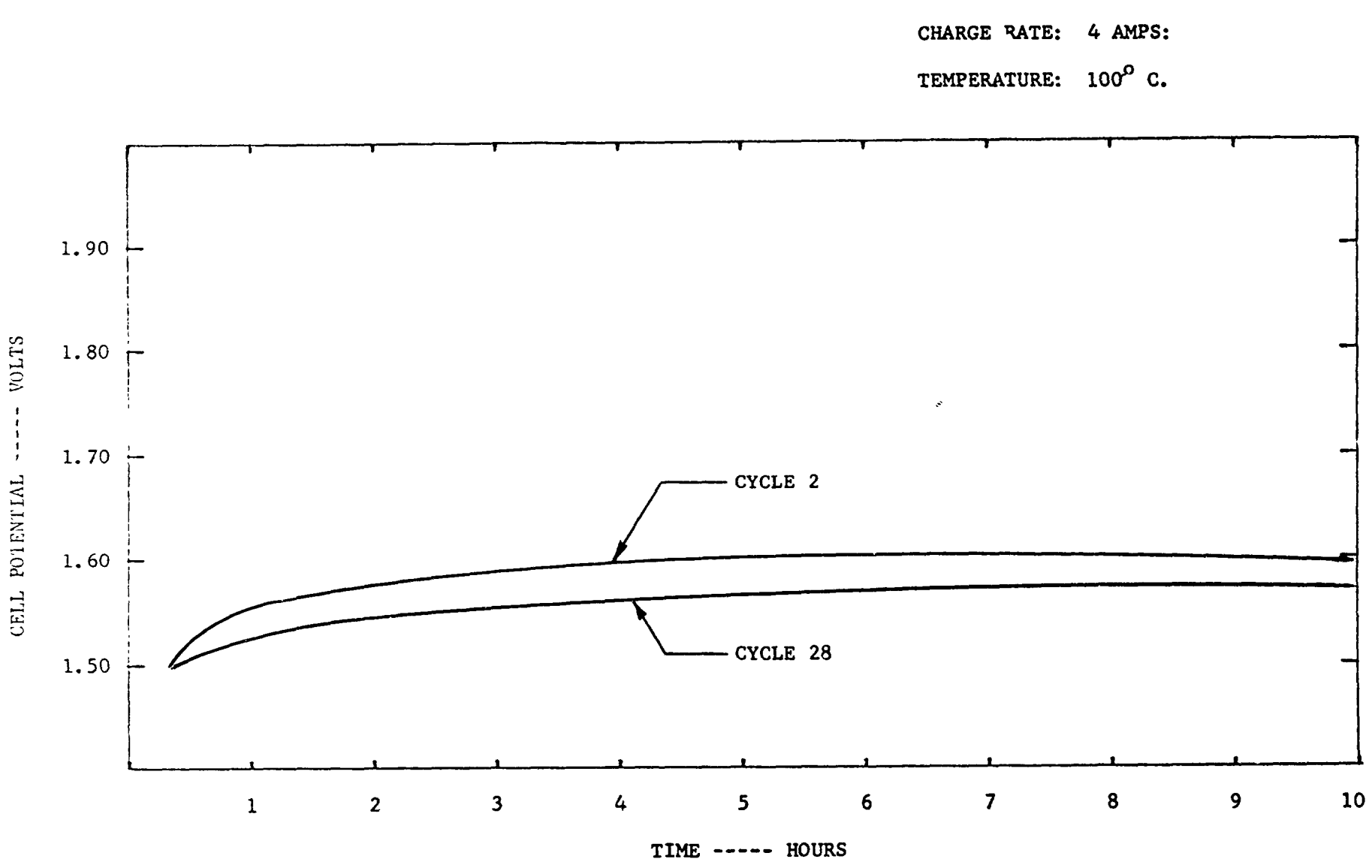

FIGURE 14. CELL NO. 4058-15 CHARGE PERFORMANCE

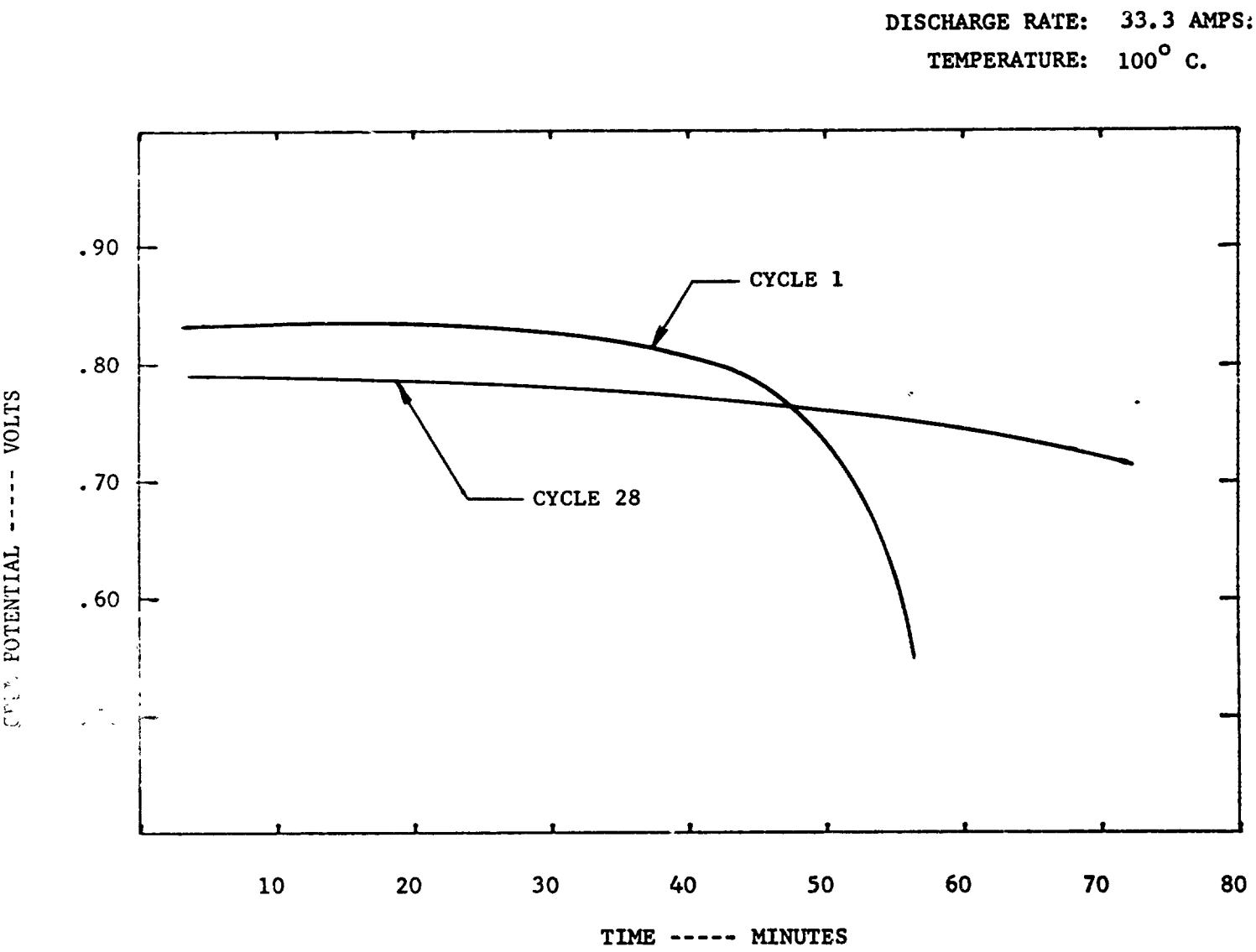

FIGURE 15. CELL NO. 4058-15 DISCHARGE PERFORMANCE

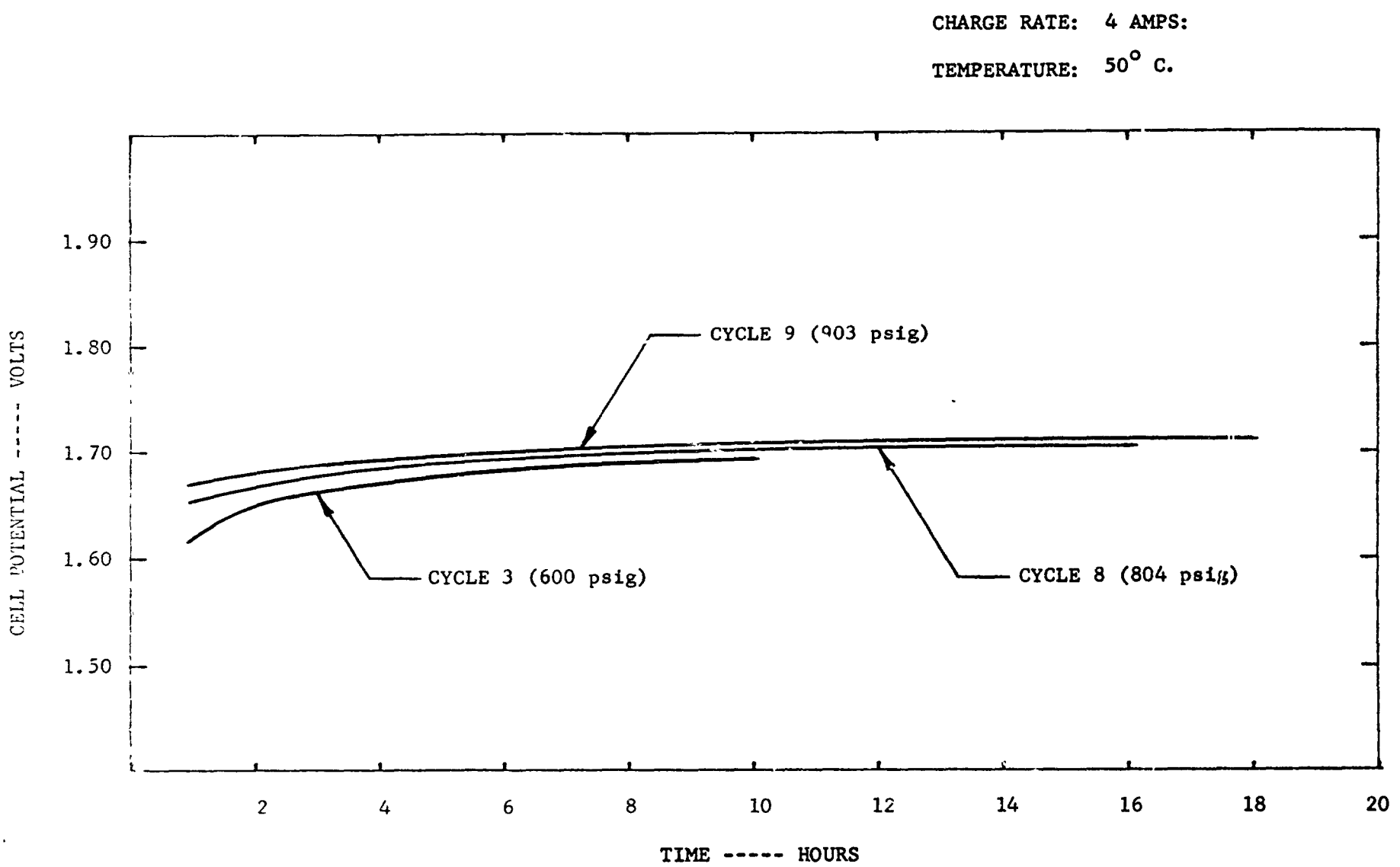

FIGURE 16. CELL NO. 4058-14 CHARGE PERFORMANCE

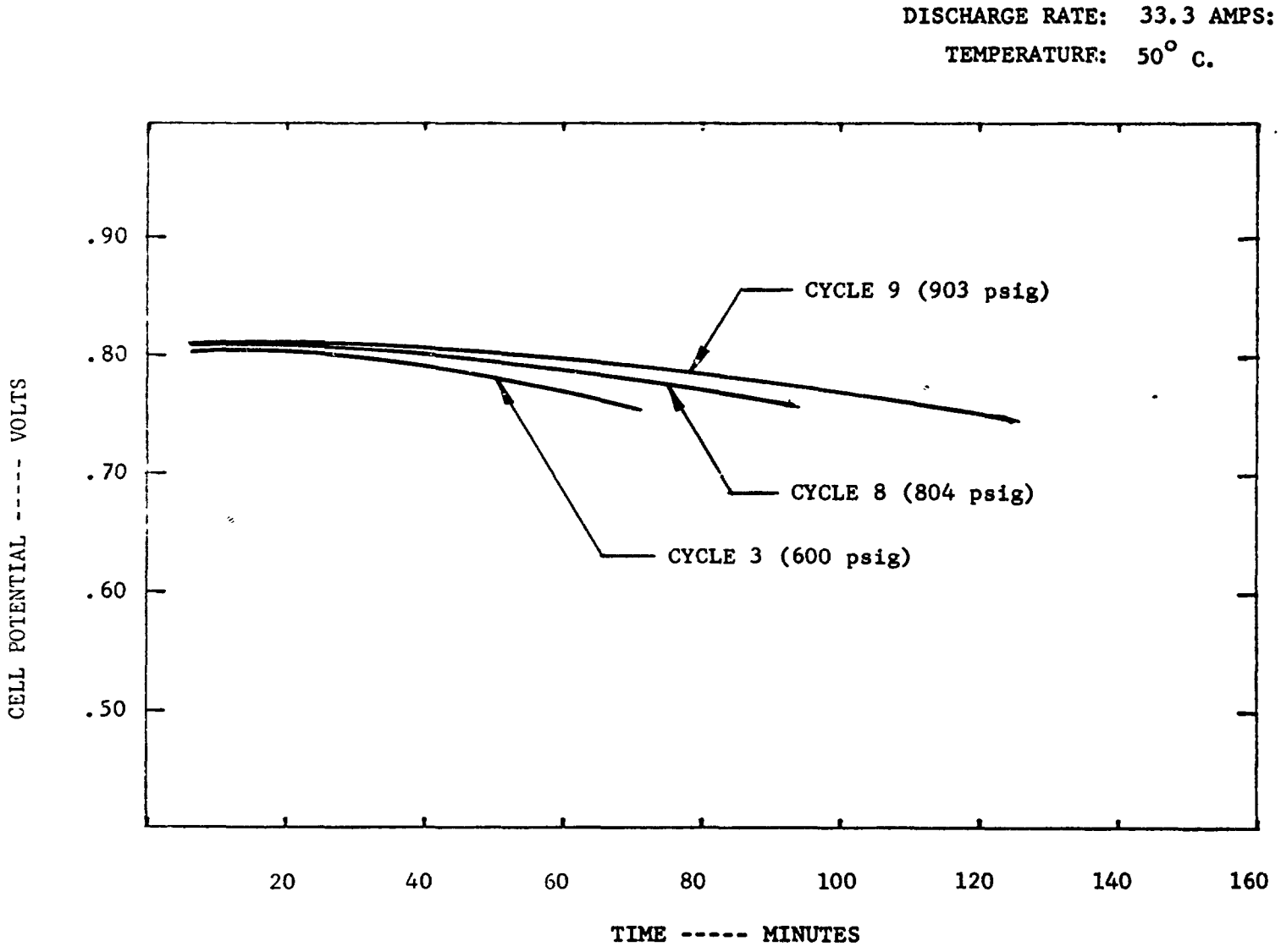

FIGURE 17. CELL NO. 4058-14 DISCHARGE PERFORMANCE

with no performance loss was demonstrated. 1000 psig was the goal of the next cycle; however, the cell failed catastrophically at 974 psig. The results of this test show that the cells can possibly be designed with smaller volumes and run at a higher pressure. Another possibility would be to use the extra capacity provided by this cell design. Both possibilities will raise the energy density characteristics of the regenerative fuel cell, the first by removing weight, and the second by adding capacity.

3.2.3 Life Testing

Cell No. 4058-6 was fabricated and instrumented in the same manner as Cell No. 4058-2. This cell was put on a 12-hour cycle at 50°C. On the first cycle, the differential pressure varied from 1 psi at the beginning of charge to 0.25 psi at end of charge, with the higher pressure on the oxygen side of the cell. During the first ten minutes of discharge, the voltage fell off from 0.75 to 0 volts at a load of 33 amps. The cell was discharged back to 0 psig by reducing the current to 1 amp. It was postulated that the oxygen pressure differential caused the electrolyte to flood the H_2 electrode, which has no teflon wetproofing. The cell was taken apart and examined. It was found that the bellows was installed as shown in position A of Figure 18. In this position, the spring constant of the bellows forces the differential to remain on the oxygen side. When the differential becomes greater than the spring constant, the bellows will flip through to the other position. The bellows was reversed to position B shown in Figure 18, and the cell was put back on test. In the subsequent cycles, the differential remained on the hydrogen side and the cell operated normally. It was observed that a three to four pound differential is required to move the bellows from one side to the other. This could be changed by using a softer rubber and, if possible, a large diameter bellows.

Cell No. 4058-6 ran 30 cycles at 50°C and then was placed on life cycle. The cell failed on Cycle No. 41. On Cycle 40, the power supply failed and the cell was not fully charged. The cell was discharged and developed a differential pressure of over 5½ psi near the end of discharge. The bellows was found to leak and was replaced. The cell failed on the following cycle. During the 41st cycle, total pressure dropped from 518 to 132 psi in 10 minutes, indicating internal leak and gas recombination. Post failure inspection revealed a hole burned through the matrix and both electrodes about one inch from the top.

The performance characteristics of this cell are depicted in Figures 19 and 20, and indicate a small amount of performance degradation in both the charge and discharge modes during the 30 cycle span. Figure 21 shows the polarization scans for Cycles 17 and 29. The charge polarization scan rose slightly, but the discharge scan remained essentially unchanged.

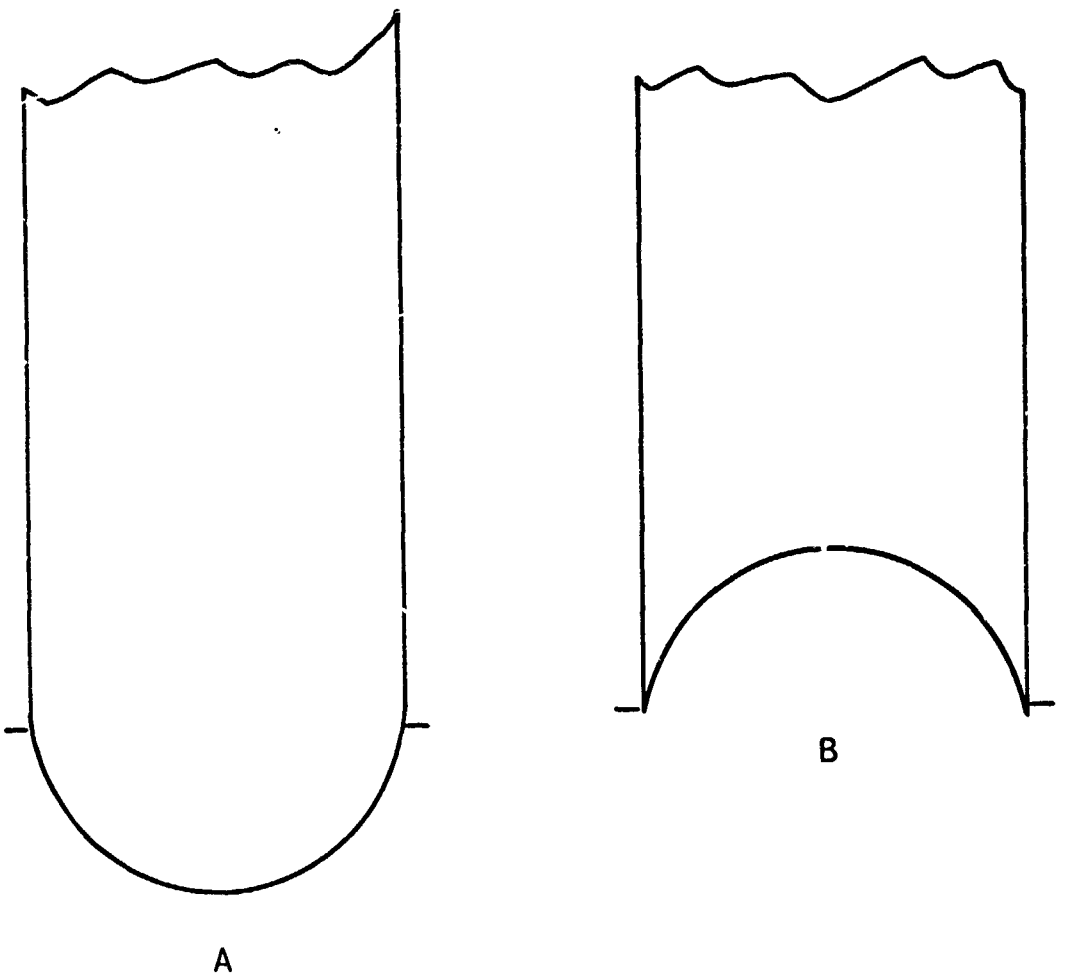

41719

FIGURE 18. SET POSITION OF BELLOWS (DIAPHRAGM)

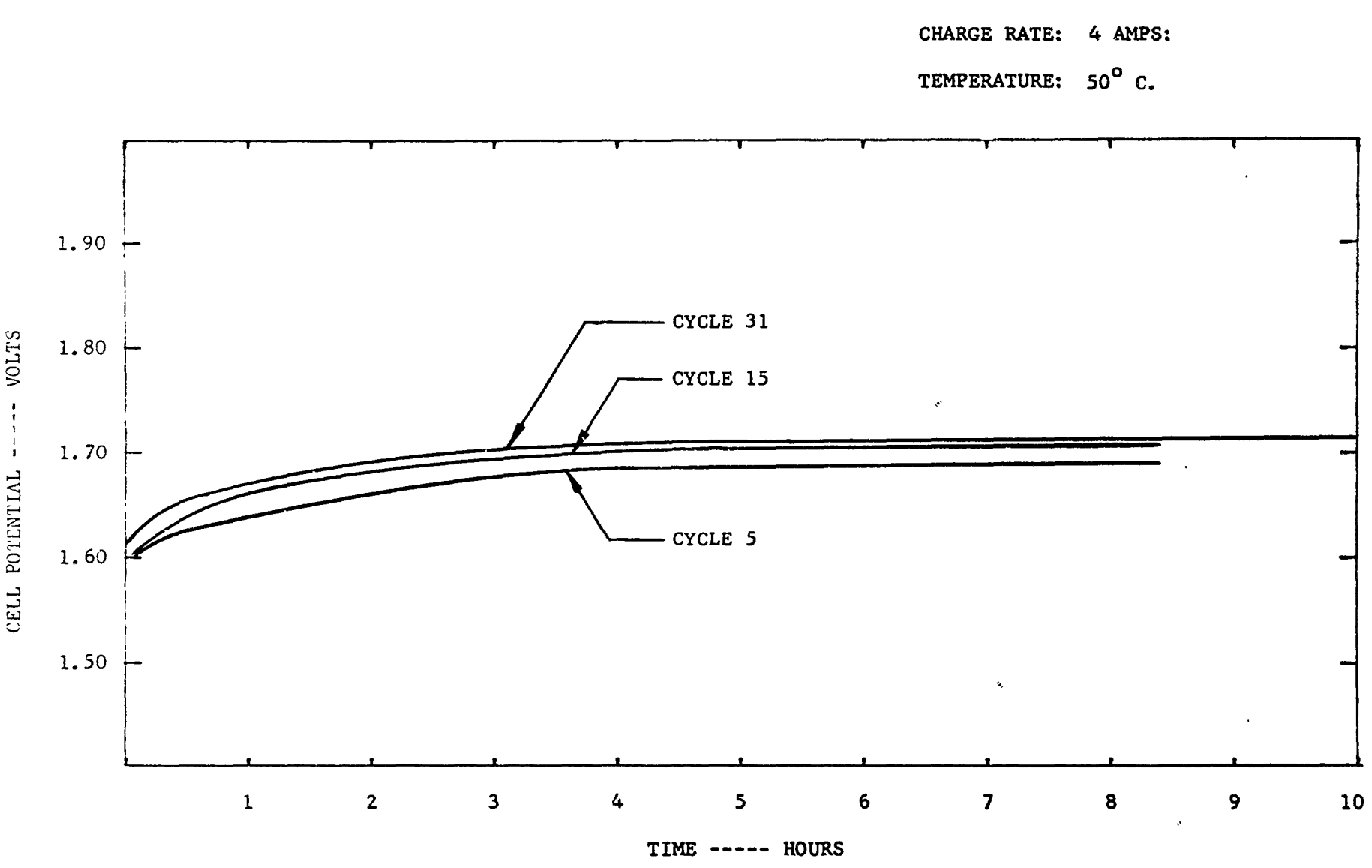

FIGURE 19. CELL NO. 4058-6 CHARGE PERFORMANCE

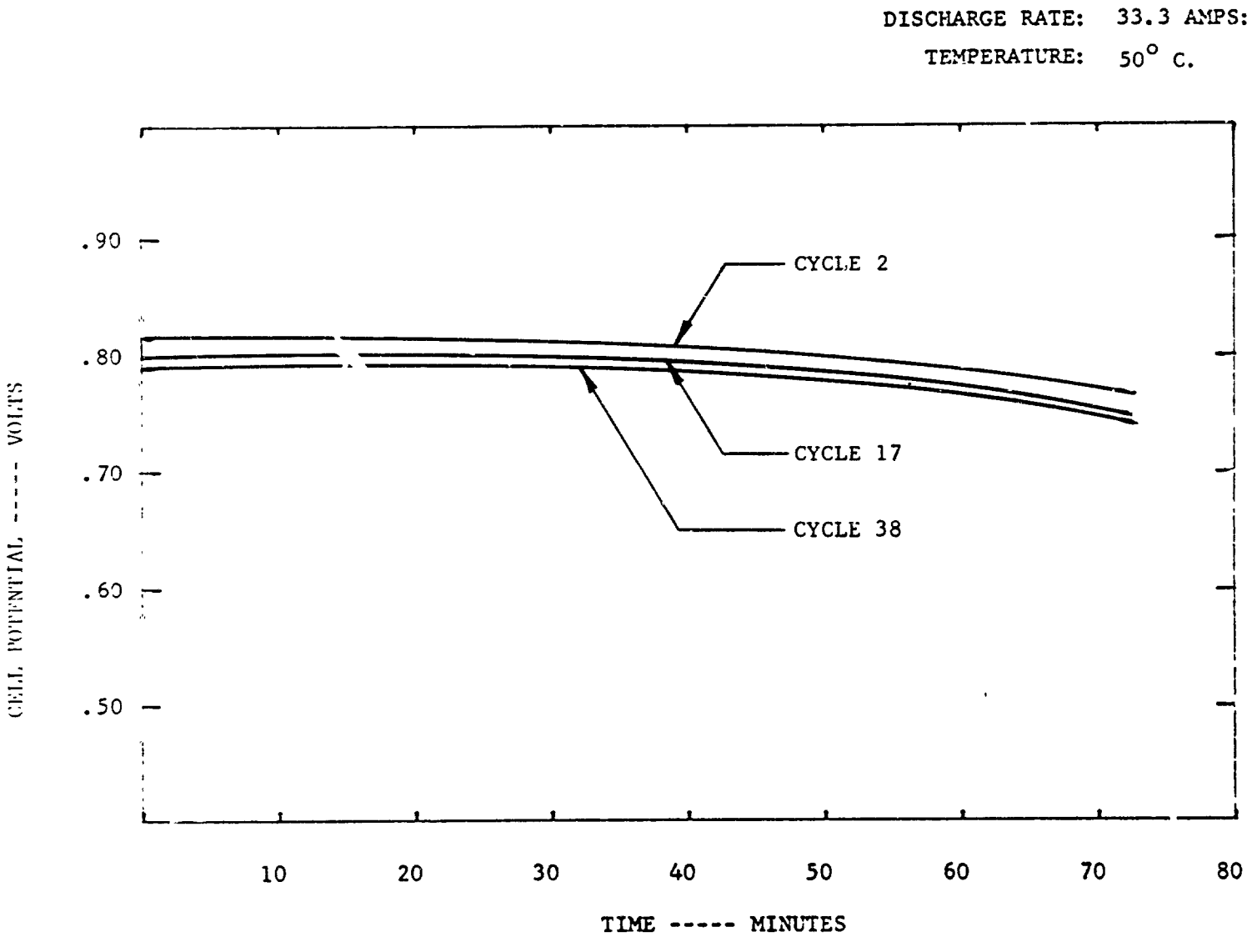

FIGURE 20. CELL NO. 4058-6 DISCHARGE PERFORMANCE

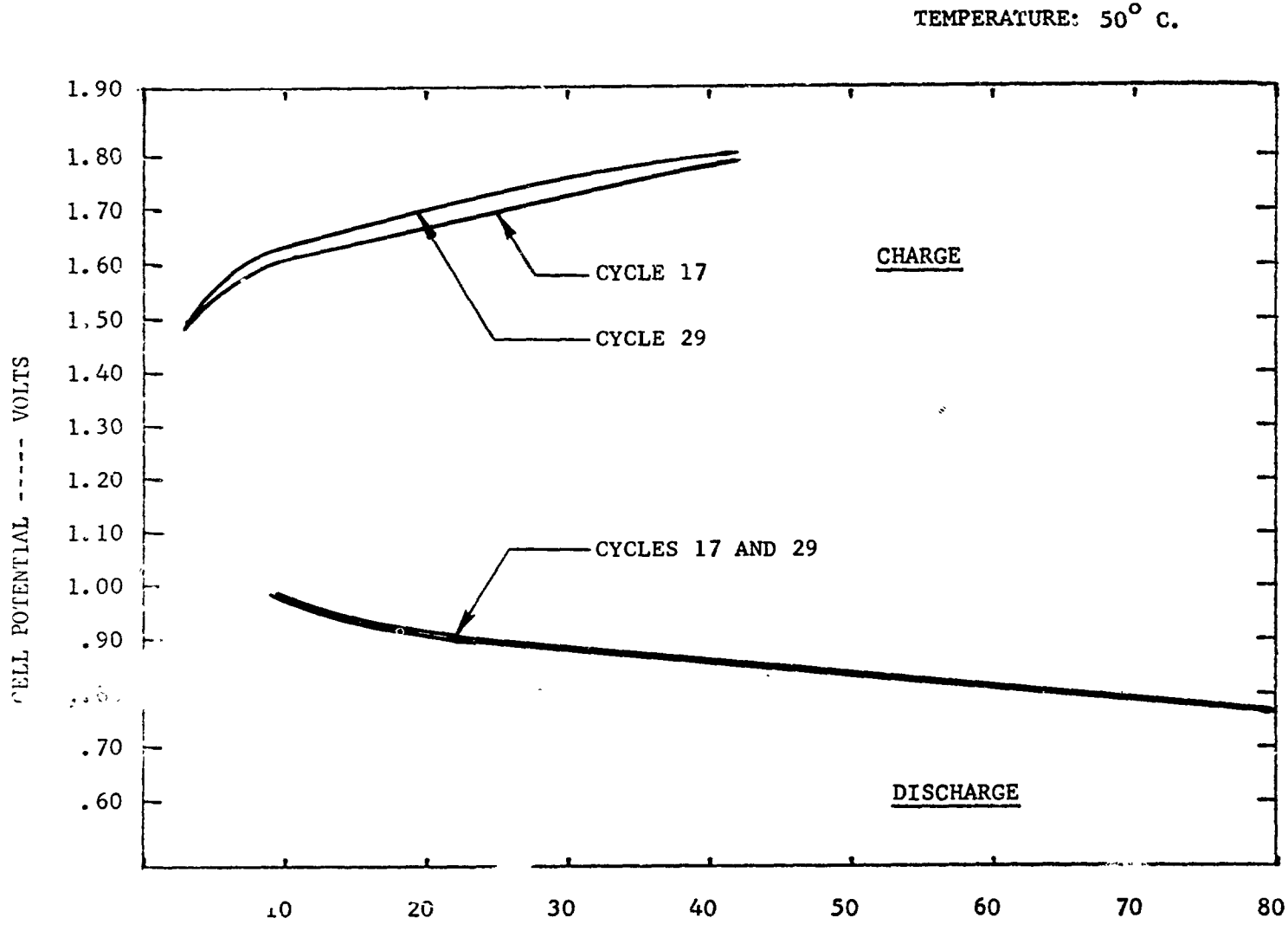

FIGURE 21. CELL NO. 4058-6 POLARIZATION SCANS

Cell No. 4058-10 was fabricated and instrumented in the same manner as the previous cells. This cell was put on a 12-hour cycle at 50°C, and 1.5 in^3 of volume was added to the hydrogen side of this cell in order to balance volumes. This cell ran for 30 cycles at 50°C and was then allowed to continue cycling for life evaluation.

Cell No. 4058-10 had completed 221 cycles prior to shutdown on 5 April 1971 for test equipment service and calibration. The cell was opened for inspection and a new Hypalon bellows was substituted. The cell was started on test on 29 April 1971 by flushing the cell five times with hydrogen and oxygen from 10 to 95 psig. During the first few hours on charge, the total pressure of the cell dropped a significant amount. The cell was removed from test for inspection, which revealed a series of leaks through the electrodes-matrix assembly. The nickel wire windings were very loose due to either wire elongation (stretching) with time and thermal cycling or shrinkage of the matrix volume with time. The effect, for either reason, results in a poor electrode-matrix interface with a resultant poor cell performance. The oxygen electrode was carefully removed to expose the matrix surface. An irregular coloration indicated nonuniformity of electrode-matrix interfacing. This could mean that the electrode has been functioning with a very poor current distribution over its surface area. The lack of any discoloration of the matrix on the lower portion of the cylinder core (bellows end) could mean a substantial loss of effective area for the cell reaction mechanism to function.

Figures 22, 23, and 24 depict the performance characteristics of this cell on charge and discharge through the cycle life duration. The average degradation in the charge half-cycle, based on readings at 5 hours of a 10 hour charge, is 0.41 millivolts per cycle (at 92 cycles, it was 0.47 mv), showing a slight decrease in the rate of charge degradation. The average degradation based on readings at 40 minutes is 0.63 millivolts per cycle (at 92 cycles, it was 0.67 mv), or a slight decrease in rate of discharge degradation.

The final complete cycle showed a voltage efficiency of approximately 40 percent. This efficiency compared favorably with Cycle No. 186 of slightly over 40 percent.

3.3 CELL COMPONENT OPTIMIZATION

Optimization of the various cell components fell into two general categories, namely; mechanical and electrochemical. In the mechanical groups were considerations such as weight, strength, radiation-induced degradation of strength, and other degradation of properties caused by exposure to the particular component's environment. The electrochemical group includes the electrodes, matrix, electrolyte, and all electrical components that contribute to resistive power losses. The mechanical components were initially evaluated as separate entities independent of fuel cell application and operation. The work effort related to mechanical component testing was

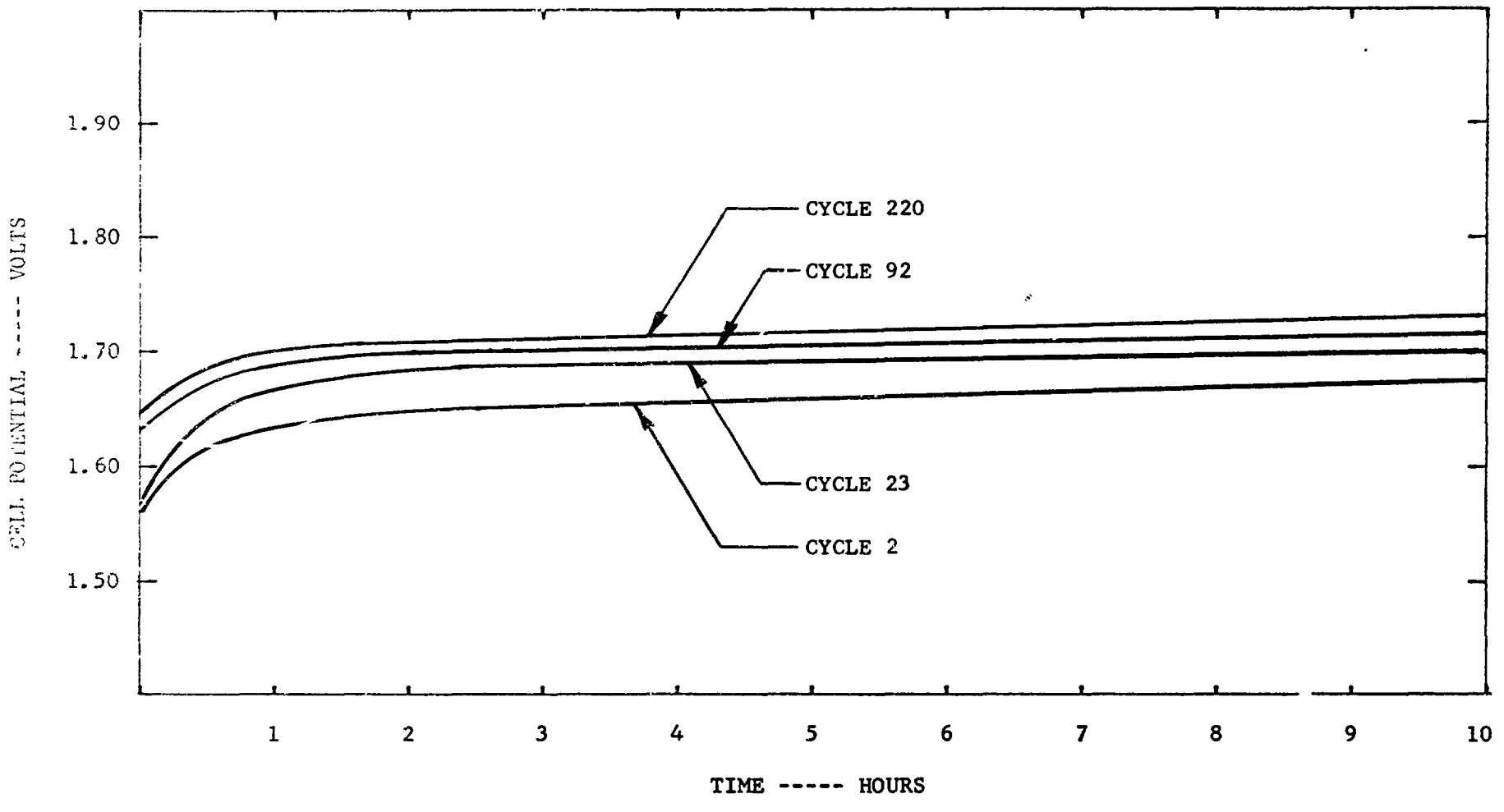

FIGURE 22 . CELL NO. 4058-10 CHARGE PERFORMANCE

DISCHARGE RATE: 33.3 AMPS:
TEMPERATURE: 50° C.

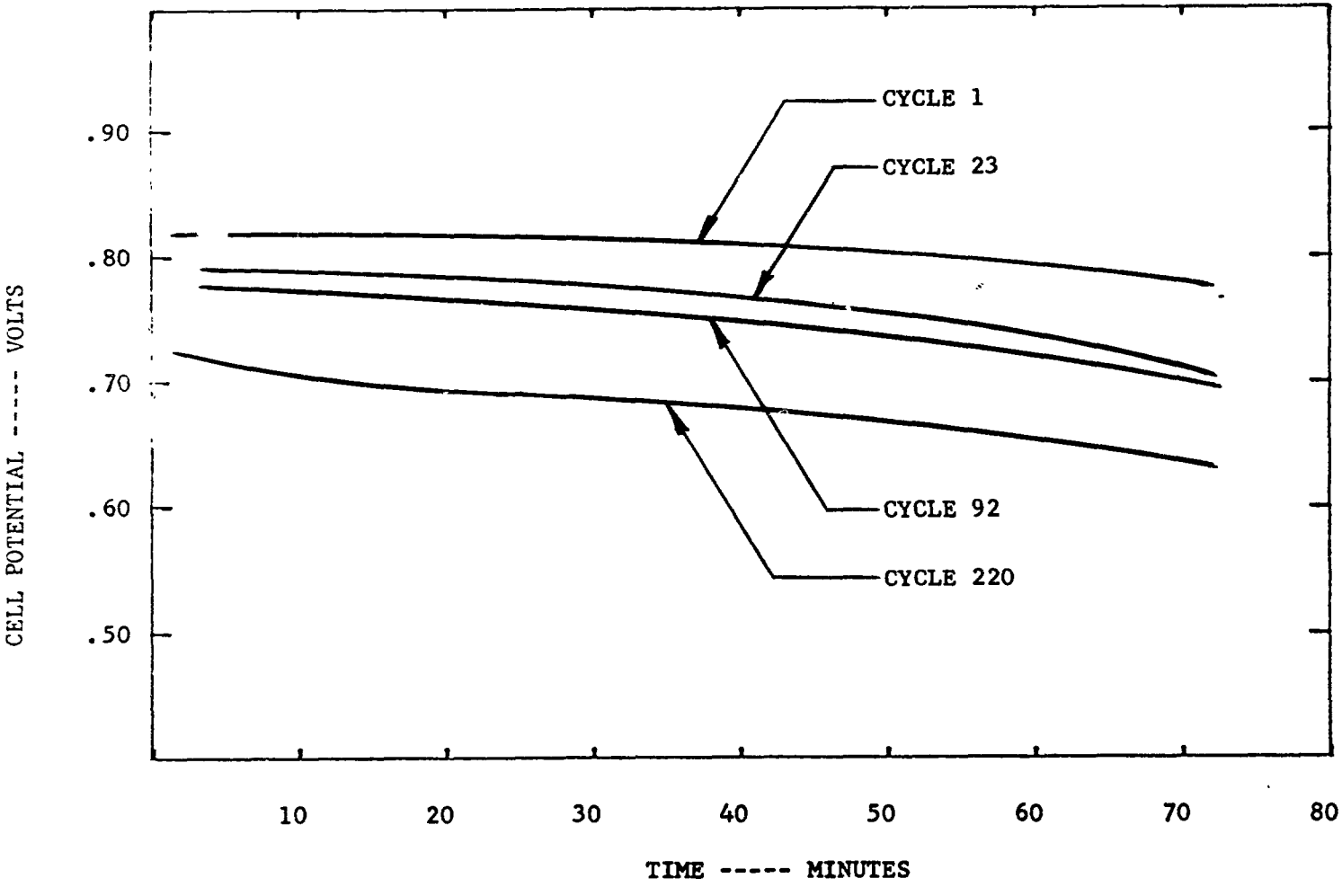

FIGURE 23. CELL NO. 4058-10 DISCHARGE PERFORMANCE

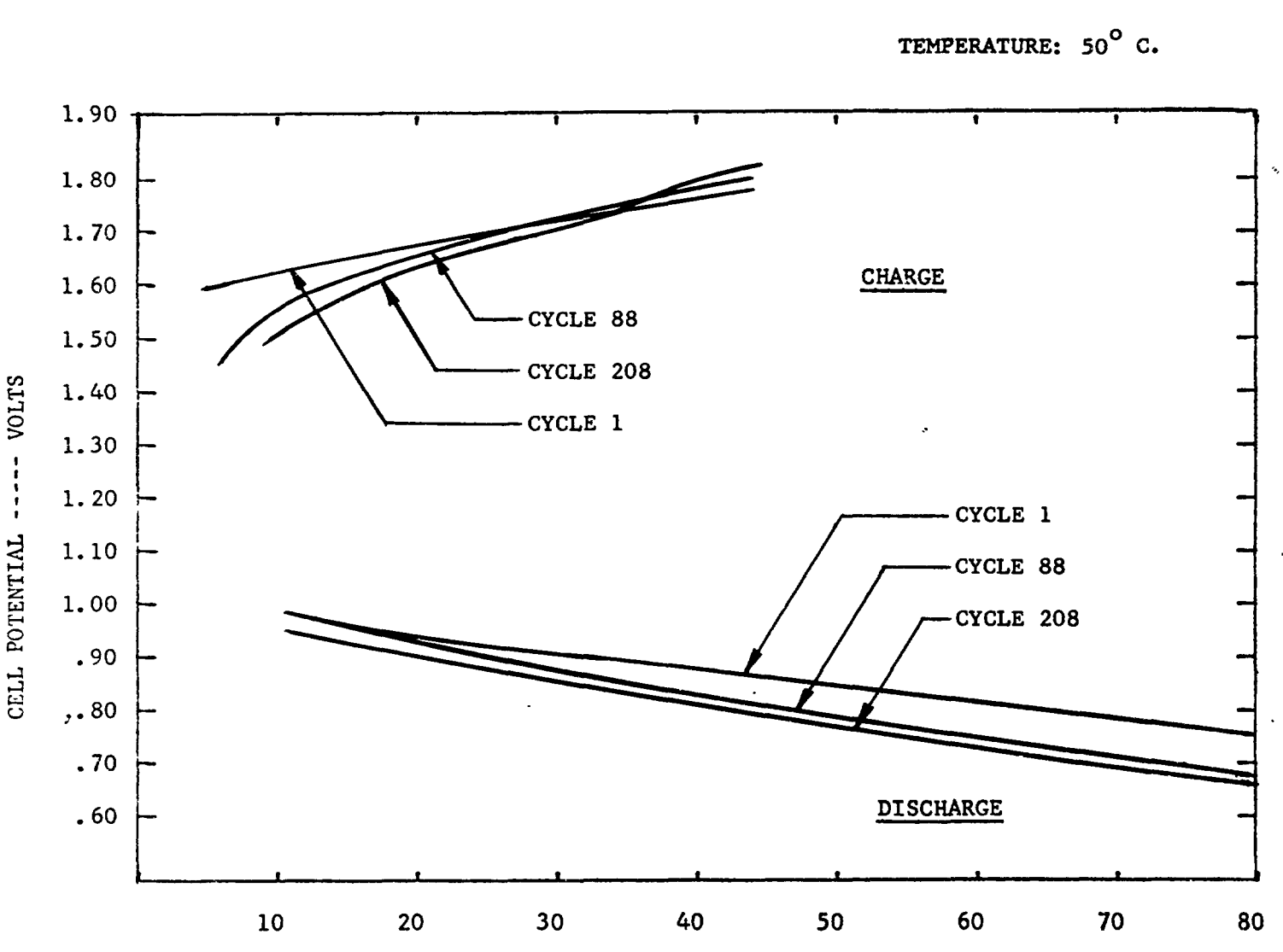

FIGURE 24. CELL NO. 4058-10 POLARIZATION SCANS

interspersed throughout the program with the single cell activities of the program. The electrochemical components were evaluated by their effect on the performance of an operating fuel cell, and the results of this effort are reported in the description of the additional single cells which were fabricated and tested.

3.3.1 Mechanical Components

3.3.1.1 Bellows. - A test fixture was designed and fabricated to cycle test various types of bellows as to life integrity. Figure 25 is a diagram showing the fixture with the timer-cycle control and pressure feed.

3.3.1.1.1 Electroformed Bellows. - Two electroformed nickel bellows obtained from Servometer Corporation were immersed in 30 percent KOH at 100°C for 48 hours. They were then washed with distilled water, dried and cycle tested using the fixture shown in Figure 25. Figure 26 shows the bellows design. The first bellows was cycled 1227 times at the 3 psid level. The pressure was then raised in increments of 1 psi and cycled until failure occurred. The bellows began to leak at 12 psi after completing a total of 4116 cycles. An inspection analysis revealed a crack in the third convolution of the bellows. The second electroformed bellows was cycled 2060 times at 3 psid then at incrementally increased pressures. The bellows failed at 15 psi after 3200 total cycles. The bellows failure was due to two noticeable cracks in the third convolution.

3.3.1.1.2 Hypalon Rubber Diaphragms. - Two Hypalon rubber diaphragms of the design shown in Figure 4 of this report were immersed in 30 percent KOH at 100°C for 48 hours. They were then washed clean with distilled water, dried and cycle tested. The diaphragm was cycled 2000 times at 3 psid. The pressure was raised in increments of 1 psi until the limit of the test apparatus, 15 psi, was reached. After a total of 5175 cycles, the test was discontinued with no damage done to the Hypalon diaphragm. The second Hypalon rubber diaphragm was cycled 1,725 times at 3 psid. The pressure was raised in increments of 1 psi until the limit of the test apparatus, 15 psid, was reached. A total of 3,525 cycles was demonstrated with no damage to the diaphragm.

3.3.1.1.3 Welded Metal Bellows. - Two welded inconel bellows had been obtained from Metal Bellows Corporation. Figure 27 shows the bellows design. The first welded bellows sample was cycled 1,320 times at 2 psid. 100 times at 3 psid, 180 times at 4 psid, and 114 times at 5 psid to give a total of 1,694 cycles. At the end of test, the bellows was intact with no leaks. The second welded inconel bellows was not cycle tested, but was incorporated into test Cell No. 4058-19 for actual cell operation evaluation. The bellows mount was welded directly to the bottom end of the core support, where normally a Hypalon diaphragm had been employed.

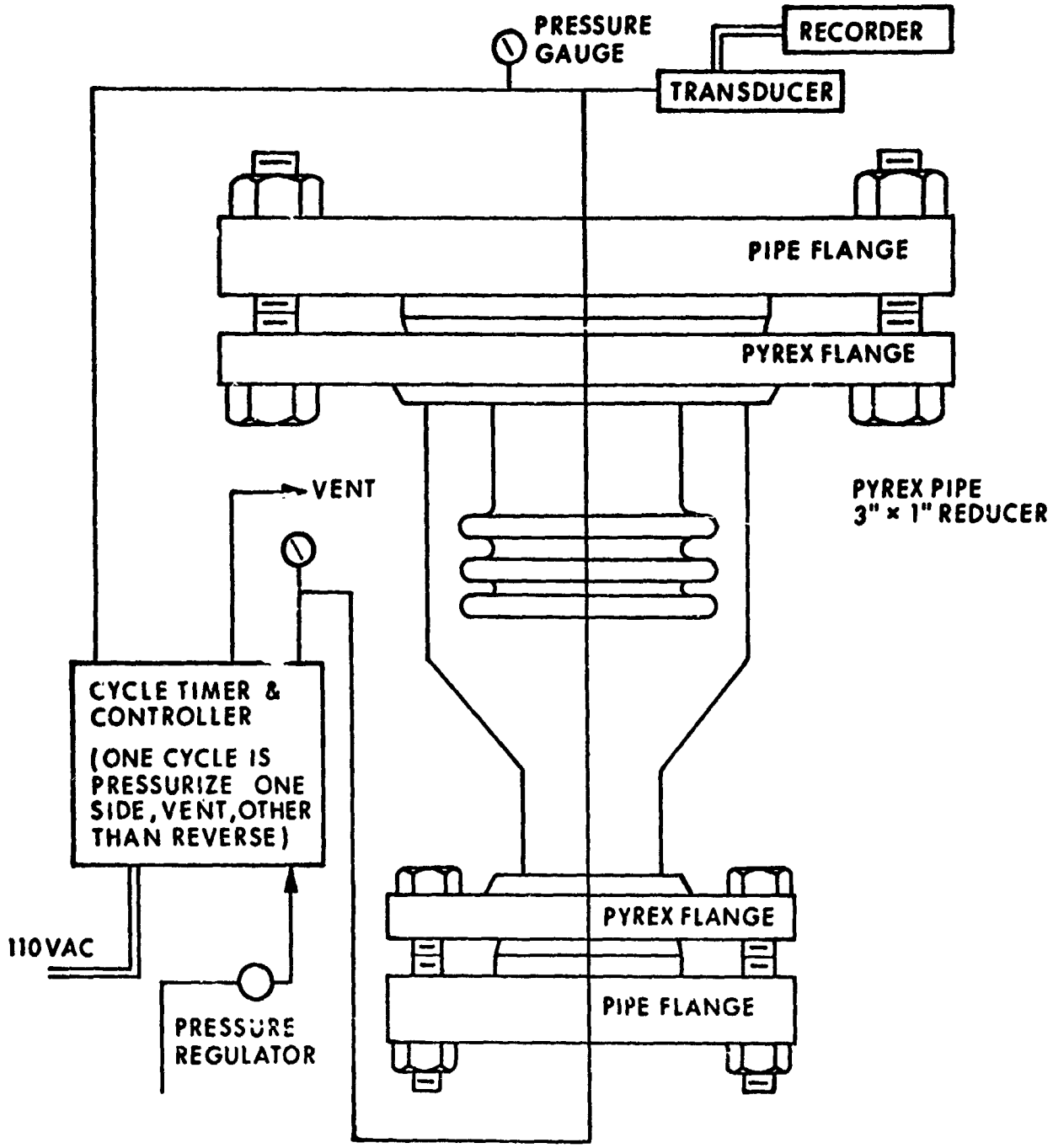

FIGURE 25. FUEL CELL BELLOWS TEST FIXTURE

41718

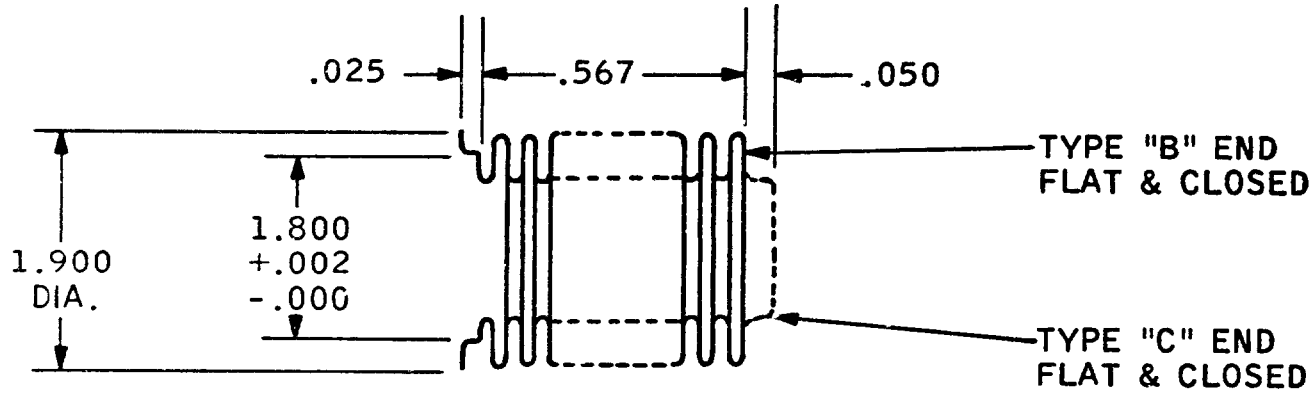

BELLOWS O.D.	1.900"
BELLOWS I.D.	1.400"
WALL THICKNESS	.003"
CONVOLUTION PITCH	.189"
ACTIVE CONVOLUTIONS	3
ALLOWABLE AXIAL STROKE:	
COMPRESSION	.250"
EXTENSION (75%)	.187"
PRESSURE RATINGS (PSIG):	
MAXIMUM ($\frac{1}{2}$ STROKE)	47
PROOF (1.75)	82
BURST (2.50)	117
SPRING RATE LBS/INCH	25.65
LIFE EXPECTANCY (CYCLES)	100 K
MAX. OPERATING TEMP.	350°F.
MATERIAL	NICKEL

FIGURE 26. ELECTROFORMED BELLOWS DESIGN

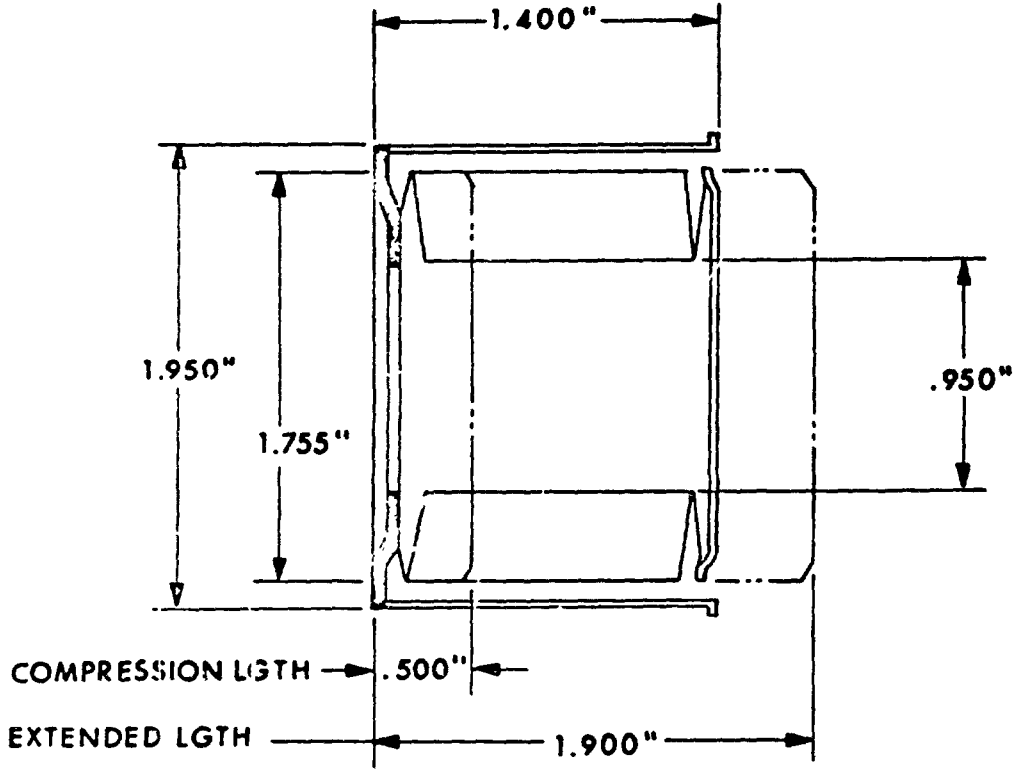

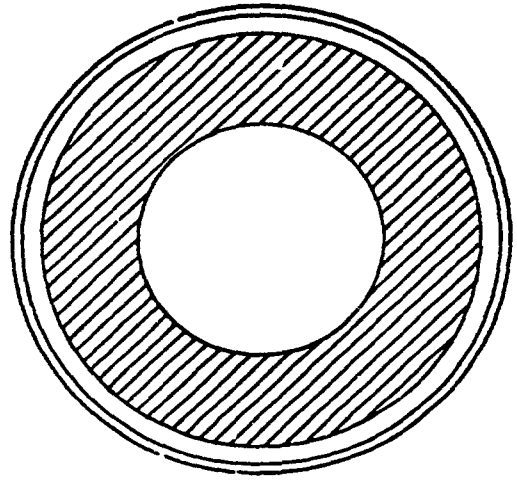

MATERIAL : BELLOWS CONVOLUSIONS — .003" INCONEL
SKIRT & TERMINAL — .010" INCONEL
OPEN FLANGE — .030" INCONEL

REQUIREMENTS

1. LEAK CHECK 2×10^{-9} cc/sec
2. PROOF PRESSURE TEST 15 PSIG
3. 1.4" LINEAL TRAVEL ≅ 2 $IN.^3$ VOL.
4. DISPLACE 1.0 IN^3 WHEN SUBJECTED TO 2.0 PSIG EITHER DIRECTION OF RELAXED POSITION

FIGURE 27. WELDED METAL BELLOWS DESIGN

The initial operation of test Cell No. 4058-19 exhibited a wider differential pressure swing than the cells which employed Hypalon rubber diaphragms. It appeared as if the inconel had too great a spring constant, as its volume displacement is less than 0.2 cu. inch per psid. The cell was cycle tested at 80°C for 12 cycles, at which time the temperature was reduced to 50°C and continued on test.

Cell No. 4058-19 had completed 113 cycles at 50°C. Early during charge Cycle No. 114, while charging at 12.0 amp rate to a pressure of 129 psig, the cell suddenly began to lose pressure slowly. The charging potential of the cell had not changed, and the charging current was turned off. The pressure of the cell continued to slowly drop and the pressure differential slowly rose from approximately 2 psid on the hydrogen side to a maximum of approximately 3.5 psid on the hydrogen side. The open circuit potential of the cell remained above 1.0 volt for approximately 40 minutes as the pressure of the cell dropped to approximately 5 psig. At this point, the O.C.V. dropped to approximately zero and the differential pressure returned to a zero value. The cell was removed from test to be analyzed for its apparent failure.

Visual analysis of the core revealed a possible scorch area of the oxygen electrode at the upper portion of the core along the seam. A leak check of the core indicated a fair leak at a 2 psid at this part of the core. The oxygen electrode was carefully peeled away from the matrix at the seam, which revealed a discolored portion of the matrix (burn) which had dried and become very hard.

An attempt was made to salvage this cell by removing a portion of the matrix which had dried out, and patching the matrix with a thick slurry of potassium titanate and water mix. After application of the patch, the portion of the oxygen electrode which had been peeled away from the matrix, was returned to its original position and rewound with wire. The core was then saturated with KOH by submerging in a KOH solution. A leak check revealed no leak at the matrix patch, but a slight (almost negligible) leak at the upper edge of the core.

Under these conditions, the cell was again assembled and placed on test. The performance of the cell on this initial cycle (Cycle #114) is illustrated in Figures 28 and 29, and demonstrates performance comparisons of the cell with Cycle #113 (just prior to failure) and with Cycle #3 (initial performance of the cell). This data is significant in that degradation of performance is primarily due to changing conditions of operation rather than deterioration of cell components. Cycle 2 (115) of this rejuvenated cell showed performance characteristics approximating Cycle #114; however, during charge of Cycle 115, at a 5 amp rate, the pressure of the cell suddenly dropped from 313 psig to 273 psig with a pressure differential buildup of 50 psi on the oxygen side. The cell remained on charge for approximately an additional one hour, during which time the pressure dropped to 102 psig, the differential pressure decreased to 35 psi, and the voltage was maintained at a reasonable charging potential (1.600 volts).

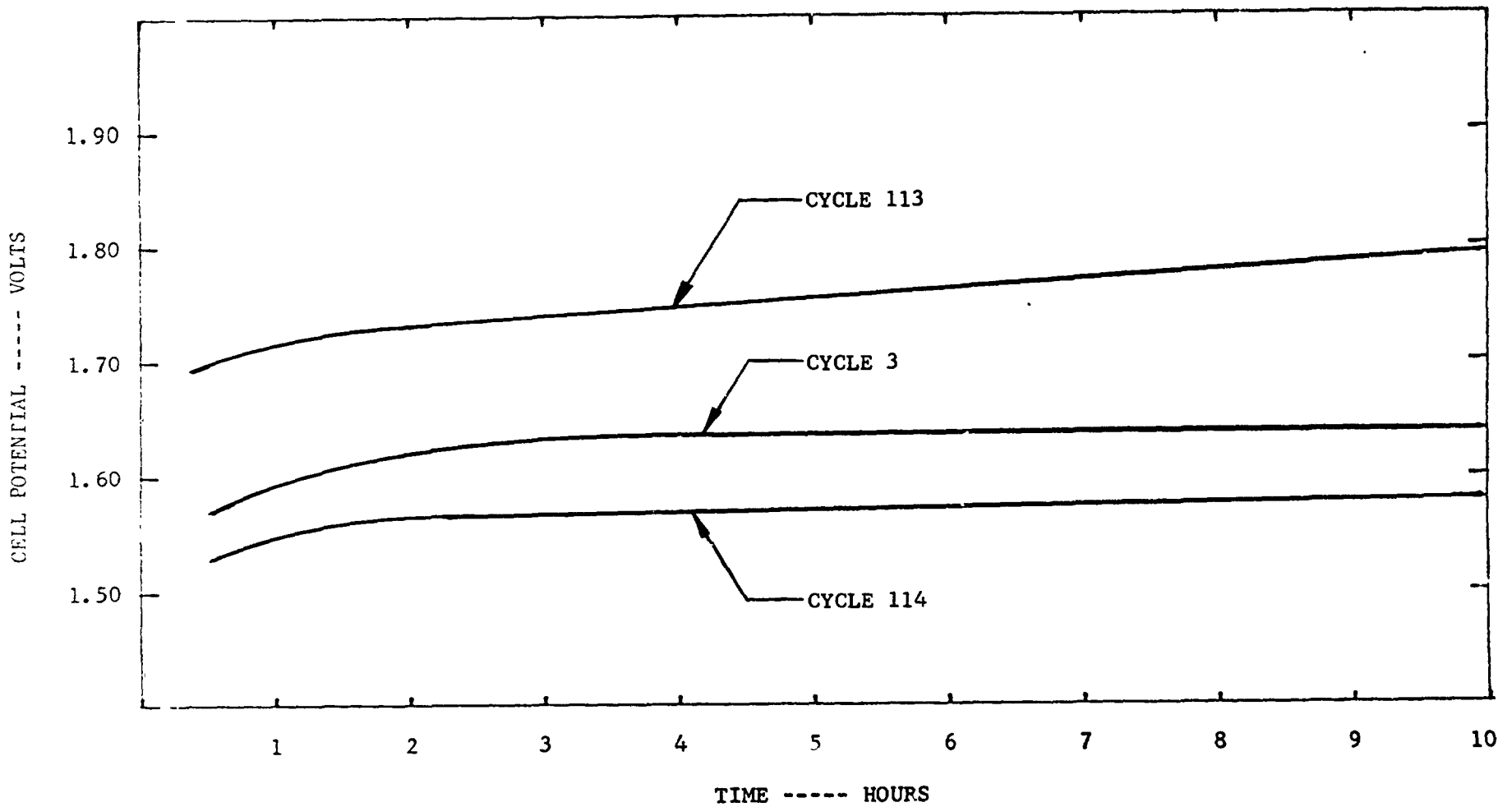

FIGURE 28. CELL NO. 4058-19 CHARGE PERFORMANCE

DISCHARGE RATE: 33.3 AMPS:

TEMPERATURE: 50° C.

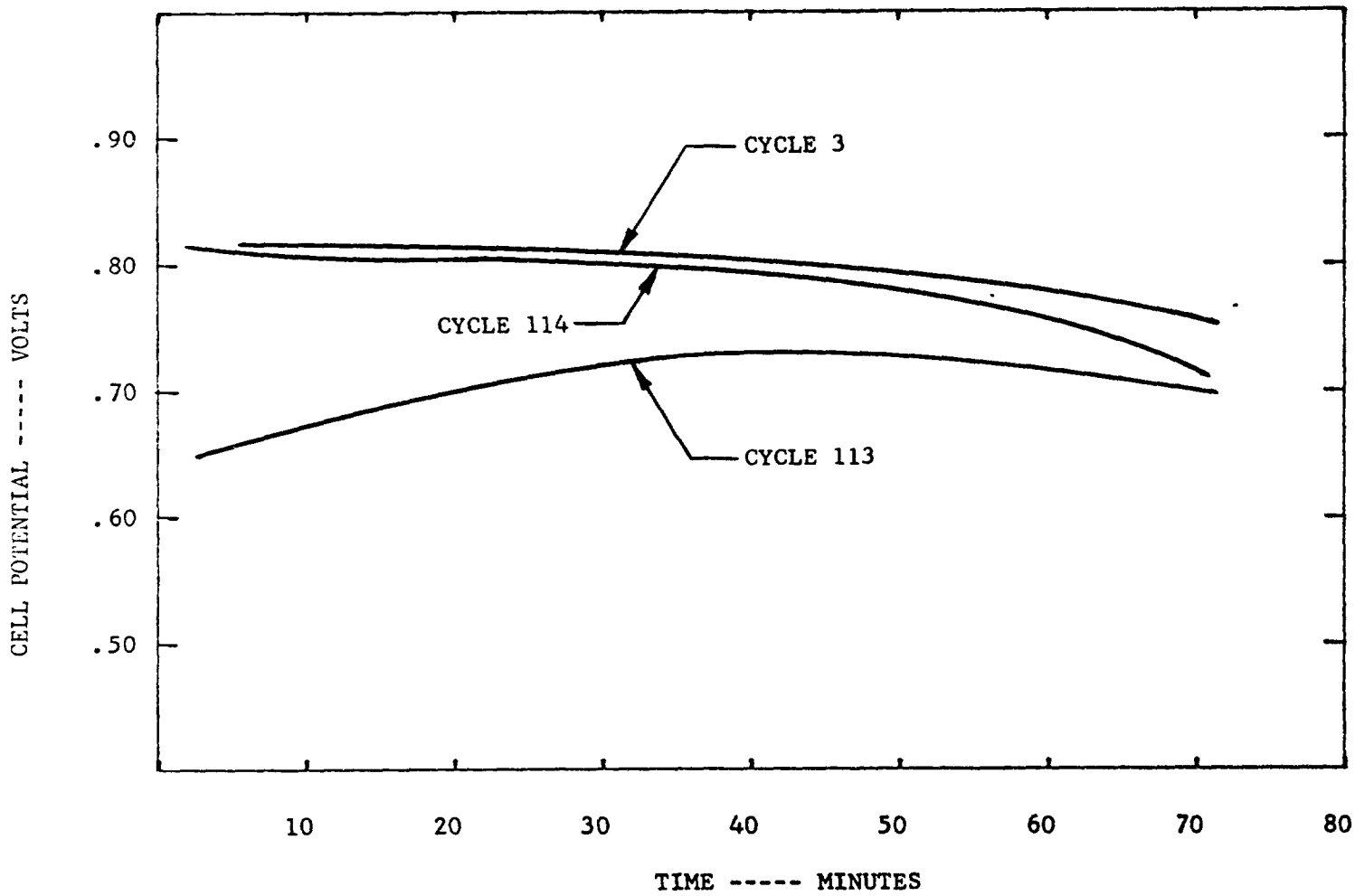

FIGURE 29. CELL NO. 4053-19 DISCHARGE PERFORMANCE

An additional hour of charging showed a pressure drop to 66 psig and a constant differential pressure of approximately 35 psi; however, the charging potential escalated to a level of 5.00 volts, and suddenly dropped to .296 volts, indicating a direct short internally. The cell was unattended during this period, but the cause of failure was an external leak in a welded fitting on the hydrogen feedthrough.

The inspection analysis of this cell revealed a severe internal combustion occurrence at the upper edge seal. An examination of the bellows showed no apparent deterioration, even being subjected to this adverse condition.

A second test cell, No. 4058-18, had also been fabricated with an inconel metal bellows for test evaluation. This cell differed from Cell 4058-19 in that the bellows used was subjected to an annealing process whereby its relaxed position was altered. Secondly, the orientation of the bellows was reversed from that in Cell No. 4058-19. The cell was flushed five times with hydrogen and oxygen from 10 to 95 psig. It was then filled to 95 psig with the respective gases and put on charge at 50°C.

Cell No. 4058-18 had completed 37 cycles, operated as a 40 A.H. cell in a pressure range of 100 to 600 psig. After 37 cycles, the cell had been cycling as a 48 A.H. cell in a pressure range of 150 to 750 psig. The cell operated for a total of 80 cycles and its performance data is illustrated in Figures 30, 31, and 32.

The trend of the curves indicate a water management problem; i.e., a drying condition of the matrix or, probably more significant, a changing position of the liquid interface in the electrodes proper. This is indicative of the cell with a low potential at the beginning of the discharge cycle, improved potential during charge to an optimum value, and then a small decrease in potential to the end of the discharge cycle, with the final voltage value being somewhat greater than the voltage at the beginning of discharge.

Cell No. 4058-18 had operated for a total of 80 cycles prior to a catastrophic failure. A severe internal combustion occurred at the bottom edge seal of the core adjacent to the bellows. The bellows suffered burn holes through several convolutions and the entire capsule was extended into the hydrogen compartment approximately 1.0 inch beyond its normal relaxed position. Except for the few burn holes, the bellows was intact.

It has been demonstrated that Hypalon bellows cannot be used for high temperature (80°C and above at 600 psig oxygen) or oxygen pressures above 900 psig. Based on this, it seems reasonable to assume that the rate of oxygen attack on Hypalon at lower temperatures and pressures, although much slower, is significant in terms of several years required performance; therefore, Hypalon has been disqualified as a material of bellows fabrication.

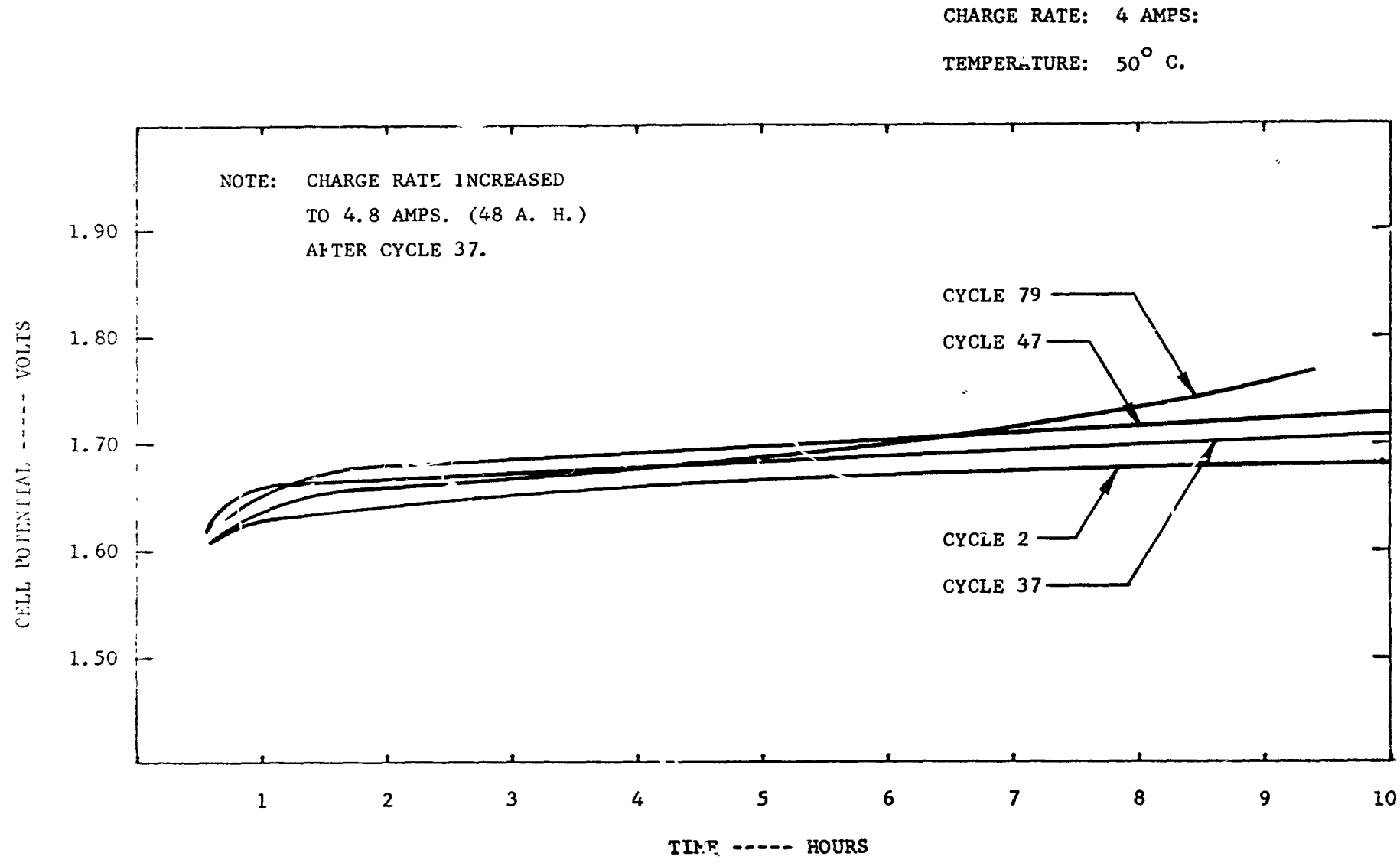

FIGURE 30. CELL NO. 4058-18 CHARGE PERFORMANCE

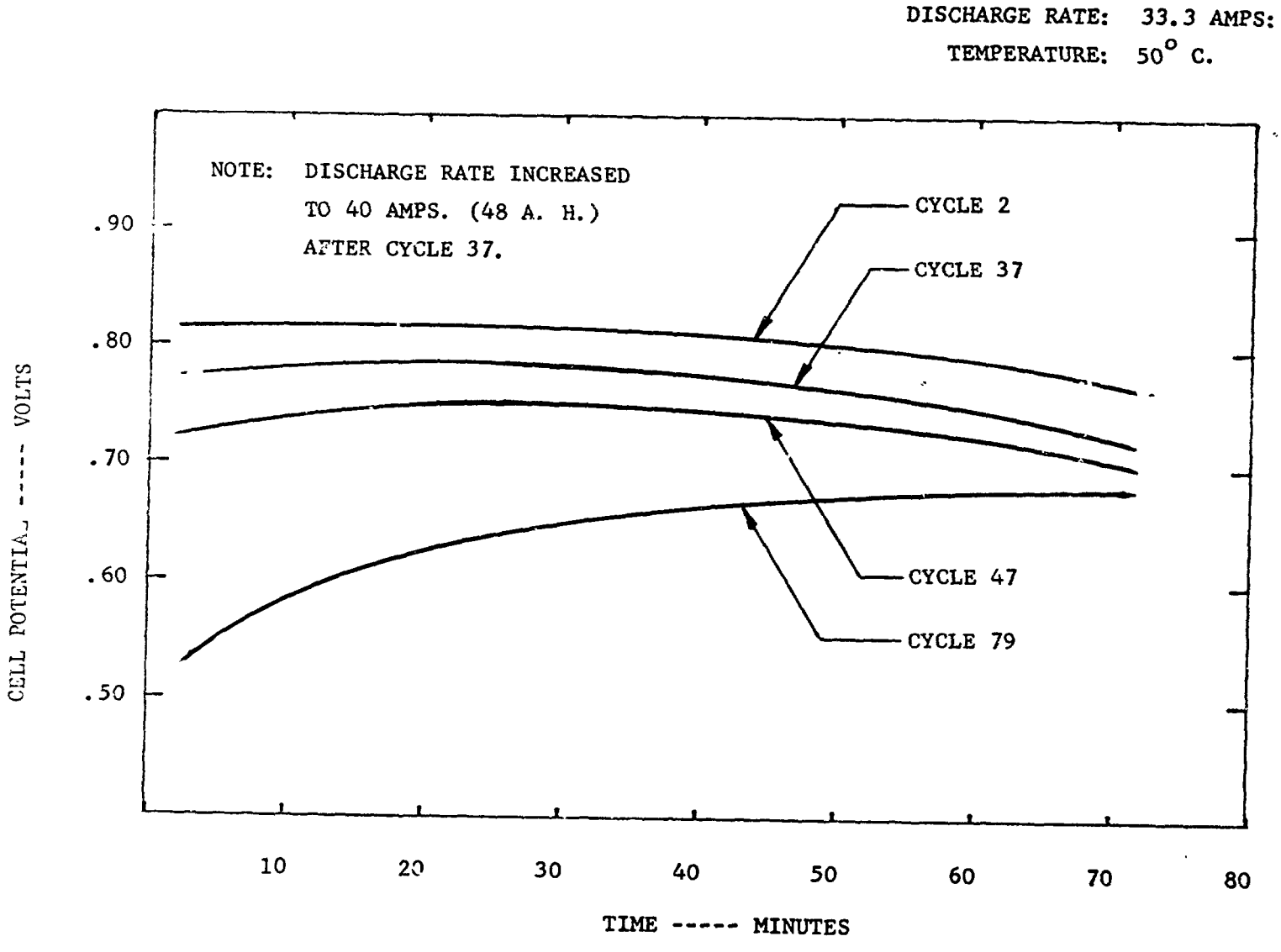

FIGURE 31. CELL NO. 4058-18 DISCHARGE PERFORMANCE

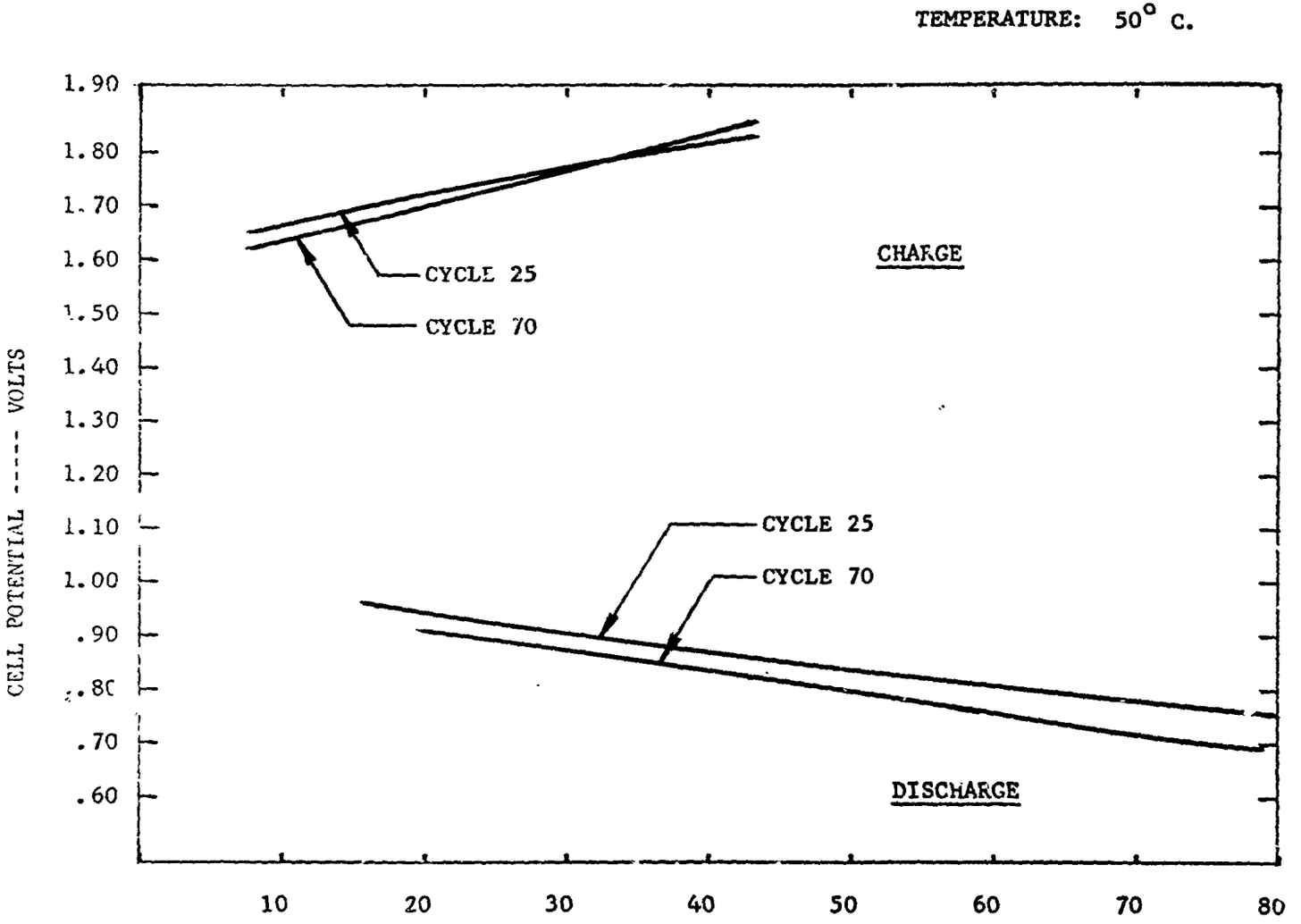

FIGURE 32. CELL NO. 4058-18 POLARIZATION SCANS

As compared to the Hypalon bellows, the metal bellows operates much more uniformly during differential pressure changes. The welded metal bellows has greatly enhanced the reliability factor of non-leakage in this area. The metal bellows is much more durable and not subject to charring in the oxygen environment. The metal bellows is a significant improvement as compared to the Hypalon bellows.

3.3.1.2 Pressure Housing. - An inconel pressure vessel of flight hardware design to house the fu' cell core assembly was fabricated and subjected to hydrostatic rupture test. The vessel is constructed of .020" inconel sheet rolled and welded into a 2.500" O.D. cylinder 12.5" long. The ends of the cylinder have been sealed with spun eliptical inconel caps that are .025" thick and welded to the cylinder.

The results of this test show a yield strength of approximately 1200 psig, and a burst pressure of approximately 1930 ps.g, which exceeds the burst strength requirement of 200 percent of full charge. The raw data of this test is shown in Table II, and a curve plotting the yield versus pressure is illustrated in Figure 33.

3.3.1.3 Core Support. - Crush tests to determine the actual strength of the different core structures were proposed as one of the fuel cell parameters. These tests were performed by applying a differential pressure to the outside of the core until the core yields.

3.3.1.3.1 Standard Perforated Core Support. - The core support, which EOS fuel cells employ, consists of a perforated .020" thick inconel sheet rolled and welded into a 2.00" diameter x 12.500" long cylinder (standard 40 A.H.). A sample core of this configuration was assembled with a hydrogen electrode, a matrix, and a simulated oxygen electrode; the entire assembly being wrapped with nickel wire at a tension of 4.5 pounds. This assembly was held at a differential pressure of 30.0 pounds for a period of 5 minutes with no damage. It was felt that 30.0 psig pressure differential is sufficiently greater than that seen by normally operating cells.

3.3.1.3.2 Core with no Support. - A core was prepared by spot welding H_2 electrode plaque material into a cylinder and spot welding 5/8" stainless steel rings on either end for cap and bellows mounts. A matrix was then formed and pressed at 250 psig and a simulated O_2 electrode, consisting of 60 mesh / mil Ni wire, was put in place and the whole core was wrapped with Ni wire at a tension of 4.5 pounds. This core crushed under 19.5 pounds pressure differential. This approach to fabricating a weight saving core concept was abandoned, but the results of this test substantiated the feasibility of fabricating a sintered nickel tubular structure that would serve as both the core support and the hydrogen electrode.

TABLE II

FUEL CELL PRESSURE SHELL HYDROBURST TEST

"Top" of Shell is end with 0.25" Tube Connection

PRESSURE PSIG	DIAMETER Two Places at approx. 90° apart						
	TOP WELD	1/6	1/3	MIDDLE	2/3	5/6	BOTTOM WELD
0	2.500	2.500	2.508	2.508	2.510	2.507	2.500
100	2.500	2.500	2.508	2.508	2.510	2.510	2.500
200	2.500	2.504	2.508	2.508	2.510	2.510	2.500
300	2.500	2.504	2.508	2.508	2.510	2.510	2.500
400	2.500	2.504	2.508	2.508	2.510	2.510	2.500
500	2.500	2.504	2.508	2.508	2.510	2.510	2.500
600	2.500	2.504	2.508	2.508	2.510	2.510	2.500
700	2.500	2.504	2.508	2.508	2.510	2.510	2.500
800	2.500	2.504	2.508	2.508	2.510	2.510	2.500
900	2.500	2.505	2.508	2.508	2.510	2.510	2.500
1,000	2.502	2.511	2.510	2.511	2.511	2.511	2.500

TABLE II (Concluded)

FUEL CELL PRESSURE SHELL HYDROBURST TEST

"Top" of Shell is end with 0.25" Tube Connection

PRESSURE PSIG	DIAMETER Two Places at approx. 90° apart						
	TOP WELD	1/6	1/3	MIDDLE	2/3	5/6	BOTTOM WELD
1,100	2.505	2.514	2.515	2.515	2.516	2.517	2.503
1,200	2.508	2.517	2.516	2.517	2.518	2.524	2.510
1,300	2.508	2.522	2.520	2.523	2.524	2.525	2.510
1,400	2.506	2.540	2.540	2.541	2.542	2.542	2.512
1,500	---	2.570	---	2.575	---	2.572	---
1,600	---	2.615	---	2.618	---	2.620	---
1,700	---	2.680	---	2.683	---	2.680	---
1,800 Photos	---	2.765	---	2.790	---	2.764	---
Stretch 1930 ⇆ 1860	---	---	---	---	---	---	---
2,000		BURST AT 1930 PSIG FRACTURED DOWN CENTER OF WELD					

MATERIAL: INCONEL 625

DIMENSIONS: 2.5"O.D. x .020 x 12.5"

TEMPERATURE: AMBIENT

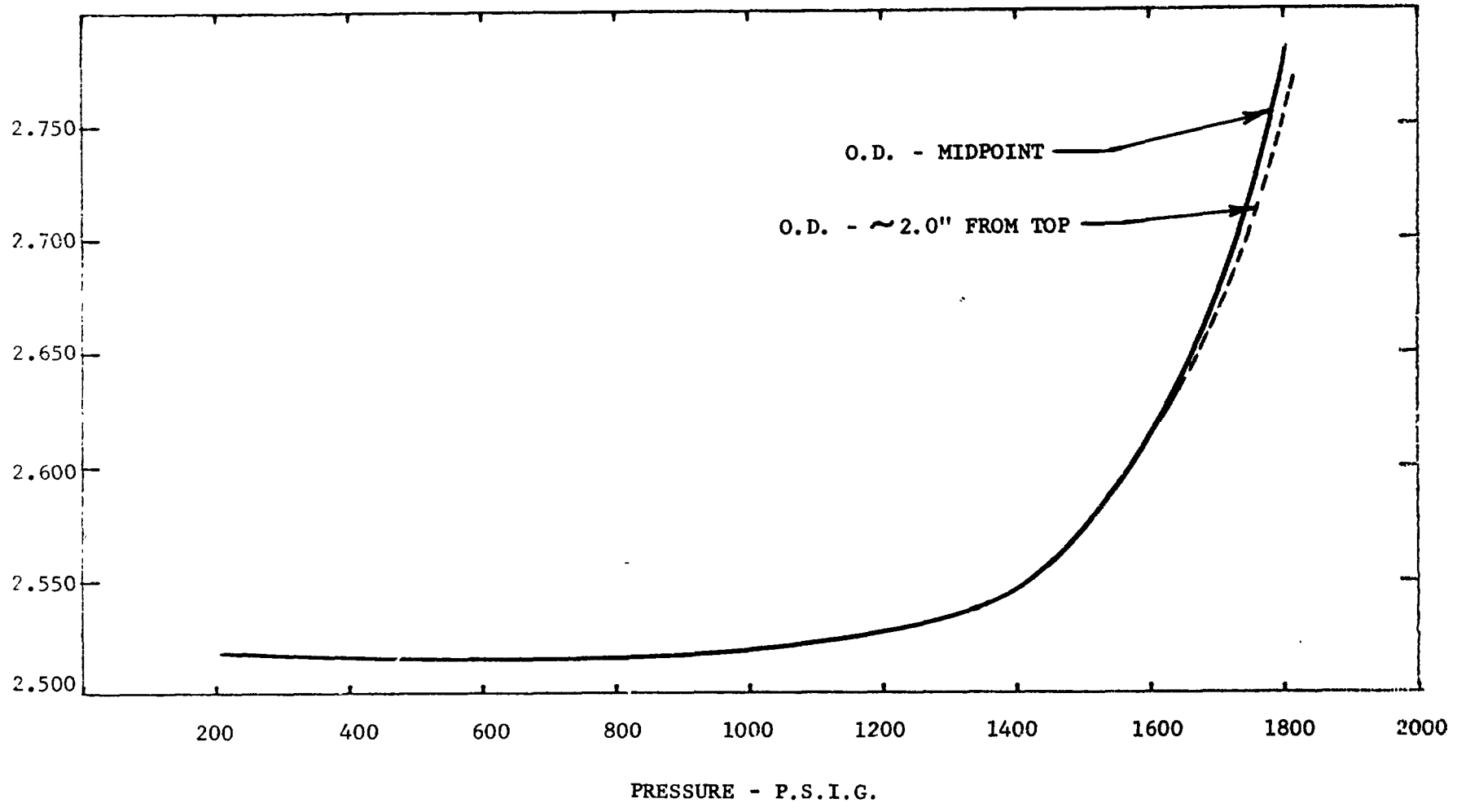

FIGURE 33. FUEL CELL PRESSURE SHELL - HYDROBURST TEST

3.3.1.3.3 Sintered Nickel Core Support. - During this contract period, a development effort was established to fabricate sintered nickel tubular structures to serve as both the core support and the hydrogen electrode. A number of tubes were made to evaluate problems and develop techniques for sintering powder in a cylindrical configuration.

Nickel powder Carbonyl "B" Type 287 is the raw material which is employed in the tube fabrication. This is the same powder that is being used for sintering nickel plaques for fuel cell application to attain a 70 percent porosity value of the finished product.

The tooling consists of a mold with a cavity approximately 7½" deep and an inside diameter of approximately 2.000 inches. The inner core of the mold is of the same length as the cavity with an outside diameter of 1.850 inches. This allows a spacing of .075 inches to pack the powder to preform the tube prior to sintering. Using .010" thick nickel Exmet for reinforcement, several tubes have been fabricated to a fair degree of success. The packing of the powder uniformly (gravity feed), in the limited cross sectional spacing, has been difficult to attain. By eliminating the support screen in the tube, a more uniform structure resulted without any cavitation. The sintered nickel tubes reflect a certain amount of structural strength even without the support Exmet. The tubes which have been fabricated have been subjected to a sintering temperature of 850°C in a hydrogen furnace for a duration of 1 hour. The porosity of the finished tubes range from approximately 67 percent, including the nickel Exmet support, to approximately 71 percent in the unsupported sintered tube. The established shrinkage factor during the sintering process is 43.7 percent.

After the above described preliminary investigation, new tooling was designed and fabricated to make sintered nickel cores to the required configuration for the 40 A.H. test cell. A total of six sintered nickel tubes had been fabricated to a finished dimension of 11.5" x 2.00" I.D. Three of the tubes were processed using Type 287 carbonyl nickel powder and the remaining three were fabricated using Type 128 nickel powder. The tubes were all made in the same manner and in the same type of mold by packing the powder (gravity) and sintering the metal in a hydrogen furnace. None of these sintered tubes contained reinforcement screening. The two types of tubes, after sintering, had the following average physical dimensions.

	TYPE 287	TYPE 128
Length:	11.5"	11.5"
Inside Diameter:	2.000"	2.000"
Outside Diameter:	2.090"	2.120"
Total Weight:	116 gms.	253 gms.
Porosity:	75%	58 %
Total Resistivity:	7 milliohms	1.6 milliohms

The sintered nickel tubes which were fabricated with Type 287 powder proved to be very fragile and two were broken in handling. A collapse test was performed on the remaining Type 287 sintered tube, which failed at < 5 psig pressure. The Type 128 sintered tube, being more dense and heavier walled, maintained its integrity when subjected to 30 psig for a period of 5 minutes. The above indicated pressures are the pressure values which the outside of the tube was subjected to, while maintaining an ambient pressure inside the tube. A minimum of 30 psi pressure differential is considered satisfactory in terms of mechanical strength.

A Type 128 sintered nickel tube had been fabricated into a working cell core by welding nickel end rings to the tube for core cap and bellows attachment. The nickel core had been successfully platinum plated; but, because of the wall thickness of the sintered tube, 40 milligrams of platinum/sq. cm. had been applied to get greater penetration of the catalyst into the sintered core.

Cell No. 4058-30 was completely fabricated using the above described sintered core assembly. The matrix for this cell was asbestos - .052" thick. The use of a potassium titanate matrix was prohibitive, in that the normal process of KT matrix preparation requires pressing the dry mat at approximately 250 psig, beyond the strength limit of the core. The process, whereby an asbestos matrix is prepared, requires only a wet press of 20 to 30 psig pressure.

It was recognized that this task was an investigation of the feasibility of using a sintered nickel tube as both a support core and the hydrogen electrode in a cylindrical regenerative fuel cell. It was beyond the scope of this program to optimize cell performance and particularly hydrogen electrode performance with a complete development program of a sintered nickel tube to establish exact porosity and pore size distribution. After vacuum impregnating the cell with KOH solution and leak checking, Cell No. 4058-30 was started on test in the normal start-up method. The cell was charged at a 10.0 amp rate for 5 hours to a cell pressure of 512 psig. Because of the thickness and density of the core, the gas volumes within the cell were out of balance. A 1.25 cu. inch external volume was added to the oxygen side to compensate for the imbalance.

At the completion of the first cycle, this cell was removed from test to repair a minute leak which had developed. A leak check at this time revealed a pin hole in the weld of an external fitting. This was then repaired. The cell was again subjected to a leak check; and at approximately 500 psig pressure, the rupture disc in the boiler-plate assembly suddenly failed. The sudden great pressure differential across the core assembly resulted in severe damage to the core assembly. An analysis of the inner core revealed that the bellows and edge ring attachment separated cleanly from the sintered nickel core at the weld. The sintered core was still intact. The edge ring also contained the rubber seal and portions of the matrix which were wired independently to the end ring. It literally tore the entire bellows end ring assembly away from the sintered core.

A second sintered core assembly had been fabricated at the same time this first cell was made. This was an identical cell construction as Cell No. 4058-30. The complete cell was immediately constructed and placed on cycle test. This is Cell No. 4058-33. During the first three cycles, the cell performance was optimized by venting gases during electrolysis to assure proper moisture conditions for good performance in the fuel cell mode. The cell has operated for 117 cycles, to the end of the contract, without failure. The performance characteristics are depicted in Figure 34 - Charge, Figure 35 - Discharge, and Figure 36 - Polar Scan.

3.3.1.4 Insulated Feedthrough Connectors. - Two types of insulated feedthrough connectors have been designed and fabricated, and evaluated as to acceptability for flight hardware. The first type, made by Ceramaseal, Inc., was of low profile design incorporating a stress relief flange made of 52 percent Ni-Iron alloy. The second type, made by R-W Products, Inc. was also of low profile design, but used inconel for the metal portions of the hardware. Figure 37 illustrates the two design concepts. Twelve electrical insulated feedthroughs from Ceramaseal, Inc. were visually inspected and graded accordingly. The lowest graded unit was subjected to a hydrostatic pressure test of 1000 psig.

The feedthrough was silver soldered to a hollowed metal base, and a 1/4" tube was silver soldered to the top section as depicted in Figure 38. The feedthrough failed to pass this pressure test in that the insulator lifted from the bottom metal ring at the braze, at the point shown in Figure 38, and permanently set in a cocked fashion. It was felt that this test was rather inconclusive because the ceramic-to-metal braze may have been affected by the silver solder connection process.

A second insulated feedthrough was then subjected to the same type of test. In this case, the bottom of the feedthrough was electron beam welded to an inconel pressure cap as would be done in actual practice. This unit was then subjected to 1000 psig pressure, using a gas medium (nitrogen). At this pressure, it was noted that the insulated feedthrough had assumed a cocked angle to the pressure cap to which it was welded. In this condition, at 1000 psig gas pressure, the feedthrough did not leak.

A post test examination of this unit revealed that the ceramic-metal braze had indeed remained intact, but the stress relief base ring had distorted causing the unit to assume a cocked position. A close reexamination of the first unit showed the same effect of ring distortion and not the ceramic-metal braze. The failure of the braze would result in a leak, which neither of these feedthroughs developed.

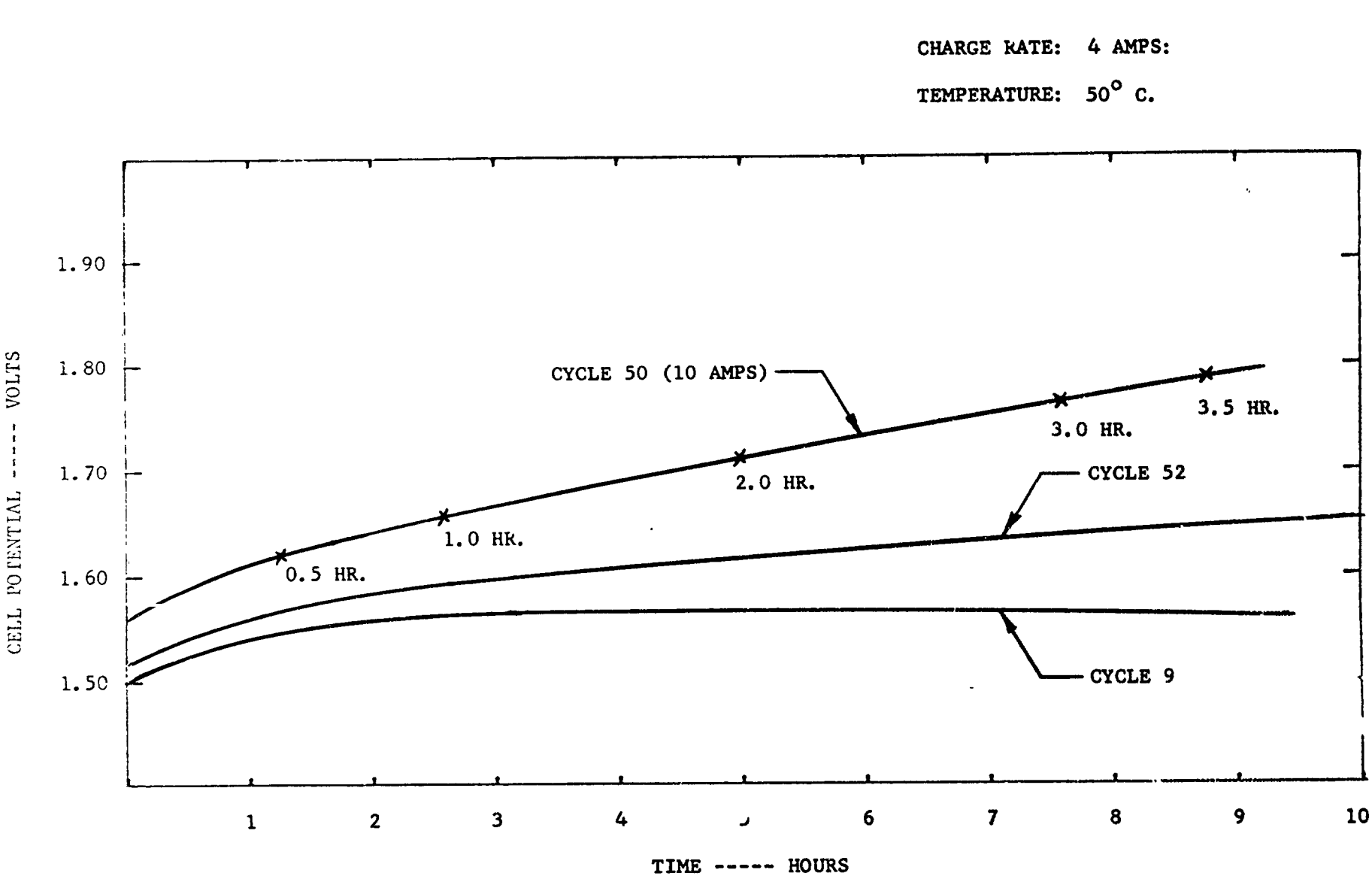

FIGURE 34. CELL NO. 4058-33 CHARGE PERFORMANCE

DISCHARGE RATE: 33.3 AMPS:

TEMPERATURE: 50° C.

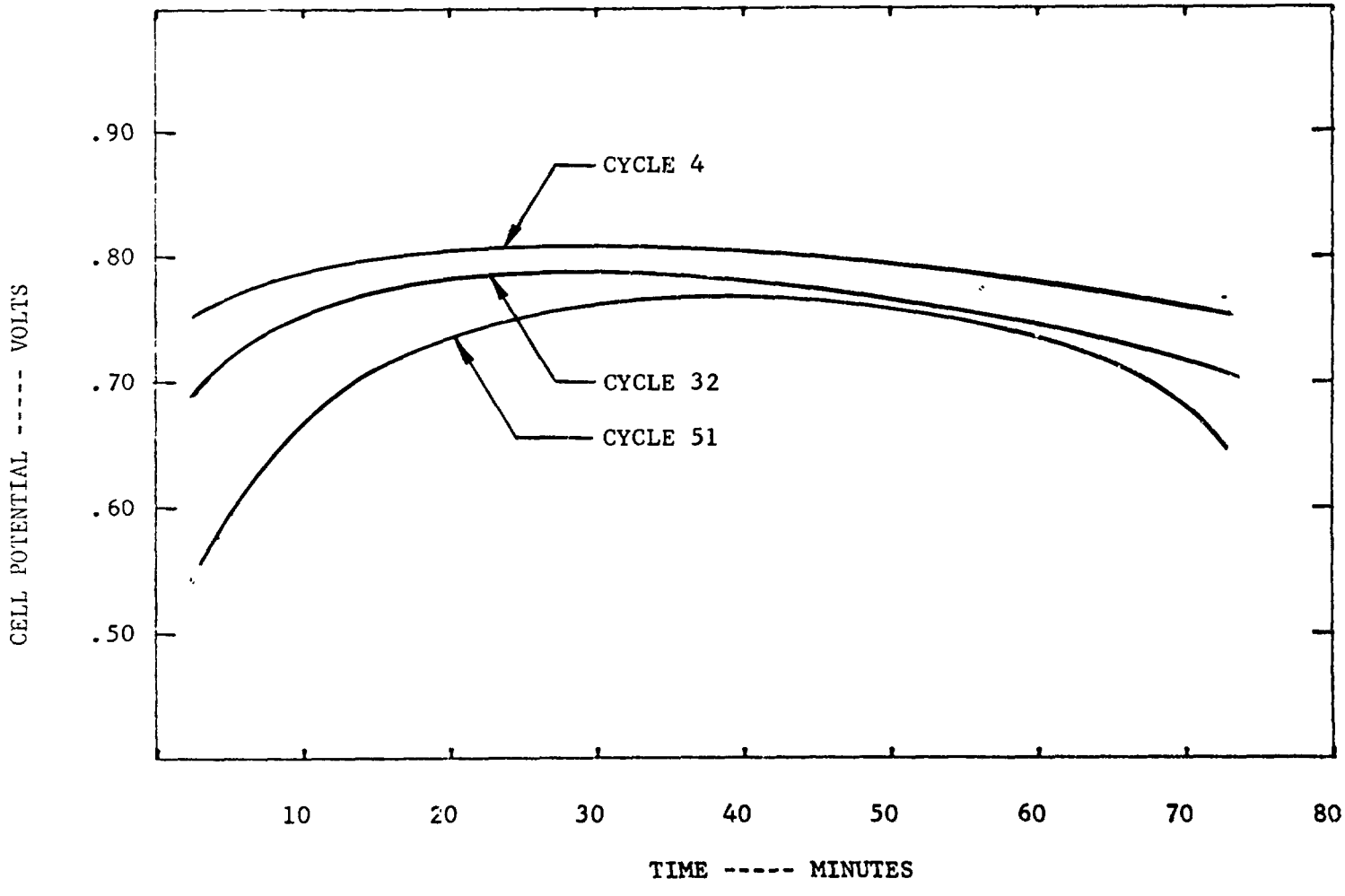

FIGURE 35 . CELL NO. 4058-33 DISCHARGE PERFORMANCE

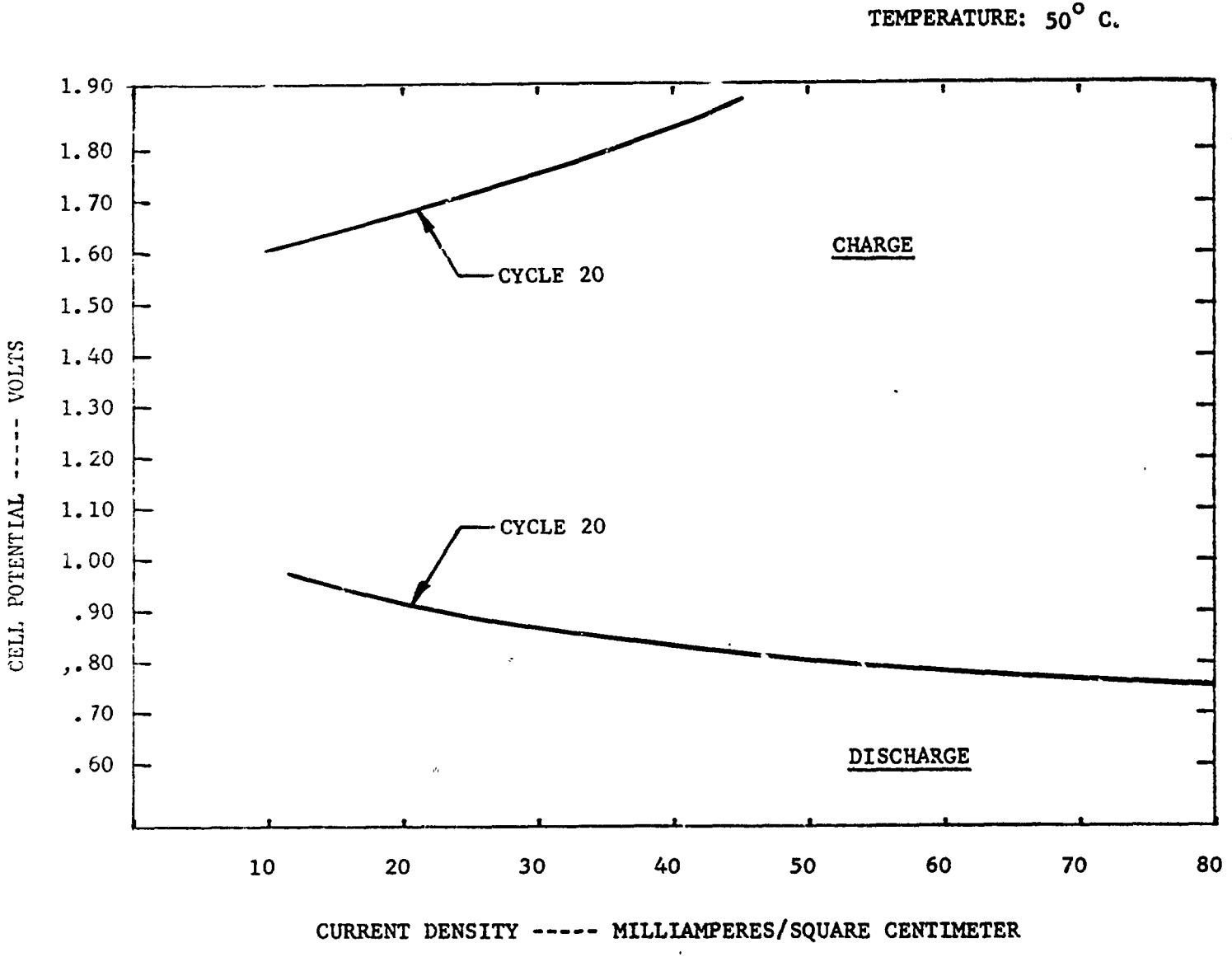

FIGURE 36. CELL NO. 4058-33 POLARIZATION SCANS

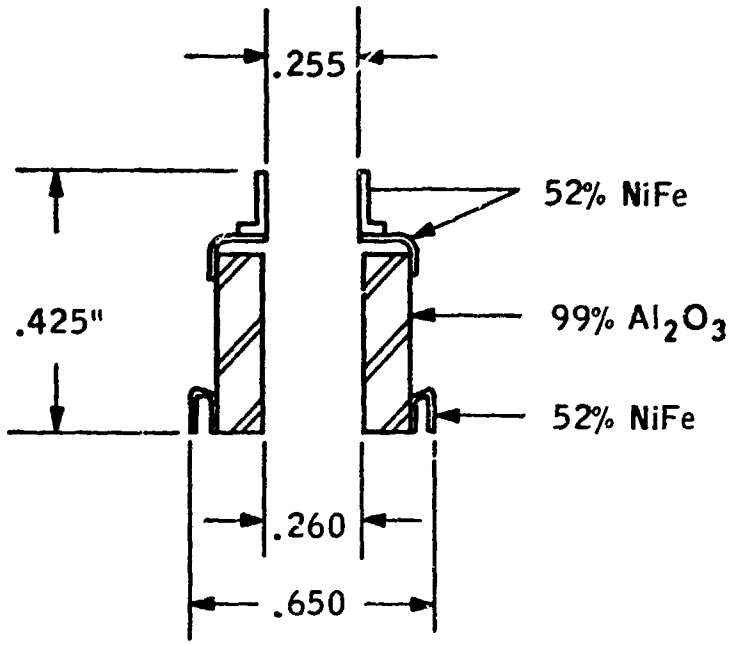

TYPE 1

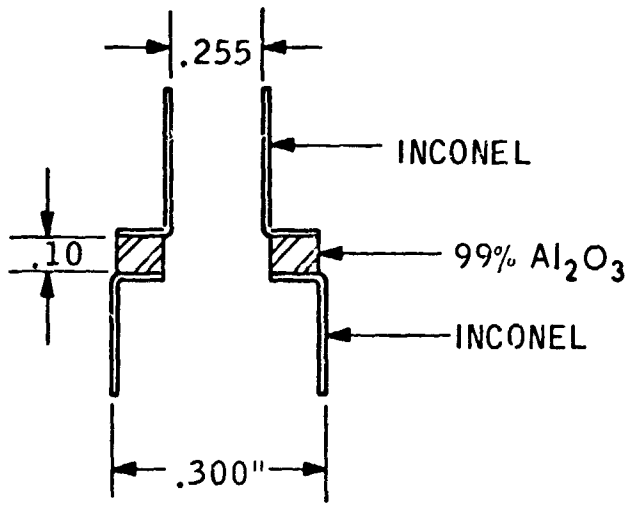

TYPE 2

FIGURE 37. CERAMIC FEEDTHROUGH DESIGNS

41715

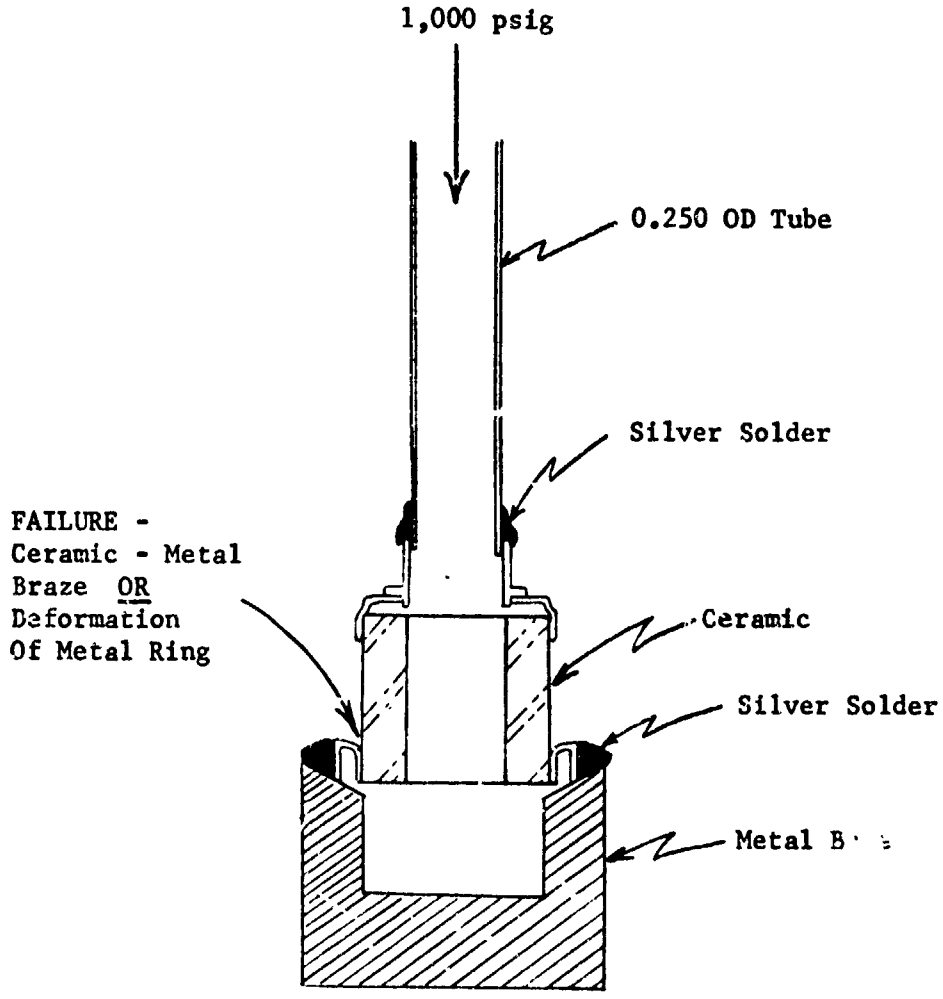

FIGURE 38. FEEDTHROUGH TEST ASSEMBLY

The vendor of these units has been notified of the ring failure, and the test samples have been submitted to them to be analyzed by their engineering group. Two prototype lightweight fuel cells were constructed, using the Ceramaseal type feedthroughs, and were subjected to environmental testing, which included the vibration acceptability test. No visible or functional damage occurred to the insulated feedthrough connectors as a result of this test.

The inconel feedthrough connectors were received late in the program, and could be only physically pressure tested as to acceptability. This unit was subjected to the same type of pressure test as depicted in Figure 38. The piece was subjected to a gas pressure of 1000 psig for 5 minutes with no leaks occurring.

The ability to bond (braze) the inconel-insulator material was of prime concern to the vendor. The accomplishment of this objective, to meet the required strength specification, resulted in a fuel cell component which is much more resistive to the corrosive environment of high pressure oxygen and KOH solution.

3.3.2 Electrochemical Components

3.3.2.1 Oxygen Electrodes. - Cell No. 4058-16 was assembled, using an Allis-Chalmers Type XIII oxygen electrode. This electrode is identical in construction to the "standard" Type VI, but contains 20 mg/cm^2 of platinum, as compared to 9 mg/cm^2 for all cells previously tested. The effect of the heavily loaded platinum oxygen electrode on initial performance as well as life cycle capability of the fuel cell was to be evaluated.

This cell had completed 50 cycles prior to shutdown on 5 April 1971. After approximately 5 weeks on standby, during which time a ceramic feedthrough and a Hypalon bellows were replaced, the cell cycle testing was resumed on 12 May 1971. During this initial charge cycle, a catastrophic failure of this cell occurred. An analysis of the printout tape, which monitors the cell data at 10 minute intervals, reveals the following information. Approximately 4 hours into the charge cycle, at a current rate of 5.28 amperes and a cell potential of 1.64 volts, the pressure of the cell was at 376 psig. The next printout reading (10 minutes) showed a total pressure drop of 268 psi to 108 psig and a pressure differential change from approximately 0.5 psi on the hydrogen side to approximately 1.5 psi on the oxygen side. The current and voltage values remained the same. This indicated a major internal leak with a recombination of the gases. The next data readout (20 minutes) indicated an additional loss of pressure from 108 psig to 76 psig; however, at this time, the cell potential dropped to 0.41 volt at the same current, indicating a direct short of the cell. No temperature excursions were observed during this short period of cell failure.

The cell was taken apart for an inspection analysis. The Hypalon bellows was badly charred with charred pieces laying in the bottom of the shell. The cell core had a burned hole through the matrix approximately 1 square inch in area. The location of the burn was at the upper ring of the core at about the 2 o'clock position of the cell orientation during test. The wraparound wires were burned through and the oxygen electrode at the burn area had formed molten pellets of metal which shorted to the hydrogen electrode. The retained matrix around the burn area was baked hard. It is concluded that a local thermal reaction caused drying of the matrix and a consequential internal leak. The charred bellows was a result of the thermal reaction of combination of the large volumes of gases in a relatively short time period.

The catastrophic failure of Cell No. 4058-16 ended the test to evaluate a high loaded platinum oxygen electrode. Comparative polarization scans of this cell and two other standard cells have been plotted in both the charge and discharge mode, and are shown in Figure 39. The voltage scale had to be expanded to recognize a difference in performance between these cells. The performance improvement of the cell using high platinum loaded oxygen electrodes is insufficient to justify using it at this time.

Two cells have been fabricated using platinum plated sintered nickel plaques as oxygen electrodes. Both of these cells utilized asbestos matrices in their construction. Cell No. IR&D-2 has an asbestos matrix approximately .043 inches thick, and Cell No. IR&D-3 has an asbestos matrix approximately .026 inches thick.

Cell No. IR&D-2 was put on cycle test to evaluate the sintered nickel plaque as an oxygen electrode. The cell was subjected to normal start up by evacuating and electrolyzing to ambient pressure three times, and then continuing the charge to full pressure of approximately 600 psig. However, during the initial charge, a small external volume was added to the hydrogen side as the pressure differential slowly built up on the hydrogen side. The rate of pressure differential build-up on the hydrogen side increased as the cell pressure increased. This was compensated for by adding increased external volumes on the hydrogen side of the cell. At approximately 300 psig cell pressure, an external volume of 2 cubic inches had been added to the hydrogen side. Continued charging of the cell demanded periodic bleeding of hydrogen gas to maintain a differential pressure less than 2 psi. In this manner, the cell was completely charged to 579 psig, the extreme of the pressure switch control.

The initial discharge cycle showed an average cell voltage of .752 volts during the 72 minute discharge cycle at 33.3 amps; however, a reversal of pressure differential to the oxygen side was immediately noted. During the 72 minute discharge cycle, it was necessary to bleed oxygen gas from the cell on five occasions to prevent the differential pressure from surpassing 2 psi.

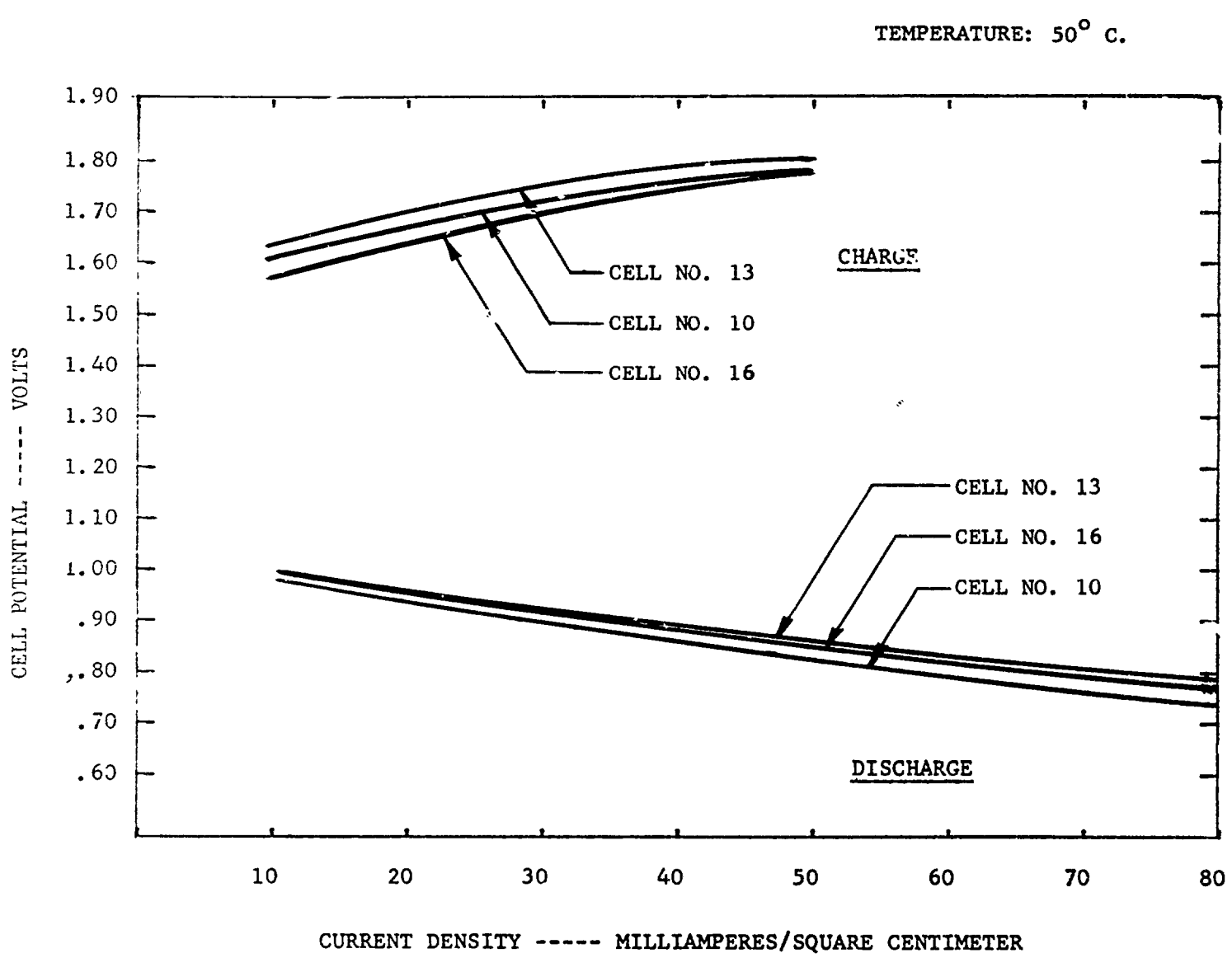

FIGURE 39. COMPARATIVE CELL POLARIZATION SCANS

Charge cycle #2 was a repeat of the initial charge, but to a much greater degree. The hydrogen gas had to be bled approximately every ten minutes through the 10 amp rate charge cycle. The discharge cycle #2 showed a drastic performance degradation, and again entailed the bleeding of oxygen from the cell to maintain a minimum pressure differential.

Although sintered nickel plaques have been used as oxygen electrodes in primary fuel cells, their use in regenerative fuel cells is prohibitive in that a conversion of the nickel to nickel oxide occurs in the cell, similarly to that of a Ni-Cad battery. On charge, the nickel is converted to some oxide of nickel rather than generated O_2 gas as such. On discharge, the oxide is reduced to some lower level of nickel oxide, rather than utilizing the O_2 gas which had been generated. This process of converting the nickel oxygen electrode into partially active material has a decided effect of reducing the electrode capability of functioning as a good fuel cell oxygen electrode. The effect of oxidation of the nickel may have inactivated the platinum catalyst, either by masking off the catalyst or possibly isolating the catalyst from the nickel substrate.

3.3.2.2 Electrical Connections. - An investigation into the high internal resistances which have been characteristic of the EOS regenerative fuel cell has revealed design shortcomings whereby high ohmic resistances have been built into the cell. Inconel 625 has an electrical resistivity approximately 10 times as great as nickel metal. In fact, the resistivity of a .020" thick inconel sheet is 30 percent greater than that of a .025" thick, 70 percent porous, sintered nickel plaque. In effect, the perforated inconel core in the EOS cell is three times more resistive than the sintered nickel plaque (hydrogen electrode) itself. Consequently, the nickel plaque is getting very little help from the core as far as current carrying capability, and results in a significant voltage loss.

The inconel cap of the inner core, which serves as a current collector to the hydrogen terminal, also shows significant voltage loss due to high resistivity.

The oxygen electrode is primarily dependent on a 50 mesh, .005" thick, wire nickel support screen to carry the accumulated electrical load to the terminal cap. This electrode has an electrical resistivity approximately 50 percent greater than that of the .025" thick sintered nickel plaque.

The calculated voltage losses due to ohmic resistance in the presently designed EOS regenerative cell and the projected losses with material and design modifications are as follows:

		Present	Proposed
(1)	Inconel cap current collector	20 mv	---
	Nickel cap current collector	---	4 mv
(2)	Inconel perforated core plus H_2 electrode	51 mv	---
	Nickel perforated core plus H_2 electrode	---	13 mv
(3)	Oxygen electrode	70 mv	---
	Oxygen electrode plus nickel screen current collector		25 mv
	Total Voltage Loss	141 mv	42 mv

Minimizing the ohmic resistance in the cell not only enhances cell performance in terms of power output, but will have a beneficial effect thermally. Less heat generation and thermal gradients will result in less gas pressure differentials and possibly affect moisture balance with greater life cycle expectancy.

Cell No. 4058-29 was fabricated as a low resistance cell. The modifications of this cell were solely to reduce ohmic resistance in the current carrying components of the cell. This was accomplished by making the following changes to the standard fabricated cell.

1. Nickel plate the perforated inconel support core to lower the resistance of the hydrogen electrode current collector.

2. Wrap the outer oxygen electrode with a 16 mesh .015" wire nickel screen to serve as an additional current collector to the oxygen electrode itself.

3. Substitute a nickel core cap for the inconel core cap to reduce resistance on the hydrogen electrode side of the cell.

4. Substitute 1/4" nickel feedthrough terminals for the 3/16" nickel terminals previously used. These tubes constituted a 50% increase in cross sectional area and consequently decreased resistivity.

The cell was fabricated into a boiler-plate cell configuration. However, prior to performance testing, this cell was subject to a leak check. This cell suffered damage as the rupture disc in the boiler-plate assembly failed at approximately 600 psig. This was the second cell in the same day that had failed due to a premature rupture diaphragm failure. Apparently, the diaphragms have deteriorated over a period of operating time in the KOH and high pressure environment. Consequently, all new rupture discs were substituted into all the test assemblies, with periodic replacements to be made after a set number of operating hours.

The extent of the damage to the inner core of this cell was limited to the weld of the bellows breaking loose and dislodging the bellows assembly from the bottom of the core. A new bellows was substituted and welded to the core and the cell was then operable. Considering the magnitude of this adverse accident to tear the weld apart, the edge seal of the matrix was not affected. This fact implies some great improvement in the new technique of edge sealing as described on page 86.

The repaired cell was placed on cycle test after again leak checking. The cell has operated for 120 cycles, to the end of contract, and is still in operating condition. The initial performance characteristics were better than any cell which had been made during this contract. The performance characteristics are illustrated in Figure 40 - Charge, Figure 41 - Discharge, and Figure 42 - Polar Scan. Also included is Figure 43, wherein cell degradation is plotted as a function of cycles.

A steady voltage degradation is noted as a function of cycles. The discharge of Cycle #33 shows a much different performance profile has developed, especially in the beginning of the discharge cycle. This indicates a substantial difference in moisture balance of the cell throughout this testing period. The performance changes indicate a drying action in the matrix of the sealed cell. Based on this assumption, Cell No. 4058-29 was allowed to discharge an additional 11 A.H using O_2 and H_2 from an external bottle supply. This would add to the cell assembly an equivalent 11 A.H. of water or approximately 3.6 grams. The results of this water addition are directly reflected in the very next discharge curve (Cycle 34), wherein definite performance improvement had occurred. Figure 43, wherein cell performance degradation is plotted, also reflects this step improvement.

3.3.2.3 Matrix and Electrolyte Loading. - During the course of the contract, a procedure modification was made in applying electrolyte to the matrix of the cell. The standard procedure had been to add a given weight of 30 percent KOH (function of matrix weight), by use of a squeeze bottle, into the center portion of the inner core. This allowed the electrolyte to be absorbed through the hydrogen electrode into the matrix by the wicking ability of the matrix.

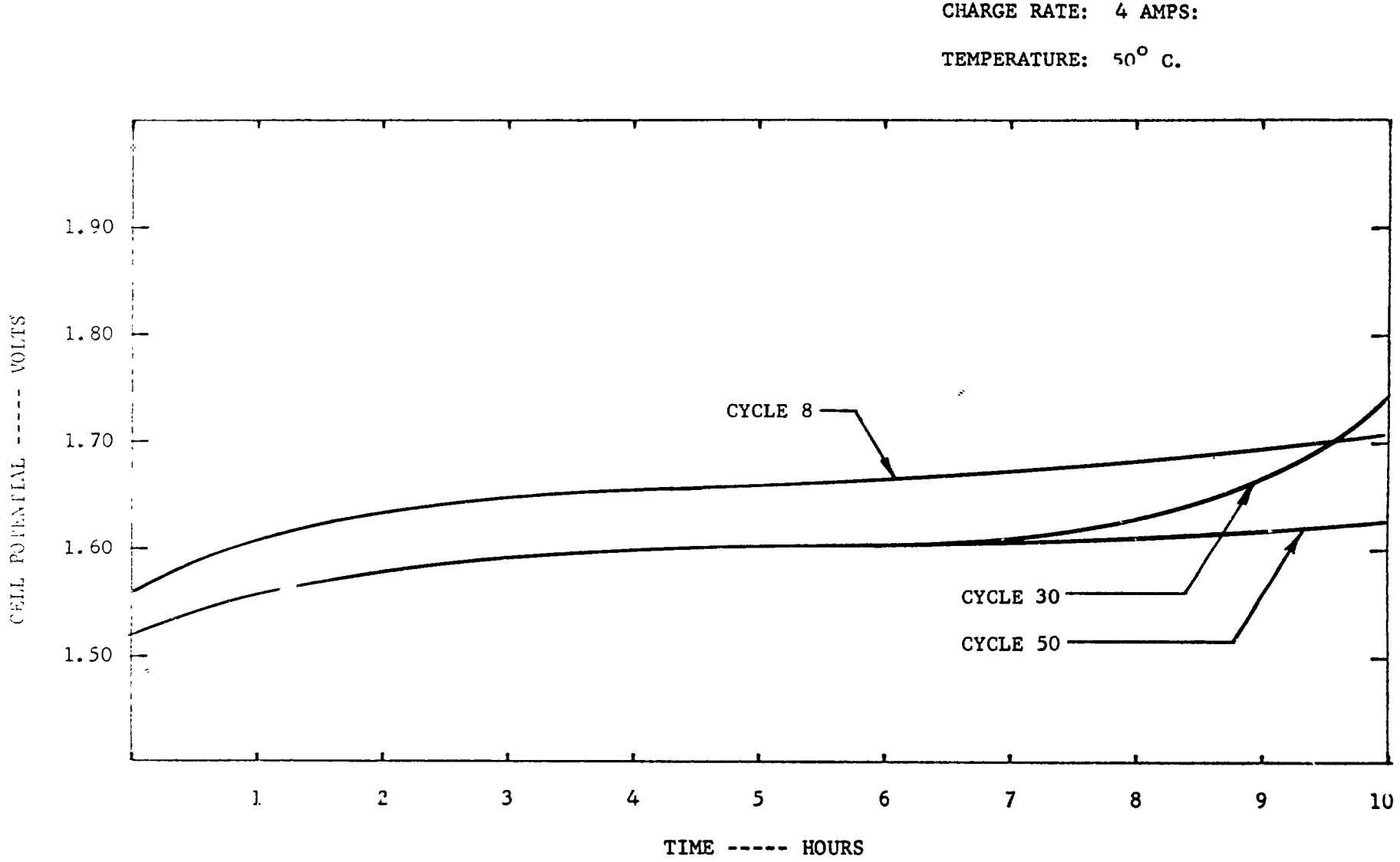

FIGURE 40. CELL NO. 4058-29 CHARGE PERFORMANCE

DISCHARGE RATE: 33.3 AMPS:

TEMPERATURE: 50° C.

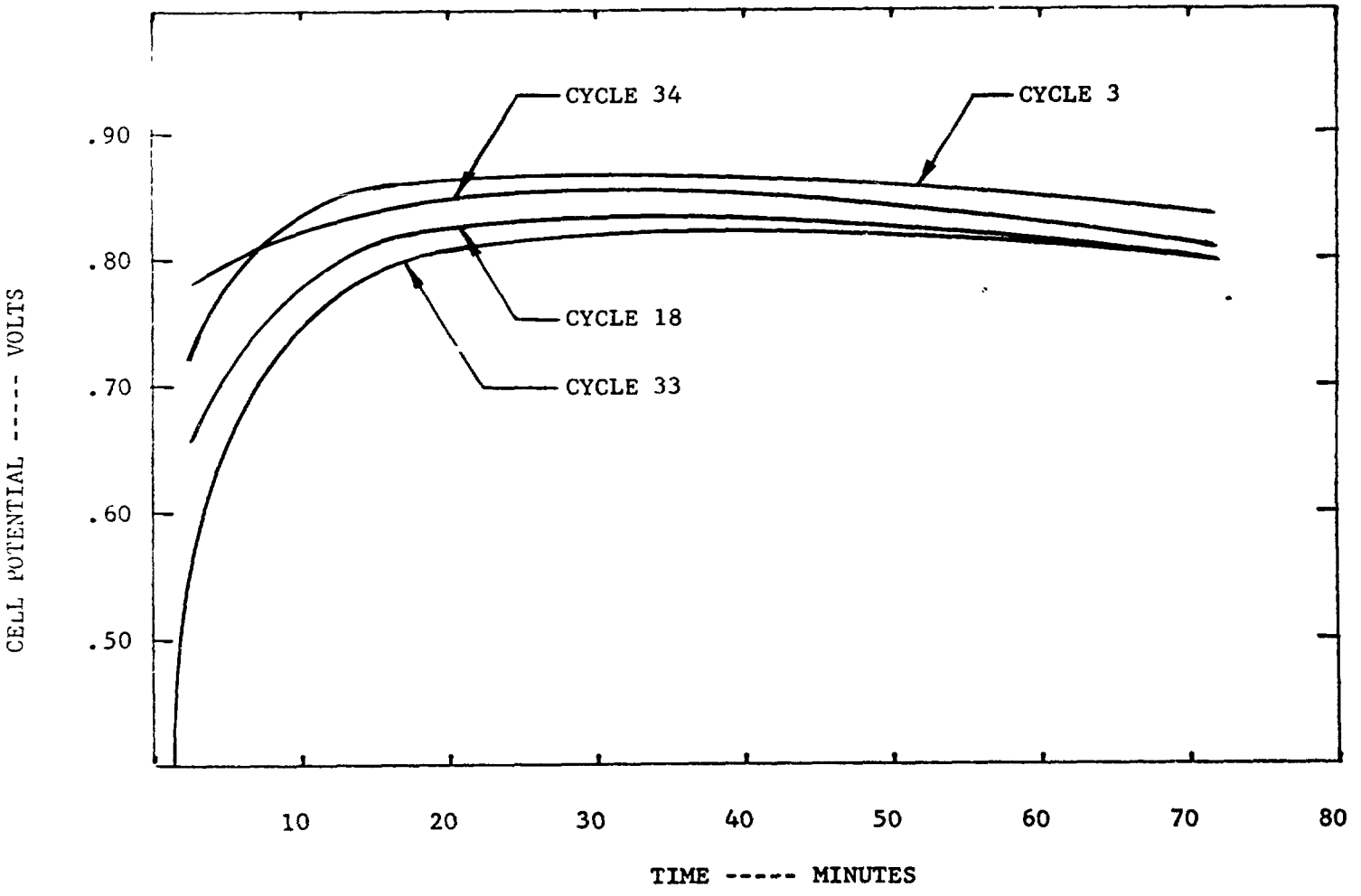

FIGURE 41. CELL NO. 4058-29 DISCHARGE PERFORMANCE

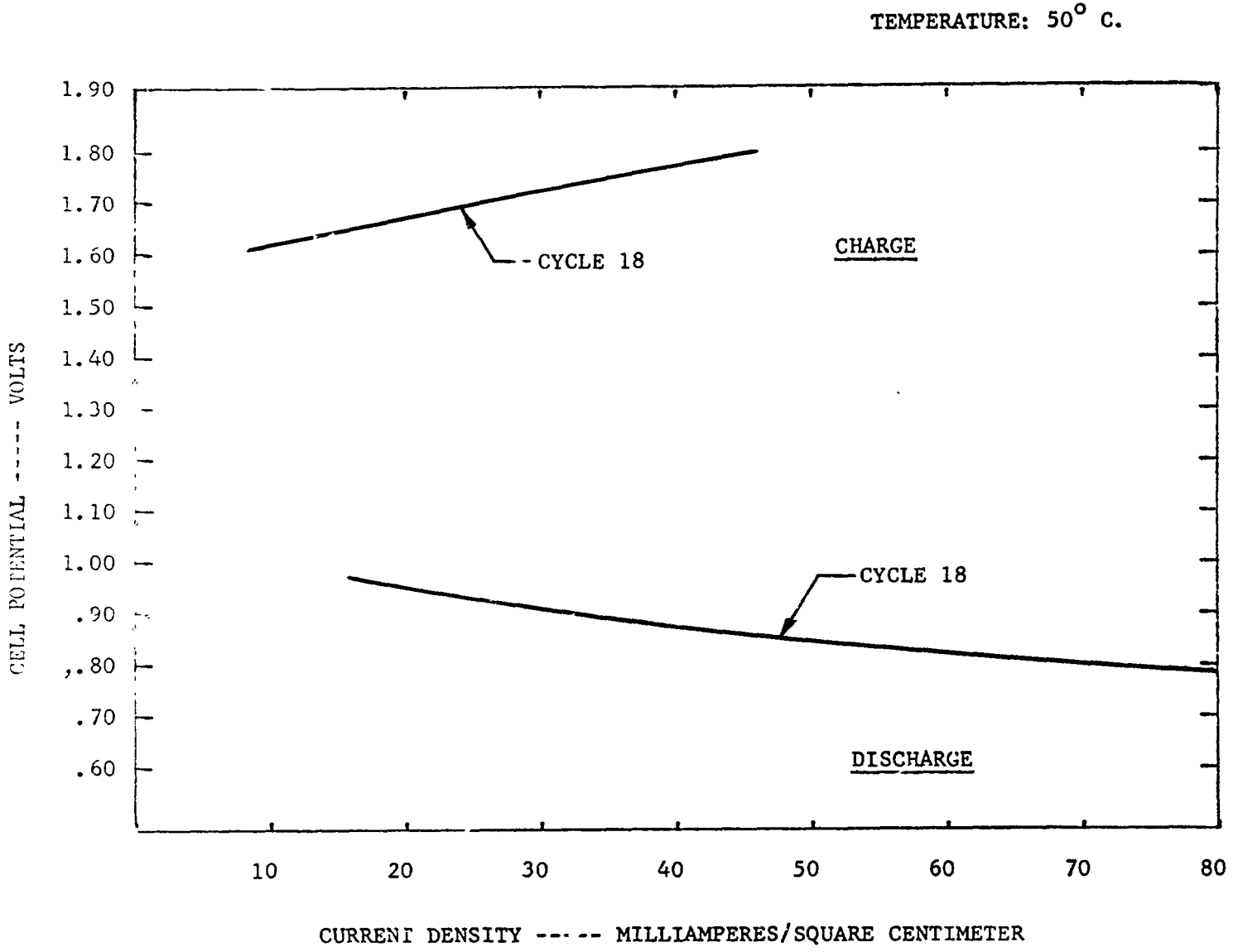

FIGURE 42. CELL NO. 4058-29 POLARIZATION SCANS

DISCHARGE RATE: 33.3 AMPS.

TEMPERATURE: 50°C

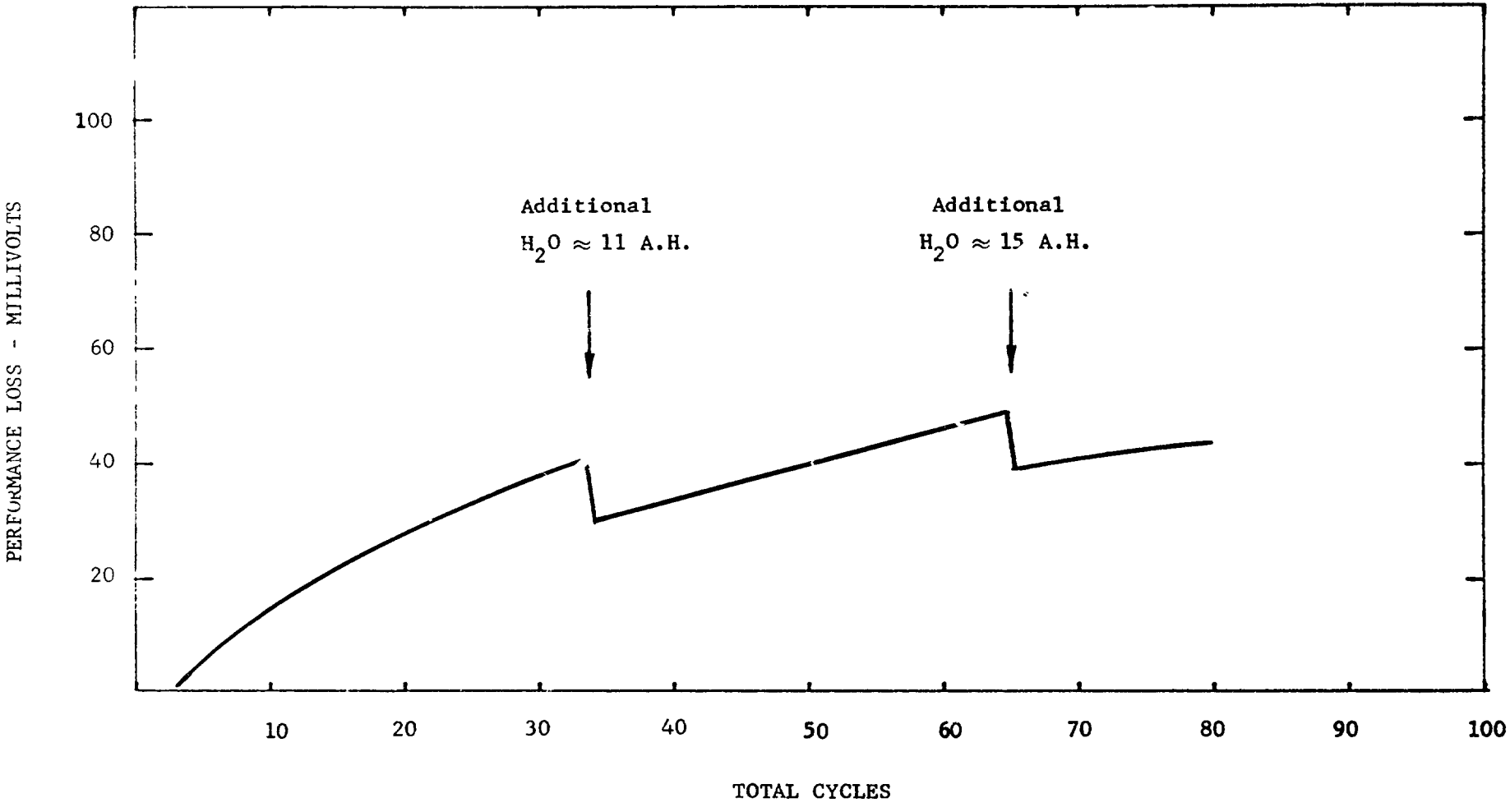

FIGURE 43. CELL NO. 4058-29 PERFORMANCE DEGRADATION

It is now standard practice in cell fabrication to vacuum load KOH solution into the cell matrix after final cell assembly. This method is to assure uniform wetting of the matrix with electrolyte, which has proved statistically to minimize cross leaks through the matrix. The result of this method of electrolyte loading is a saturated condition of KOH solution in the electrode-matrix assembly and requires a cell conditioning operation, whereby moisture is removed by venting gases during electrolysis to attain a proper electrolyte balance for optimum cell performance.

3.3.2.4 Temperature Measurements. It was deemed necessary that an effort be made to verify the assumptions concerning internal thermal conditions used in the cell design calculations. This task entailed monitoring the temperature of the innermost working components of an operating cell in both the charge and discharge modes.

Cell No. IR&D-3 had been fabricated with a platinum plated sintered nickel oxygen electrode, to evaluate the nickel plaque as an oxygen electrode. The test results of a cell of similar construction, No. IR&D-2 discussed in Section 3.3.2.1 of this report, demonstrate the prohibitiveness of using a sintered nickel plaque as the oxygen electrode in a regenerative fuel cell. Consequently, this cell was used on test with provisions to monitor temperature measurements at several locations on the core. Four thermocouples were introduced into the cell in the following positions.

TC-1 - Approximately 1.0" from the top of the core assembly, and mounted on the insde of the core directly to the perforated inconel core support (hydrogen electrode).

TC-2 - Approximately 1.0" from the bottom of the core assembly, and mounted on the inside of the core assembly directly to the perforated inconel core support (hydrogen electrode).

TC-3 - Approximately 2.0" from the top of the core assembly, and mounted on the outside of the core assembly directly in contact with the oxygen electrode.

TC-4 - Approximately 2.0" from the bottom of the core assembly, and mounted on the outside of the core assembly directly in contact with the oxygen electrode.

After fabrication of the cell and the application of thermocouples to the cell, it was put on test in the charge mode. Because of the thermocouple penetrations into the cell, complete sealing of the cells was not undertaken and the cells were operated at ambient pressure conditions, venting the generated gas during charge and supplying gases from an external source during discharge.

The temperature profile of the cell during initial charge at the 4.0 amp rate is illustrated in Figure 44. The cell seems to be sufficiently wet to operate quite efficiently as indicated by the cell voltages during

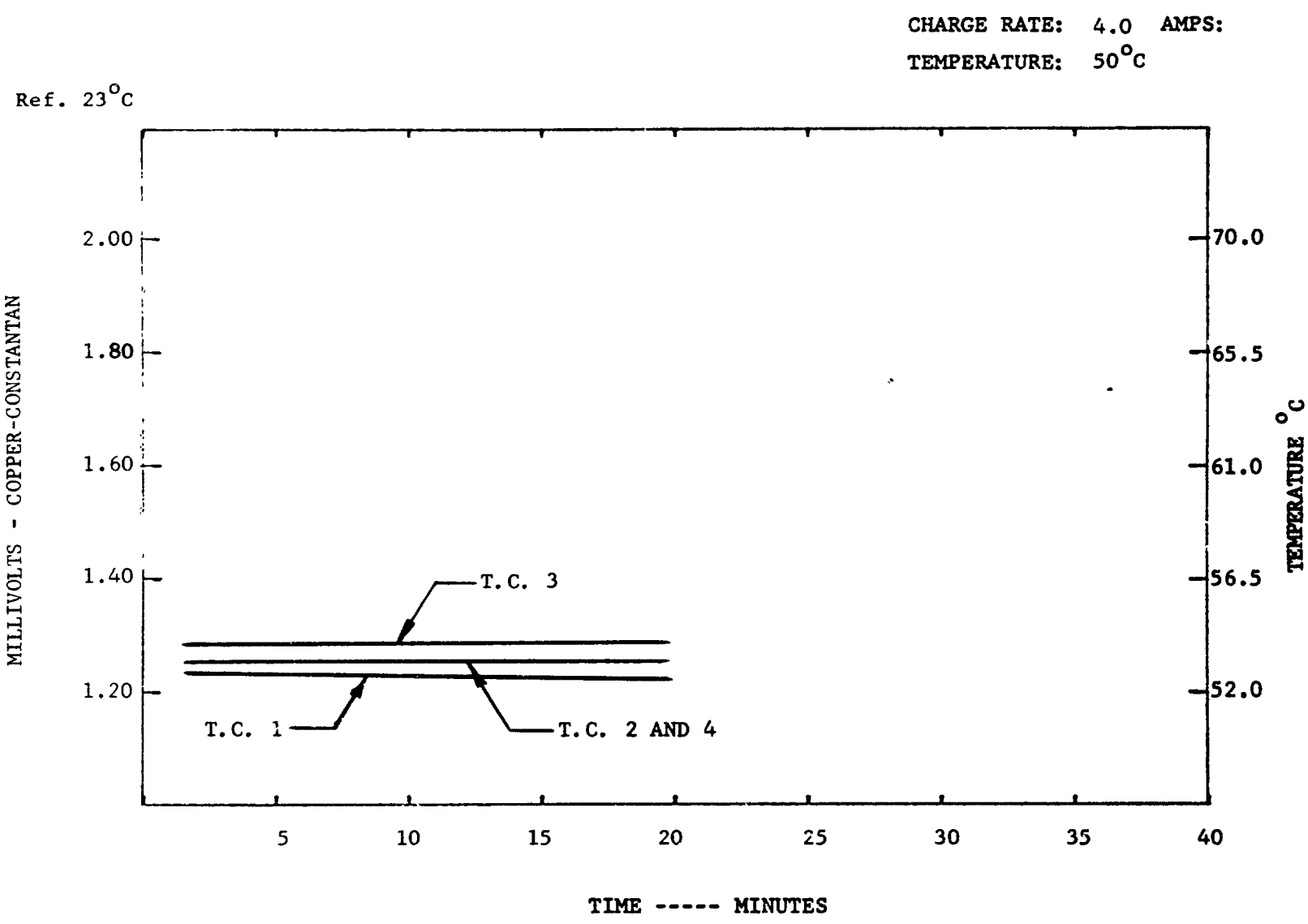

FIGURE 44. CELL NO. IR&D 3 TEMPERATURE PROFILE DURING CHARGE

this electrolysis mode. No temperature fluctuations were noted through this charge cycle. Two additional charge cycles of 30 minutes duration each were made at the 8.0 amp rate (average voltage $\approx$ 1.521 VDC) and at the 12.0 amp rate (average voltage $\approx$ 1.566 VDC). The temperature curves for these two cycles duplicate those at the 4.0 amp rate with a slight displacement of the curves ($\approx 1.0^{o}$ - 1.5^{o}C) for each of the increased increments of charging rate. No apparent deviation of temperature was noted through the charging cycles.

The cell was then allowed to function in the fuel cell mode by introducing the hydrogen and oxygen from an external supply. The cell initially performed very poorly in this mode, but continuous conditioning of the cell by cycling for short periods of time improved the cell to be able to plot the temperature profile of the cell at a discharge rate of 20.0 amps at a voltage efficiency that the cell would normally operate. These temperatures are plotted in Figure 45. These temperatures are at a discharge rate of 20.0 amps, wherein actual operation the cell will be delivering 33.3 amps.

The temperature profile of TC-3 shows the greatest rise during the discharge cycle. This position is the top of the oxygen electrode where the accumulated current approaches the maximum value. The oxygen electrode, with no current carrying support, is more resistive than the sintered nickel plaque (hydrogen electrode). Both electrodes need additional support to carry the current to prevent the resultant temperature gradients. At 33.3 amps discharge, the temperature gradients will be much more severe and no doubt affect moisture balance in the cell.

3.4 DELIVERABLE SINGLE CELLS

Two complete "boiler-plate" prototype fuel cells were fabricated, acceptance tested, and delivered to WPAFB, Aero Propulsion Laboratory in Dayton, Ohio. The cell core assembly consisted of the following components:

1. 2.00" OD x 13.0" x .020" cylindrical perforated inconel support core.
2. 6.25" x 11.5" x .025" sintered nickel hydrogen electrode plated with 20 milligrams platinum/sq. cm. A new plating technique has been used to assure a more uniform catalyst distribution throughout the nickel plaque.
3. .060" thick EOS potassium titanate matrix.
4. 6.50" x 11.5" x .010" Allis Chalmers Type VI wetproofed electrode 10 milligrams platinum/sq. cm.
5. .020" inconel wrapping wire - 14 turns to the inch at a drag pressure of six pounds.

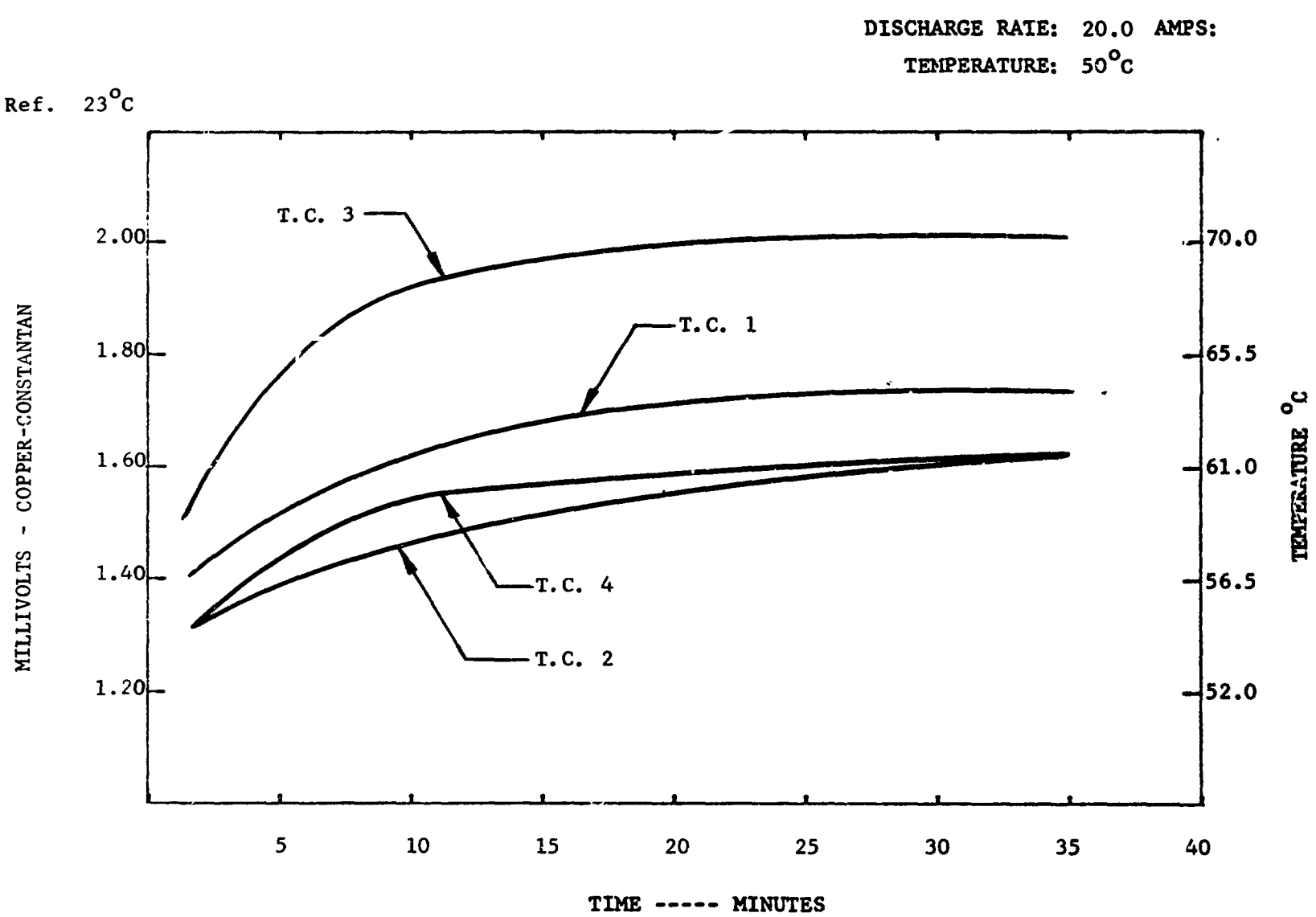

FIGURE 45. CELL NO. IR&D 3 TEMPERATURE PROFILE DURING DISCHARGE

6. Welded inconel bellows welded to the bottom of the support core.

7. 30 percent potassium hydroxide solution vacuum loaded into the matrix - approximately 142 grams.

The boiler-plate cell units were equipped with Dynascience Model P7D Differential Pressure Transducers and were supplied with Model CD10 Carrier Demodulators. The cells also included total pressure transducers connected to the oxygen side, pressure switches set at approximately 650 psig, and replaceable disc burst diaphragm assemblies rated at 1400 psig. The hydrogen and oxygen connections were equipped with valves. See Figure 46.

The cells were leak tested and subjected to acceptance testing with the following start-up procedure. The cells were evacuated to approximately 27 in. Hg and pressurized to ambient conditions by electrolysis of the cell. This function was performed three times to assure removal of all inert gases and to establish a mass balance of hydrogen and oxygen gas in the pressure vessel. After three evacuations, the cells were allowed to charge to approximately 600 psig, followed by a 33.3 amp discharge rate for 72 minutes. The temperature of the cell was maintained at 50°C throughout the test program.

The cells delivered to WPAFB were identified as Cells No. 4058-22 and No. 4058-27. Curves depicting the performance characterisitcs of the cells during acceptance testing are included as Figures 47, 48, 49, and 50.

The effort to fabricate and test two cells to be delivered to WPAFB resulted in numerous cell failures. The series of failures of cells, whereby 7 cells were fabricated to effectively produce 2 acceptable cells, had been costly in terms of schedule and materials. The failure mode in practically all cases was a matrix edge seal leak and reemphasized a major problem area.

A modification in the wire winding of the core assembly was made to help alleviate this situation. Previously, the core assembly had been wound with a single strand of wire with a 6 pound drag on the wire. The winding started on the rubber seal gasket and continued along the core assembly and terminated on the rubber seal gasket at the other end. Cell No. 4058-27 was wound similarly to the above method, but did not include the rubber seals. The continuous wire winding was used only as a means of forming an intimate contact between the electrodes and the matrix. The rubber seals themselves were each wound with 5 individual wire loops and twisted to enhance a much greater force on the rubber seal than the mere 6 pounds drag in the single continuous winding process. Using 5 individual loops, rather than a continuous 5 loop winding on the rubber seals, adds redundancy for greater seal integrity. A test sample, using a single twisted wire loop on a rubber seal mounted on an inconel core, showed no leak at a pressure differential of approximately 15 psid.

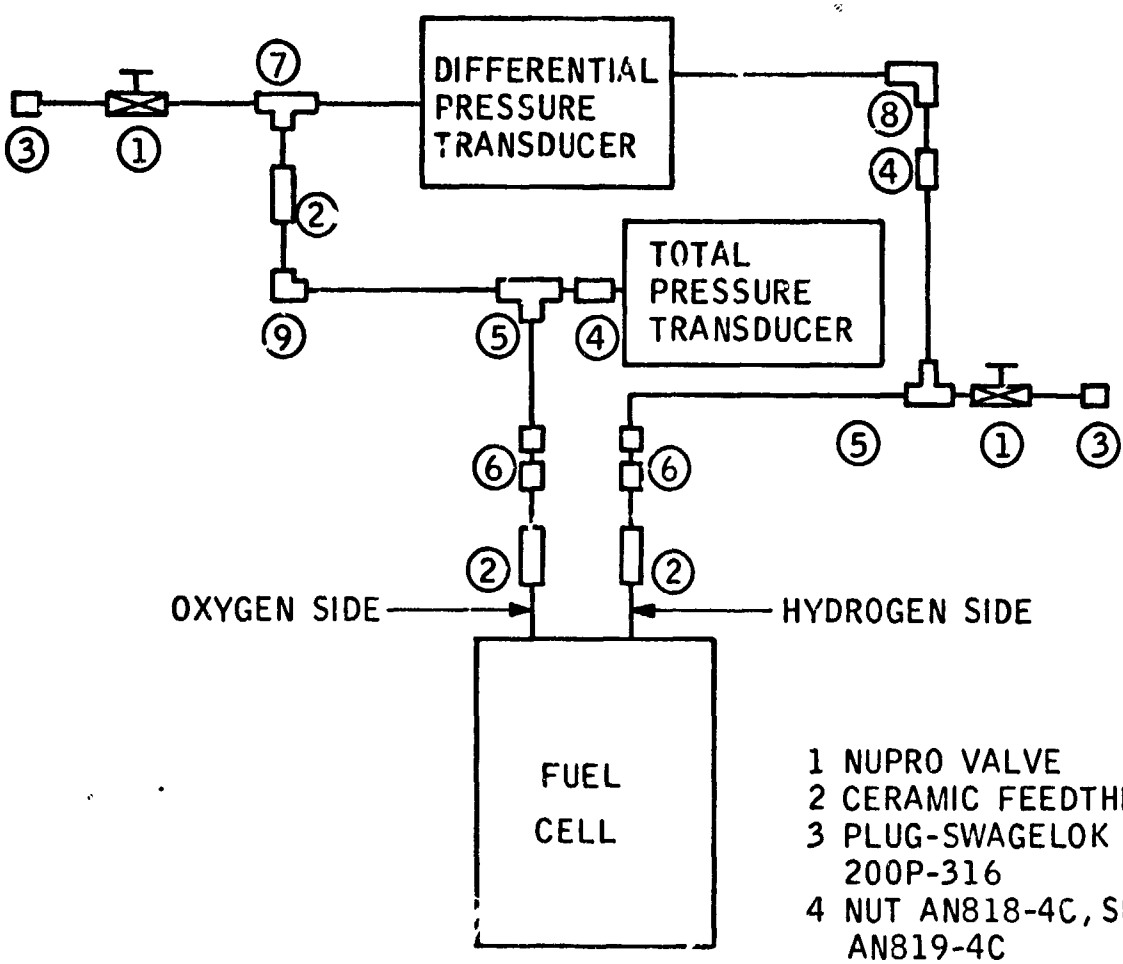

41714

FIGURE 46. EXTERNAL PLUMBING - BOILERPLATE FUEL CELL

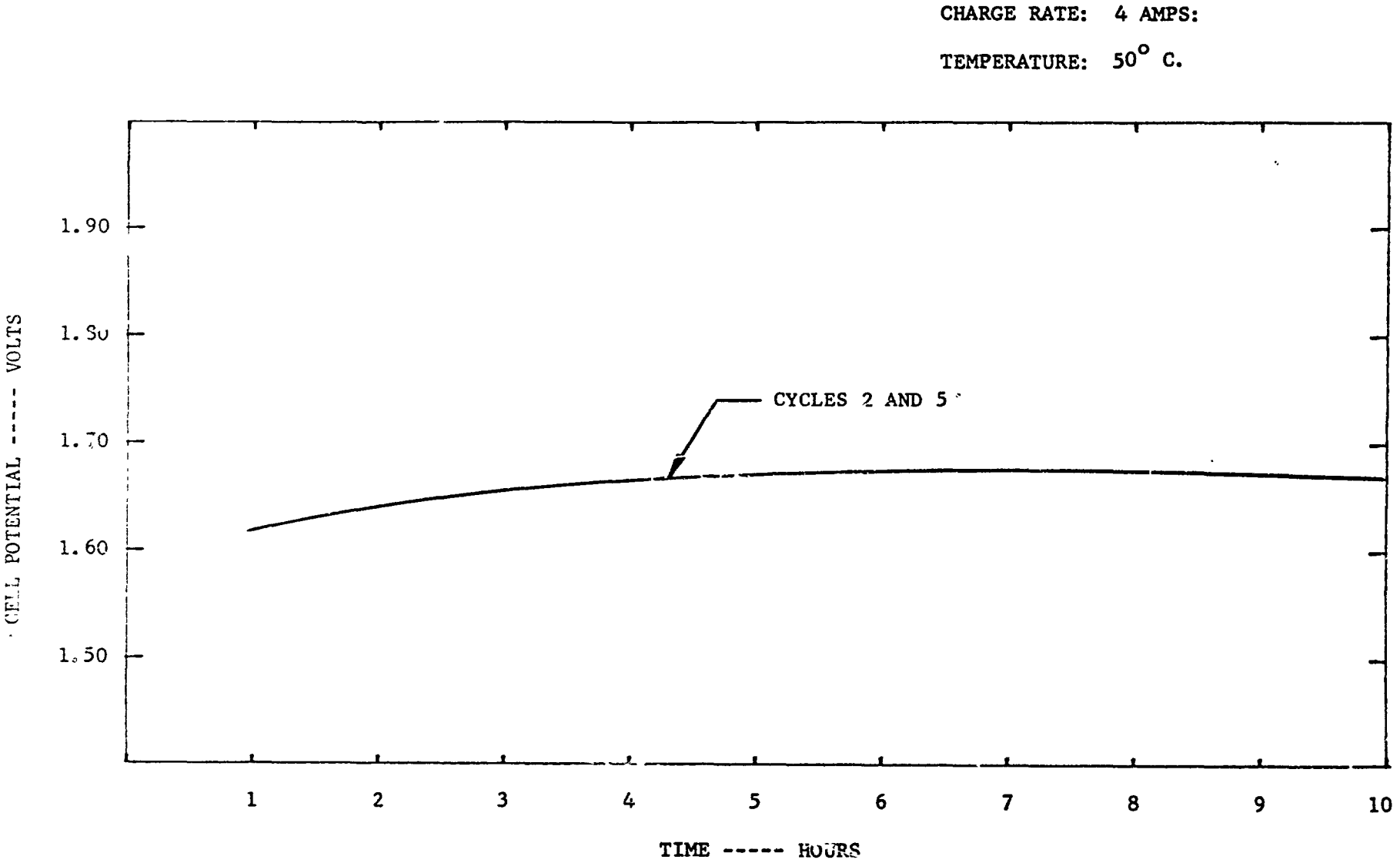

FIGURE 47. CELL NO. 4058-22 CHARGE PERFORMANCE

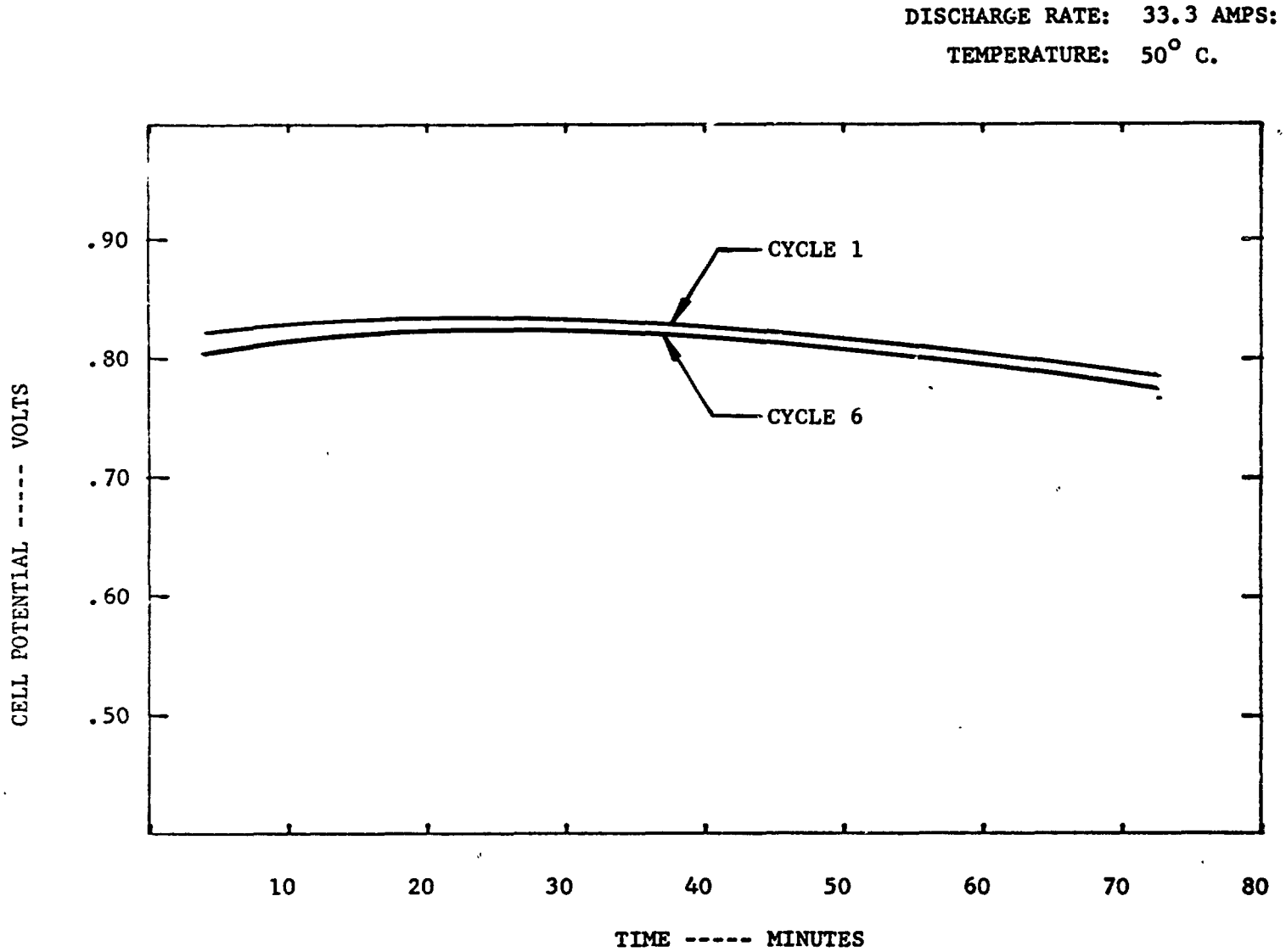

FIGURE 48. CELL NO. 4058-22 DISCHARGE PERFORMANCE

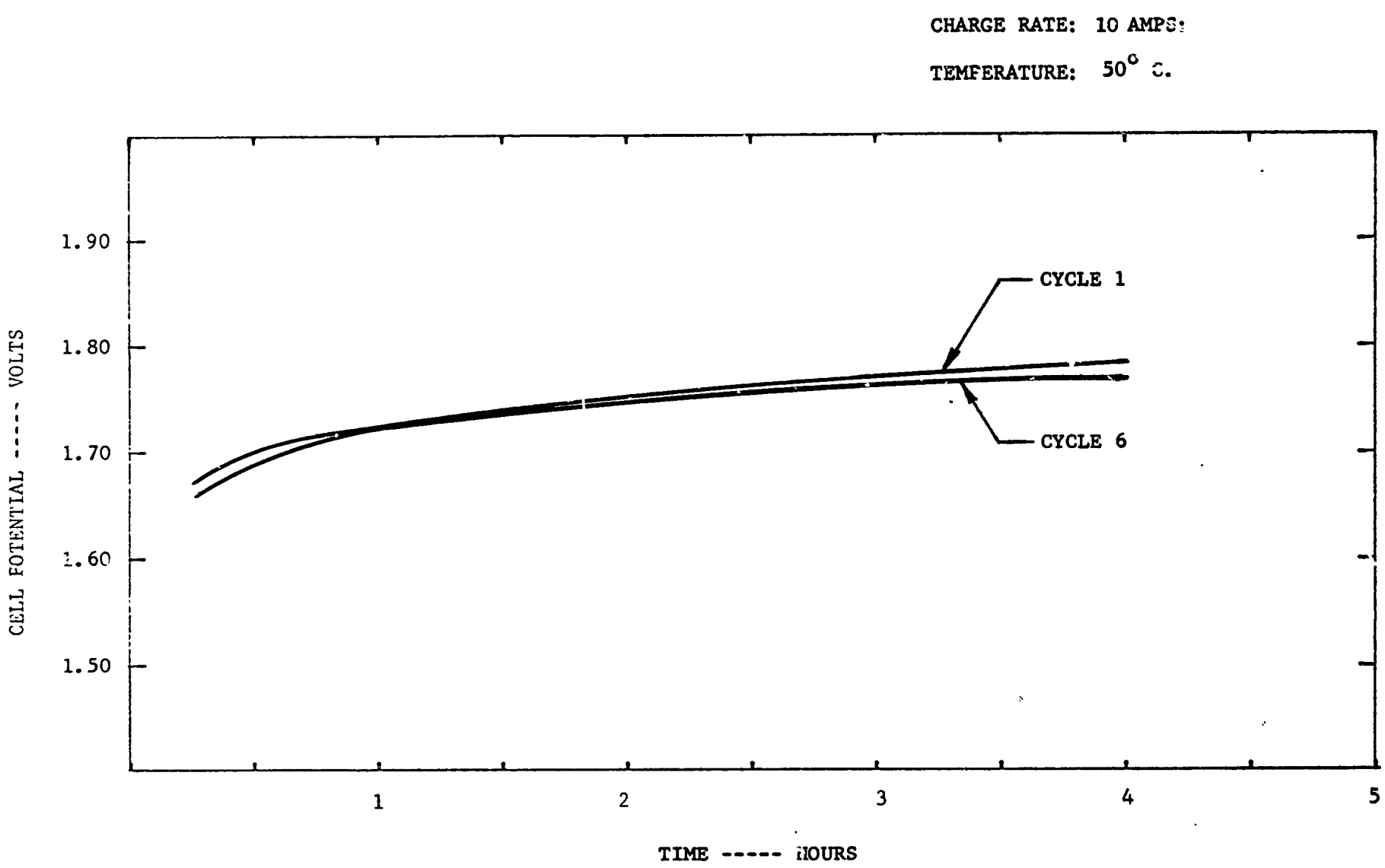

FIGURE 49. CELL NO. 4058-27 CHARGE PERFORMANCE

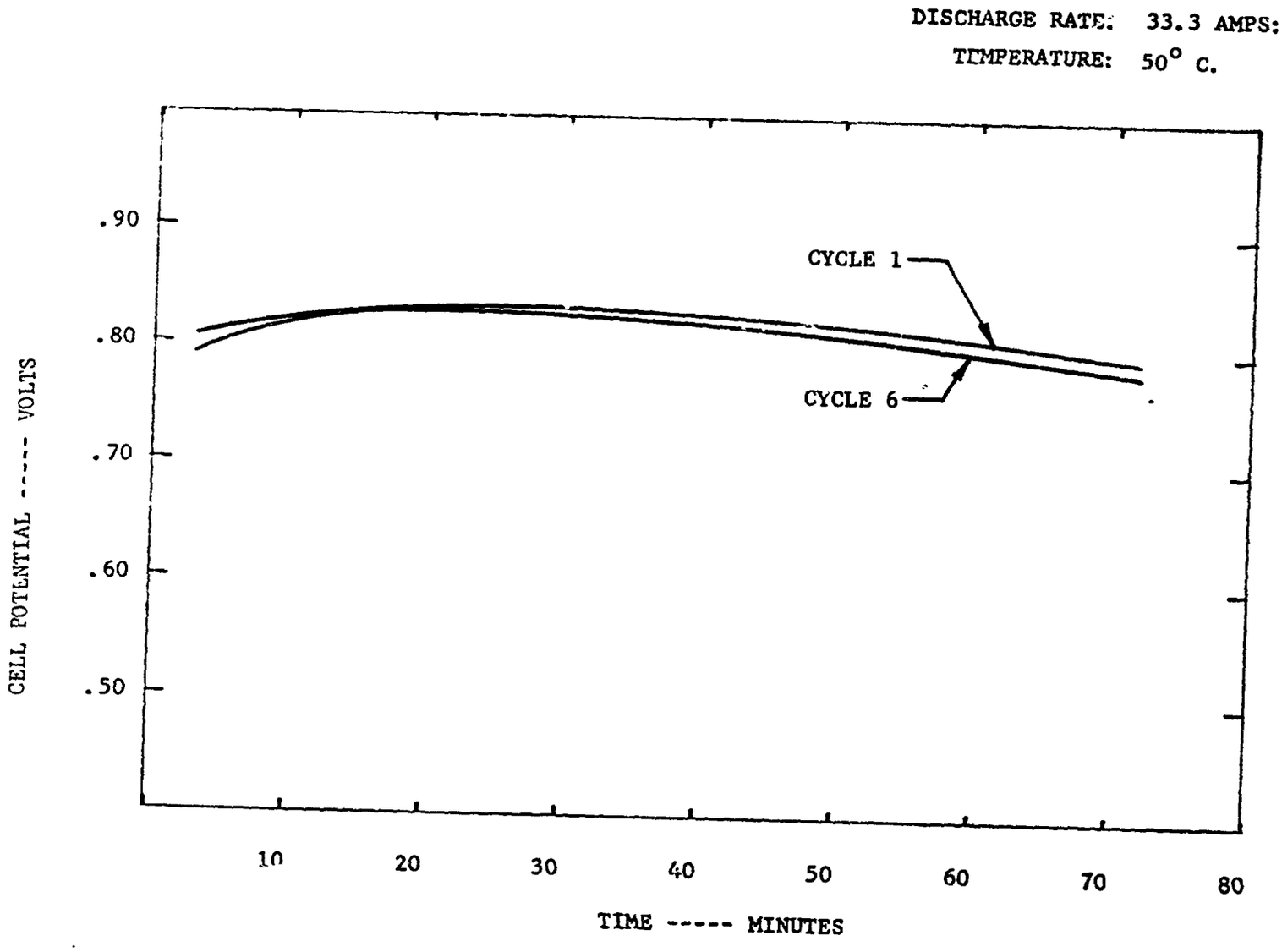

FIGURE 50. CELL NO. 4058-27 DISCHARGE PERFORMANCE

SECTION IV

LIGHTWEIGHT CELLS

4.1 CELL DESIGN AND ANALYSIS

The properties of the materials, which were selected for use in the fuel cell, have essentially been verified as to their compatibility in the chemical as well as the static and dynamic environments to which they are subjected. Total optimization of the cell materials and design configuration has not been attained during this contract effort; however, single cell analysis has been undertaken to generate recommendations for eventual cell optimization.

4.1.1 Stress and Dynamic Analysis

A random vibration analysis was performed to verify the lightweight regenerative fuel cell design. The report of this analysis is included herein as Appendix III.

4.1.2 Thermodynamic Analysis

A thermodynamic analysis program has been developed to calculate the oxygen and hydrogen fuel cell pressure as a function of time. The various parameters controlling pressure such as mass, volume, charge and discharge rates, bellows stiffness, and ambient temperature can be varied within the program to determine the effect on fuel cell performance, and to define optimum fuel cell configurations.

Appendix IV describes the thermodynamic analysis, and includes a flow diagram depicting the analysis procedure, temperature expression, various plots of gas pressures throughout the discharge cycle, and a computer printout representative of a fuel cell discharge cycle at 30.3 amps for 1.2 hours, followed by a charge cycle at 2.0 amps for 22.8 hours and a 24 hour dwell time after charge. The program computes the oxygen and hydrogen temperatures and pressures as a function of time with a given set of input parameters.

SECTION V

FABRICATION AND TESTING OF LIGHTWEIGHT CELLS

5.1 PROTOTYPE FABRICATION AND CHECKOUT

Two lightweight fuel cells have been fabricated using standard components for the cell core assembly, but incorporating a modified matrix end seal technique, and incorporating the welded metal bellows and the Ceramaseal short profile insulated feedthroughs with 1/4" nickel tube feedthrough terminals. These cells have been leak checked and identified as Cells No. 4058-31 and 4058-32. Both cells were constructed of used oxygen electrodes, which were sufficiently good to verify the survivability of the fuel cells when subjected to the environmental tests.

5.1.1 Vibration Test

Cell No. 4058-31 was subjected to six cycles of operation which constituted the preliminary performance test prior to random vibration of the cell. The cell was depressurized to ambient conditions, sealed, and mounted in a double clamping fixture. The cell was vibrated per the specified random vibration spectrum for 5 minutes in each of the three axis. A post vibration analysis of the cell showed no apparent damage to the external components of the cell.

After vibration, the cell was again put on test to compare performance characteristics before and after vibration. The cell was charged to full pressure of 595 psig. The pressure buildup during the charge at 10 amps was very uniform (18 psi/10 minutes) and the pressure differential was maintained at less than 1.0 psid during the entire cycle. The cell was then put into the discharge mode; two minutes into the discharge cycle, the following parametric measurements were monitored.

.622 volts
35.6 amps
590 psig
0.05 psid (O_2 side)
49°C oven temperature
49°C cell temperature

Immediately following the 2 minute reading, this cell failed with an internal explosion. A visual examination of the cell revealed a hole burned through the outer shell approximately 1/2" from the bottom end of the core (bellows end) and on the bottom side of the cylinder in its particular horizontal orientation. The inner core revealed a badly charred bottom rubber edge seal, with part of the oxygen electrode edge melted

away, and 4 of the individual wire wraps on the rubber seal either broken or burned. The metal bellows appeared normal and showed no effect of a large pressure differential which usually accompanies an explosion of this type. The lower teflon core support ring showed some melting effect on the side of the edge seal, but generally was intact.

Although the pressure differential just prior to the failure was quite small, the failure appears to be due to an edge seal leak. A possible explanation of the cause of failure could be the loss of edge seal during the vibration mode, whereby the individually wrapped wires may have broken. Of the 5 wires which were wrapped around the rubber edge seal, only 1 wire was intact. Three of the wires were broken at the twist, (point of stress) which could indicate breakage during vibration. The fourth wire was badly burned (half of it melted away), which may or may not have been broken at the time of combustion.

The performance characteristics of this cell is illustrated in Figure 51. The overall performance of this cell was below normal, and has been attributed to the "used" electrodes.

5.1.2 Temperature Test

Cell No. 4058-32, the second prototype lightweight cell, was also subjected to 6 cycles of operation to establish the preliminary performance characteristics prior to thermal and vacuum testing of the cell.

The cell was installed in a thermal chamber and thermally cycled twice between -20°F and 100°F, with a 12 to 24 hour storage duration at each extreme. The cell was nonoperational during this thermal storage period, but was subject to cycle test immediately following the thermal soak. The discharge performance curves before and after thermal cycling are depicted in Figure 52. A small degradation of performance is noted after thermal cycling, but this may be attributed to the handling of the cell in removing it from the test station, setting it up in the thermal chamber, removing the cell from the thermal chamber, and again setting the cell up in the test station. Approximately seven days elapsed between running the pre-environmental and post environmental functional tests.

5.1.3 Vacuum Test

After successfully completing the thermal test, Cell No. 4058-32 was installed in a vacuum chamber to be operated for one complete cycle at an environmental pressure of 1×10^{-5} mm Hg. or lower.

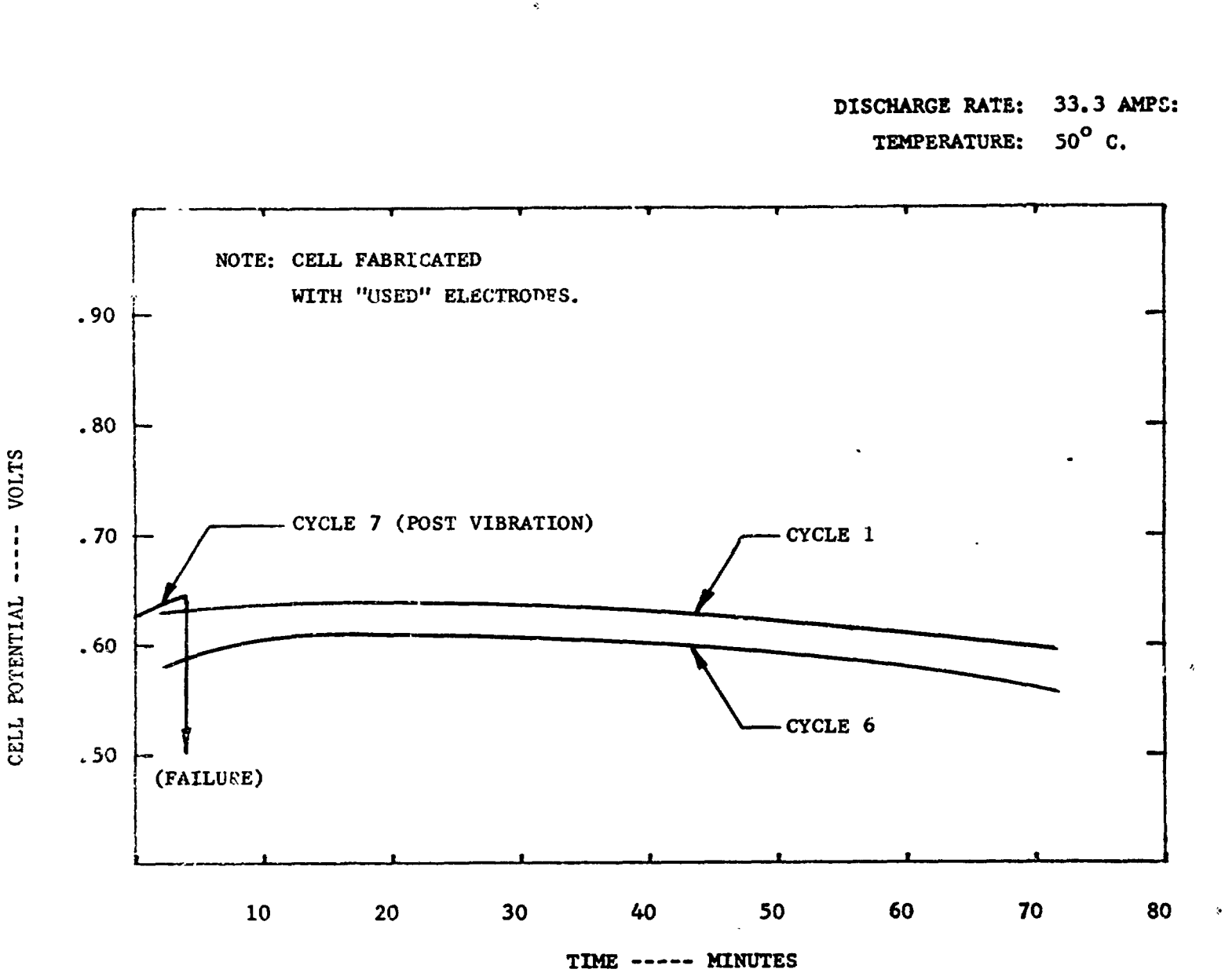

FIGURE 51. CELL NO. 4058-31 DISCHARGE PERFORMANCE

The cell was wrapped with heater tape to maintain a 50°C environmental temperature. The cell was then mounted in the vacuum chamber and provided with connector penetrations for current leads, voltage leads, heater leads, pressure switch leads, and thermocouples. A portable load bank was provided to discharge the cell, a power supply to charge the cell at a controlled rate, and a digital voltmeter to monitor cell voltage.

The chamber was evacuated to 1×10^{-5} mm Hg. pressure and the cell charging cycle began at a 5 amp rate. After approximately 8 hours of charge, the activation of the pressure switch on the cell opened the circuit to indicate full charge. The temperature during the charge mode was maintained at 123°F (50°C). The potential of the cell rose from 1.617 VDC to 1.686 VDC at the 5.0 amp rate. The discharge performance of the cell is demonstrated in Figure 52, Cycle #8, which compares the post vacuum test to that of the pre-environmental tests. A greater than normal increase in cell temperature during discharge was noted due to the heater tape which blanketed the cell (insulation) and was a constant source of heat to the cell.

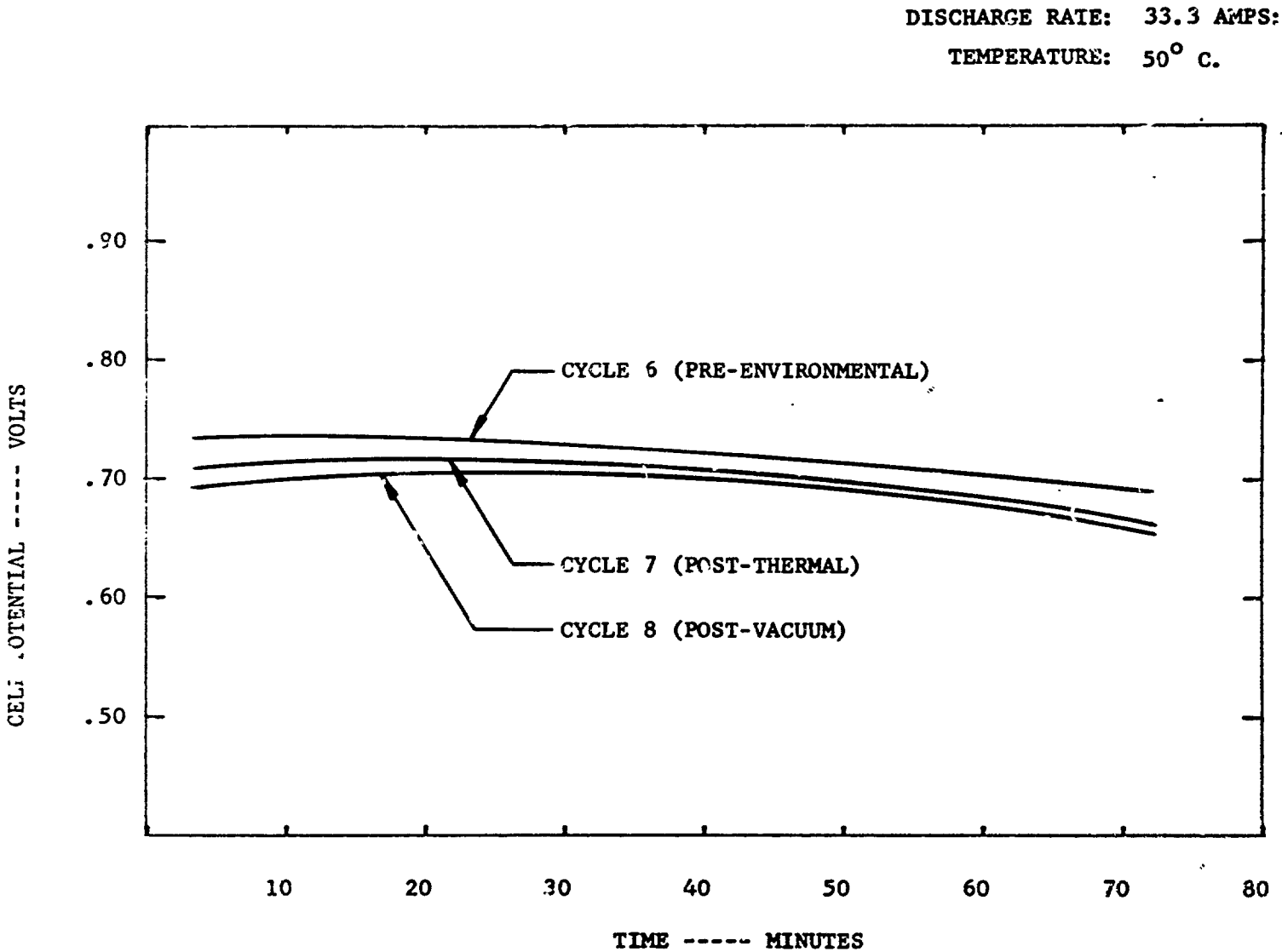

FIGURE 52. CELL NO. 4058-32 DISCHARGE PERFORMANCE

SECTION VI

BREADBOARD REGENERATIVE FUEL CELL ENERGY STORAGE SYSTEM

6.1 DESIGN AND FABRICATION

A complete breadboard regenerative fuel cell energy storage system has been designed, based on the data and information generated during this contract effort. The breadboard is a 133 watt hour system and consists of 4 cylindrical fuel cells mounted in a lightweight clamping frame. The cells are electrically connected in series to deliver 33.3 amperes for a 72 minute duration at a potential of 3.2 volts (0.8 volt per cell). The breadboard includes pressure transducers on each of the cells to indicate state-of-charge, a pressure switch on one of the cells to control full charge condition of the system, and interconnections between the individual cells.

The voltage requirement of fuel cells in the charge mode is approximately twice as great as the voltage of cells delivering power. It is recognized that switchgear is required in the system to select series or parallel connections of groups of cells to stay within the required voltage range of an energy storage system. Switchgear components have not been included in the present breadboard; however, a schematic drawing of a typical switching arrangement is shown in Figure 53.

Six fuel cells were fabricated in the lightweight configuration and individually functionally tested to select four cells to be used in the breadboard energy storage system. Figure 54 is a picture of the E.O.S.-40 AH cylindrical regenerative fuel cell. No attempt was made to weight optimize these cells; but rather, the cells were fabricated with overemphasis of quality control and incorporating better edge seal techniques to assure greater cell integrity. In processing the core assemblies, the heart of the fuel cell, slight deviations of matrix thickness resulted, primarily due to the method used for this application. Any deviation of matrix thickness from the design dimension results in an imbalance in hydrogen and oxygen gas storage volumes, with a consequent excessive pressure differential buildup during the charge mode. To compensate for the deviations in matrix thicknesses, each core assembly was carefully measured and fitted into an outer pressure shell dimensionally designed to maintain proper gas volume balance. As a result, the outer length dimension of each of the four cells in the breadboard system do vary. However, no external volumes were required for any of these cells, and no greater pressure differential than 2.5 psi developed in these cells when charged from zero to approximately 600 psig.

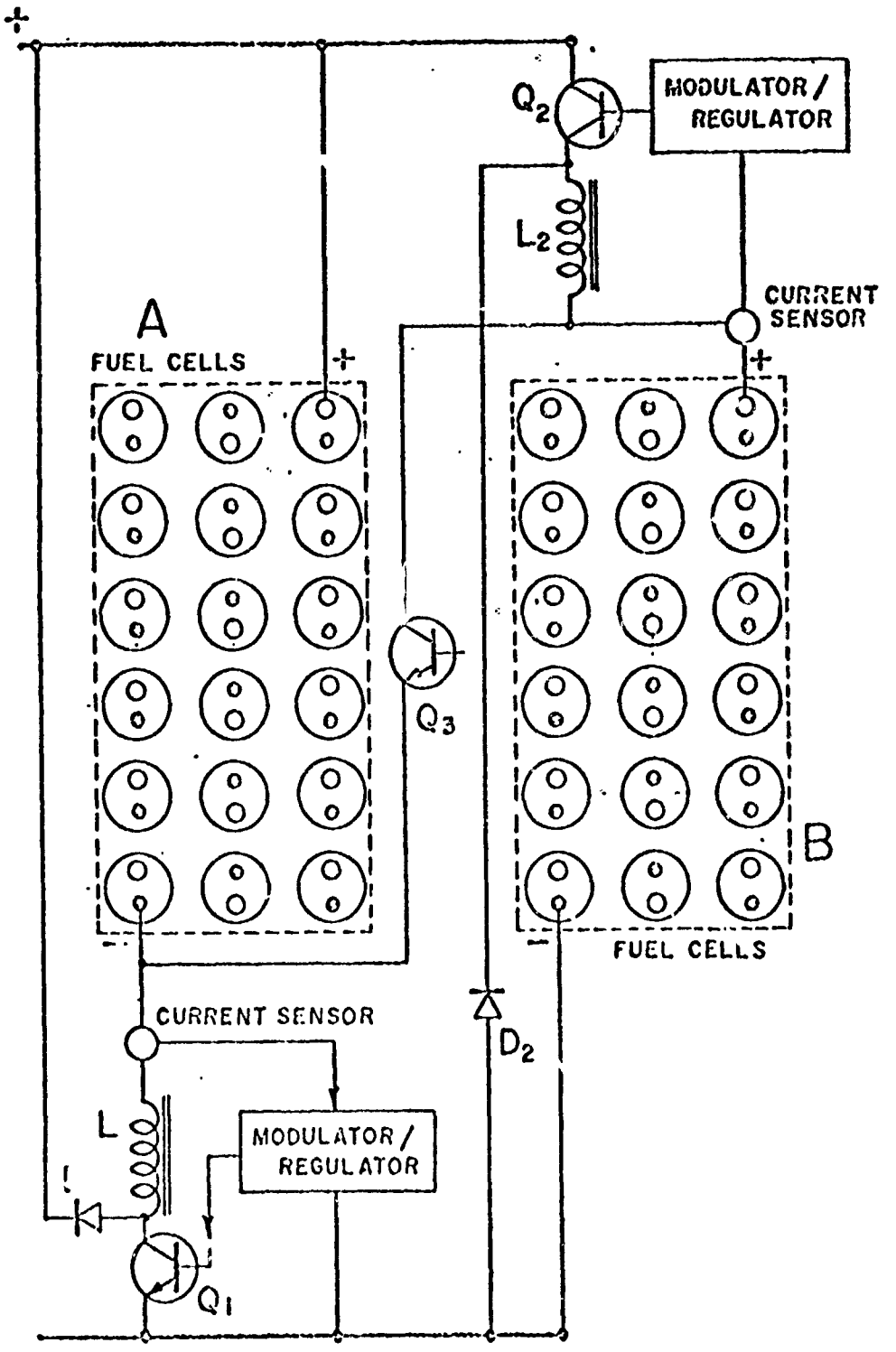

FIGURE 53. BASIC CIRCUIT OF SWITCH AND CHARGE REGULATOR

6.2 PERFORMANCE OF BREADBOARD CELLS/SYSTEM

6.2.1 Cell Acceptance Tests

The six fabricated fuel cells were individually subjected to acceptance testing which comprised at least one complete cycle of charge at 4.0 amperes to a cell pressure of 600 psig and a discharge of 33.3 amperes for a period of 72 minutes. The cell environmental temperature was maintained at approximately 50°C during the tests. Table III summarizes the discharge performance characteristics of these cells during acceptance testing.

TABLE III

BREADBOARD CELLS - ACCEPTANCE TEST DATA

CELL NO.	AMPS.	FUEL CELL VOLT			REMARKS
		INIT.	MAX.	FINAL	
4058-34	33.3	.817	.828	.828	Operated for 26 minutes
4058-35	33.3	.832	.838	.791	
4058-36	33.3	.837	.838	.783	
4058-37	33.3	.744	.843	.767	
4058-38	33.3	.865	.865	.851	Operated for 52 minutes
4058-39	33.3	.880	.881	.824	

Cell No. 4058-34 was discharged for a period of only 26 minutes, at which time the test was discontinued due to an excessive cell temperature rise and a corresponding excessive pressure drop during the discharge mode. The cell did not catastrophically fail on test, but the abnormal temperature rise and gas pressure drop indicated an internal cross leak and recombination of gases. This cell was consequently rejected for breadboard usage.

Cell No. 4058-36 showed good performance characteristics during the acceptance test. This cell, however, was inadvertently subjected to a large pressure differential due to the operator's misjudgement during removal of the fuel cell from the test setup. The bellows of the cell was destroyed by over-extension, with a resultant cross leakage. This cell was rejected from any further testing at this time.

Cell No. 4058-38 was discharged for a period of only 52 minutes. The test was discontinued due to faulty test equipment which prevented maintaining a constant discharge rate. The faulty equipment proved to be a low capacity battery which is electrically connected in series with the test fuel cell to control the discharge rate. The fuel cell was consequently rated as acceptable without any further testing.

6.2.2 System Cyclic Testing

The fuel cell acceptance test data resulted in selecting cells No. 4058-35, 37, 38, and 39 to be electrically integrated as a four cell system to be operated for a number of cycles representative of synchronous orbit operation. To accelerate the cycle testing, the 24 hour cycle duration was reduced to 12 hours by increasing the charge rate from 2.0 to 4.0 amperes. The individual cells were electrically integrated in a series circuitry with a common power supply for charging the system and a common load bank for the system discharge mode. Each cell, however, utilized the boiler plate external plumbing components for monitoring differential pressure as well as total cell pressure. Only one cell (No. 4058-35) was equipped with a pressure switch in place of the pressure transducer to limit the charge duration of the four cell system to approximately 600 psig per cell. The breadboard system was fully charged and then subjected to the cyclic regime as shown in Figure 56.

During the initial charge of the 4 cell breadboard system, Cell No. 4058-39 developed an internal cross-leak with a recombination of gases at a pressure of approximately 265 psig, at which time no further pressure buildup occurred during the continued charge mode. The system was then electrically inactivated and allowed to remain on open circuit for a period of approximately 1 hour, in which time the cell pressure dropped to 210 psig. Cell No. 4058-39 was replaced with Cell No. 4058-36, which had previously been acceptance tested but had been subject to bellows damage and had been repaired.

The 4 cell breadboard system consists of Cells No. 4058-35, 4058-37, 4058-38, and 4058-36, and was subjected to 23 cycles of testing per the specified single eclipse season. Table IV lists the individual cell voltages during discharge for each of the 23 cycles. A small variation of performance characteristics of the individual cells is indicated by the maximum recorded voltage difference in the initial cycle of 39 millivolts. It is noted, however, that in Cycle 23, the maximum recorded voltage difference of the cells has risen to 160 millivolts. A variation of individual cell performance degradation during cycling is also evident in that a voltage difference of each of the cells during the 1st cycle and Cycle 23 has values of 31 millivolts, 42 millivolts, 88 millivolts, and 141 millivolts. These values are approximate, based on the average cell voltage of the initial and final values recorded during each cycle.

TABLE IV

4 CELL BREADBOARD SYSTEM - CYCLIC DISCHARGE DATA

CYCLE NO.	DISCHARGE		VOLTAGE					
	Duration Min.	Rate Amps.		4 Cell System	Cell 4058-35	Cell 4058-37	Cell 4058-38	Cell 4058-36
1	12	33.3	Initial	3.305	.819	.838	.842	.806
			Final	3.311	.824	.835	.845	.807
2	16	33.3	Initial	3.303	.820	.838	.840	.805
			Final	3.333	.838	.832	.858	.805
3	21	33.3	Initial	3.296	.820	.837	.839	.800
			Final	3.305	.830	.822	.848	.805
4	26	33.3	Initial	3.291	.827	.839	.836	.789
			Final	3.250	.823	.791	.840	.796
5	30	33.3	Initial	3.272	.822	.836	.834	.780
			Final	3.273	.824	.822	.840	.787
6	34	33.3	Initial	3.252	.817	.834	.829	.772
			Final	3.238	.820	.796	.834	.788
7	39	33.3	Initial	3.245	.820	.833	.832	.764
			Final	3.259	.820	.820	.834	.785
8	43	33.3	Initial	3.237	.813	.832	.834	.758
			Final	3.211	.815	.786	.835	.775
9	47	33.3	Initial	3.210	.803	.824	.834	.749
			Final	3.198	.817	.805	.829	.768
10	50	33.3	Initial	3.215	.811	.828	.829	.747
			Final	3.191	.812	.794	.823	.762
11	53	33.3	Initial	3.213	.812	.830	.827	.744
			Final	3.154	.805	.772	.818	.759
12	57	33.3	Initial	3.210	.813	.830	.826	.741
			Final	3.175	.807	.800	.819	.749
13	60	33.3	Initial	3.193	.805	.827	.826	.735
			Final	3.141	.793	.792	.815	.736
14	63	33.3	Initial	3.165	.805	.828	.824	.708
			Final	3.129	.782	.804	.813	.730

TABLE IV (Concluded)

CYCLE NO.	DISCHARGE		VOLTAGE					
	Duration Min.	Rate Amps.		4 Cell System	Cell 4058-35	Cell 4058-37	Cell 4058-38	Cell 4058-36
15	65	33.3	Initial	3.059	.780	.834	.747	.698
			Final	3.055	.798	.803	.739	.715
16	67	33.3	Initial	3.017	.755	.824	.739	.699
			Final	3.013	.787	.803	.721	.702
17	68	33.3	Initial	3.043	.759	.833	.754	.697
			Final	3.030	.794	.808	.725	.703
18	69	33.3	Initial	2.991	.746	.827	.732	.686
			Final	3.015	.795	.802	.724	.693
19	70	33.3	Initial	3.030	.756	.829	.748	.697
			Final	3.019	.778	.801	.742	.698
20	71	33.3	Initial	3.009	.751	.827	.740	.691
			Final	3.044	.793	.798	.749	.704
21	71	33.3	Initial	3.020	.772	.822	.738	.688
			Final	3.030	.789	.792	.755	.694
22	72	33.3	Initial	3.004	.802	.807	.732	.663
			Final	2.983	.763	.775	.774	.671
23	72	33.3	Initial	2.996	.806	.808	.734	.648
			Final	3.016	.775	.782	.775	.684

The discharge performance characteristics of the 4 cell breadboard for 23 cycles are depicted in Figure 54. These are straight line plots using initial and final voltage values of each of the specified cycles. The performance degradation of the system is 302 millivolts for the specified 23 cycles of operation.

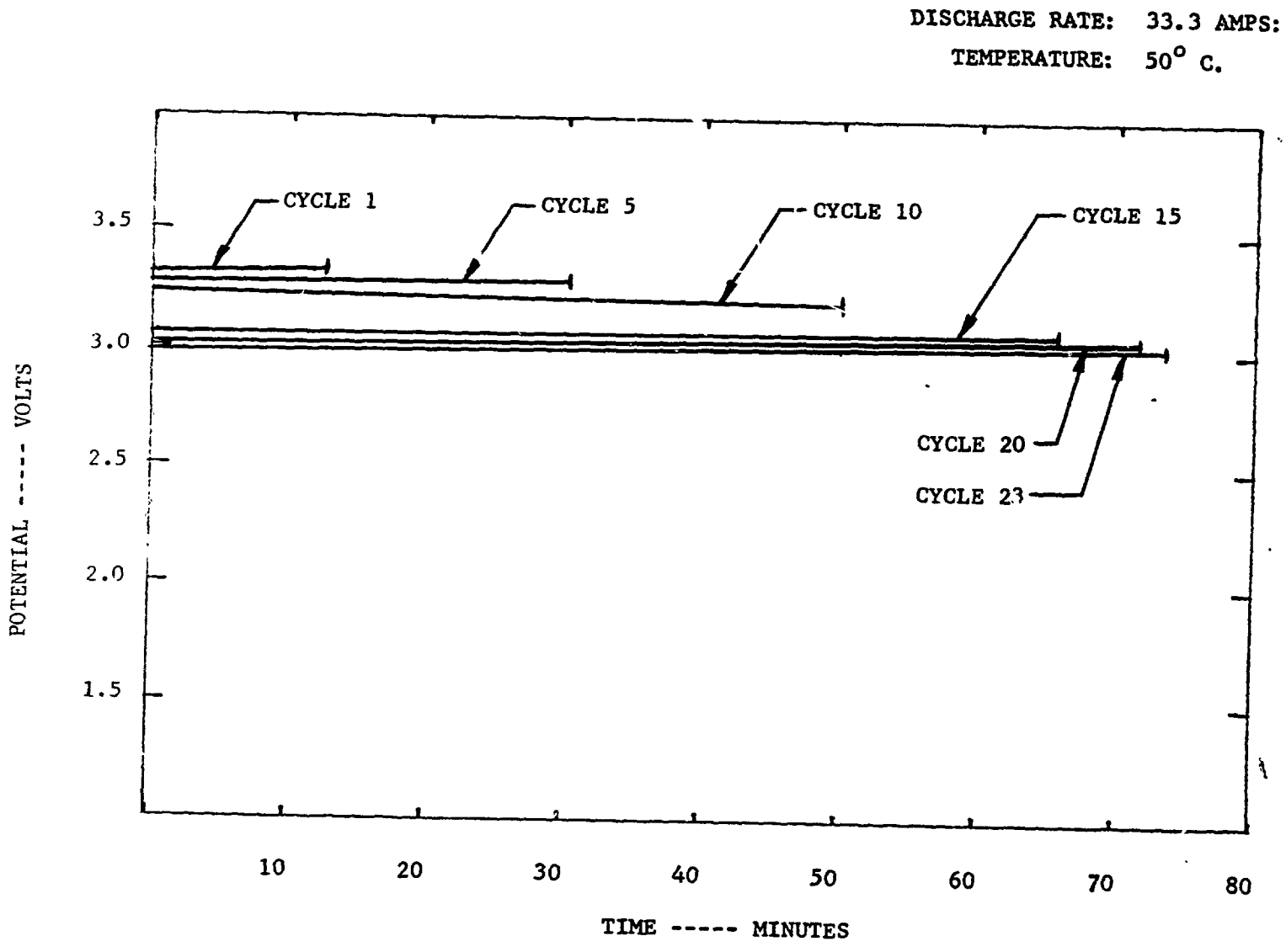

FIGURE 54. 4 CELL BREADBOARD SYSTEM - DISCHARGE PERFORMANCE

SECTION VII

CONCLUSIONS AND RECOMMENDATIONS

The cylindrical regenerative hydrogen-oxygen fuel cell has been demonstrated as a practical concept for a lightweight secondary battery. The cylindrical fuel cell, with its integral gas tankage, is a self-contained sealed unit that can be the modular base to build a large energy storage system. It has the advantages which are common to other single cells which are assembled into large batteries. The most significant are:

(1) Each cell can be inspected prior to assembly into a battery and matched sets can be assured.

(2) Extensive testing of single cells can be performed in the actual final configuration.

(3) Defective or failed cells can be removed from a battery and replaced (a few redundant cells are cheaper and lighter than a redundant battery)

(4) The hazard of a large and violent internal reaction is reduced since the reactants are stored in many small vessels rather than large pressure tanks common to all cells. In addition, location of the cells is not limited to a single battery configuration.

It has been recognized that regenerative fuel cells, which must operate in both a charge and discharge mode, are subject to greater performance degradation than primary fuel cells. This is primarily due to two reasons; (1) a more rapid oxidation occurs on the oxygen electrode side of the cell during the charge mode, and (2) lack of proper water management for optimum performance, which demands a flooded condition during the charge mode and a somewhat drier condition in the fuel cell mode. Past development programs of the regenerative fuel cell have resulted in nonoxidizable materials being used for the oxygen electrode and improved matrices for better water management within the cell. The net result of these improvements was cells which attained life-duration in the 500 to 1000 cycle range with some minimal deterioration. This development effort was performed on test cells of flat plate configuration.

The introduction of a cylindrical designed fuel cell has created problems which affect the performance characteristics and integrity of the cells, and which were nonexistent or of minimal consequence in the flat plate construction. This factor has been borne out during this contract effort, wherein many cells failed in less than 50 cycles of operation, several cells exceeded 100 cycles, and only one cell passed 200 cycles of operation. The principal failure modes were sudden failure rather than wear out degradation. During the final phase of this contract effort, some of the failure modes of the cylindrical regenerative fuel cells have been

identified, and some of these have been corrected by design modification, and others need additional development work. At the end of this program, two cells which had been subject to mechanical design modification were still on test with over 115 cycles on each.

The principal failure related factors are an internal mixing of reactant gases due to failures of mechanical structures such as the Hypalon bellows and the cell edge seal. The secondary failure related factor is the internal mixing of reactant gases through the electrolyte contained matrix. This phenomena occurs due to loss of electrolyte from the matrix, due to misting during electrolysis (gas evolution), local loss of electrolyte due to cell orientation (gravity), or possibly loss of water due to thermal conditions or of local hot spots in the cell. The loss of liquid from the matrix reduces the gas barrier effect of the matrix.

It appears that additional development effort is required to reduce the failure modes to assure greater system reliability, wherein these cells are utilized. This effort should include mechanical and design analysis of the fuel cell components to resolve structural failures. It should also include experimental approaches to the mechanisms which cause failures of the electrolyte as a gas barrier. The development of a technique for controlled water management would enhance cell performance degradation as well as increase cycle life.

The program has resulted in the identification of cylindrical regenerative fuel cell problems, and a better understanding of resolutions to the problems. Although the cells which were delivered, as the end product of the contract, consisted of some design modifications to alleviate the failure modes, no effort was made to weight optimize these cells; however, several significant weigh saving areas have been identified, such as the inconel pressure vessel which has a strength factor much greater than necessary; and the elimination of the perforated inconel support core by incorporating a sintered nickel tube to serve as both the core support and the hydrogen electrode. It is also anticipated that with increased integrity of the electrolyte gas barrier, a thinner matrix with a corresponding decrease in electrolyte volume can be utilized for further weight reduction.

It is projected that with additional design analysis and development efforts, substantial increases in cycle life and improvement in performance degradation can be attained in the cylindrical regenerative fuel cell.

APPENDIX I

SCOPE OF WORK

TASK I - CONTRACT REVIEW

Contract F33615-70-C-1671 will be reviewed by all technical and administrative personnel that will be involved in the performance of the program. Based on this review, a Program Plan had been instigated and a Program Master Schedule was prepared as a Milestone Forecast.

TASK II - DESIGN AND FABRICATION OF BOILER-PLATE CELL

2.1 DESIGN

A heavyweight, or "boiler-plate", test cell will be designed capable of internal pressures of at least four times that anticipated in the fully charged condition for operational lightweight cells. The internal configuration of the cell will be essentially the same as the EOS Rechargeable Fuel Cell Model RHO-24AH-Mod I, modified so as to simplify the replacement of any or all components. The pressure shell shall be designed so as to permit removal of the top head, with all of the connections and internal parts attached, for inspection, replacement of parts, or any other operation followed by easy reassembly.

2.2 FABRICATION

For simplicity of fabrication, the boiler-plate shell will be built of heavy wall stainless steel pipe with flanges at both ends, a blind flange at the bottom, and a blind flange perforated for all connections at the top. Fabrication of a prototype boiler-plate cell and two cores will be done. The prototype will be cycle tested before fabrication of the following five units. Upon completion of the prototype test, five more boiler-plate cells will be fabricated with modifications, if necessary.

2.3 TEST

To insure that the design and fabrication is adequate, all boiler-plate pressure vessels will be hydraulically pressure tested to 4,000 psig (double the anticipated maximum operating pressure) using a plug in place of the burst diaphragm.

Preliminary testing of one boiler-plate cell will be done using similar internal components as are used in the Model RHO-24AH-Mod I. Based on this work, a determination will be made as to whether the design meets all of the intended goals, or if redesign is required. If an improved design is needed, it too will be subjected to the same test program.

2.3.1 Deliverable Hardware

Two "boiler-plate" cells will be completely fabricated, leak tested, and operated through a minimum of six complete twelve-hour cycles, each cycle being 20 hours of charge at 2.0 amperes, 2.8 hours of open-circuit stand at 600 psig pressure, and 1.2 hours of discharge at 33.3 amperes, with data on voltage, amperes, total pressure, and differential pressure recorded on tape at 10 minute intervals. Following the sixth cycle, the cells will be fully discharged, vented to reduce pressure to atmospheric, and a shorting strap connected to the terminals. The valves will be closed to prevent air from entering the cells. The cells will be delivered to AFAPL by, or before, 30 July 1971.

TASK III - PARAMETRIC STUDIES OF ELECTROCHEMICAL PERFORMANCE

Using the "boiler-plate" shell and internal cell configuration designed in Task II, cells will be assembled for evaluation of the electrochemical performance of the materials and components used in EOS Rechargeable Fuel Cell Model RHO-24AH-Mod I. Evaluation tests will be performed as a function of environmental temperature and pressure, and will be instrumented as follows:

1.	Voltmeter	$\pm$ 1%
2.	Ammeter	$\pm$ 1%
3.	Total Pressure Transducer	$\pm$ 2%
4.	Differential Pressure Transducer	$\pm$ 2%
5.	Cell Temperature Thermocouple	$\pm$ 1%
6.	Chamber Temperature Thermocouple	$\pm$ 1%

The data will be periodically recorded throughout each test.

A voltage-current scan on charge and discharge will be done in the middle of the discharge cycle during the initial, final, and every sixth cycle. The scan will range from 1 ma/cm^2 to 100 ma/cm^2. The discharge portion of the scan will be done by manually varying the load on the fuel cell. The cell will be allowed to discharge for 30 seconds at each of the following current densities, starting with the lowest value: 1 ma/cm^2, 5 ma/cm^2, 10 ma/cm^2, 25 ma/cm^2, 50 ma/cm^2, 75 ma/cm^2, 100 ma/cm^2. For the charge scan, a constant current power supply will be manually operated to charge the fuel cell for 30 seconds at each current density listed above, starting with the lowest value. The cell will then be allowed to finish out the 1.2 hour discharge cycle. The voltage current scan will be performed manually during the discharge portion.

The 24 hour cycle will be as follows: charge @ 1.85 amps for 22.8 hours. When the 600 psig pressure switch removes the cell from charge it will remain at open circuit during the remaining charge period. The discharge will be at 33.3 amps for 1.2 hours. The cell pressure at the beginning of each cycle will be approximately 100 psig.

3.1 TEMPERATURE TESTS

Two cells using the materials and components listed above, with a 600 psig pressure switch and a 900 psig burst diaphragm, will be cycled a maximum of 30 cycles at each of the following temperatures: 30°C, 50°C, 80°C, 100°C. The testing at these temperatures will give information pertinent to the electrochemical performance of the cells. The choice of these temperatures was based on previous experience with flat plate cells: 100°C was selected as the higher limit to minimize material degradation, while at temperatures below 50°C electrochemical performance was poor, i.e., high charge voltage and low discharge voltage. In the flat plate cell investigations, a charge voltage higher than 1.90 or a discharge voltage below 0.70 was considered a failure, and at the lower temperatures there were many "early failures".

3.2 HIGH PRESSURE TESTS

The RHO-24AH-Mod I fuel cell has an average matrix weight of 29.5 g, and is loaded with 67.5 g of 30% KOH solution. This results in an electrolyte-to-matrix ratio of 2.28. Using this ratio, the cell electrodes will flood at approximately 100 psig during discharge. 100 psig was chosen as the lower pressure limit because the cell performance decreases at lower pressures. However, since the thermodynamic effect of pressure is small, lower pressures will be considered.

During the charge or electrolysis period, water is decomposed at the rate of 0.336 gm/amp-hr. The capacity limit of a fuel cell is below the point where enough water is removed from the matrix to allow the gases to readily migrate across and react chemically; this will vary with pressure and temperature.

The 24AH fuel cell is originally loaded with 67.5 g of KOH solution containing 47.5 g of H_2O. To attain initial full charge (including purging of the cell and pressurization of 100 psig), 9.95 g of H_2O is electrolyzed, or 21.1% of the total water present. This represents 35.0% maximum KOH concentration at nominal full charge of 600 psig.

The high pressure tests are designed to determine the capacity limit of the PHO 24AH Mod I fuel cell matrix and to determine the feasibility of increasing the capacity by using a thicker matrix, a thicker H_2 electrode, or an additional electrolyte storage bed. The resulting increase in resistivity with a thicker matrix will also be determined.

3.2.1 Two cells will be fabricated using the standard components listed above without pressure switches and with 1500 psig burst diaphragms. The cells will be mounted in the test stations and the controls will be run manually. The cells will be tested at 50°C, 80°C, and 100°C in the following manner:

1. Charge to 600 psig at 10 amps; discharge at 33.3 amps until the voltage falls below 0.7 volts.

2. Charge to 800 psig or until cell charge voltage shows a steep rise characteristic of a dry matrix. Discharge at 33.3 amps until the voltage falls below 0.7 volts.

3. Charge to 1000 psig or until the cell voltage shows a steep rise characteristic of a dry matrix. Discharge at 33.3 amps until the voltage falls below 0.7 volts.

4. If possible, charge beyond 1000 psig and repeat the test listed above.

This information will be used in calculating the volume and weight of the lightweight cells in Task 7.

3.2.2 Using the data obtained from 3.2.1, design data will be determined for cells with a thicker matrix, a thicker H_2 electrode, and/or additional electrolyte storage. The cells will be fabricated in a boiler-plate housing. All other materials and components will be the same as used in the RHO-24AH-Mod I fuel cell.

3.3 LIFE TESTING

3.3.1 Based on the data collected in 3.1 and 3.2, modifications to the materials and components will be evaluated in the boiler-plate cells to determine the best choice for further cyclic testing, and also the optimum choice of operating conditions. These choices will be verified by construction of cells and several cycles of operation under the tentatively chosen conditions. Two or more of these cells will be placed on test fixtures for life testing, which will be carried out continuously from this time throughout the rest of the program duration, using a twelve hour cycle with a 1.2 hour discharge period in order to subject the cells to more cycles. The tests will be continued either until the end of the program or until the energy efficiency of the cells falls significantly below 45 percent. The pressure limit will be 600 psig. It should be recognized that the 12-hour cycle is more severe than the simulated synchronous orbit cycle (Fig. NR1, Exhibit A, Contract F33615-70-C-1671) because the cell will be charged for more than 20 hours each day at twice the normal current, and discharged for a full 2.4 hours each day.

3.3.2 The cells that are on life test will be subjected to a voltage-current scan as previously described in both charge and discharge modes, after each 30 cycles. This will give an accurate record of the extent of degradation with cycling when compared to the same type of data observed before the cells were extensively cycled.

3.4 INSPECTION AND FAILURE ANALYSIS

All cells that have been cyclically tested and have completed a particular sequence will be dismantled in a glove box with an inert atmosphere for inspection and failure analysis. The inspection will consist of:

1. Core and bellows visually inspected for any detectable change or damage.
2. The core will be pressure tested at 2 to 4 psig to determine whether any leaks have developed. The inside of the core will be pressurized with nitrogen gas. A bourdon gauge will be connected to the core. If a pressure drop is observed within 15 minutes, the location of the leak will be traced.
3. The oxygen electrode will be carefully removed, and this electrode and the matrix visually inspected.
4. A section of the matrix will be removed and analyzed for electrolyte (KOH) concentration. A few drops will be squeezed from the matrix, diluted in distilled water and titrated to the phenolphthalein end point with standardized HCI.

On selected cells, particularly those that have been on cyclic life test for extended periods, sections of both electrodes and the matrix will be chemically analyzed for platinum.

TASK IV - CELL COMPONENT OPTIMIZATION

4.1 MECHANICAL COMPONENTS

4.1.1 Bellows Evaluation

Since the Hypalon bellows may not meet the life requirement of the ESS, and may be marginal in regard to radiation-induced damage, both electroformed and welded metal bellows will also be evaluated.

4.1.1.1 Two of each of the following type of bellows will be immersed in a 30% KOH solution at 100°C for 48 hours:

1. Hypalon bellows
2. Electroformed nickel bellows
3. Welded nickel bellows

The KOH solution will be washed off and the bellows dried. The bellows will be mounted in a test device that will alternately put a 3 psi differential on each side. The test mounting will be glass pipe so that the flexing at the bellows can be visually observed. The cycle frequency will be 1/2 minute/side. Timer controlled solenoid valves will control the pressure cycles. The test fixture will be instrumented with either a piston operated veeder counter or a pressure transducer with a recorder. The test will run until the test part passes 2000 cycles or fails.

4.1.1.2 A literature search will be made to evaluate the radiation tolerance of the various bellows materials.

4.1.2 Pressure Housing

The thickness of the pressure housing of the cells will be designed for a proof-pressure of 150 percent of the full-charge pressure, and burst strength of 200 percent of full-charge pressure. These figures are conservative, and may be somewhat reduced in the future when overall system reliability has been demonstrated to the extent that lower safety factors are warranted.

The material used will be an inconel alloy because of its excellent compatibility with KOH.

4.1.2.1 A sealed pressure housing with all the accessories, except a burst diaphragm, will be hydraulically tested to experimentally verify the yield and burst pressures. The pressure housing will be tested as described in paragraph 2.3.1, except it will be pressurized to the yield and burst pressures.

4.1.2.2 A literature search will be made to evaluate the radiation tolerance of the pressure housing material.

4.1.3 Perforated Core Support

The perforated core, which supports the electrodes and matrix, will be redesigned to minimize its weight. Several alternatives will be investigated. Thinner metal than used in the RHO-24AH-Mod I is the simplest, most direct approach. However, the nickel plaque which is the basis of

the hydrogen electrode may have adequate strength if supported only by a metal ring at each end to serve as sealing edges as well as circular support. In this latter approach, the nickel plaque will be welded to the rings. Another approach to evaluate will be a sintered nickel core attached to nickel rings, as manufactured by Union Carbide. A removable plastic core will be used to support the inner electrode while forming the matrix and winding the wire around the outer electrode.

4.1.3.1 Complete cores with dummy electrodes will be fabricated as follows:

1. Core with standard RHO-24AH-Mod I support
2. Core with lighter support
3. Core with no support

The cores will be wet with electrolyte and subjected to increasing differential pressures on each side until a mechanical failure occurs. The results of the core pressure tests will be used to help determine the final selection of core design.

4.1.3.2 As an alternate to the perforated core support, a study will be made of the feasibility of fabrication of a sintered nickel tubular structure that would serve as both the core support and the hydrogen electrode. Analytical studies will be done to determine the method of attachment of end rings to an expanded metal screen, and the tooling required to apply nickel powder to the screen to be sintered while maintaining the required dimensional tolerances. Tooling will be fabricated to produce a structure 2.00" I.D. and approximately 40 to 60 mils thick.

A few preliminary parts will be fabricated to evaluate the tooling, and experimentally determine the optimum sintering conditions. A limited number of parts will be fabricated to determine the ability of the tooling and process techniques to vary the porosity of the finished cores within controlled limits. Based on these preliminary tests, one set of operating conditions will be established, and 4 to 6 cores fabricated.

The cores produced above will be subjected to crush tests to verify adequate strength; a minimum of 30 psi pressure differential in either direction will be considered satisfactory in terms of mechanical strength. Following the mechanical testing, a series of chemical tests will be run to establish that the sintered nickel can be platinized, and any modifications to the present techniques that might be required will be determined.

Four more sintered cores will then be made, and platinized. Two of these will be processed as completed fuel cell cores, complete with welded metal bellows, top caps, matrix and oxygen electrodes, and installed in boiler-plate shells for actual cyclic testing.

4.1.4 Pressure Switch

The pressure switch on the RHO-24AH-Mod I is a modification of a commercial switch. Alternate sources of pressure switches, lighter in weight and vendor-qualified to the environmental requirements, will be sought.

4.1.5 Pressure Transducer

Regenerative Fuel Cell Model RHO-24AH-Mod I includes a pressure transducer to indicate state-of-charge. As in the case of the pressure switch, sources of adequately qualified components will be sought.

4.1.6 Insulated Feedthrough Connectors

The insulated feedthrough connections used on RHO-24AH-Mod I are a commercial item, subject to wide dimensional tolerance, and are not acceptable for flight hardware. The Advanced Technology Division of EOS will design and fabricate a new feedthrough connector for the regenerative fuel cell. At the same time, alternate sources of commercial feedthrough connectors suitable for this application will be investigated.

4.2 ELECTROCHEMICAL COMPONENTS

4.2.1 Oxygen Electrodes

A basic limiting factor of electrochemical performance of the regenerative fuel cell is the electrode activity. Higher current densities without increased voltage losses would permit higher energy-to-weight ratios at the same energy efficiency.

4.2.1.1 Two cells will be fabricated in the boiler-plate shells and cycle tested using increased platinum loading on the oxygen electrodes; these will tentatively be with 20 mg/cm^2 of platinum, compared to the presently used 9 mg/cm^2. All other materials and components will be the same as used in the RHO-24AH-Mod I fuel cell.

4.2.1.2 One cell will be fabricated using a platinized nickel plaque (EOS) electrode as the oxygen electrode. This type electrode is not "wetproof", and is thicker than the Allis-Chalmers Type 6 material, thus will hold more electrolyte and permit the gas-liquid interface to move in and out (with reference to the matrix) while maintaining adequate 3-phase contact zones. It is recognized that non-gold plated nickel will corrode in the KOH-oxygen environment, but the rate of corrosion of the platinized nickel may be sufficiently low to permit extensive evaluation of this type electrode. The rate of corrosion may be low enough that it is not a limiting factor in performance; this will be evaluated by life testing within the duration of the program.

4.2.1.3 One or more cells will be fabricated in the same manner as those described under 4.2.1.2, except that the matrix will be made from 100% fuel cell grade asbestos. It is recognized that asbestos is more reactive to KOH than potassium titanate, but the rate of attack is believed to be sufficiently low that deterioration of the asbestos is not considered a pertinent factor in life testing at the present state-of-the-art. The purpose of these tests is to demonstrate any advantages of asbestos such as higher capillary potential, greater swelling contact, ability to resist gas permeation with reduced thickness and lower resistive losses, and better uniformity throughout the matrix (one component vs. three). It is proposed to run extended tests on one of these cells, to try to determine the life limiting characteristic(s).

4.2.2 Electrical Connections

All electrical connections in and on the cell will be investigated in an attempt to reduce the electrical resistive losses in the system and improve upon the earlier design. All cell connections will be measured with a milliohmeter. An effort will be made to reduce the total cell resistance to an absolute minimum.

4.2.2.1 One or more cells will be fabricated to evaluate the merits of current collectors on the oxygen electrode to minimize IR losses. The construction of the cell and the collectors will be based on data analyses of cell component variables to optimize performance. Parametric tests will be run to determine the electrical properties of the cell in charge and discharge modes compared to earlier tests. If time permits, testing will be continued for the duration of the program.

4.2.3 Compression of Electrodes and Matrix

Compression of the electrodes and matrix will be investigated. Lack of uniformity of compression, and contact, of the matrix and both electrodes may be a factor in limiting electrochemical performance.

4.2.3.1 The tension used in the nickel wire windings is now five pounds. Dummy cores will be wound at increased tension. The limit will be determined at which physical damage is done to the core. This test is to determine the upper limits of wire tension on the core winding. A cell will then be assembled, using the maximum tension, and cyclic tests will be run to confirm if electrochemical performance is improved by providing a closer contact between the electrodes and matrix.

4.2.4 Matrix and Electrolyte Loading

The thickness of the matrix and its electrolyte loading will be investigated experimentally in Task 3, although the results of the tests will be used in this task, Cell Component Optimization. The optimum matrix thickness and electrolyte loading, as a function of operating pressure, will be determined in Task 3.

4.2.5 Temperature Measurements

A cell will be fabricated with provision for temperature measurements at several locations on the core. Thermocouples will be mounted in contact with the core, and the leads will be brought out of the cell through one of the gas connection tubes.

During electrolysis, or charge mode, the total pressure of the cell will be held very slightly above ambient pressure, and the gases generated will be vented continuously. Similarly, during discharge, or fuel cell mode, the pressure will be held slightly above ambient, and the required hydrogen and oxygen will be supplied from external sources. This will alleviate the problem of gas leakage at the multiple-wire feedthrough for the thermocouple leads.

Although a small error will be introduced by the heat content of the gases leaving or entering the cell, it is assumed that this will be small compared to the total polarization and resistive electrical losses which generate the heating effects being measured in this test. It is anticipated that a reasonable approximation to internal cell temperatures will be observed in this test, and the data will be used to verify the assumptions concerning internal thermal conditions used in design calculations.

TASK V - ESS CENTERLINE DESIGN

A functionally complete breadboard regenerative fuel cell energy storage system, modular at the single cell level, that is fully representative of a larger system in all performance aspects, will be designed, fabricated, and tested. Consistent with and appropriate to the EOS single cell approach, the Centerline Design will be based on a system comprising four regenerative fuel cells, each of which will be of the same size and configuration as the basic elements of the proposed ESS. The four cells will be arranged in two groups of two cells each, with the two cells in each group connected electrically in series. The two groups will be in parallel for charging and in series for discharging. Each cell will have a discharge current of 33.3 amperes, and have a current-time rating of 40 ampere-hours.

The breadboard that will be built, tested, and delivered in this program will be rated at 111 watts, or 133 watt-hours. It will operate at charge and discharge voltages between the limits of 3.0 volts minimum and 3.67 volts maximum. In this respect, it is exactly one-ninth of a one-kilowatt system in energy storage and busbar voltage.

Each of the cells will be provided with a total pressure transducer. Either cell in a group can signal to discontinue the charging of its group. Each of the cells' transducer will indicate state-of-charge. The transition from charge to discharge will be controlled by a double-pole double-throw switch, with the connections to the busbars directly from the switch. Provisions for instrumentation will be made for the breadboard prototype, but will not be considered as part of the flight-weight ESS. The ESS Centerline Design will be periodically reviewed and updated to incorporate all new information throughout the duration of the program.

TASK VI - ESS COMPONENT SELECTION

Following the first review and improvement of the Centerline Design, all components of the ESS will be selected and identified by manufacturer, model number, drawing number, etc. A revised Centerline Drawing will be prepared with complete identification of all components. Wherever possible, components that have been vendor-qualified to comply with the environmental requirements of the ESS will be specified.

Following each revision of the Centerline Design, the ESS Component List will be reviewed and any changes incorporated.

TASK VII - DESIGN OF LIGHTWEIGHT CELLS

This task is divided into two major subtasks. The first includes the work required to optimize the single cell configuration. The second subtask will include parametric analyses, spacecraft integration considerations, and the generation of a conceptual design of a 1 kw energy storage system.

7.1 SINGLE CELL DESIGN AND ANALYSIS

The following specific tasks will be undertaken to optimize the single cell configuration.

7.1.1 Stress and Dynamic Analysis

7.1.1.1 Random Vibration. - The response of the fuel cell into the specified random vibration spectrum will be predicted and the resulting deflections and stresses checked. The location and type of supports required to insure that the core assembly will survive the vibration environment will be defined by this analysis. Survivability of the electrical feedthroughs and other attachments will also be determined.

7.1.1.2 Pressure Vessel Design. - This analysis will define the minimum weight configuration which will meet the following criteria:

- Proof pressure of 1.5 times the maximum normal operating pressure.
- Burst pressure of 2.0 times the maximum normal operating pressure.
- Strain levels which control the O_2 volume changes under pressure to values which do not cause unacceptable pressure differentials between the hydrogen and oxygen chambers.

7.1.2 Thermodynamic Analysis

This analysis will be performed in three steps.

7.1.2.1 Develop General Equations. - The general equations which define the relations between the system variables as shown in the flow diagram will be derived. A heat transfer analysis will be performed to define the temperatures within the cell as a function of time. Consideration will be given to the effect of strain in the pressure vessel, bellows deflections, and thermal expansion in the determination of the volume relationships. The gas compressibility factor will be included in the gas law.

7.1.2.2 Program for Digital Computer. - The number of interrelated variables included in the analysis is such that a numerical analysis, using the digital computer, will be required to determine the hydrogen and oxygen pressures as a function of time.

7.1.2.3 Run the Program to Determine Conditions for Minimum ΔP. - Using the geometry of the centerline configuration and various conditions, the ΔP between the hydrogen and oxygen chambers will be calculated. The sensitivity to molar imbalance, volume imbalance, temperature, pressure vessel stiffness, bellows stiffness, etc. will be evaluated and set(s) of conditions which produce acceptable performance determined.

7.1.3 Material Analysis

The properties of the materials selected for use in the fuel cell will be reviewed to insure compatibility in the chemical, radiation, and static and dynamic environments specified.

7.1.4 Detail Design of Lightweight Cell

The recommendations of the foregoing analyses will be incorporated into such documentation, drawings and/or sketches as required for the manufacture of the prototype and breadboard lightweight cells.

7.2 1 KW ESS DESIGN AND ANALYSIS

The following tasks will be undertaken to define potential thermal interface problems which may arise with the spacecraft in the integration of an energy storage system using a fuel cell of the design optimized in Task 7.1.

7.2.1 Parametric Heat Transfer Analysis

7.2.1.1 Predict Equivalent Ambient Temperature for Single Cell as a Function of Time - $T_A(t)$. - This task will require the use of a three dimensional, transient, heat transfer analysis computer program. The equivalent ambient temperature for each cell of the 1 kw system will be determined for a limited number of cell groupings and spacecraft temperatures and heat rejection system configurations.

7.2.1.2 Determine ΔP Versus $T_A(t)$. - Using the temperature predictions from the previous task, the computer routine developed in Task 7.1.2 will be reentered with T_A as a time variable and the resulting gas pressures calculated.

7.2.1.3 Define Thermal Integration Requirements. - Iterations of Task 1 and 2 will be performed to determine the conditions required for compatibility of the fuel cell ESS in various spacecraft configurations.

7.2.2 Conceptual Design and Integration of 1 kw ESS

7.2.2.1 Description of System and Basis for Selection. - The results of Task 7.2.1.3 will be reviewed and the system which best satisfies the required conditions will be selected for the conceptual design.

7.2.2.2 Conceptual Drawing. - A drawing depicting the configuration of the 1 kw PSS and its integration into a typical spacecraft will be generated in sufficient detail to demonstrate feasibility.

TASK VIII - FABRICATION AND TESTING OF LIGHTWEIGHT CELLS

8.1 PROTOTYPE FABRICATION AND CHECKOUT

After completion of the cell design in Task 7, two cells will be fabricated. All manufacturing and quality control procedures will be reviewed during the fabrication. These two cells will be pressure-leak tested in a vacuum chamber, with the internal part of the cell pressurized to a full-charge pressure with helium, flushed to remove inert gases, sealed, and subjected to at least a two cycle preliminary performance test.

8.2 VIBRATION TESTS

After the preliminary performance test, one of the cells will be mounted in a fixture for the random vibration test in each of three mutually perpendicular planes for five minutes in each plane at the frequencies and spectral densities given in Figure 55. After completion of the random vibration test, the cell will be functionally tested using one standard charge-discharge cycle, after which it will be disassembled for complete examination of all internal parts.

8.3 THERMAL TESTS

The other cell of the two described above will be tested by obtaining a voltage-current scan at a predetermined temperature, then thermally cycled twice between -20°F and 100°F, with at least 12 hours storage at each extreme, following with a second voltage-current scan which will be run at the same test temperature as before.

8.4 VACUUM TEST

Following successful completion of the temperature cycling test, the cell will be installed in a vacuum environmental test chamber, and operated for one complete 24 hour charge-discharge cycle at a pressure of 10^{-5} mm Hg or lower with instrumentation to record voltage, current, and temperature.

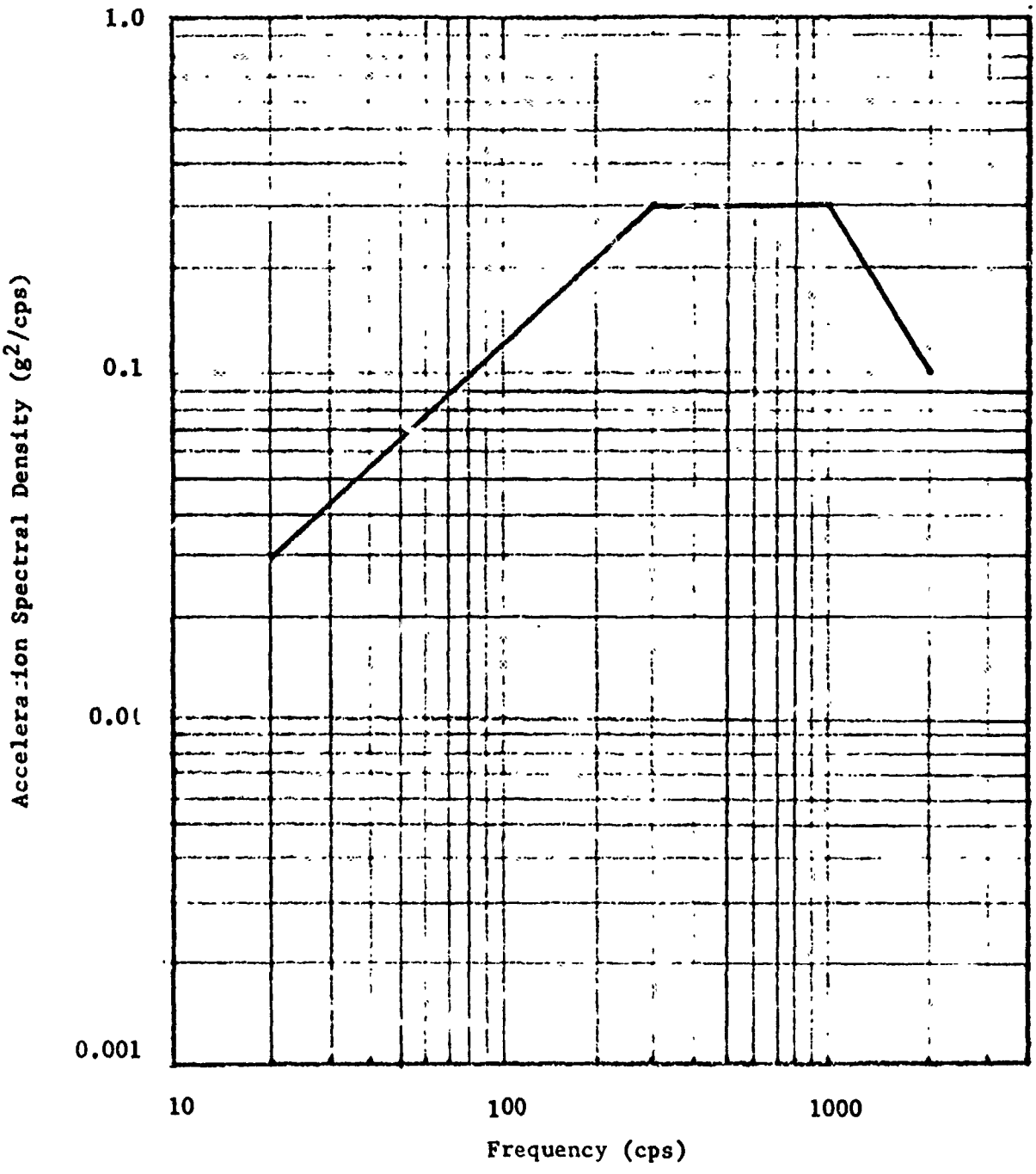

FIGURE 55. RANDOM VIBRATION ENVIRONMENT

8.5 CYCLE TEST

After successful completion of the environmental tests, two more cells will be fabricated. The helium leak test will be considered a standard quality control check before the cells are sealed. These two cells will be subjected to a two-cycle preliminary test, using the standard 24-hour charge-discharge cycle. Upon the successful completion of this test, the cells will be subjected to a 30-cycle test, using either the standard 24-hour cycle or a shorter (6- or 12-hour) cycle, with each cycle running from full discharge to full charge.

8.6 HYDROSTATIC TEST

In addition to the two cells fabricated for electrochemical testing, two or more cells will be fabricated without electrodes or matrix. These "empty" cells, complete in all external details and with full standard assembly and inspection of all welding, case penetrations, burst diaphragm, etc., will be subjected to a proof pressure hydrostatic test. The cells will be tested using the fixtures and instrumentation described in paragraph 2.3.1. The pressure will be increased until the burst diaphragm ruptures, which should be at the design proof pressure. In addition, one of the empty cells will be assembled without a burst diaphragm, and will be hydrostatically tested to burst pressure. (One of the cells used for proof pressure testing may be used by welding a solid plate in place of the released diaphragm).

8.7 BREADBOARD CELL FABRICATION

Upon the successful completion of the 30-cycle tests, 6 lightweight cells will be fabricated, using the same manufacturing and quality control procedures as used for the two test cells. Each of the cells will be subjected to a minimum of two 24-hour cycles under standardized conditions. Each of the cells will be equipped with total pressure transducers. Four of the cells will be used to assemble the breadboard ESS.

TASK IX - CRITICAL COMPONENT TESTING

The critical components of the energy storage system are the regenerative fuel cells, pressure switches for charge control, switchgear to select the charge or discharge mode, and the current control device. Representative samples of each of the critical components will be subjected to both functional and environmental testing to assure compliance to the temperature, pressure, and random vibration requirements.

All parts subjected to any or all of the environmental test regimens will be functionally tested to assure proper operation after the environmental tests. This includes the regenerative fuel cell. The functional tests will be to the full rating of the particular component; in the case of the fuel cell, this will consist of at least one complete charge-discharge cycle (see Task VIII).

Although no tests will be run to demonstrate radiation resistance, this requirement will be considered in all design work. As discussed in Task VII, little or no problem is anticipated due to this environment.

TASK X - DESIGN OF BREADBOARD REGENERATIVE FUEL CELL ENERGY STORAGE SYSTEM

Concurrent with Task VIII, Fabrication and Testing of Lightweight Cells, the design of the complete breadboard regenerative fuel cell energy storage sytem will be done. The design will be based on the data and information generated in Tasks III through IX, and will be for a 111 watt (133 watt hours) system.

The breadboard will include all the components from the regenerative fuel cells to the ESS electrical terminals for connection to the host vehicle bus bars. This includes pressure transducers to indicate state-of-charge and to signal or control full charge condition, interconnections between individual cells, and switchgear to select series or parallel connections of groups of cells.

Preliminary analysis of the 111 watt system indicates that 4 cells in series connection will be required to achieve the required voltage in the discharge mode. Each cell, and the group of 4 in series, will deliver 40 ampere-hours at 33.3 amperes. A double-pole double-throw switch will be used to realign the cells into two groups of two for the charge mode; each group of two will be in series, and the two groups will be in parallel. This arrangement will permit the cells to be charged, using a power conditioning device to maintain constant current in each group of cells, using bus bar voltage.

The supporting structure of the 111 watt (133 watt-hour) breadboard system, including the 4 cells, interconnections, switches, bus bar connections, and instruments will be included in the design of the breadboard, but will not be representative of the final design, nor will it be designed for the environmental test conditions.

The instrumentation and controls required for the time-cycle controllers and the transducers, the power supply for the charging current, and the electrical load with its controls for discharging will all be external to the breadboard, and not considered part of it.

TASK XI - DESIGN REVIEW

Upon completion of Task X, a design review will be conducted. Specialists in material and stress analysis, radiation and other environmental problems, electrical and electronic control, manufacturing engineering, quality control, thermal analysis, and solar panel interface problems will be on the review team.

The design review package will include engineering drawings of the cells, specifications and certifications (where available) of all other components, data from environmental and functional tests, and the breadboard design.

All members of the Design Review Team will be asked to submit recommendations for improvements and/or modifications to the design package. These will be reviewed by the Program Manager and Principal Investigator, considering the effect of the recommended changes on performance, system weight and power density, schedule, and cost.

The Program Manager will issue a report based on the results of the Design Review, including all recommendations, how they were incorporated into the design package, and a justification of rejection of any of the suggestions.

The Breadboard Design will then be updated to include the work of the Design Review Team prior to fabrication of the breadboard.

TASK XII - BREADBOARD FABRICATION AND TEST

12.1 ASSEMBLY

Based on the design of Task X and the design improvements of Task XI, the complete breadboard system will be assembled.

12.2 CIRCUITRY CHECKOUT

Prior to functional testing, all electrical circuitry will be checked, all instrumentation tested and standardized where required, and all switchgear tested for proper operation. The breadboard system will be installed in a protected remote location in the "fuel cell blockhouse" (EOS Bldg. 100, Room 122) with all power and instrumentation leads brought out to the control center. As discussed in Task VIII, all of the regenerative fuel cells will have been tested for two complete cycles before being assembled into the breadboard.

12.3 PRELIMINARY TESTING

Preliminary functional testing will consist of two complete cycles, using the standard 22.8 hour (or slightly less) charge and 1.2 hour discharge, for a total of 24.0 hours. The charging current will be slightly more than required to attain full charge in 22.8 hours, so that the pressure control switches will interrupt the charging current when the full charge condition is reached; the cells will then remain dormant in the fully charged condition until the beginning of discharge. After the two complete cycles, all components of the system will be inspected to the extent possible.

12.4 CYCLE TEST

The breadboard system will be subjected to the cyclic regime of Figure 56, modified to permit two cycles per day, for two complete eclipse seasons. The modification of the cyclic regime will be that charging of the 40 ampere-hour cells will be done at 4.0 amperes (10 hours maximum) and discharging at 33.3 amperes for the time indicated for the particular day of the eclipse season. Charge will be immediately after completion of the discharge; there will be a period of storage at full charge in each cycle between charge and discharge.

During this testing, system voltage and current will be continuously recorded. Individual cell voltages will be recorded to determine whether any individual cell is degrading at a different rate than the overall system; if this occurs, the cell will be replaced and subjected to extensive examination to determine the cause of degradation.

TASK XIII - DELIVERABLE HARDWARE

The breadboard regenerative fuel cell energy storage system fabricated and tested in Task XII will be delivered to the Air Force Aero Propulsion Laboratory as specified in Paragraph 6.3 of Exhibit A, Contract Number F33615-70-C-1671.

In addition, representative samples as described in Paragraph 6.4 will be delivered upon request. These samples will not be specifically fabricated for this purpose, but shall be items which are no longer needed for their original purpose because of failure, completion of test, or design change.

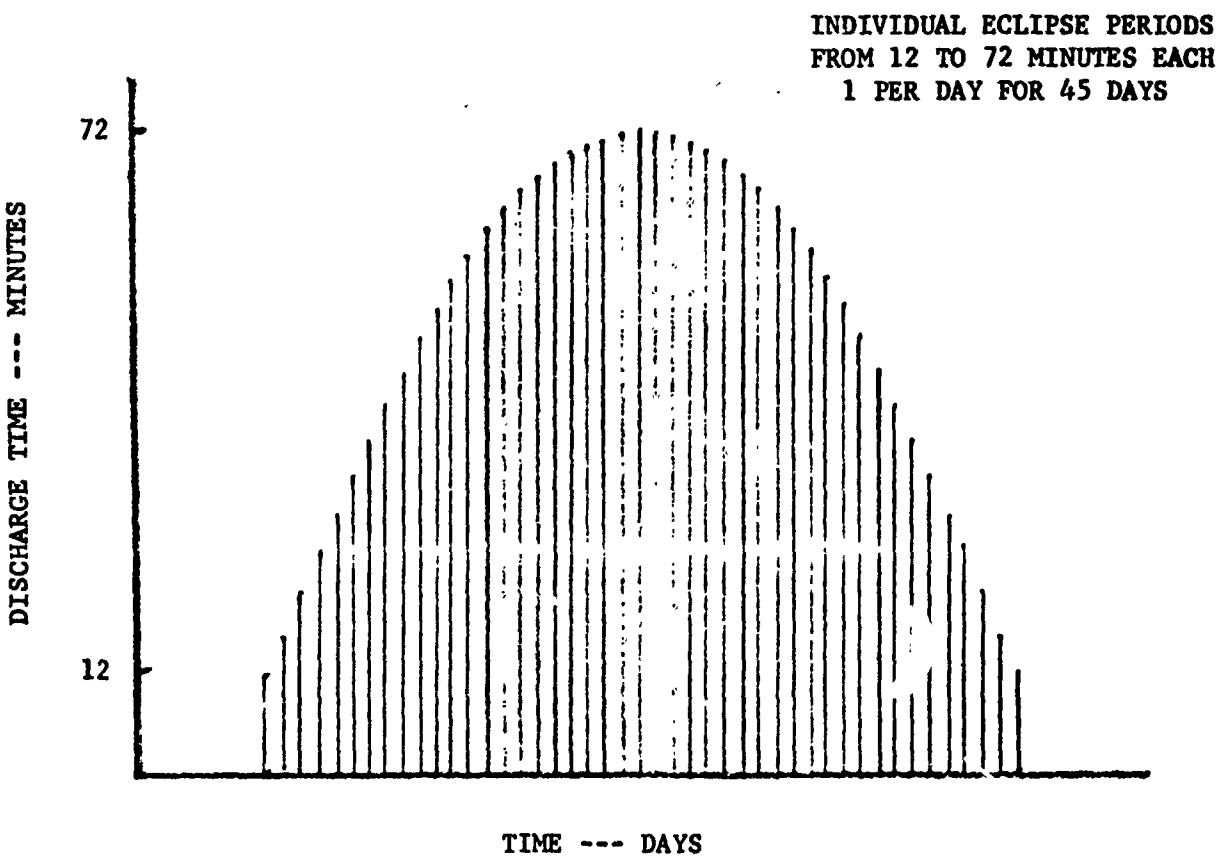

FIGURE 56. SINGLE ECLIPSE SEASON

APPENDIX II

BOILER-PLATE DESIGN ANALYSIS

1.0 PRELIMINARY DESIGN CALCULATIONS

The preliminary design calculations establish the dimensional parameters of a 40 A.H fuel cell at a discharge rate of 33.3 amps and subject to 600 psig at full charge.

1.1 Electrode Area

$$\frac{33{,}300 \text{ ma}}{78.5 \text{ ma/cm}^2} = 450 \text{ cm}^2 = 70 \text{ in}^2$$

1.2 Volume H_2

$$PV = ZNRT$$

$$N_{H_2} = 40 \text{ A-hr} \times 0.0374 \frac{\text{gm } H_2}{\text{A-hr}} \times \frac{\text{mole}}{2.016 \text{ gm/}H_2} = 0.75$$

$T = 50^{\circ}C = 323^{\circ}K$

$R = 82.057$

$P_1 = 100$ psi

$P_2 = 600$ psi

$A_P = 500$ psi $= 34$ atm.

$Z_{H_2} = 1.0395 \quad Z_{O_2} = 0.9849$

$$V_{H_2} = \frac{0.75\ (82.057)\ (323)\ (1.0195)}{34} = 596 \text{ cc} \qquad 36.4 \text{ in}^3$$

1.3 Volume O_2

$$\text{Required } V_{O_2} = Z \frac{V_{H_2}}{2}$$

$$V_{O_2} = (0.9849)\ (298\text{cc}) = 294\text{cc} \qquad 17.95 \text{ in}^3$$

1.4 CORE ID

$$\pi r^2 \ell = 36.4 \text{ in}^3$$

$$2 \pi r (\ell - 0.75) = 70 \text{ in}^2 \qquad \ell = \frac{36.4 \text{ in}^3}{\pi r^2}$$

$$2 \cancel{\pi} \cancel{r} \frac{36.4}{\cancel{\pi} r^{\cancel{2}}} - 1.5 \pi r = 70$$

$$\frac{72.8}{r} - 1.5 \pi r - 70 = 0$$

$$-1.5\pi r^2 - 70V + 72.8 = 0$$

$$r^2 + 14.9r - 15.5 - 0$$

$$r = - 14.9 \pm \sqrt{\frac{(14.9)^2 - 4 (-15.5)}{2}}$$

$$r = - 14.9 \pm \sqrt{\frac{222 + 662.0}{2}} = - 14.9 \pm \sqrt{\frac{284.0}{2}} = \frac{-14.9 \pm 16.85}{2}$$

$$r = \frac{1.95}{2} = 0.975$$

$$D = 1.95$$

$$\ell = \frac{36.4}{\pi (0.975)^2} = 12.2 \text{ in}$$

1.5 Dimensions of Pressure Vessel Using 2.45" ID

Required O_2 V = 17.95 in^3

Displaced Volumes

V core Assembly = $(1.11)^2 \pi$ (11.5) = 44.50 in^3

H_2 and O_2 tubes	=	0.03
O_2 current collector	=	0.05
Bellows clamping	=	0.08
Bellows	=	0.29
Edges $\pi(1)^2(.75)$	=	2.34
Total displaced vol.		47.29

Using 2.45 in. diameter

Va = 12.23 (π) $(1.225)^2$ - 47.53

57.7 in^3 - 47.29 = 10.41 in^3

$$V_b = \begin{array}{r} 17.95 \\ -10.41 \\ \hline = 7.54 \text{ in}^3 \end{array}$$

$$\ell_b = \frac{7.54}{\pi (1.225)^2} = 1.64 \text{ in}$$

$$\ell_a + \ell_b = 12.23 + 1.64 = 13.87 \text{ in.}$$

2.0 STRESS ANALYSIS

A stress analysis was performed on the flange of the boiler-plate pressure vessel using equations 32 shown in Figure 57. Values for the variables were calculated using the Fortran time share computer. This analysis showed the flange was not the critical area. The yield and burst pressures at the weakest section, the end plate, were calculated as follows:

2.1 YIELDING OF END PLATE

$$S_{r\ max} = \frac{3\ p\ \beta\ b^2\ (m+1)}{(4)\ 8\ \beta\ m\ h^2}$$

$b = 4.60$

$m = 1/\nu = 1/.33 = 3$

$h = .375$

$$S_{r\ max} = \frac{\beta\ (4.0)^2\ (4)^2}{(4)\ 2\ \beta\ (3)\ (.375)^2} \cdot p = \frac{8\ (64)}{9\ (4)} = \frac{128}{9}\ p$$

$$S_{r\ max} = 14.22\ P$$

2.2 YIELD PRESSURE

$$P_Y = \frac{S_Y\ p}{14.22} = \frac{42000}{14.22} = 2,953$$

M.S. at 2000 PSI with F.S. = 2

$$\text{YIELD M.S.} = \frac{S_Y\ p}{14.22\ (2000)\times 2} - 1 = \frac{42,000}{56,880} - 1 = -.2616$$

2.3 BURST PRESSURE

$$P_{BURST} = \frac{S_u}{14.22} = \frac{81,000}{14.22} = 5,696$$

M.S. at 2000 PSI with F.S. = 2

$$\text{BURST M.S.} = \frac{S_u}{56,880} - 1 = .42405$$

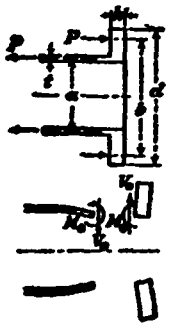 Flanged and bolted pipe	23. Uniform internal pressure, p lb. per sq. in.; longitudinal tension P lb.	$V_0 = \dfrac{\left(f^3 - \frac{h^3}{2k}T_1\right)(t + 0.2325f/T_1)p - 2T_2(h + 0.5577f)P}{1.866ft + T_1\left[h^3\left(2 + 0.1169\dfrac{f}{t}T_1\right) + 1.5108fh + 0.866f^2\right]}$ $M_0 = \dfrac{(h^2T_1 + 1.56ft)V_0 + hT_2P - 0.5kp\left(f^3 - \frac{h^3}{2k}T_1\right)}{1.5T_1h - 2.464t}$ where $f = \sqrt{ab}$; $T_1 = \dfrac{P(3a^2 + 5b^2)}{h^2(b^2 - a^2)}$; $T_2 = \dfrac{3.5b^2}{h^2(b^2 - a^2)}\left[\dfrac{a^2}{3}\log_e\dfrac{b}{a} + 0.1(b^2 - a^2)\right]$ Long. bending stress in cylinder: $s_1' = \dfrac{6M_0}{t^2}$. Radial bending stress in flange: $s_1' = \dfrac{6}{h^2}\left(M_0 - \dfrac{1}{2}Vsh\right)$ Long. direct stress in cylinder: $s_1 = \dfrac{P + p\pi(\frac{1}{2}a - \frac{1}{2}t)^2}{\pi at}$. Radial direct stress in flange: $s_1 = \dfrac{V_0}{h} + p$ Max long. stress in cylinder $= s_1' + s_1$ (tension at outer surface, at junction with flange). Tangential bending stress in flange: $s_2' = s_1' + \dfrac{0.78}{h^2(b^2 - a^2)}\left[a^2\left(-15.4M_0 + 7.5fV_0 + 1.462P\log_e\dfrac{b}{a}\right) + 0.4475p(b^2 - a^2)\right]$ Tangential hoop stress in flange: $s_2 = \dfrac{h^2}{4b^2}T_2(V_0 + kp)$ Max radial stress in flange $= s_1' + s_1$ (compression at outer face at junction with cylinder) Max tangential stress in flange $= s_2' + s_2$ (tension at inner face at junction with cylinder) (Ref. 19)

FIGURE 57. FORMULAS FOR STRESSES AND DEFORMATION IN PRESSURE VESSELS

3.0 THERMODYNAMIC ANALYSIS SUMMARY

The fuel cell configuration analyzed is shown in the attached Fig. 58. As shown, the fuel cell basically is a pressure vessel containing oxygen and hydrogen gases. These two gases are separated by a matrix material. The fuel cell design incorporates a flexible bellows between the two gases as means of minimizing pressure differences across the matrix material.

The first step in the analysis was to derive the governing equations. This was done in the following manner: First, the equations were derived for calculating the pressure difference across the matrix if there were no compensating bellows. Second, an equation for calculating necessary bellows volume was derived. Third, a total energy balance equation was established for the fuel cell. Solution of the third equation is required prior to evaluating the first two equations. Derivation of these equations follows:

3.1 Maximum Pressure Difference, No Bellows:

(The no-bellows infers a constant volume system)

Equation of State:

$$p_i V_i = w_i R_i T_i \qquad (1)$$

$$i = H_2;\ O_2$$

Taking the differential and dividing through by eq. (1), obtain:

$$\frac{dp_i}{p_i} = \frac{dw_i}{w_i} + \frac{dT_i}{T_i} \qquad (2)$$

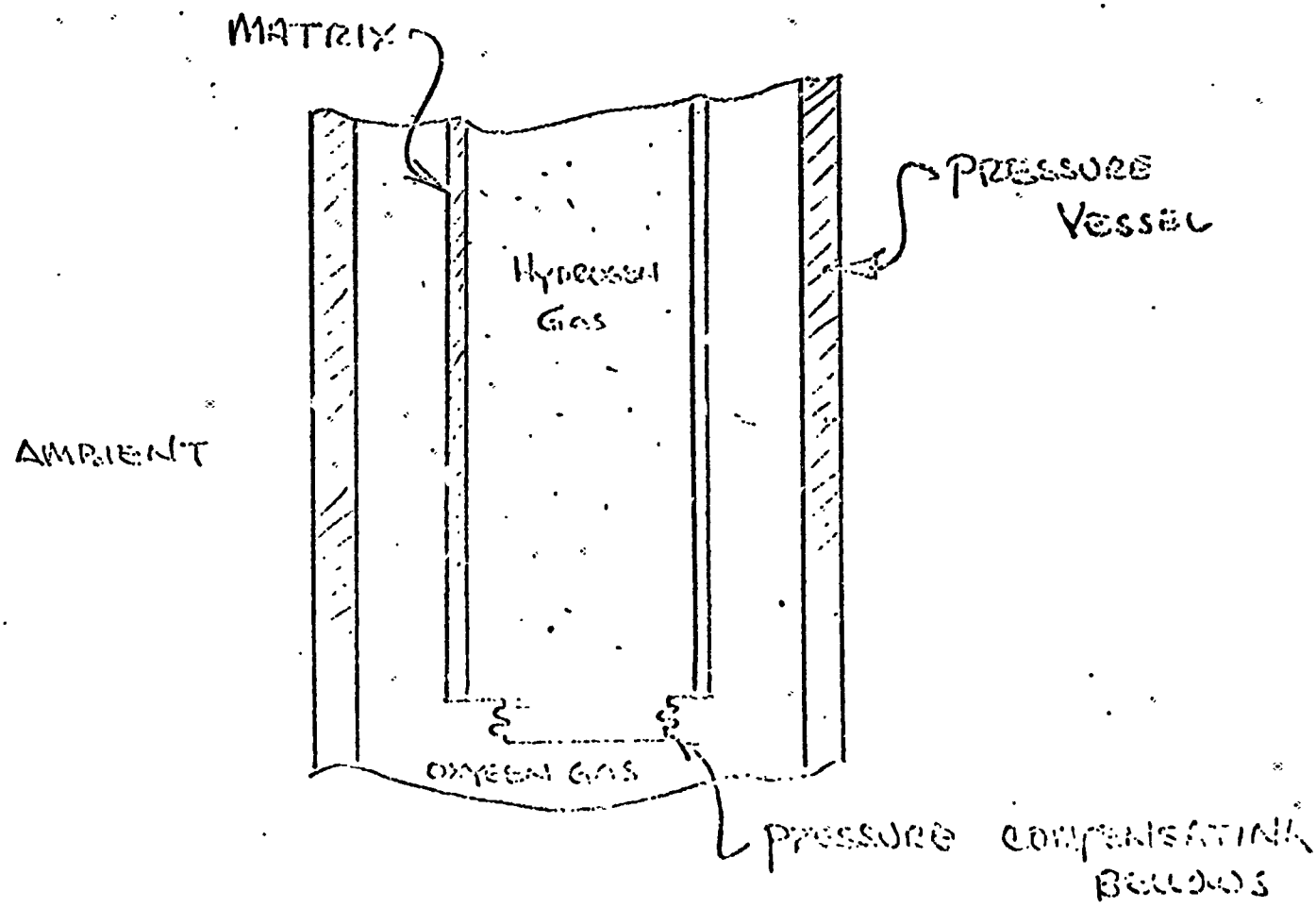

FIGURE 58. FUEL CELL CONFIGURATION

Note that: $$w_i = w_{0_i} + \dot{w}_i t \quad (3)$$

$$dw_i = \dot{w}_i \, dt \quad (4)$$

for $\dot{w}_i$ = constant

Substituting equations (3) and (4) into equation (2) and integrating, obtain:

$$p_i/p_{o_i} = T_i/T_{o_i} \left(\frac{w_{o_i} + \dot{w}_i \{t - t_o\}}{w_{o_i}} \right) \quad (5)$$

where: $p_i = p_{o_i}$; $T_i = T_{o_i}$ @ $t = t_o = 0$

Equation (5) may be used to calculate the hydrogen and oxygen gas pressures as a function of time once the temperature ratio (T_i/T_{0_i}) is known.

3.2 Required Bellows Volume:

The bellows volume required for pressure compensation is calculated in the following manner:

Equation of State:

At some point in time:

$$p_{O_{2_1}} V_{O_{2_1}} = w_{O_{2_1}} R_{O_2} T_{O_{2_1}} \quad (6)$$

$$p_{H_{2_1}} V_{H_{2_1}} = w_{H_{2_1}} R_{H_2} T_{H_{2_1}} \quad (7)$$

at some other point in time:

$$p_{O_{2_2}} V_{O_{2_2}} = w_{O_{2_2}} R_{O_2} T_{O_{2_2}} \quad (8)$$

$$p_{H_{2_2}} V_{H_{2_2}} = w_{H_{2_2}} R_{H_2} T_{H_{2_2}} \quad (9)$$

The bellows swept volume; ΔV:

$$\Delta V = \Delta V_{O_2} = V_{O_{2_2}} - V_{O_{2_1}} \tag{10}$$

$$\Delta V = \Delta V_{H_2} = V_{H_{2_2}} - V_{H_{2_2}} \tag{11}$$

and

$$\Delta V_{H_2} = - \Delta V_{O_2} \tag{12}$$

Note that:

$$P_{O_{2_1}} = P_{H_{2_1}} \; ; \; P_{O_{2_2}} = P_{H_{2_2}} \tag{13}$$

Therefore:

$$\frac{W_{O_{2_2}} R_{O_2} T_{O_{2_2}}}{V_{O_{2_2}}} = \frac{W_{H_{2_2}} R_{H_2} T_{H_{2_2}}}{V_{H_{2_2}}} \tag{14}$$

and:

$$V_{O_{2_2}} = V_{O_{2_1}} - \Delta V \tag{15}$$

$$V_{H_{2_2}} = V_{H_{2_1}} + \Delta V \tag{16}$$

Substituting equations (15) and (16) into equation (14) obtain the following equation for the swept volume of the bellows:

$$\Delta V = \frac{\left(W_{H_{2_2}} R_{H_2} T_{H_{2_2}}\right) V_{O_{2_1}} - \left(W_{O_{2_2}} R_{O_2} T_{O_{2_2}}\right) V_{H_{2_1}}}{\left(W_{H_{2_2}} R_{H_2} T_{H_{2_2}}\right) + \left(W_{O_{2_2}} R_{O_2} T_{O_{2_2}}\right)} \tag{17}$$

Equation (17) may be used to calculate the bellows swept volume necessary to equalize the H_2 and O_2 gas pressures for a given set of initial conditions $\left(V_{O_{2_1}} \text{ and } V_{H_{2_1}}\right)$ and a known or calculable set of different conditions $\left(W_{H_{2_2}} \; ; \; T_{H_{2_2}} \text{ and } W_{O_{2_2}} \; ; \; T_{O_{2_2}}\right)$.

3.3 Total Energy Balance

The energy balance for the fuel cell system is based on the premise that:

Heat is dissipated uniformly in the matrix during a charge or discharge condition and is ultimately lost to the surrounding environment by convection from the outer pressure vessel shell.

The heat dissipated by the matrix is either stored in the matrix material or transferred to the O_2 and H_2 gas:

$$Q = (wc)_M \frac{dT_M}{dt} + (hA)_M \left(T_M - T_{O_2}\right) + (hA)_M \left(T_M - T_{H_2}\right) \qquad (18)$$

An energy balance on the H_2 gas:

$$(hA)_M \left(T_M - T_{H_2}\right) = (wc)_{H_2} \frac{dT_{H_2}}{dt} \qquad (19)$$

An energy balance on the O_2 gas:

$$(hA)_M \left(T_M - T_{O_2}\right) = (wc)_{O_2} \frac{dT_{O_2}}{dt} + (hA)_{O_2} \left(T_{O_2} - T_s\right) \qquad (20)$$

An energy balance on the pressure vessel:

$$(hA)_{O_2} \left(T_{O_2} - T_s\right) = (wc)_s \frac{dT_s}{dt} + (hA)_s \left(T_s - T_a\right) \qquad (21)$$

The temperature history of the hydrogen and oxygen gas, the matrix material, and the pressure vessel may be obtained through the simultaneous solution of the four differential equations, (18), (19), (20), and (21). Obtaining the four simultaneous solutions as a function of time is a task for a rather sophisticated, 3-dimensional, transient, heat transfer computer program* and is beyond the scope of the present exercise. As a result some simplification was required.

*There are several such programs currently in use within the aerospace industry.

In evaluating system parameters, it is apparent that the significant heat dissipation is during the 72-minute discharge period, and that the dominant and controlling thermal mass in the system is that of the containment vessel. By neglecting 1) the thermal mass of the gases (a good assumption) and (2) the mass of the matrix (this is a reasonable assumption, but not nearly as legitimate as neglecting the mass of the two gasses), we may write:

$$Q = (wc)_s \frac{d T_s}{dt} + (hA)_s (T_s - T_a) \tag{22}$$

$$Q = (hA)_{O_2} \left(T_{O_2} - T_s\right) \tag{23}$$

$$Q = (hA)_M \left(T_M - T_{O_2}\right) \tag{24}$$

$$T_{H_2} = T_M \tag{25}$$

By further assuming that at the beginning of discharge:

$$T_{H_{2_o}} = T_{O_{2_o}} = T_{M_o} = T_{s_o} = T_a = T_o$$

equation (22) may be integrated to result in the following equation:

$$T_s = T_o + \frac{Q}{(hA)_s} \left(1 - e^{-(hA)_s t/(wc)_s}\right) \tag{26}$$

After solving equation (26) for T_s as a function of time, the remaining temperatures may be calculated:

$$T_{O_2} = T_s + \frac{Q}{(hA)_{O_2}} \tag{27}$$

$$T_M = T_s + \frac{Q}{(hA)_{O_2}} + \frac{Q}{(hA)_{H_2}} \tag{28}$$

Equations (5), (26), (27), (28), and (25) have been programmed for parametric evaluation and solved on the time share computer to obtain gas temperature and pressure histories during discharge. Having once obtained this data, the required bellows volume can be calculated from equation (17).

3.4 BELLOWS USING FULL BOILER PLATE VOL. AT 600 PSIG AND 100°C

$$\Delta V = \frac{N_{H_{2_2}} T_{H_{2_2}} V_{O_{2_1}} - N_{O_{2_2}} T_{O_{2_2}} V_{H_{2_1}}}{N_{H_{2_2}} T_{H_{2_2}} + N_{O_{2_2}} T_{O_{2_2}}}$$

$T_{H_{2_2}} = 1.133 \; T_{H_{2_2}} = 423°K$

$T_{O_{2_2}} = 1.088 \; T_{O_{2_1}} = 406°K$

$N_{H_{2_2}} = 0.90 \text{ M}, \; N_{O_{2_2}} = 0.45\text{M}$

$V_{H_{2_1}} = 596 \text{ cc}, \; V_{O_{2_1}} = 294 \text{ cc}$

$$\Delta V = \frac{(0.90\text{M})(423°K)(294\text{cc}) - (0.45\text{M})(406°K)(596\text{cc})}{(0.90\text{M})(423°K) + (0.45\text{M})(406°K)}$$

$$\Delta V = \frac{112{,}000 - 109{,}000}{381 + 182\text{-}5} = \frac{3000}{563.5} = 5.32 \text{ cc}$$

$.325 \text{ in}^3$

3.5 BELLOWS USING FULL BOILER PLATE VOL. AT 600 PSIG AND 50°C

$T_{H_{2_2}} = 1.153 \; T_{H_{2_1}} = 372$

$T_{O_{2_2}} = 1.10 \; T_{O_{2_1}} = 356$

$$\Delta V = \frac{(0.90)(372)(294) - (0.45)(356)(596)}{(0.90)(372) + (0.45)(356)}$$

$$\Delta V = \frac{95{,}900 - 93{,}800}{335 + 160} = \frac{2{,}100}{495} = 4.24 \text{ cc}$$

$.259 \text{ in}^3$

3.6 BELLOWS ADJUSTING BOILER PLATE VOL. TO 40 AH AT 1000 PSIG

$$PV = Z\,NRT$$

$P = 900$ psig $= 61.2$ atm.

$T = 373^{\circ}K$

$N = 0.75$ moles

$Z_{H_2} = 1.0312$

$R = 82.057$

$$V_{H_2} = \frac{1.0312\ (0.75)\ (82.057)\ (373)}{61.2} = 387\text{ cc}$$

23.6 in^3

$$V_{O_2} = Z_{O_2}\ \frac{V_{H_2}}{2} \qquad V_{O_2} = .9745\left(\frac{387}{2}\right) = 188\text{ cc}$$

$Z_{O_2} = .9745$ $\qquad 11.45\text{ in}^3$

3.7 BELLOWS VOLUME AT 100°C, 1000 PSIG, (40 AH)

$$\Delta V = \frac{N_{H_{2_2}}\ T_{H_{2_2}}\ V_{O_{2_1}} - N_{O_{2_2}}\ T_{O_{2_2}}\ V_{H_{2_1}}}{N_{H_{2_2}}\ T_{H_{2_2}} + N_{O_{2_2}}\ T_{O_{2_2}}}$$

$T_{H_{2_{1000}}} = 1.133\ (373^{\circ}K) = 423^{\circ}K$

$T_{O_{2_{1000}}} = 1.088\ (373^{\circ}K) = 406^{\circ}K$

$N_{H_{2_2}} = 0.825M$, $N_{O_{2_2}} = 0.4125M$

$V_{H_{2_1}} = 3.87$cc, $V_{O_{2_1}} = 188$ cc

$$\Delta V = \frac{(0.825M)\ (423^{\circ}K)\ (188\text{ cc}) - (0.4125M)\ (406^{\circ}K)\ (387\text{ cc})}{(0.825M)\ (423^{\circ}K) + (0.4125M)\ (406^{\circ}K)}$$

$$\Delta V = \frac{65,500 - 64,600}{349 + 167.5} = \frac{900}{516.5} = 1.74\text{ cc}$$

0.0106 in^3

3.8 BELLOWS USING FULL BOILER PLATE VOLUME AND CHARGING TO 1000 PSIG.

$$\Delta V = \frac{\left(N_{H_{2_2}} \; T_{H_{2_2}} \; V_{O_{2_1}} - N_{O_{2_2}} \cdot T_{O_{2_2}} \; V_{H_{2_1}}\right)}{\left(N_{H_{2_2}} \; T_{H_{2_2}} + N_{O_{2_2}} \; T_{O_{2_2}}\right)}$$

For 100°C and 1000 psig use in 40 AH volume.

$$T_{H_{2_2}} - 1.133 \; T_{H_{2_1}} = 1.133 \; (373) = 423^{\circ}K$$

$$T_{O_{2_2}} = 1.088 \; T_{O_{2_1}} = 1.088 \; (373) = 406^{\circ}K$$

$$N_{H_{2_2}} = 1.50 \text{ moles}$$

$$N_{O_{2_2}} = 0.75 \text{ moles}$$

$$V_{H_{2_1}} = 596 \text{ cc}$$

$$V_{O_{2_1}} = 294 \text{ cc}$$

$$\Delta V = \frac{(1.50M)\ (423^{\circ}K)\ (294\ cc) - (0.75M)\ (406^{\circ}K)\ (596cc)}{(1.50M)\ \ (423^{\circ}K) + (0.75M)\ (406^{\circ}K)}$$

$$\Delta V = \frac{(186{,}000cc) - (151{,}200cc)}{(6.35) \quad + (304)}$$

$$\Delta V = \frac{34{,}800cc}{939} = 36.1 \text{ cc}$$

$$2.265 \text{ in}^3$$

TABLE V

NOMENCLATURE DEFINITION

A - Area

c - Specific heat

h - Heat Transfer coefficient

p - Pressure

Q - Heat dissipation rate

R - Gas constant

T - Temperature

V - Volume

w - Weight

APPENDIX III

RANDOM VIBRATION ANALYSIS

1.0 INTRODUCTION

A random vibration analysis was performed to verify the lightweight regenerative fuel cell design,shown in Figure 59, and to optimize the mounting configuration for the stacking of the cells in series. The extent of the analysis was limited to the outer shell and the core, which is the inner tube with the electrodes.

2.0 SUMMARY

The design for the lightweight fuel cell is structurally sound, provided that added supports are made to both the forward and aft ends of the core. The locations of the supports on both the core and outer shell are not critical. Figure 71 shows a free-body diagram of the recommended design.

3.0 DISCUSSION

3.1 DESIGN PARAMETERS

Figure 60 shows the acceleration spectral density spectrum to be used for the design analysis. During the random vibration excitation, the internal pressure of the shell and the pressure drop across the core were assumed to be 600 and 0 psi, respectively.

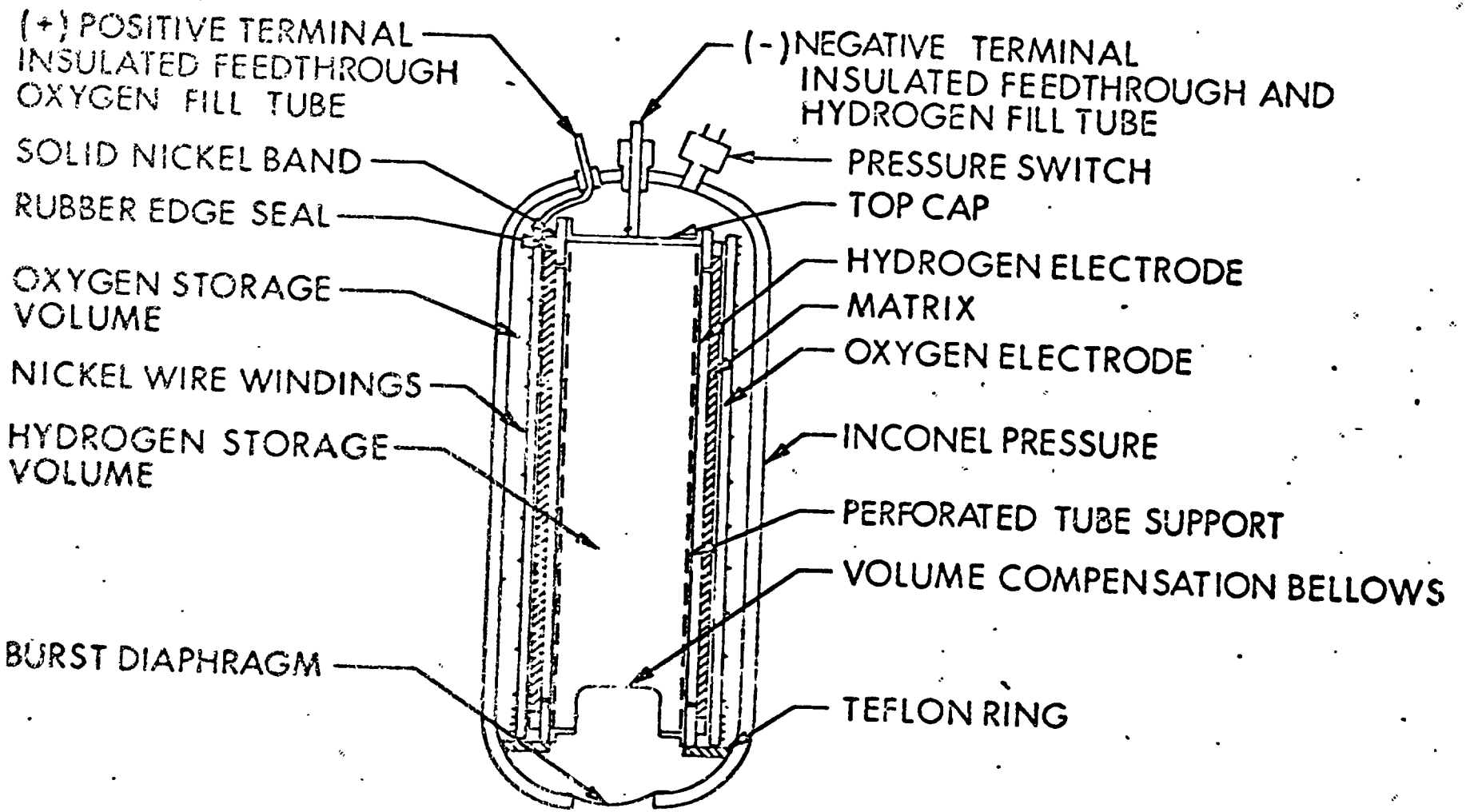

Figure 59. Cylindrical Regenerative Fuel Cell Construction

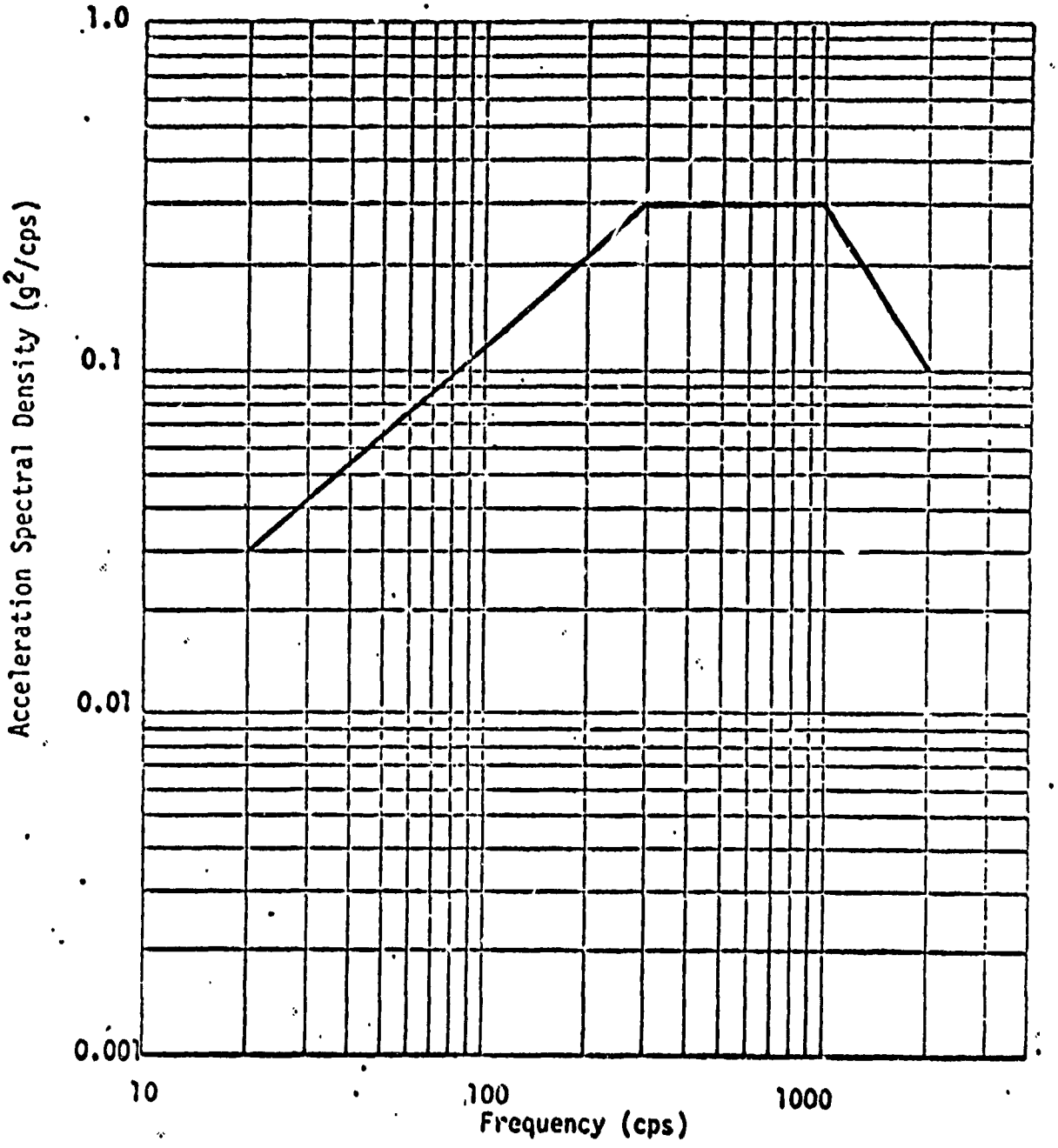

Figure 60

Random Vibration Environment

3.2 PEAK CRITERION IN RANDOM VIBRATION TESTING

3.2.1 Overall Acceleration Spectral Density

The overall spectrum is given by:

$$grms = \left(\Sigma \int_{f_1}^{f_2} W(f)df\right)^{\frac{1}{2}}$$

$$= \left(\int_{20}^{300} .00236\ f^{.849}df\right)^{\frac{1}{2}} + \left(\int_{300}^{1000} .3df\right)^{\frac{1}{2}} + \left(\int_{1000}^{2000} 17700f^{-1.59}df\right)^{\frac{1}{2}}$$

$$grms = 6.95 + 14.5 + 13.1 = \underline{34.55\ g's}$$

3.2.2 Equivalent Peak Sinusoidal Vibration

The equivalent sinusoidal vibration based on the random vibration spectrum is given by:

$$Ae = 3\left(\frac{\pi}{2}\ \frac{W(fn)\ fn}{Q}\right)^{\frac{1}{2}}$$

where

Ae = Equivalent sinusoidal input, g's rms
W(fn) = Acceleration spectral density at resonance
fn = Resonant frequency
Q = Dynamic magnification

The factor 3 is used to envelope the 3σ peaks of the random spectrum. The 0-peak sine vibration is:

$$A = \sqrt{2}\,Ae$$

$$A = 3\left(\frac{\pi W(fn)fn}{Q}\right)^{\frac{1}{2}}$$

The maximum acceleration response is:

$$\ddot{W} = QA$$

$$\ddot{W} = 3\sqrt{\pi QW(fn)fn} \qquad (1)$$

If the natural frequency is greater than 2000 Hertz, the maximum acceleration response is tabulated below at the transition points of the spectrum. The dynamic magnification (Q) is equal to one.

f	W(f)	W(f)f	$\ddot{W}(gs)$
300	.3	90	50.4
1000	.3	300	92
2000	.1	200	75

The maximum response for a natural frequency greater than 2000 Hertz is 92 g's. This response exceeded the overall spectrum input of 34.55 g's (see Section 3.2.1).

3.3 OUTER SHELL ANALYSIS

3.3.1 Natural Frequency of Shell

The outer shell will be secured at two locations as shown in Figure 61.

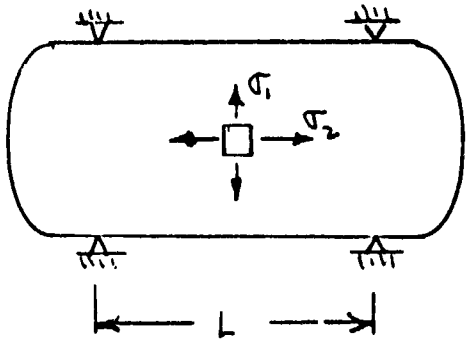

OUTER SHELL FREE-BODY DIAGRAM

Figure 61

The distance between the supports will be treated as a variable.

The internal pressure will greatly influence the natural frequency of the system. The expression for the natural frequency of a pressurized cylinder is given by:

$$\frac{\rho r^2}{E}\omega_n^2 = \frac{\lambda^4}{(n^2+\lambda^2)^2} + \frac{(t/r)^2(n^2+\lambda^2)^2}{12(1-\nu^2)} + \bar{n}_x\lambda^2 + \bar{n}_\varphi n^2 \qquad (2)$$

and $f_n = \frac{\omega_n}{2\pi}$

where

ω_n = Angular natural frequency, rad/sec

$\bar{n}_x = \frac{pr}{2Et}$ $\qquad \bar{n}_\varphi = \frac{pr}{Et}$ $\qquad \lambda = \frac{m\pi r}{L}$

p = Internal pressure = 600 psi

r = Tube radius = 1.23 inch

t = Tube wall thickness = .020 inch

E = Modulus of Elasticity = 31×10^6 psi

L = Length between supports, in.

ν = Poisson's ratio = .32

m = Number of axial half waves = 1

n = Number of circumferential waves = 2

ρ = Mass density = .307/386 = .000795 lb-sec^2/in^4

Figure 62 is a plot of the natural frequency (f_n) versus the length (L). The frequencies are all near 2000 Hz, and the responses will have small amplitudes.

FIGURE 62. OUTER SHELL NATURAL FREQUENCY

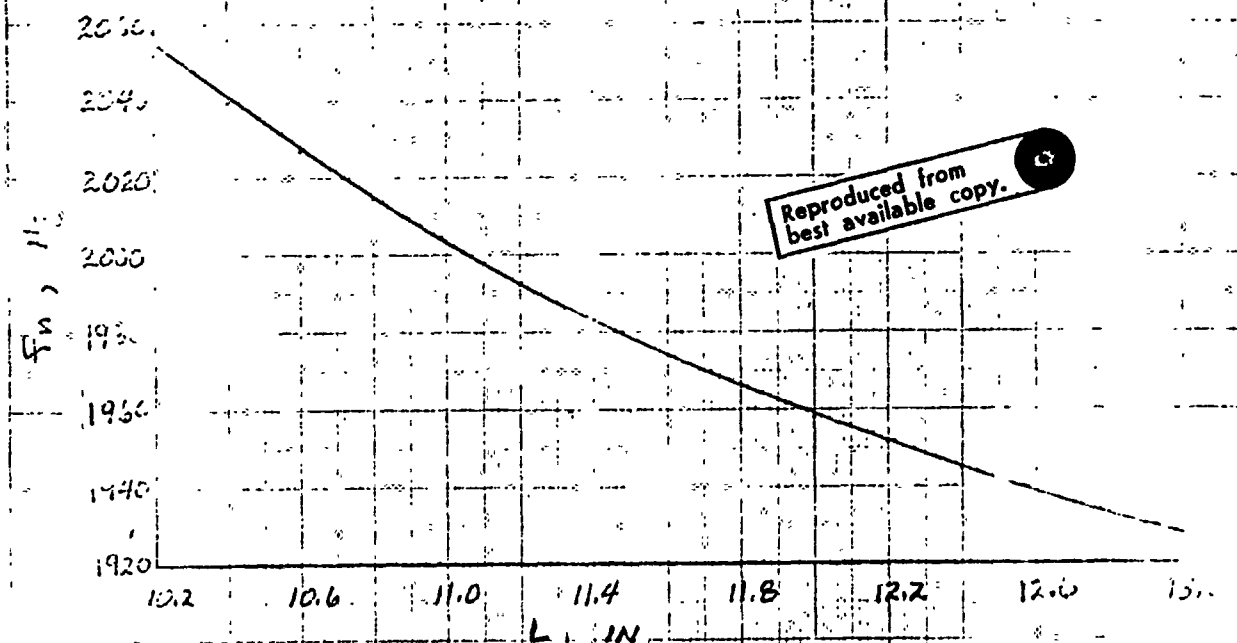

FIGURE 63. OUTER SHELL STRESS

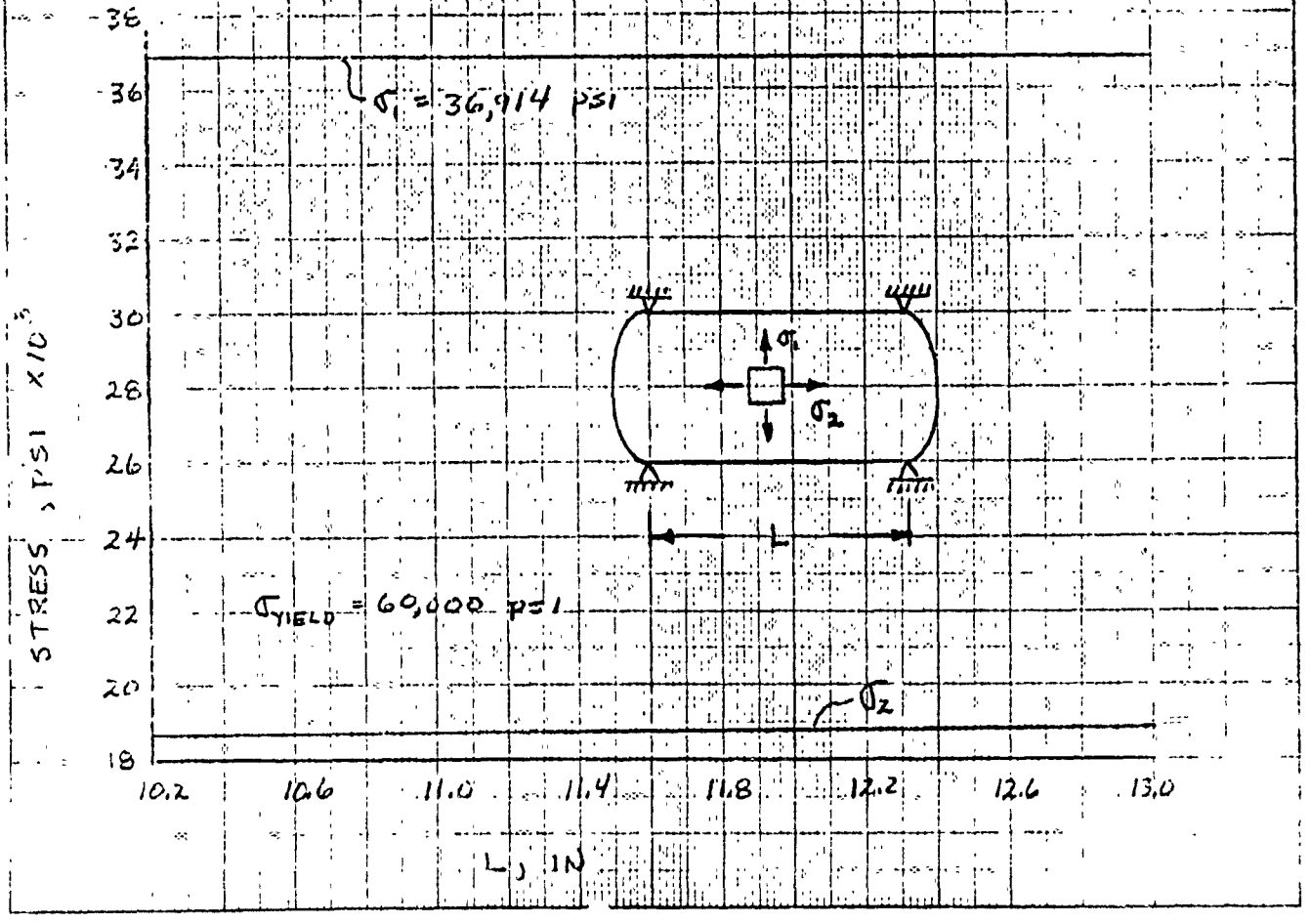

3.3.2 Stress on Shell

With the extremely high natural frequency of the shell, the maximum acceleration from the random vibration is 92 g's (see Section 3.2.2). As shown in Figure 61, the two stress components are given by:

$$\sigma_1 = \frac{qr}{t} + \frac{pr}{t} \qquad (3)$$

$$\sigma_2 = \frac{qL^2}{4rt} + \frac{pr}{2t} \qquad (4)$$

where

p = 600 psi

q = Inertia loading component normal to the surface

$= \ddot{W}_{ave}\,\omega$

Assuming the acceleration response to have sinusoidal distribution over the length of the shell

$$\ddot{W}_{ave} = \frac{4}{\pi^2}\,\ddot{W} = \frac{4}{\pi^2}(92) = 37.4 \text{ g's}$$

$$\omega = \rho t = .307 \frac{\text{lb}}{\text{in}^3} \times .020 \text{ in} = .00614 \text{ lb/in}^2$$

Substituting

$$q = (37.4)(.00614) = .25 \text{ lb/in}^2$$

The resulting stresses are shown in Figure 63. The length between the supports (L) has very little effect on the σ_2 stress. As shown, the stresses are below the yield strength of Inconel 625.

3.3.3 Buckling of Shell

The critical buckling stress of a pressurized cylinder is given by:

$$\sigma_{cR} = (C_b + \Delta C_b) \frac{Et}{r} \qquad (5)$$

The constants C_b and ΔC_b are a function of r/t and $\frac{P}{E}(\frac{r}{t})^2$, respectively. The internal pressure increases the critical buckling stress. From "Shell Analysis Manual" by E. Baker

$$C_b = .325$$

$$\Delta C_b = .23$$

Solving

$$\sigma_{cR} = 270{,}000 \text{ psi}$$

The buckling stress exceeds the design stresses by a large margin.

3.4 CORE ANALYSIS

As shown in Figure 59, the core is a multi-layer cylinder. It is assumed that the perforated Inconel tube provides the strength and stiffness for the entire assembly. No pressure drop across the surface of the core is assumed.

3.4.1 Equivalent Core Wall Thickness

Since the Inconel tube is perforated, an equivalent wall thickness is calculated to simulate the same stiffness and load carrying capability. Figure 64 shows a typical perforated surface.

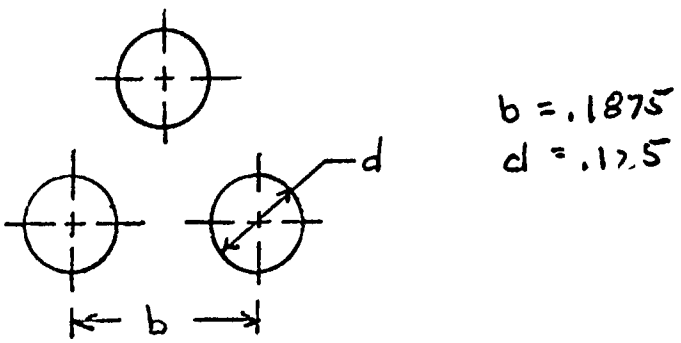

TYPICAL PERFORATED SURFACE

Figure 64

The equivalent thickness is calculated as follows:

$$bt_{EQ} = (b-d)t$$

$$t_{EQ} = \frac{(b-d)t}{b} = \frac{(.0625)\ t}{.1875} = .333\ t$$

$$= .00667 \quad \text{(for } t = .020\text{")}$$

$$= .00334 \quad \text{(for } t = .010\text{")}$$

10% is added for the plaque, matrix and sintered nickel.

$$t_{EQ} = .00734 \text{ in.} \quad \text{(for } t = .020\text{")}$$

$$= .00367 \quad \text{(for } t = .010\text{")}$$

3.4.2 Natural Frequency of Core

As shown in Figure 59, the core is restrained by a tube in the axial direction. The lowest frequency mode occurs at the top cap which acts as a diaphragm with a concentrated load in the center. Figure 65 shows a model of the top cap.

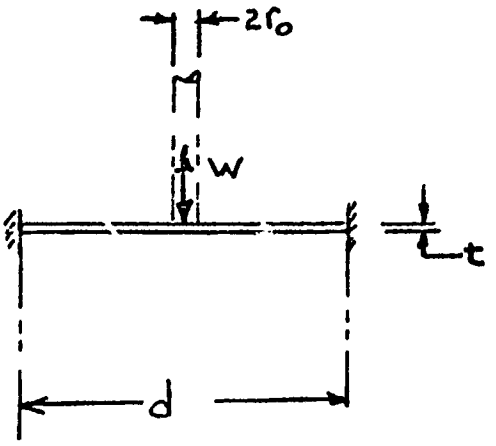

MODEL OF TOP CAP

Figure 65

The natural frequency is given by:

$$fn = \frac{4.09}{2\pi}\sqrt{\frac{Et^3g}{Wd^2(1-\nu^2)}}$$

where

$E = 30 \times 10^6$ psi

$t = .020$ in

$d = 1.96$ in

$\nu = .3$

$W = .77$ lb

substituting

$fn = 123$ Hertz

Two configurations were analyzed for vibration in the lateral direction. They are shown in Figure 66.

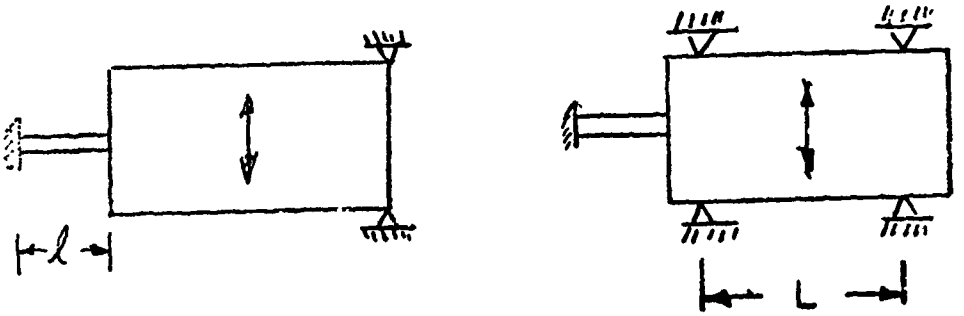

Configuration 1 Configuration 2

LATERAL VIBRATION OF CORE

Figure 66

Configuration 1 depicts the current design. The tube length (ℓ) has not been selected. Since the core is much stiffer than the tube, the effect of the core can be ignored in the frequency equation. The natural frequency is given by:

$$f_n = \frac{1}{2\pi}\sqrt{\frac{6EI}{W\ell^3}}$$

where

$E = 30 \times 10^6$ psi

$I = .785(r_o^4 - r_i^4) = .785(.125^4 - .030^4) = .000191 \text{ in}^4$

W = Total weight of core = .77 lb

ℓ = Length of tube, in.

Substituting

$$f_n = 660\sqrt{1/\ell^3} \qquad (6)$$

The frequencies are plotted in Figure 67.

FIGURE 67. NATURAL FREQUENCY OF CORE - CONF. 1

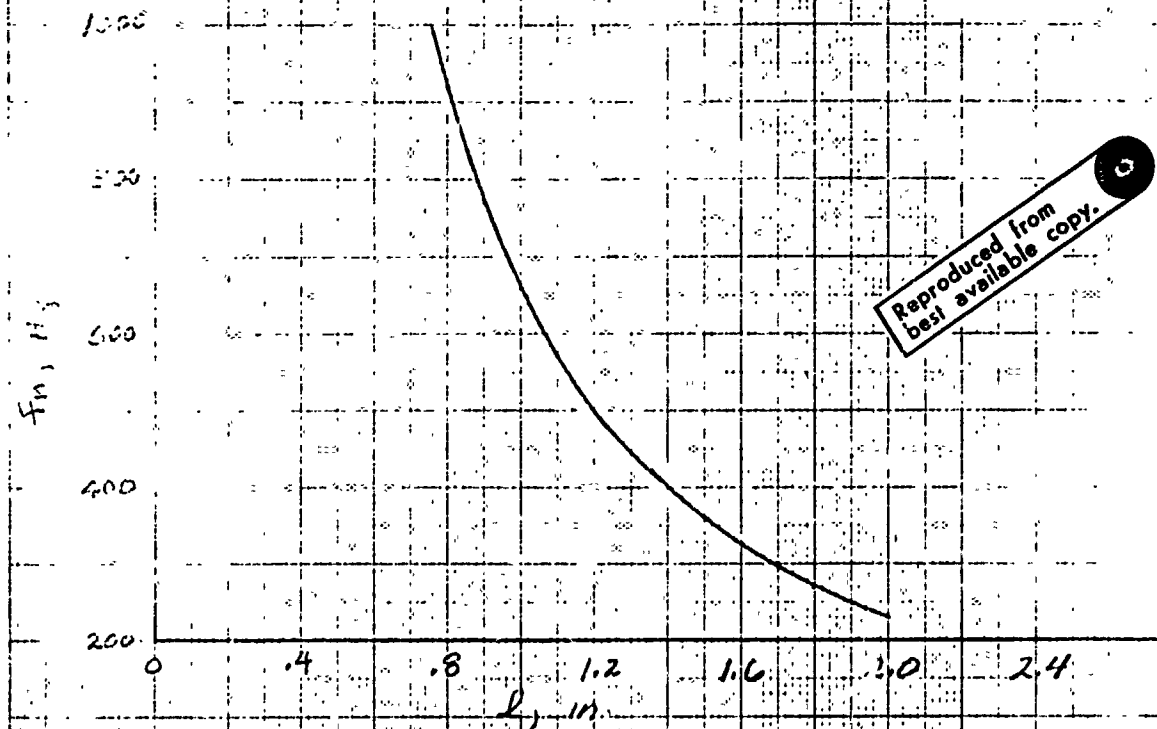

FIGURE 68. NATURAL FREQUENCY OF CORE - CONF. 2

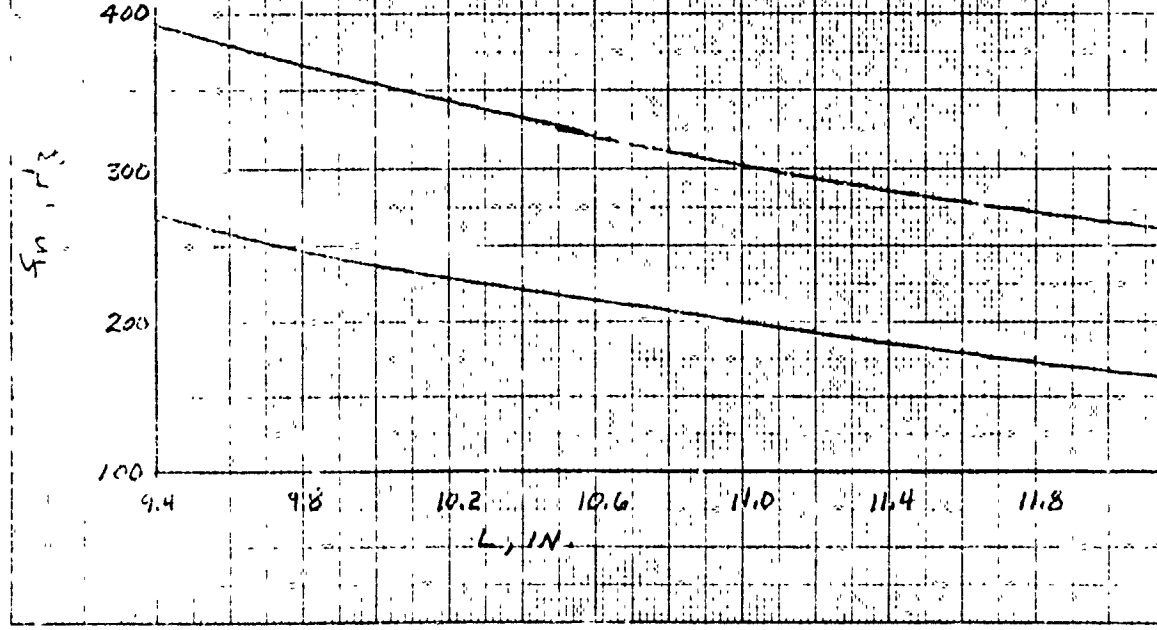

The natural frequency for Configuration 2 is given by Equation 2. Since the perforated cylinder is also made from Inconel 625, the mechanical properties are the same as the outer shell. The different variables are:

$r = .98$ in.

$t = .00734$ in (See Section 3.4.1)

$p = 0$ psi

$$\rho = \frac{(\rho t)}{tg} = \frac{\omega}{tg} = \frac{.01149}{(.00734)(386)} = .00407 \text{ lb-sec}^2/\text{in}^4$$

The results are plotted in Figure 68.

3.4.3 Stress on Core

For vibration in the axial direction (see Figure 65), the maximum stresses on the top cap are:

$$\sigma_r = \frac{3W}{2\pi t^2}\left(1 - \frac{2r_o^2}{d^2}\right)$$

$$\sigma_t = \frac{3W}{2\pi m t^2}\left(1 - \frac{2r_o^2}{d^2}\right)$$

where

σ_r = Radial stress

σ_t = Tangential stress

$W = \ddot{W}\, W_{core}$

$$\ddot{W} = 3\sqrt{\pi Q W (f_n) f_n} \qquad \text{(Equation 1)}$$

Assume $Q = 15$

$W(f_n) = .00236\ f_n^{.849}$ (See Section 3.2.1)

$f_n = 123$ Hertz (See Section 3.4.2)

Substituting

$W'' = 83.6$

$W = 83.6 \times .77 = 63.3$ lb

r_o = Tube radius = .125 in.

$m = 1/\nu = 1/.3 = 3.33$

$d = 1.96$ in

$t = .020$ in

Substituting into the stress equations

$\sigma_r = 75{,}000$ psi

$\sigma_t = 22{,}600$ psi

The yield strength of the Inconel 625 is 60,000 psi. Therefore, failure is predicted unless an additional support is made to restrain the core in the axial direction.

The tube stress from the lateral vibration on Configuration 1, shown in Figure 66, is given by:

$$\sigma = \frac{Md}{2I}$$

where

$$M = \ddot{W} \frac{W}{2} \ell$$

$$\ddot{W} = 3\sqrt{\pi Q W(f_n) f_n} \qquad \text{(Equation 1)}$$

$$W(f_n) = .00236\, f_n^{.849} \qquad \text{(See Section 3.2.1)}$$

$$f_n = 660\sqrt{1/\ell^3} \qquad \text{(Equation 6)}$$

$$W = .77 \text{ lb}$$

$$d = .25 \text{ in}$$

$$I = .000191 \text{ in}^4$$

Figure 69 shows the results of the tube stress. The stresses are all above the yield strength of pure nickel which is 50,000 psi. Therefore, the current design, depicted by Configuration 1 in Figure 66, will not work.

The stresses on the core for Configuration 2 are given by Equations 3 and 4. Since the pressure drop across the surface is zero, the equations are reduced to:

$$\sigma_1 = \frac{qr}{t}$$

$$\sigma_2 = \frac{qL^2}{4rt}$$

where

$$q = \ddot{W}_{ave}\, \omega$$

$$\ddot{W} = 3\sqrt{\pi Q W(f_n) f_n} \qquad \text{(Equation 1)}$$

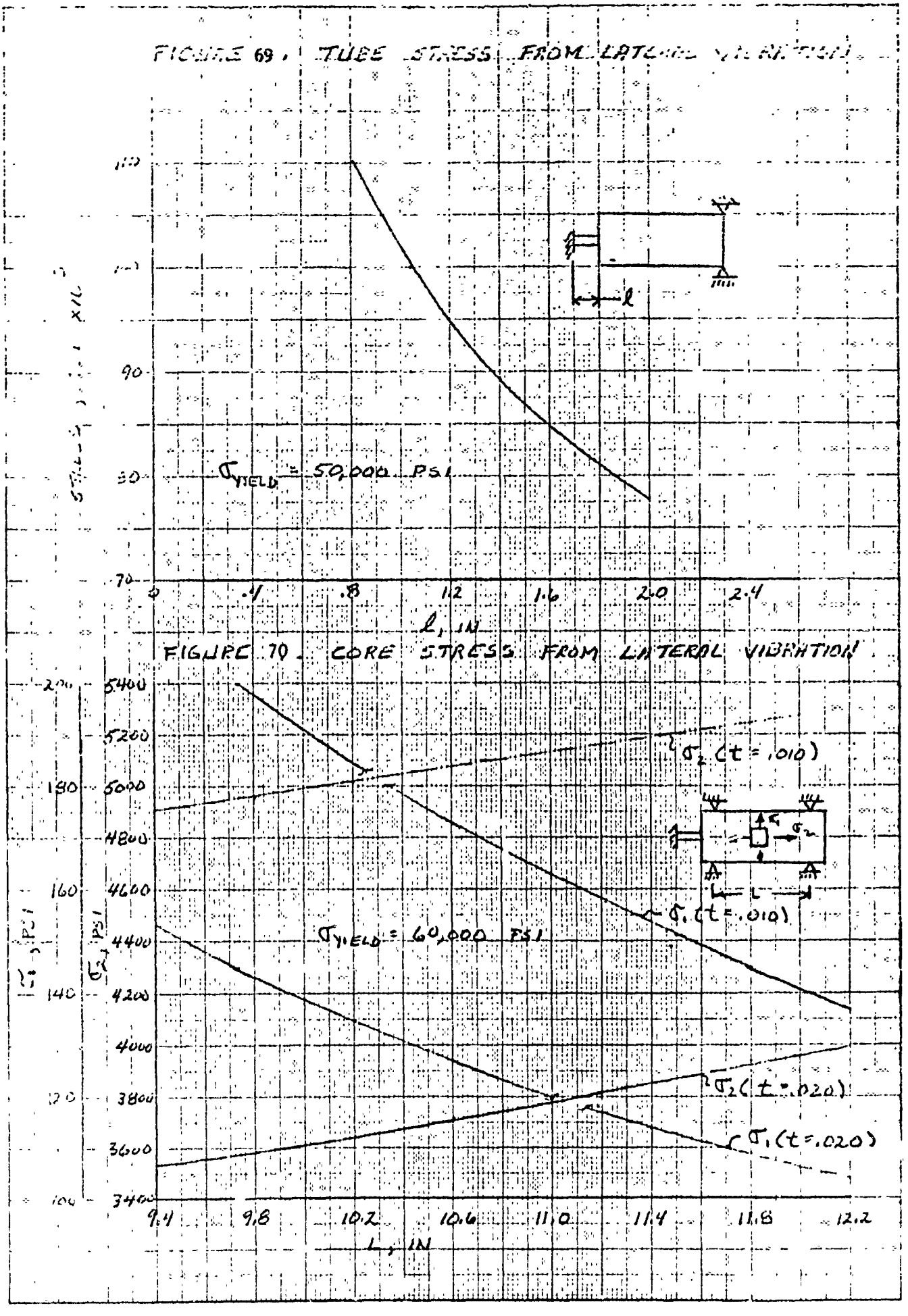

Assume Q = 15

$W(f_n) = .00236\ f_n^{.849}$ (See Section 3.2.1)

f_n = Figure 9

$\ddot{W}_{ave} = \frac{4}{\pi^2} \ddot{W}$ (Assume Sinusoidal Distribution)

r = .98 in

t = .00734 in (for t actual = .020)

= .00367 in (for t actual = .010)

The results are plotted in Figure 70. As shown, the stresses are below the yield strength of Inconel 625 which is 60,000 psi. Therefore, an additional support at the front end of the core is needed for the lateral vibration.

3.4.4 Buckling of Core

Equation 5 is used to determine the critical buckling stress of the perforated Inconel cylinder. With no pressure drop (p=0), the equation is:

$$\sigma_{CR} = C_b E \frac{t}{r}$$

where

C_b = .325 (for t actual = .020)

= .28 (for t actual = .010)

r = .98 in.

t = .00734 in. (for t actual = .020)

= .0036 (for t actual = .010)

Substituting

σ_{CR} = 73,000 psi (for t actual = .020)

= 32,400 psi (for t actual = .010)

The buckling stresses exceed the design stresses by a large margin.

3.5 CONCLUSION

Results from the dynamic and stress analyses indicate that:

(1) An additional restraint is necessary on the aft end of the core for vibration in the axial direction.

(2) An additional restraint is necessary on the forward end of the core for vibration in the lateral direction.

(3) The unsupported lengths of the core and outer shell are not critical. The supports should be in line, as shown in Figure 71, for continuity of the load path.

Figure 71 shows the recommended design.

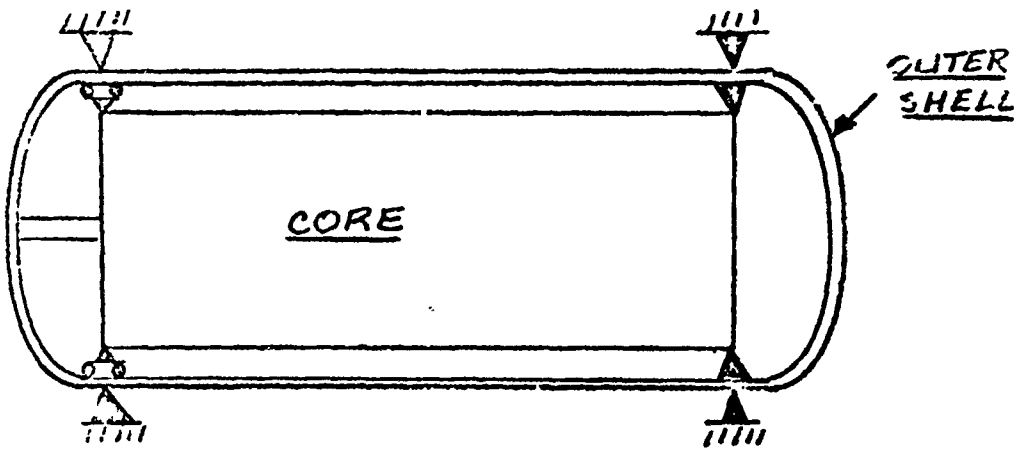

FIGURE 71. RECOMMENDED DESIGN - FREEBODY DIAGRAM

APPENDIX IV

THERMODYNAMIC ANALYSIS

A flow diagram depicting the anlaysis program to calculate respective gas pressures as a function of time is shown in Table VI. The thermodynamic analysis procedure has been explained in Appendix II as a segment of the boiler-plate design analysis.

An initial computed plot of gas pressures as a function of time during the discharge mode is shown in Figure 72. The plots of pressure differentials of the hydrogen gas and the oxygen gas during discharge are shown in Figure 73. The latter figure demonstrates the effect of mass imbalance on the pressure differential during discharge. Figure 74 demonstrates a series of plots of gas pressures of a balanced system and the pressure effect of systems with deliberate mass and volume imbalance. An explanation of each of the curves of Figure 74 is as follows:

Curve #1 - Balanced System

This curve represents a molarity balance between the H_2 and O_2. The H_2 volume is twice the O_2 volume (corrected for compressibility) representing the theoretical (no tolerances considered) volume of the current fuel cells. The initial mass of H_2 and O_2 is calculated from:

$$W_{O_2} = \left(\frac{PV}{ZRT}\right)_{O_2} \quad \text{and} \quad W_{H_2} = \left(\frac{PV}{ZRT}\right)_{H_2}$$

Where the initial pressure for each gas is 600 psi, the volumes are balanced as described above, the temperature is T = 582°R (50°C), and the gas constants and compressibility factors are values for the respective gases. It should be noted the initial pressures are not balanced since we have a small ΔP at time zero in Curve #1. This is due to the heat transfer portion of the original computer program which predicts immediate temperature differentials in the cell. This inaccuracy has been corrected with a new and more sophisticated heat transfer portion of the program.

Curve #2

The balanced mass of H_2 calculated for Curve #1 was arbitrarily increased 1 percent, thus slightly increasing the pressure of the H_2. The program calculates the initial increased pressure of the H_2 and the resulting effect upon the initial O_2 pressure due to bellows deflection. All other input parameters are the same as Curve #1.

TABLE VI

FLOW DIAGRAM FOR SYSTEM ANALYSIS - H_2 O_2 FUEL CELL

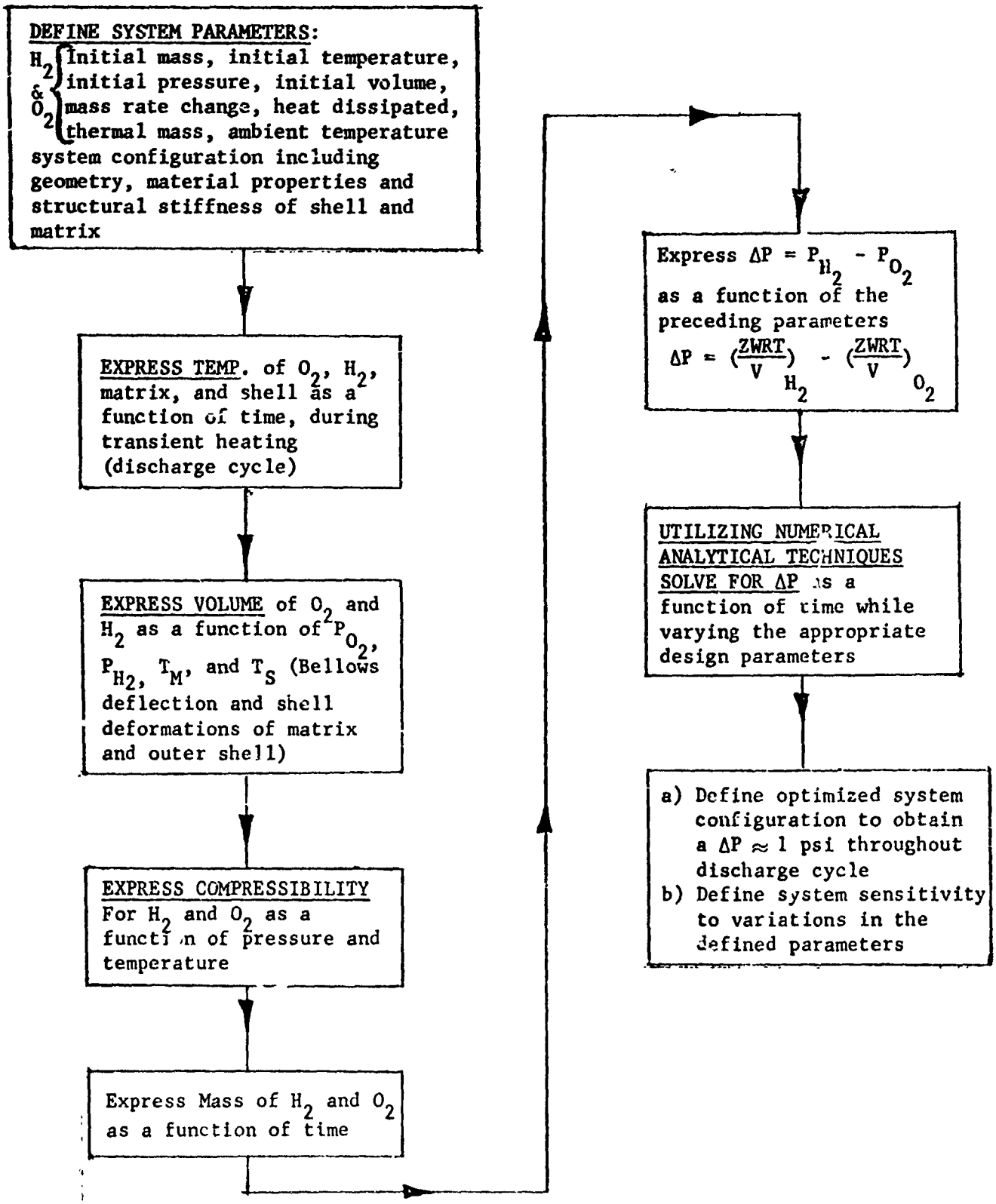

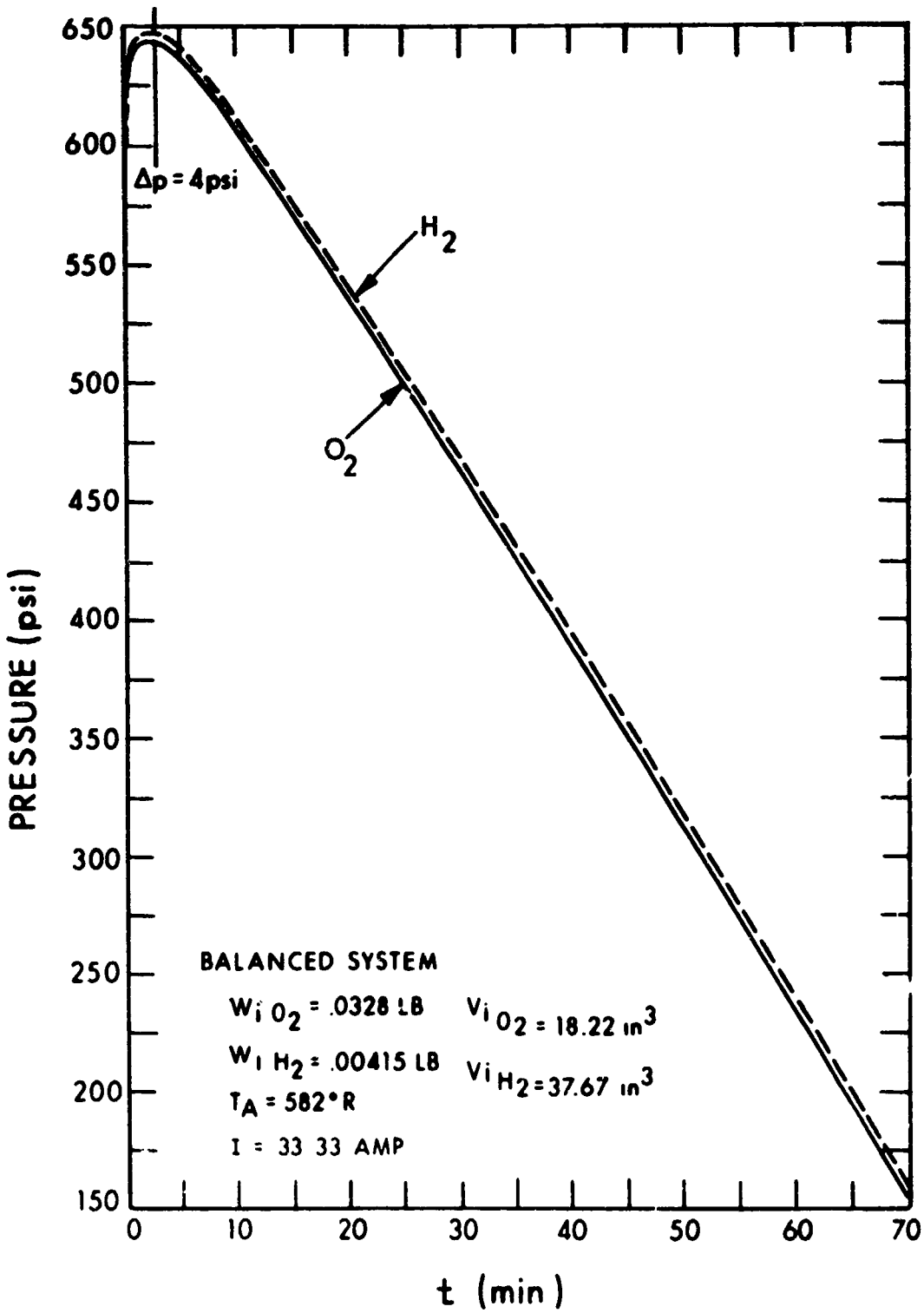

FIGURE 72. PRESSURE PLOTS OF BOILERPLATE FUEL CELL DISCHARGE CYCLE

41713

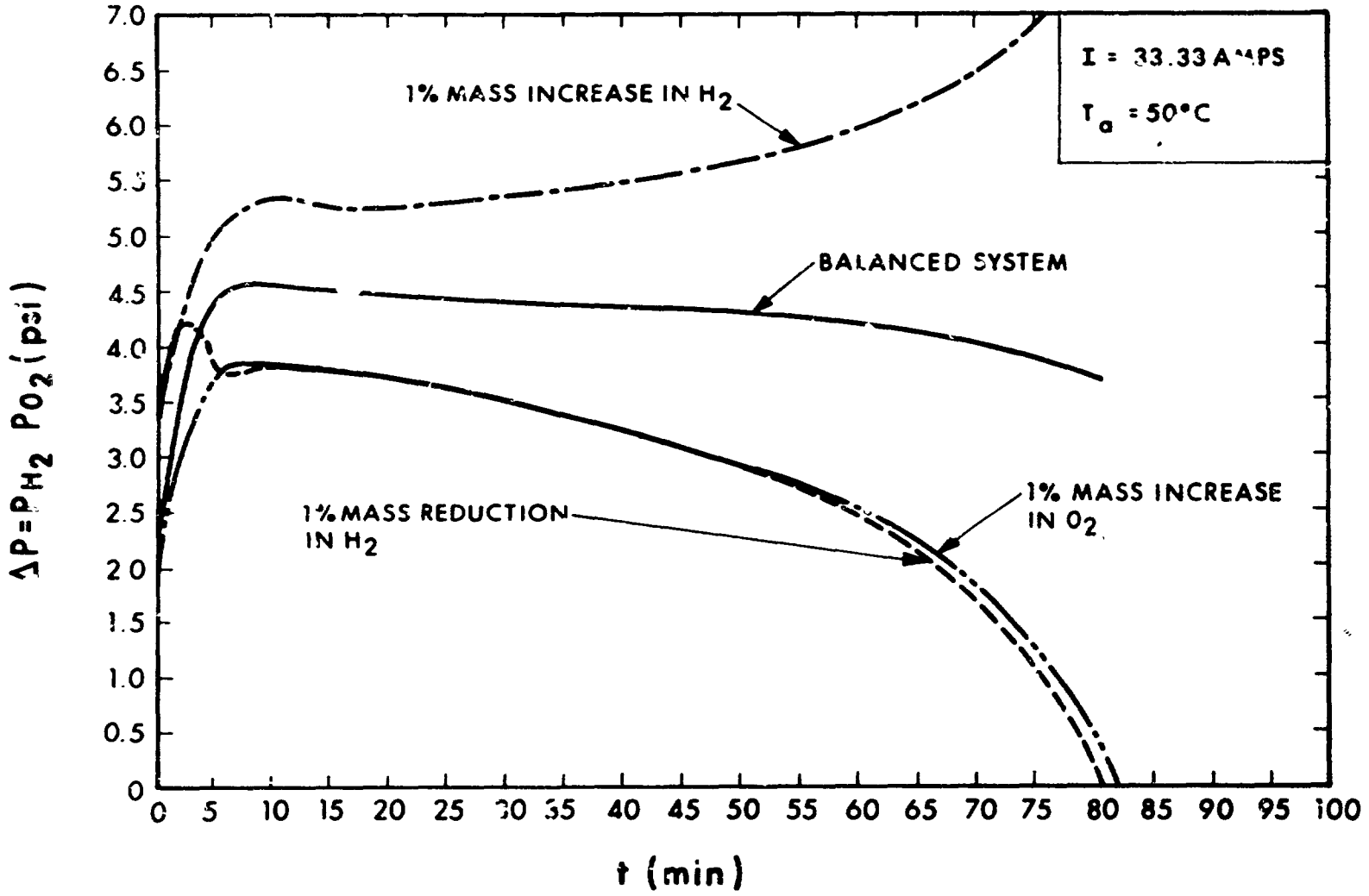

FIGURE 73. PRESSURE DIFFERENTIAL PLOTS OF BOILERPLATE FUEL CELL DISCHARGE CYCLE

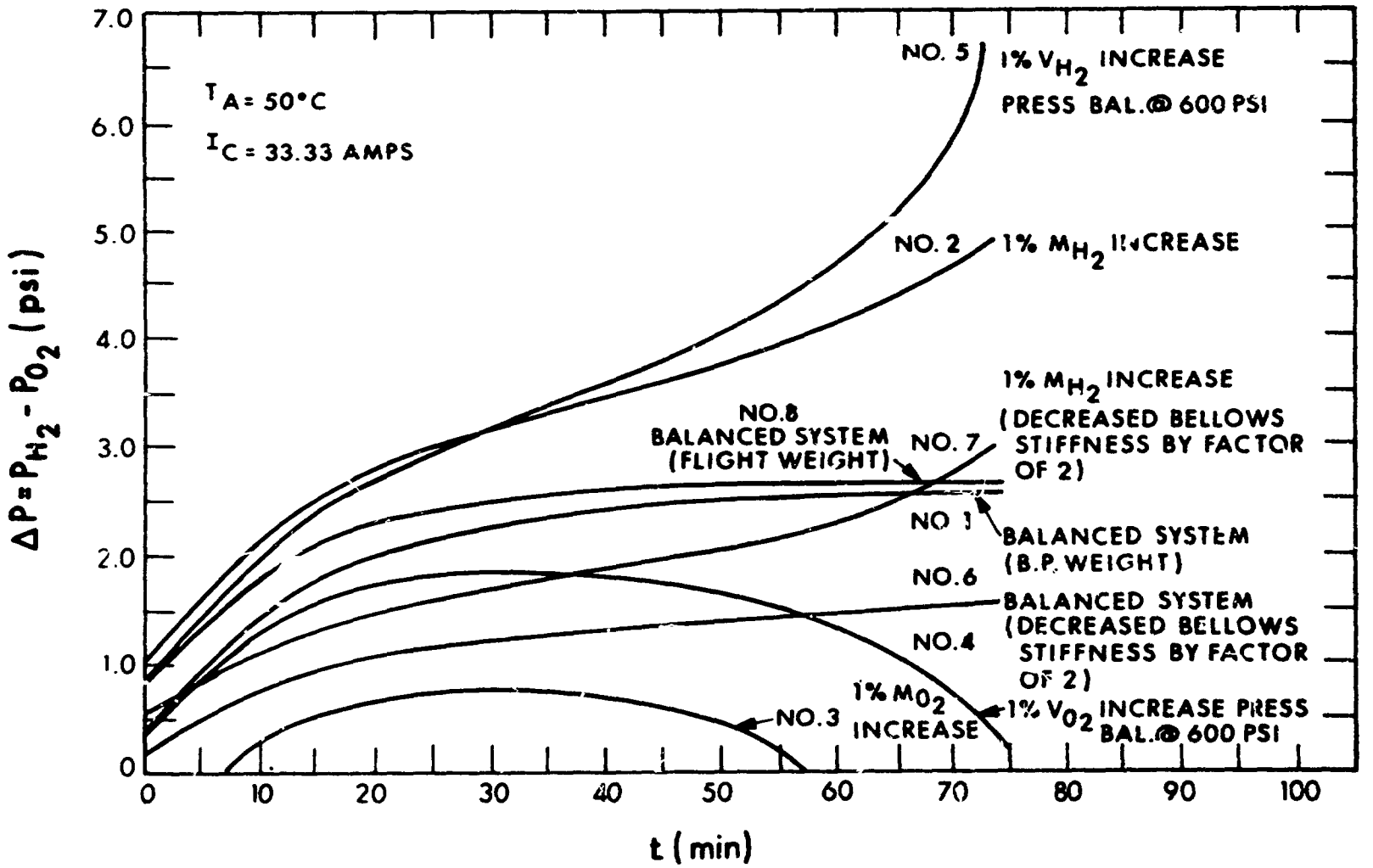

FIGURE 74. GAS PRESSURE PLOTS OF A BALANCED SYSTEM

Curve #3

The balanced mass of O_2 calculated for Curve #1 was arbitrarily increased 1 percent affecting initial pressures slightly (again, calculate in the program). All other input parameters are the same as Curve #1.

Curve #4

The O_2 volume was arbitrarily increased 1 percent with new initial masses calculated for the O_2 and H_2 at 600 psi by:

$$W_{O_2} = \left(\frac{PV'}{ZRT}\right)_{O_2} \quad \text{and} \quad W_{H_2} = \left(\frac{PV'}{ZRT}\right)_{H_2}$$

(all other parameters are the same as Curve #1).

Curve #5

The balanced H_2 volume was arbitrarily increased 1 percent with new masses calculated as in Curve #4. All other parameters are the same as Curve #1.

Curve #6

The same balanced system as Curve #1, except the bellows stiffness is decreased by a factor of two.

Curve #7

The same 1 percent mass increase as Curve #2 except the bellows stiffness is decreased by a factor of two.

Curve #8

Balanced system as in Curve #1 except the flight weight shell is analyzed.

Subroutines in the program have been upgraded to better predict temperatures in the oxygen and hydrogen during the discharge cycle. Includes at the end of this appendix is a printout which represents a fuel cell discharge cycle at 33.33 amperes for 1.2 hours, followed by a charge cycle at 2.0 amperes for 22.8 hours and a 24-hour dwell time after charge. The program computes the oxygen and hydrogen temperatures and pressures as a function of time with a given set of input parameters.

TEMPERATURE EXPRESSIONS

A) CHARGE CYCLE

$$P_{O_2} = \left(\frac{ZWRT}{V}\right)_{O_2} \qquad P_{H_2} = \left(\frac{ZWRT}{V}\right)_{H_2}$$

REVISED TERMS

$$W'i_{O_2} = X \text{ (variable)}$$

$$\frac{dWo_2}{dt} = -\frac{.298}{454} I_c \text{ (lb/hr)(variable)}$$

$$T'_{O_2} = T_O + \frac{Q_c}{h_s A_s}\left(1-e^{\frac{-h_s A_s t_c}{(WC)_s}}\right) + \frac{Q_c}{h_s A_s}\left(1-e^{-\frac{t_c}{T_c}}\right)$$

$$T'_{O_2} = T_O + \frac{Q_c}{h_s A_s}\left(2-e^{\frac{-h_s A_s t_c}{(WC)_s}} - e^{-\frac{t_c}{T_c}}\right)$$

$$\text{or} \quad T'_{O_2} = T_s + \frac{Q_c}{h_s A_s}\left(1-e^{-\frac{t_c}{T_c}}\right)$$

---

where

$$Q_c = VI$$

when $V = 0.4$ volts

$$Q_c = 0.4\, I_c \quad \text{(variable)}$$

For $I_c = 2$ amps $\quad Q_c = .8$ watt

$$T'_{H_2} = T_O + \frac{Q_c}{h_s A_s}\left(1-e^{\frac{-h_s A_s t_c}{(WC)_s}}\right) + \frac{2Q_c}{h_s A_s}\left(1 - e^{-\frac{t_c}{T_c}}\right)$$

$$\text{or} \quad T'_{H_2} = T_s + \frac{2Q_c}{h_s A_s}\left(1 - e^{-t_c/T_c}\right)$$

$$W'_{i_{H_2}} = Y \text{ (variable)}$$

$$\frac{dW_{H_2}}{dt} = -\frac{.0376}{454} I \text{ (lb/hr)}$$

B) DWELL END CHARGE

$$W''_{i_{O_2}} = \left(-\frac{dW_{O_2}}{dt}\right)_c t_c + W'_{i_{O_2}} \qquad W''_{i_{H_2}} = \left(-\frac{dW_{H_2}}{dt}\right)_c t_c + W'_{i_{H_2}}$$

$$\frac{dW''_{O_2}}{dt} = 0 \qquad \frac{dW''_{H_2}}{dt} = 0$$

$$T''_{O_2} = T_o + (T'_{O_2} - T_o)\, e^{\frac{-h_s A_s}{(WC)_s} t_D}$$

$$T''_{H_2} = T_o + (T'_{H_2} - T_o)\, e^{\frac{-h_s A_s}{(WC)_s} t_D}$$

C) DISCHARGE

$$W_{i_{O_2}} = \left(-\frac{dW_{O_2}}{dt}\right)_d t_d + W'_{i_{O_2}} \qquad W_{i_{H_2}} = \left(-\frac{dW_{H_2}}{dt}\right)_d t_d + W'_{i_{H_2}}$$

$$\frac{dW_{O_2}}{dt} = \frac{.298}{454} I_d \text{ (lb/hr)} \qquad \frac{dW_{H_2}}{dt} = \frac{.0376}{454} I_d \text{ (lb/hr)}$$

$I_d = 33.3$ amps

$$T''_{O_2} = T_o + \frac{Q_d}{h_s A_s} + \frac{Q_d\left(1 - e^{-\frac{t_d}{Tc}}\right)}{h_s A_s} + e^{\frac{-h_s A_s t_d}{(Wc)_s}}\left[T''_{O_2} - T_o - \frac{Q_d}{h_s A_s}\right]$$

$$T''_{H_2} = T_o + \frac{Q_d}{h_s A_s} + \frac{2Q_d\left(1-e^{-\frac{t_d}{Tc}}\right)}{h_s A_s} + e^{\frac{-h_s A_s t_d}{(WC)s}} \left[T'_{H_2} - T_o - \frac{Q_d}{h_s A_s}\right]$$

D) DWELL END DISCHARGE

$$W_{i_{o_2}} = \left(-\frac{dW_{o_2}}{dt}\right)_d t_d + W'_{i_{o_2}}$$

$$W_{i_{o_2}} = \left(-\frac{dW_{H_2}}{dt}\right)_d t_d + W'_{i_{H_2}}$$

$$\frac{dW_{o_2}}{dt} = 0 \qquad \frac{dW_{H_2}}{dt} = 0$$

$$T'''_{o_2} = T_o + (T'''_{o_2} - T_o)\, e^{-\frac{h_s A_s t'_d}{(WC)_s}}$$

$$T''_{H_2} = T_o + (T'''_{H_2} - T_o)\, e^{-\frac{h_s A_s t'_d}{(WC)_s}}$$

AMB. TEMP. (F) =?582.
SHELL WALL THICK. (IN) =?.25
K1 (BTU/HR F) =?.725
K2 (BTU/HR F) =?3.48
K3 (BTU/HR F) =?4.43
K4 (BTU/HR F) =?1.26
WM (LB) =?.428
WS (LB) =?13.50
CH2 (BTU/LB F) =?3.44
C02 (BTU/LB F) =?.221
CM (BTU/LB F) =?.80
CS (BTU/LB F) =?.11
INITIAL WT. OF OXYGEN (LB) =?.0328
INITIAL WT. OF HYDROGEN (LB) =?.00415
INITIAL 02 VOL =?18.22
INITIAL H2 VOL =?37.67
CB =?.168
DISCHARGE TIME (HRS) =?1.2
Q (BTU/HR F) =?78.3
CURRENT (AMP) =?33.33
DWELL AFTER DISCHARGE TIME (HRS) =?0.
CHARGE TIME (HRS) =?22.8
Q (BTU/HR F) =?.75
CURRENT (AMP) =?-2.
DWELL AFTER CHARGE TIME (HRS) =?24.

DISCHARGE TIME

T(HR)	T(MIN)	T02	TH2	P02	PH2
.00	.00	.582E+03	.582E+03	.600E+03	.600E+03
.05	3.00	.587E+03	.589E+03	.586E+03	.587E+03
.10	6.00	.590E+03	.596E+03	.570E+03	.572E+03
.15	9.00	.593E+03	.603E+03	.554E+03	.556E+03
.20	12.00	.596E+03	.608E+03	.536E+03	.539E+03
.25	15.00	.600E+03	.613E+03	.518E+03	.521E+03
.30	18.00	.602E+03	.616E+03	.499E+03	.503E+03
.35	21.00	.605E+03	.619E+03	.480E+03	.484E+03
.40	24.00	.606E+03	.622E+03	.461E+03	.465E+03
.45	27.00	.607E+03	.625E+03	.442E+03	.445E+03
.50	30.00	.610E+03	.627E+03	.422E+03	.425E+03
.55	33.00	.611E+03	.629E+03	.402E+03	.406E+03
.60	36.00	.613E+03	.631E+03	.382E+03	.385E+03
.65	39.00	.614E+03	.633E+03	.361E+03	.365E+03
.70	42.00	.617E+03	.635E+03	.341E+03	.345E+03
.75	45.00	.618E+03	.636E+03	.320E+03	.324E+03
.80	48.00	.619E+03	.638E+03	.300E+03	.303E+03
.85	51.00	.620E+03	.640E+03	.279E+03	.282E+03
.90	54.00	.622E+03	.641E+03	.258E+03	.261E+03
.95	57.00	.623E+03	.643E+03	.237E+03	.240E+03
1.00	60.00	.622E+03	.644E+03	.215E+03	.219E+03
1.05	63.00	.626E+03	.645E+03	.194E+03	.198E+03
1.10	66.00	.627E+03	.647E+03	.173E+03	.176E+03
1.15	69.00	.629E+03	.648E+03	.151E+03	.155E+03
1.20	72.00	.629E+03	.649E+03	.130E+03	.133E+03

CHARGE TIME

T(HR)	T(MIN)	TG2	TH2	PG2	PH2
.00	.00	.629E+03	.649E+03	.130E+03	.133E+03
1.00	60.00	.602E+03	.605E+03	.149E+03	.150E+03
2.00	120.00	.592E+03	.594E+03	.171E+03	.172E+03
3.00	180.00	.589E+03	.589E+03	.194E+03	.195E+03
4.00	240.00	.585E+03	.586E+03	.217E+03	.218E+03
5.00	300.00	.584E+03	.584E+03	.241E+03	.242E+03
6.00	360.00	.584E+03	.584E+03	.265E+03	.265E+03
7.00	420.00	.584E+03	.583E+03	.289E+03	.289E+03
8.00	480.00	.582E+03	.583E+03	.313E+03	.313E+03
9.00	540.00	.581E+03	.583E+03	.337E+03	.337E+03
10.00	600.00	.583E+03	.583E+03	.361E+03	.361E+03
11.00	660.00	.583E+03	.583E+03	.385E+03	.385E+03
12.00	720.00	.581E+03	.583E+03	.409E+03	.409E+03
13.00	780.00	.582E+03	.583E+03	.433E+03	.433E+03
14.00	840.00	.583E+03	.583E+03	.457E+03	.457E+03
15.00	900.00	.583E+03	.583E+03	.481E+03	.481E+03
16.00	960.00	.583E+03	.583E+03	.505E+03	.505E+03
17.00	1020.00	.583E+03	.583E+03	.529E+03	.529E+03
18.00	1080.00	.582E+03	.583E+03	.553E+03	.553E+03
19.00	1140.00	.583E+03	.583E+03	.577E+03	.577E+03
20.00	1200.00	.582E+03	.583E+03	.601E+03	.601E+03
21.00	1260.00	.583E+03	.583E+03	.625E+03	.625E+03
22.00	1320.00	.583E+03	.583E+03	.649E+03	.649E+03
22.80	1368.00	.583E+03	.583E+03	.668E+03	.669E+03

DWELL AFTER CHARGE TIME

T(HR)	T(MIN)	TG2	TH2	PG2	PH2
.00	.00	.583E+03	.583E+03	.668E+03	.669E+03
1.00	60.00	.583E+03	.582E+03	.668E+03	.668E+03
2.00	120.00	.582E+03	.582E+03	.667E+03	.668E+03
3.00	180.00	.581E+03	.582E+03	.667E+03	.668E+03
4.00	240.00	.581E+03	.582E+03	.667E+03	.668E+03
5.00	300.00	.582E+03	.582E+03	.667E+03	.668E+03
6.00	360.00	.582E+03	.582E+03	.667E+03	.668E+03
7.00	420.00	.582E+03	.582E+03	.667E+03	.668E+03
8.00	480.00	.581E+03	.582E+03	.667E+03	.668E+03
9.00	540.00	.582E+03	.582E+03	.667E+03	.668E+03
10.00	600.00	.583E+03	.582E+03	.667E+03	.668E+03
11.00	660.00	.582E+03	.582E+03	.667E+03	.668E+03
12.00	720.00	.582E+03	.582E 03	.667E+03	.668E+03
13.00	780.00	.582E+03	.582E+03	.667E+03	.668E+03
14.00	840.00	.581E+03	.582E+03	.667E+03	.668E+03
15.00	900.00	.580E+03	.582E+03	.667E+03	.668E+03
16.00	960.00	.582E+03	.582E+03	.667E+03	.668E+03
17.00	1020.00	.582E+03	.582E+03	.667E+03	.668E+03
18.00	1080.00	.581E+03	.582E+03	.667E+03	.668E+03
19.00	1140.00	.582E+03	.582E+03	.667E+03	.668E+03
20.00	1200.00	.582E+03	.582E+03	.667E+03	.668E+03
21.00	1260.00	.581E+03	.582E+03	.667E+03	.668E+03
22.00	1320.00	.582E+03	.582E+03	.667E+03	.668E+03
23.00	1380.00	.581E+03	.582E+03	.667E+03	.668E+03
24.00	1440.00	.582E+03	.582E+03	.667E+03	.668E+03